Environmentally Malleable Epigenomic Regions in the Mammalian Brain

A Dissertation

Presented to the Faculty of the Weill Cornell Graduate School

of Medical Sciences

in Partial Fulfillment of the Requirements for the Degree of

Doctor of Philosophy

by

Shifra Liba Klein

February 2016

ENVIRONMENTALLY MALLEABLE EPIGENOMIC REGIONS IN THE MAMMALIAN BRAIN

Shifra Liba Klein, Ph.D.

Cornell University 2016

Understanding the development of epigenetic patterns that underlie neural development and differentiation is an essential foundation for understanding what occurs in "abnormal" situations. DNA methylation, in concert with other epigenetic regulators, controls the accessibility of transcription factors to DNA and/or their function. While extensively studied in neuronal progenitors *in vitro*, the role of methylation/demethylation in neuronal lineage/subtype specification *in vivo* is not known. By profiling two distinct neuronal lineages, and five neuron subtypes in the hippocampus and striatum, we uncovered a set of five principles that govern DNA methylation-dynamics in neurodevelopment. By dividing neurodevelopment to three alternating methylation and demethylation periods and applying the principles to each of these stages, we created a matrix that comprehensively describes the targets, genomic contexts, functional consequences and putative mechanisms of methylation/demethylation events. The overarching theme is that the developmental methylation program is remarkably similar in the hippocampus and striatum, with significant divergence only occurring during subtype specification. Our matrix can be cross-referenced with disease-associated methylation changes to specify possible events and underlying principles compromised in disease.

Adverse environmental conditions, particularly during early life, are associated with increased risk for behavioral and/or psychiatric disorders. However, the molecular basis that can potentially link environmental conditions to psychopathologies are unknown, complicating diagnosis and therapeutic measures. We identified differentially methylated regions (DMRs) in mammalian offspring exposed to an adverse maternal environment associated with anxiety in both the mother and offspring. We hypothesized the presence of metastable "hotspots" in the genome that display an inherent sensitivity to environmental cues. These hotspots would enable an adaptive/maladaptive molecular response to multiple environmental conditions by modifying appropriate gene expression patterns and cellular phenotypes. Using several animal models of early life adversities, which result in a common offspring anxiety phenotype, we used genome-wide DNA methylation sequencing to detect common environmentally sensitive DMRs (E-DMRs). E-DMRs displayed several DNA features including: Exonic enrichment, intermediate methylation, and enhancer activity. Interestingly, E-DMRs did not perturb the overall patterning of DNA methylation that takes place during neural development. The experience dependent variations in DNA methylation at E-DMRs may prime the genome for differential transcriptional response to later events. This metaplasticity may be especially important in brain regions responsible for processing environmental input to elicit a behavioral response.

Since maternal conditions impact the offspring during gametogenesis and through fetal/early-postnatal life, the resultant phenotype is likely the aggregate of consecutive germline and somatic effects; a concept that hasn't been previously

studied. We dissected a complex maternally-transmitted phenotype, reminiscent of comorbid generalized anxiety/depression, to elementary behaviors/domains and their transmission mechanisms. We show that four anxiety/stress-reactive traits are transmitted via independent iterative-somatic and gametic epigenetic mechanisms across multiple generations. Somatic/gametic transmission alters DNA methylation at enhancers within synaptic genes whose functions can be linked to the behavioral-traits. Traits have generation-dependent penetrance and sex-specificity resulting in pleiotropy, often seen in psychiatry. A transmission-pathway based concept can refine current inheritance models of psychiatric diseases and facilitate the development of better animal models and new therapeutic approaches.

BIOGRAPHICAL SKETCH

Shifra Liba Klein completed her undergraduate degree in Biology at Yeshiva University in 2008. During her first two years she focused on completing her program requirements to build up her knowledge and skills in her areas of interest. In her junior and senior year she was involved in a variety of academic and research activities including work as an Organic Chemistry teachers assistant. In the summer of 2007 she was accepted as a University Scholar at the Albert Einstein College of Medicine's Summer Undergraduate Research Program, and in the Spring of 2008 she interned at Columbia University in the laboratory of Dr. Songtao Jia, studying techniques used in epigenetic research. She continued to build her practical research skill after graduating in 2008 when she accepted a position as a research assistant at the NYU School of Medicine, in the laboratory of Dr. Derya Unutmaz, which focuses on mechanisms of human T-cell biology and HIV pathogenesis. Simultaneously, she accepted an offer from Yeshiva University to serve as a Physiology Lab Instructor transmitting knowledge and expertise she values and cherishes to others. After looking into several graduate schools for the Fall of 2009 she decided that the environment at Weill Cornell was an ideal choice for her to continue her studies. After spending some highly productive and informative time in the labs of Drs. David Allis and Mary Goll she joined the lab of Dr. Miklos Toth in the Fall of 2011. During her time in the Toth lab she has made substantial scientific contributions that have led to the identification and characterization of several novel patterns of DNA methylation during neural development and subtype differentiation. Additionally, her work has revealed environmentally sensitive regions in the mammalian genome that display increased sensitivity to early life environmental adversity.

ACKNOWLEDGEMENTS

I want to extend my gratitude to a number of people who have helped me during my graduate school progress. Firstly, I would like to acknowledge my PI, Dr. Miklos Toth. His encouragement and advice toward all aspects of my academic career, have aided me tremendously to grow as a scientist and an independent thinker. I would also like to thank all the past and present members of the Toth lab who have been a wonderful group to learn and work with. Furthermore, a very special thanks to the members of my special committee, Drs. Olivier Elemento, Mary Goll and Barry Kosofsky, for the valuable feedback and advice. Also I would like to thank Drs. David Allis and Mary Goll for the mentorship I received in their labs in my first two years of graduate school. In addition, I would like to thank Drs. Jason Banfelder, Luce Skrabnek and Friederike Dundar at the Applied Bioinformatics Core facility for their computational guidance. Lastly, I would like to thank the Dr. Kirk Deitsch for his advice over the years.

TABLE OF CONTENTS

LIST OF FIGURES

CHAPTER 4

CHAPTER 5

LIST OF TABLES

CHAPTER 1

INTRODUCTION

1.1 Non-genetic foundation of Psychiatric Disorders

Psychiatric disorders affect nearly one third of the human population at some point in their lives[1]. However, despite the prevalence of these disorders, little is known regarding the underlying causes. The majority of psychiatric disorders cannot be traced to genetic abnormalities, and are believed to arise, at least partly, from epigenetic changes caused by environmental factors, often during early life[2-5].

The mammalian brain is a complex system with a highly choreographed developmental process. The process is guided by distinct stages of gene expression by transcription factors, and morphogens[6,7]. In addition, external factors including resources from the mother during early stages of life, such as hormones and cytokines, influence neuronal development[8-10]. Environmental perturbations during early life are believed to result in the dysregulation of the developmental process, giving rise to abnormal brain structure/function and subsequent behavioral and/or neuropsychiatric abnormalities[9]. Early environmental adversities, such as maternal stress, maternal deprivation or maternal infection are associated with increased neurophysiological and behavioral abnormalities in adult offspring[11-13]. Due to the vulnerability of certain neuronal systems and circuits during development, different early-life environmental adversities often result in similar phenotypes. However, little is known regarding the convergence point, whether at the molecular, circuit or behavioral level, that explain the observed convergent phenotype[14,15]. Furthermore, recent studies have demonstrated that the behavioral abnormalities can be multigenerationally inherited[4,9,16-20].

The behavioral consequences of early life adversity can most plausibly explained by epigenetics. Dysregulation of key epigenetic modifiers results in gross behavioral abnormalities[21-23]. Several studies have shown differential methylation at candidate genes following early life environmental adversity, and adult environmental changes[24-26]. Moreover, the early-life adversity induced behavioral phenomena discussed above, including convergent phenotypes and multigenerational transmission, can have an epigenetic origin. Epigenetic modifications alter gene expression and phenotype in response to environmental perturbations and occur without a change in DNA sequence. Epimutations are based on changes in DNA methylation and/or histone modifications, and can remain stable through embryonic development and adult life[27,28].

1.2 DNA methylation dynamics during neural development

One limitation in studying the early development of environmentally induced behavioral abnormalities is our limited understanding of the epigenetics of neural development and differentiation. While many of the morphogens and transcription factors have been well studied and documented[6,7], little is known regarding the epigenetic factors, particularly DNA methylation, one of the most stable epigenetic modifications. While the dynamics of DNA methylation from germ cells to fertilization and through early embryonic development have been well documented and are characterized by distinct waves of methylation and demethylation[28,29], the dynamics during neural development remains unclear. Recently, epigenetic modifications associated with *in-vitro* development and differentiation of neural progenitors to glia and neuronal cells have been described[30]. We expanded upon these data by profiling DNA methylation in vivo and our study is the first to describe the

dynamics that take place during distinct stages of neural development in multiple regions and lineage subtypes in the brain.

1.3 Link between early life adversity, epimutations, and behavioral abnormalities

Neural development is associated with the formation of epigenetic patterns that are essential for proper differentiation[31,32]. Neural differentiation continues late in development, with many regions undergoing differentiation through the late prenatal to early postnatal period[33,34]. Environmental interference within this period often results in localized developmental and behavioral abnormalities associated with these developing regions, including anxiety[35], depression[36] and ADHD[37]. Since these psychiatric phenotypes are not due to genetic abnormalities, they are believed to result from stable epigenetic changes[13]. In fact dysregulation of key epigenetic modifiers, such as MECP2, results in gross behavioral abnormalities[21-23]. Additionally, several studies have shown differential methylation at candidate genes following early life environmental adversity, and adult environmental changes[24-26]. For instance, maternal deprivation in rats results in demethylation of the CRH promoter[38]. However, no studies to date have shown the environmental effect of early life adversity at the global level.

Studies described in Chapters 3 and 4 utilize three animal models of early life adversity that result in adult behavioral abnormalities, resembling neuropsychiatric disease. These models differ in timing, duration and severity. However, despite some differences in the physiological and behavioral phenotypes, all three models are associated with increased anxiety. This leads to the question of how such differing environmental triggers give rise to a phenotypic convergence on an anxiety phenotype. The convergence of non-genetic permanent behavioral abnormalities following early

life adversity suggests a common molecular and/or cellular phenotype in neuronal tissue. We hypothesized that the convergence of the various early life challenges occurs at specific regions in the genome that are inherently sensitive to environmental cues through development, particularly in the brain, and which can respond in an adaptive manner to modify gene expression and cellular phenotype. In chapters 3 and 4 we identified regions that undergo similar epigenetic changes in response to the different early life environmental challenges.

1.4 Propagation of epigenetic signatures across multiple generations

Several studies have documented the multigenerational inheritance of behavioral phenotypes[8,16,17,39,40]. Transmission can occur either through the germline due to epigenetic changes in the gametes, or somatically due to the exposure of the offspring to the affected parent. Due to technical difficulties separating the germ-line from somatic inheritance, most studies using rodent models have focused on the paternal inheritance[18,19,41].

However, many studies indicate that non-genetic transmission via the maternal line may be a more prominent mode of multigenerational inheritance of behavioral phenotypes[4,39,42,43]. Chapter 5 examines the multigenerational transmission of a complex maternally transmitted behavioral phenotype, reminiscent of the symptoms of anxiety and stress disorders. We show that transmission of the epigenetic signatures tracks the propagation of the behavioral phenotype across generations and that the individual traits are transmitted via parallel but segregated gametic and somatic pathways.

CHAPTER 2

PRINCIPLES GOVERNING DNA METHYLATION DURING NEURONAL LINEAGE AND SUBTYPE SPECIFICATION

** Sharma A.[**], Klein S.L.[**], Barboza L., Lodhi N., and Toth M. 2015. Principles governing DNA methylation during neuronal lineage and subtype specification. Manuscript submitted for review.*
[**] These authors contributed equally

2.1 Introduction

An important question in neuroscience is to understand how neuronal lineages, and the large number of neuronal subtypes, are established in the CNS during development and how this program is perturbed in neurodevelopmental disorders. Neuronal development is driven by a transcriptional program consisting of morphogens, their downstream intracellular signaling pathways, and associated transcription factors. Accessibility of these factors to DNA, determined by epigenetic mechanisms such as DNA methylation, is believed to be a permissive requirement for regulation [44]. An alternative model is that DNA methylation is secondary to regulation but cooperates with other factors to solidify the regulatory state [45,46]. Whether a causative factor or cooperating partner in gene regulatory changes, DNA methylation allows the identification of regulatory regions and provides information on the gene regulatory landscape during neuronal lineage and subtype specification.

Compared to DNA binding proteins and co-factors, relatively little is known regarding the role of DNA methylation in neuronal development. Studies with neuronal progenitors, differentiated *in vitro* from embryonic stem cells (ESCs), showed that pluripotency genes are methylated and repressed while a subset of genes, which are active in terminally differentiated neurons, become hypomethylated and

bivalent [47,48]. Surprisingly, few methylation changes, at least in promoters, were found during the transition from progenitors to postmitotic neurons [47]. Another report described hypomethylation at enhancer-like elements and increased expression at nearby genes in similar neuronal progenitors [45]. However, an *in vitro* differentiation system may not capture the complexities of lineage and neuronal subtype diversification and corresponding DNA methylation changes occurring *in-vivo*. Therefore, our aim was to determine genome-wide DNA methylation differences between two groups of prototypical neurons, hippocampal glutamatergic and striatal GABAegic, and their precursors at single base resolution to assess the contribution of DNA methylation to neuronal development.

Hippocampal and striatal neurons represent two highly divergent neuronal subtypes differing in several fundamental characteristics, including their origin, neurotransmitter identify and function. Hippocampal principal neurons, that include CA1 and CA3 pyramidal neurons as well as dentate gyrus (DG) granule cells (GCs), derive from the most medial domain of the dorsal telencephalon. In contrast, striatal projection neurons (medium spiny neurons or MSNs) originate from the ventral telencephalon. While hippocampal neurons are involved in spatial learning/memory and navigation, MSNs are associated with coordination of movement (dorsal) and reward processes (ventral). The hippocampal circuit is often implicated in epileptic seizures and hippocampal neurons are one of the first neuronal subtypes affected in Alzheimer's disease. MSNs on the other hand, degenerate in Huntington's disease and are critical in the development of Parkinson's disease.

Differentiation of ESCs to neuron-restricted neuronal progenitors and then to subtype specific neurons in the CNS is a gradual process of diversification. ESCs in the inner cell mass of the embryonic (E) 3.5 day blastocyst undergo progressive fate restriction and sequentially give rise to tissue-specific multipotent progenitor cells,

including neural progenitors in the ventricular germinal layer in the E9.5-10.5 telencephalon (Fig. 2.1A, developmental stage-1). Hippocampal progenitors (HPs) are derived from the epithelium of the ventricular germinal layer, while striatal progenitors (SP) from the lateral ganglionic eminence [49-51] (Fig. S2.1A). The regional specification of these progenitors is regulated by morphogens produced in patterning centers. The dorsal telecephalon is patterned by Wnt via the canonical Wnt pathway and bone morphogenic proteins, both derived from the cortical hem, an area in the dorsal midline in the telencephalon [52,53]. Specification of ventral telencephalic progenitors is regulated by sonic hedgehog secreted from the rostrocaudal axis of the neural tube [54]. The graded signaling of dorsal and ventral morphogens is translated into regional transcription factor codes [49]. For example, in HPs, LEF1/TCF proteins, nuclear mediators of Wnt signaling, are required for patterning and proliferation [53]. In contrast, SP specification is controlled by the homeodomain transcription factor GSH2 and the proneural basic helix-loop-helix factor MASH1 [55,56].

The next phase in neuronal development, between E10.5 and 17.5, is neurogenesis and early differentiation that produce postmitotic "young" CA (yCA) neurons from HPs in the CA region of the hippocampus [57](Fig. 2.1A, developmental stage-2, Fig. S2.1B). Neurogenesis of yGCs in the developing DG of the hippocampus is delayed, peaking during the first week of postnatal (P) life in rodents (Altman and Bayer, 1990a). Propagation/differentiation of SPs occur between E13.5 and E17.5, producing postmitotic yMSNs in the developing striatum [58](Fig. S2.1B).
Final maturation of neurons in both the hippocampus and striatum begins prenatally and continues postnatally (Fig. 2.1A, developmental stage-3).

2.2 Results

Alternating waves of gain and loss of methylation in the telencephalon during neuronal development

We determined DNA methylation patterns in two distinct neuronal lineages across development; starting with pluripotent stem cells that produce dorsal and ventral telencephalic neural progenitors, which in turn differentiate to various hippocampal and striatal neurons (Fig. 2.1A). In principle, methylation changes can be measured in two "dimensions" during neuronal development; "vertically" through discrete steps of development in individual lineages (developmental specific) and "horizontally" across lineages/subtypes at each developmental stage (Fig. 2.1B). Differences in developmental methylation between lineages create lineage/subtype specificity. ESCs, which can be differentiated towards the neuronal fate [59] were used as reference. Mouse ESCs, presumably because of their serial propagation in culture, have a DNA methylation pattern similar to that of E6.5 epiblasts [29,47], the last of pluripotent undifferentiated cells in the embryo [60]. Indeed, we found a high concordance between methylation in our ESCs and in E6.5 epiblasts [29] at CpG sites (Fig. S2.2A). Because of its higher coverage, our ESC dataset was used in all studies. Progenitors and young neurons were isolated by microdissection from cryosectioned slices of E10.5 and 17.5 brains, respectively (Fig. S2.1A, B). Neuronal cell bodies were isolated from cryoslices of DG and CA, regions that have a low number of non-neuronal cells, from adult brains (Fig. S2.1C, D). MSNs, which are more dispersed in the dorsal and ventral striatum, were obtained by fluorescent activated cell soring (FACS)(Fig. S2.1AE, F). In addition to minimize contamination by non-neuronal cells during sample preparation, the threshold for differential methylation was set to 20% (beyond statistical difference) to further minimize that changes in methylation are due to the presence of non-neuronal cells. The ten isolated populations of cells, ranging

from pluripotent ESCs through neuronal progenitors to young and mature postmitotic neurons, were subjected to enhanced reduced representational bisulfite sequencing [61], a method that is less biased to CpG rich regions than the traditional RRBS but relatively cost effective because up to 90% of reads of full genome sequencing are not informative (i.e. have no cytosines). Differentially methylated regions (DMRs) were defined as clusters of $\geq$4 differentially methylated sites ($\geq$20%; $p<0.01$, SLIM-corrected), either at CpG or non-CpG (CpH) dinucleotides, with inter CpN distance of $\leq$1kb. The size of DMRs ranged between 1,000 and 1,400 bps and contained 5.7-7.3 differentially methylated sites across developmental stages and between neuronal subtypes (Fig. 2.1B).

We found large-scale changes in methylation, with alternating hyper-, hypo- and again hypermethylation, through the three distinct periods of neuronal development (Fig. 2.1C). During the establishment of progenitors (up to E10.5, stage-1), approximately one tenth of the 1.48 and 1.36 million profiled CpG sites were differentially methylated within clusters (10.4% and 9.6% of CpGs in HPs and SPs, respectively), with relatively few clustered changes at the ~6.5 million profiled non-CpG sites (0.1%). Most of these changes involved hypermethylation (93.4% and 92.6% in HPs and SPs, respectively, Fig. 2.1C). During neurogenesis/early differentiation (stage-2), as progenitors gave rise to young postmitotic neurons, there was a substantial loss of methylation and/or active demethylation, both in the dorsal and ventral telencephalon (Fig. 2.1C). Again, changes were almost exclusively at CpG sites. Finally, during the third period, as young neurons matured to field specific CA1/CA3 pyramidal neurons, GCs and MSNs, methylation again increased (Fig. 2.1C). Substantially more methylation occurred in the striatal than hippocampal, lineage. In contrast to the two previous developmental periods, methylation in this period involved not only CpGs but CpH sites as well (23.2% and 33.2% of the

methylated CpNs in CA1 neurons and MSN, respectively). CpH methylation took place mainly in CpA context, in agreement with previous reports [62-66]. In conclusion, the neuronal genome undergoes alternating, largely unidirectional changes, at consecutive stages of neuronal development.

Figure 2.1. Dynamics of DNA methylation during hippocampal and striatal neuron development. A. Schematic diagram of the developmental "tree" of hippocampal and striatal lineages in the telencephalon. DNA methylation changes were studied during three consecutive developmental periods that span the production of progenitors in the telencephalon (stage 1), neurogenesis and early differentiation to "young" (y) neurons (stage-2) and maturation to subtype specific neurons (stage-3). HP and SP, hippocampal and striatal progenitors; yCA, young CA neuron; yGC, GC, granule cell; MSN, medium spiny neuron; d, dorsal; v, ventral; CPu, caudate putamen; NAc, nucleus accumbens. **B**. Methylation differences are analyzed vertically, through development within lineages and horizontally, across lineages and subtypes. Differentially methylated regions (DMRs) are defined as regions with 4 or more clustered differentially methylated sites (DMSs). **C**. Hyper- and hypomethylation at CpGs (grey bars) and CpHs (black bars) during the three developmental periods, as shown in "A", in the hippocampal and striatal lineages. **D**. Extensive overlap between lineages during proliferation and early differentiation but diversification in differentially methylated sites during maturation. **E**. Lineage differences in CpG and CpH methylation across development and subtype specific methylation differences in mature neurons. **F**. Developmental time course of Tet mRNA levels. **G**. Inactivation of *Dnmt3a* in developing GCs prevents gain in methylation during GC maturation. T-cre^{-}, control; T-cre^{+}, cre-induced inactivation of *Dnmt3a*.

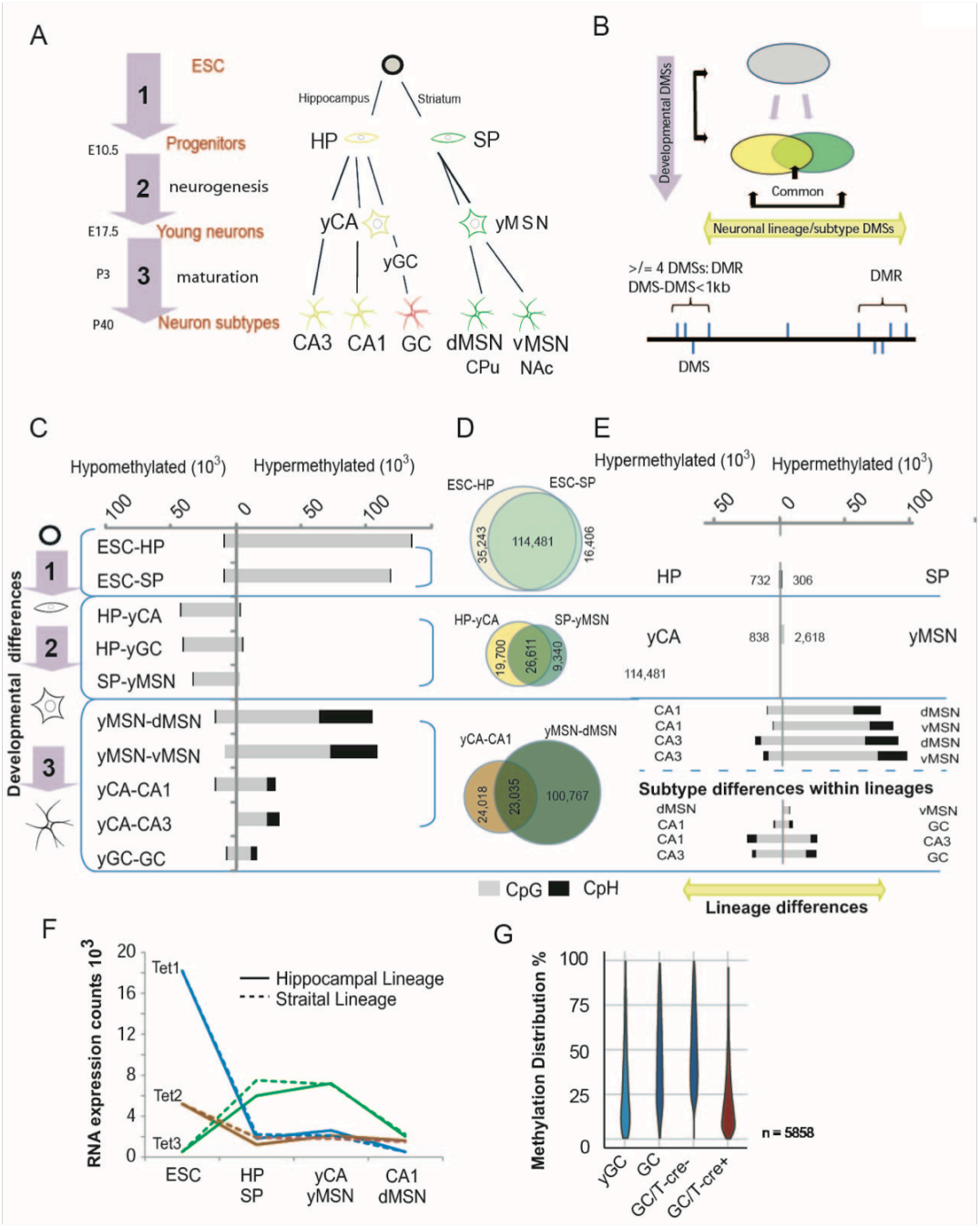
A
ESC
1
Progenitors
E10.5
2
neurogenesis
E17.5
Young neurons
3
maturation
P3
P40
Neuron subtypes
Hippocampus
Striatum
HP
SP
yCA
yMSN
yGC
CA3
CA1
GC
dMSN
CPu
vMSN
NAc
B
Developmental DMSs
Common
Neuronal lineage/subtype DMSs
>/= 4 DMSs: DMR
DMS-DMS<1kb
DMR
DMS
C
Hypomethylated (10^3)
Hypermethylated (10^3)
100
50
0
50
100
Developmental differences
ESC-HP
ESC-SP
HP-yCA
HP-yGC
SP-yMSN
yMSN-dMSN
yMSN-vMSN
yCA-CA1
yCA-CA3
yGC-GC
CpG
CpH
D
ESC-HP
ESC-SP
35,243
114,481
16,406
HP-yCA
SP-yMSN
19,700
26,611
9,340
yCA-CA1
yMSN-dMSN
24,018
23,035
100,767
E
Hypermethylated (10^3)
Hypermethylated (10^3)
50
0
50
100
HP
732
306
SP
yCA
838
2,618
yMSN
114,481
CA1
CA1
CA3
CA3
dMSN
vMSN
dMSN
vMSN
Subtype differences within lineages
dMSN
CA1
CA1
CA3
vMSN
GC
CA3
GC
Lineage differences
F
RNA expression counts 10^3
20
16
12
8
4
0
Tet1
Tet2
Tet3
Hippocampal Lineage
Straital Lineage
ESC
HP
SP
yCA
yMSN
CA1
dMSN
G
Methylation Distribution %
100
75
50
25
0
n = 5858
yGC
GC
GC/T-cre-
GC/T-cre+

Regulation of loss and gain of methylation during neuronal differentiation

To explain the mostly uniform loss of methylation during the progenitor to young neuron transition (stage-2, Fig. 2.1C), we surveyed the expression of all known enzymes with confirmed or putative DNA demethylase activity by RNA-Seq. We found a 5 and 7-fold increase in apobec2 expression in yCA neurons and yMSNs, relative to that in HPs and SPs, respectively. Although the AID/APOBEC family has been implicated in demethylation [67], more recently APOBEC2 and other members of the APOBEC family have been shown to have no or minimal activity at methylated cytosines [68]. Consistent with the latter data, differentially methylated sites that were hypomethylated in P5 WT yGCs were also hypomethylated in *apobec2*$^{-/-}$ yGCs, indicating no consequence of the absence of the protein on methylation. Alternatively, loss of methylation could be due to active demethylation by the ten-eleven translocation (TET) family of enzymes via hydroxylation, followed by reversion to unmethylated cytosines through iterative oxidation and thymine DNA glycosylase-mediated base excision repair [69]. Expression of *Tet1* and *Tet2* were high in ESCs but declined from the progenitor stage and remained low through neurogenesis and maturation. In contrast, expression of *Tet3* was initially low in ESCs, higher in progenitors and young neurons, and again low in mature neurons. This time course is most consistent with loss of methylation between the progenitor and young neuron stages and gain in methylation in the preceding and consecutive periods (Fig. 2.1F). Finally, passive loss of methylation could also be a contributing factor due to proliferation during the progenitor to young neuron transition. Overall, these data suggest that both active demethylation via Tet3 and passive demethylation may have a role in the substantial loss of methylation during early neuronal differentiation.

In the next developmental stage, characterized by the transition of young to mature neurons in the hippocampus and striatum (stage-3, Fig. 2.1C), there was an

overall gain in methylation at both CpG and non-CpG sites. The *de novo* methyltransferase DNMT3a is essential for CpH methylation [65,66,70]. Therefore, we conditionally inactivated *Dnmt3a* by tamoxifen inducible nestin-creERT2, from E13.5 in the hippocampus (75-85% knockdown efficiency), before the young to adult GC transition at E17.5. This prevented the developmental gain in methylation in GCs (Fig. 2.1G), implicating Dnmt3a in the gain of methylation during GC maturation.

Lineage specific DNA methylation differences are minimal during neuronal proliferation and early neuronal differentiation, but substantial during neuronal maturation

A large fraction of the developmentally methylated sites (76% and 88% for HP and SP, respectively), mapped to the same CpG sites, with the same direction of change, in the two lineages (Fig. 2.1D, Fig. S2.2B). Significant methylation differences between HPs and SPs were found at only 1,038 CpG sites (Fig. 2.1E), much less than the number of developmentally modified sites (lineage vs. developmental ratio of ~1:100). In contrast, lineage diversity at the transcriptome level was much greater (lineage vs. developmental specific transcript ratio of ~1:10; i.e. 946 HP-SP vs. 10,374 ESC-HP/10,640 ESC-SP, RNA-Seq, FDR <0.05). This indicates that the neuronal DNA methylation program during progenitor proliferation may only minimally contribute to lineage specification.

During the progenitor to young neuron transition (stage-2), most sites were still similarly modified in the two lineages (Fig. 2.1D). Consequently, the number of lineage, compared to development specific differentially methylated sites (Fig. 2.1E) was still low (~10:1). This is in contrast to the ~1:2 lineage vs. developmental gene expression ratio (4,114 yCA-yMSN vs. 9,165 HP-yCA/8,885 SP-yMSN). This suggests that DNA hypomethylation during the transition of progenitors to young

neurons is still primarily associated with common, lineage-independent, neuronal changes.

In contrast to the previous developmental stages, neural maturation was characterized by 3-4 times more methylated sites in the striatum. This resulted in less overlap between the lineages (Fig. 2.1D), and consecutively larger diversity across lineages (Fig. 2.1E). Modifications at CpHs contributed to these lineage and subtype specific methylation changes. As a result, the lineage and developmental methylation (Fig. 2.1C and E), similar to the lineage vs. developmental expression changes (CA1-dMSN vs. yCA-CA1/yMSN-dMSN), were in par. Methylation differences were observed not only between hippocampal and striatal mature neurons, but between neuronal subtypes within brain regions as well, particularly in the hippocampus (Fig. 2.1E). This suggests that the DNA methylation program progresses in a field specific manner in the hippocampus, while the striatal pattern remains relatively uniform in the dorsal and ventral compartments. This is consistent with the successive birth and migration of CA3, CA1 and finally GC neurons in the hippocampus. In contrast, the dorsal and ventral MSNs, destined to the caudate-putamen and nucleus accumbens, are produced and migrate simultaneously [58,71]. Taken together, the developmental methylation program is remarkably similar initially in the hippocampus and striatum, with significant divergence only occurring during neuronal maturation.

Widespread DNA methylation at partially methylated sites during neuronal progenitor proliferation

Methylation during the establishment of the progenitor pool was targeted to sites with an intermediate level of methylation (25-75%) in ESCs (and in E6.5 epiblasts). Methylation shifted to a higher level in both the dorsal and ventral progenitors (Fig. 2.2A). Intermediately methylated sites represents a minority of all CpGs in ESCs and epiblasts (Fig. S2.2A), since methylation is bimodal, with most

CpG sites either methylated (>75%) or unmethylated (<25%)(Fig. 2.2A; Controls). In inbred mice, like those used in our experiments, intermediate methylation reflects cell-to-cell variability (except at imprinted genes)[72,73]. Indeed, differentially methylated sites on the X-chromosome were also intermediately methylated in male ESCs. Intermediate/variable methylation in ESCs and E6.5 epiblasts may represent epigenetic mosaicism due to ongoing, yet uncompleted reprogramming at these sites, that follows the erasure of methylation marks in the early embryo [28].

Figure 2.2. **Characteristics of DNA methylation during progenitor proliferation.** **A.** Distribution of methylation levels at proliferation specific differentially methylated sites (DMSs) across development, as compared to the methylation of all CpG sites (Control) in ESC and HP/SP. Sites with intermediate methylation in ESCs (and in epiblasts) are preferentially targeted, while genomic CpGs overall show a bimodal distribution in ESCs and progenitors (see Controls in frame). The sites with intermediate methylation in ESC acquire high methylation level in hippocampal and striatal progenitors (HP and SP) and maintain it through neuronal differentiation. In oocytes and sperms, as well as in zygotes, CpGs at proliferation specific differentially methylated sites have the typical bimodal methylation distribution and are demethylated during reprogramming in the inner cell mass (ICM). **B.** Enrichment and depletion of proliferation-related DMSs in genomic features (fold difference, as compared to the representation of all profiled CpGs). **C**. Heat map representation of methylation levels emphasizing the permanence of most HP and SP DMSs across development. **D** and **F**. Genes with differential methylation and expression (mean methylation of differentially methylated sites within a gene). Hypermethylation during HP and SP proliferation is associated with both gene activation and repression. **E, G**. Hypermethylated/upregulated (red) and hypermethylated/downregulated (blue) genes belong to different functional categories in both the dorsal and ventral telencephalon.

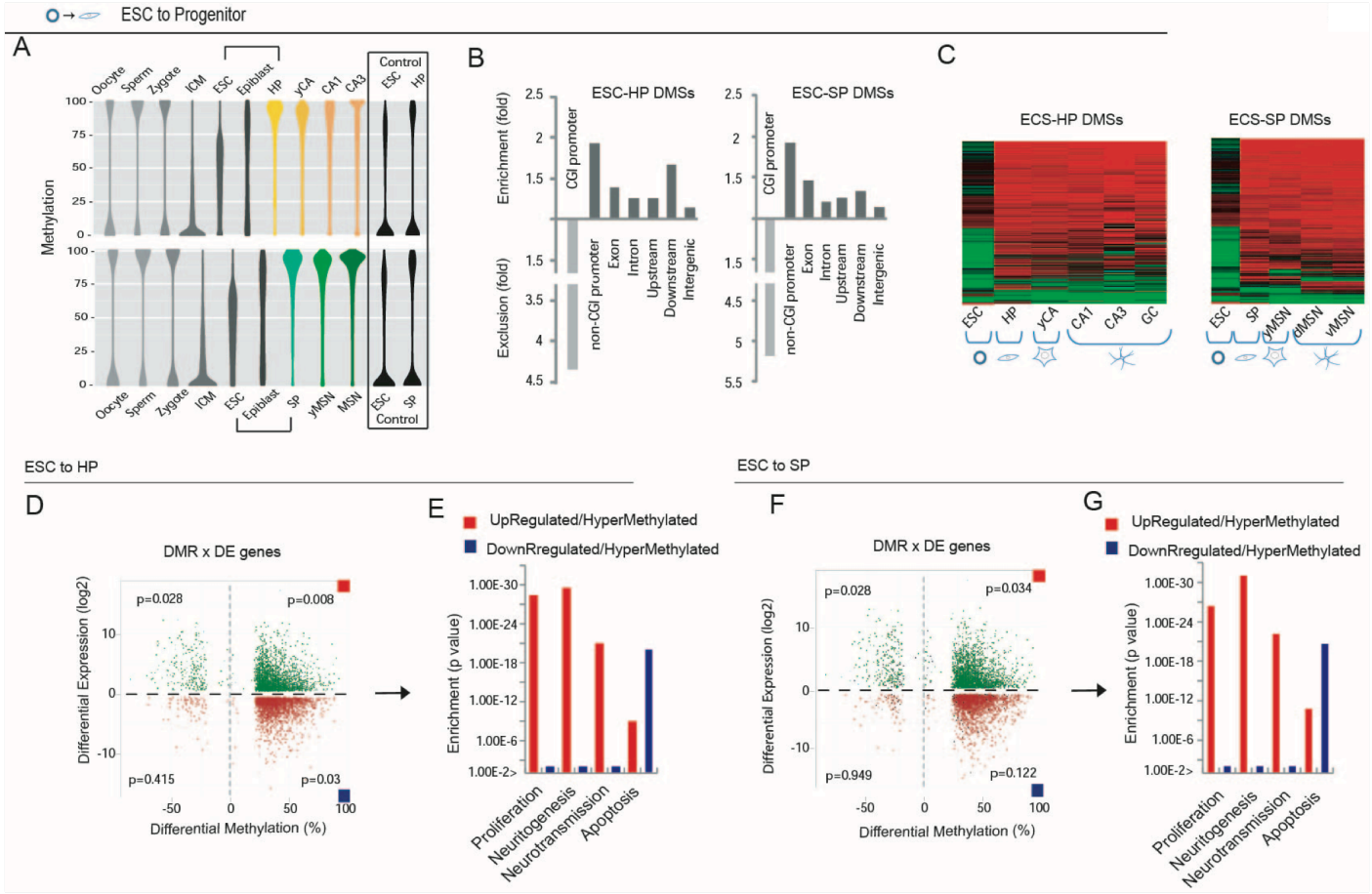
ESC to Progenitor
A
Oocyte
Sperm
Zygote
ICM
ESC
Epiblast
HP
yCA
CA1
CA3
Control
Methylation
SP
yMSN
MSN
B
ESC-HP DMSs
ESC-SP DMSs
Enrichment (fold)
Exclusion (fold)
CGI promoter
non-CGI promoter
Exon
Intron
Upstream
Downstream
Intergenic
C
ECS-HP DMSs
ECS-SP DMSs
GC
ESC to HP
ESC to SP
D
DMR x DE genes
Differential Expression (log2)
Differential Methylation (%)
p=0.028
p=0.008
p=0.415
p=0.03
E
UpRegulated/HyperMethylated
DownRregulated/HyperMethylated
Enrichment (p value)
Proliferation
Neuritogenesis
Neurotransmission
Apoptosis
F
p=0.034
p=0.949
p=0.122
G

Surveying the genomic location of differentially methylated sites between ESCs and progenitors, we noticed their exclusion from CpG rich areas, such CG island (CGI) promoters. This is consistent with the known resistance of CGIs to methylation [47,74]. However, ESC-HP/SP differentially methylated sites were enriched in multiple other genomic features (Fig. 2.2B). This included a substantial fraction of non-CGI promoters (5474 and 4498 in hippocampus and striatum, respectively) and which became predominantly methylated (87% and 90% in HP and SP) relative to ESCs. Although the enrichment was lower, extensive methylation also occurred at exons, introns and intergenic regions in progenitors. Heatmap representation of the methylation data indicated that the gain in methylation during progenitor development was mostly permanent (Fig. 2.2C). Only 9.6% and 10.2% of the ESC-HP, and 7.5% and 14.3% of the ESC-SP differentially methylated sites, were modified again during the progenitor to young neuron and young to mature neuron transitions, respectively (Fig. S2.3). Only a small fraction of sites (1.9 and 3.5%) were modified in all three stages of development in the dorsal and ventral telencephalon.

In accordance with the genome-wide methylation during proliferation, a large number of genes were differentially methylated (8,329 ESC-HP and 7,865 ESC-SP genes). Approximately 60% of differentially methylated genes were also differentially expressed (DMR x DE genes) and could be divided into four categories according to the direction of their methylation and expression change (Fig. 2.2D,F). The majority of DMR x DE genes were hypermethylated, consistent with the overall gain in methylation during this period (Fig. 2.1C), but were associated with both gene activation and repression. Gene ontology analysis by Ingenuity Pathway Analysis (IPA) showed that the upregulated/hypermethylated and downregulated/hypermethylated groups of genes were enriched in different functional categories (Fig. 2.2E,G). Upregulated genes were enriched in the cellular processes of

proliferation, *neuritogenesis* and even *neurotransmission*. This suggests that aside from stage-specific changes, epigenetic and transcriptional changes supporting later differentiation processes are also underway. In contrast, downregulated genes were solely enriched in *apoptotic* function. Thus, while there is no global correspondence between methylation and expression during progenitor proliferation, within specific functional categories methylation correlates with increased or reduced gene expression.

Intronic and intergenic methylation during neuronal differentiation

Developmental methylation changes, predominantly hypomethylation, during the progenitor to young neuron transition (Fig. 2.1A, stage-2) were concentrated in introns, and, to a lesser extent, in intergenic areas, while excluded from promoters and exons (Fig. 2.3A and Fig. S2.4). The modified sites had predominantly high methylation in progenitors, which was drastically shifted to a low methylation level in yCA neurons and yMSNs (Fig. 2.3B), as well as in yGCs. While loss of methylation during the progenitor to young neuron transition was mostly permanent in the hippocampus, a significant fraction of SP-MSN differentially methylated sites were remethylated in adult neurons (Fig. 2.3C).

During the transition from young to mature neurons (Fig. 2.1A, stage-3), intron-specific methylation changes were also more abundant (Fig. 2.3E); but instead of loss, sites gained methylation, both at CpG and CpH sites (Fig. 2.3F). Introns were also the preferred targets during GC development.

Figure 2.3. **Characteristics of DNA methylation during neuronal differentiation from progenitors to young neurons (A-D) and then from young to mature neurons (E-G). A.** Enrichment and depletion of young neuron specific differentially methylated sites (DMSs) in genomic features (fold difference, as compared to the representation of all profiled CpGs). **B**. Distribution of methylation levels in 10% bins at HP-yCA and SP-yMSN DMSs, as well as all profiled CpGs, before (blue) and after (red) the developmental transitions. **C**. Heat map representation of methylation levels at HP-yCA and SP-yMSN DMSs through development, illustrating that loss of methylation during the progenitor to young neuron transition is mostly permanent, except at a fraction of SP-yMSN DMSs that are remethylated in adult neurons. **D.** Selected young neuron specific DMRs have promoter and/or enhancer-like activity in transfected neuronal N2A cells (ANOVA: basic vector, $F_{6.14}=3.272$, $P=0.032$; promoter vector, $F_{6.14}=13.594$, $P<0.0001$, LSD posthoc, *p<0.05, **p<0.01, ***p<0.005, $^{\#}p<0.01$ trend). Luciferase expression is expressed in fold change, relative to activities in cells transfected with basic (left panel) and promoter vector (right panel). Positive controls are basic vector with EF1 promoter (left panel) and promoter vector with CMV enhancer (right panel). **E**. Enrichment and depletion of mature neuron specific DMSs in genomic features (fold difference, as compared to the representation of all profiled CpGs). **F**. Distribution of methylation levels in 10% bins at yCA-CA and yMSN-MSN DMSs, as well as at all genomic sites, before (blue) and after (red) the developmental transitions, at CpG and CpH sites. **G**. Selected mature neuron specific DMRs have no promoter but significant enhancer-like activity in N2A cells (ANOVA: promoter vector, $F_{4.10}=27.983$, $P<0.0001$, LSD posthoc, *p<0.05, ***p<0.005). Luciferase expression is expressed in fold change as indicated in D. An intergenic Drosophila control sequence has neither promoter nor enhancer activity.

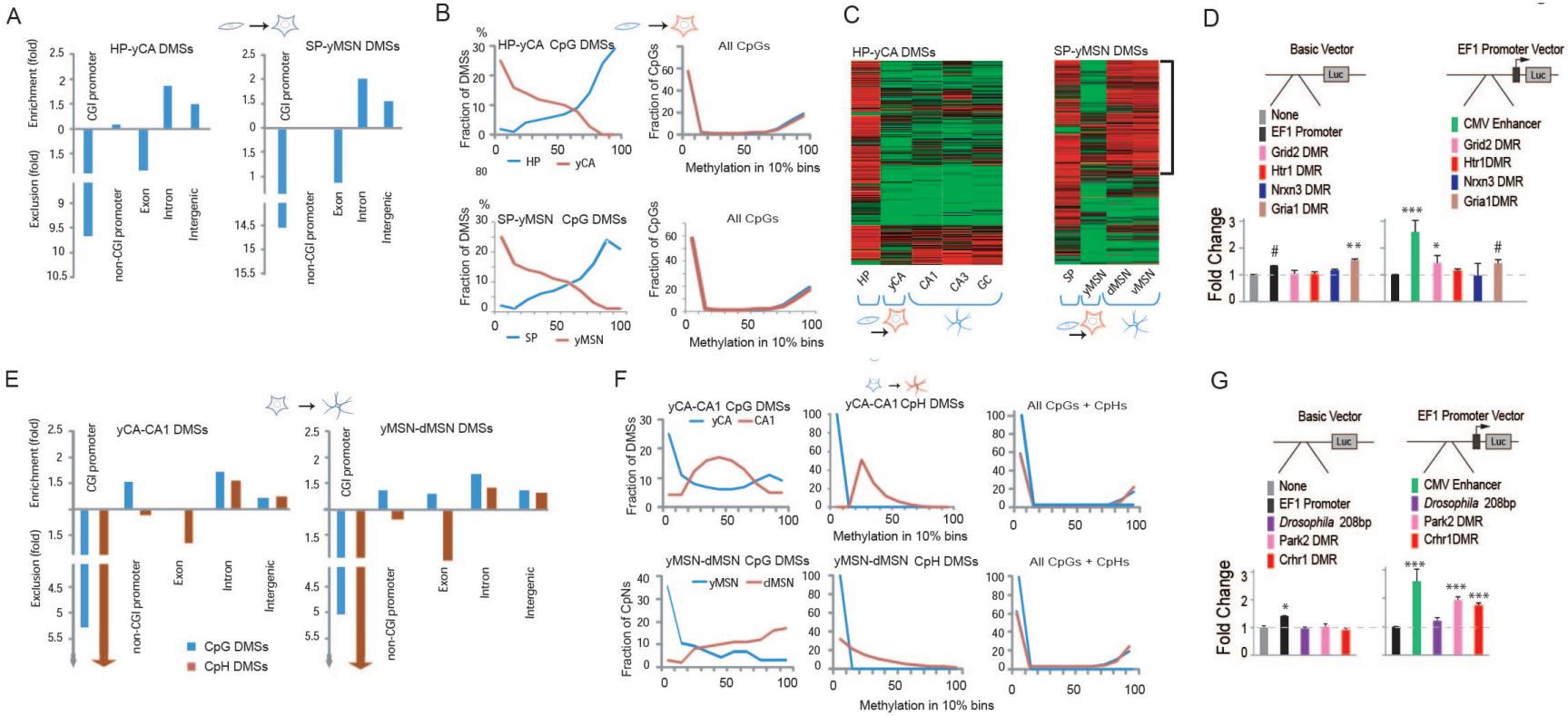
A
HP-yCA DMSs
SP-yMSN DMSs
Enrichment (fold)
Exclusion (fold)
CGI promoter
non-CGI promoter
Exon
Intron
Intergenic
B
HP-yCA CpG DMSs
All CpGs
SP-yMSN CpG DMSs
Fraction of DMSs
Fraction of CpGs
HP
yCA
SP
yMSN
Methylation in 10% bins
C
HP-yCA DMSs
SP-yMSN DMSs
HP
yCA
CA1
CA3
GC
SP
yMSN
dMSN
vMSN
D
Basic Vector
EF1 Promoter Vector
Luc
None
EF1 Promoter
Grid2 DMR
Htr1 DMR
Nrxn3 DMR
Gria1 DMR
CMV Enhancer
Grid2 DMR
Htr1DMR
Nrxn3 DMR
Gria1DMR
Fold Change
E
yCA-CA1 DMSs
yMSN-dMSN DMSs
CpG DMSs
CpH DMSs
F
yCA-CA1 CpG DMSs
yCA-CA1 CpH DMSs
All CpGs + CpHs
yMSN-dMSN CpG DMSs
yMSN-dMSN CpH DMSs
Fraction of CpNs
Methylation in 10% bins
G
Basic Vector
EF1 Promoter Vector
None
EF1 Promoter
Drosophila 208bp
Park2 DMR
Crhr1 DMR
CMV Enhancer
Drosophila 208bp
Park2 DMR
Crhr1DMR
Fold Change

Intronic DMRs exhibit promoter and enhancer activities

The preferred intronic localization of DMRs suggested alternative promoter and/or enhancer function. Therefore, we used luciferase reporter constructs in neuronal N2A cells to determine possible promoter and/or enhancer activity. One out of the four intronic DMRs (~200 bp), hypomethylated in both yCA neurons and yMSNs relative to HPs and SPs, exhibited promoter activity (*Gria1,* glutamate receptor (AMPA) 1), while two enhanced the activity of the EF1 promoter (*Grid2*, glutamate receptor, ionotropic, delta 2 and *Gria1*, trend only) (Fig. 2.3D). Additionally, two selected intronic DMRs, hypermethylated in CA1 neurons and dMSNs relative to yCA neurons and yMSNs, exhibited significant enhancer activity (*Park2*, parkin 2 and *Crhr1*, corticotrophin receptor 1; Fig. 2.3G), but no promoter activity. In contrast, an arbitrary 208 bp long intergenic drosophila sequence had neither promoter nor enhancer activity. These data indicate that at least some of the intronic DMRs associated with the transition of progenitors to young neurons, and young to mature neurons, have promoter and/or enhancer activity and could thus regulate isoform and/or overall gene expression.

Intersecting DNA methylation and gene expression changes across differentiation identifies developmental stage-specific functional gene clusters

Functional analysis was performed with genes which were differentially methylated in intronic/intergenic regions during the progenitor to young neuron transition. They exhibited enrichment in a wide range of developmental functions, including *proliferation*, *migration*, *neuritogenesis*, and *synaptic transmission*, in both the hippocampal (Fig. S2.5A) and striatal lineages. These functional categories were still strongly represented in the next, final maturation stage (Fig. S2.5B). Overall, these functional categories aligned with the consecutive steps along neuronal

differentiation, indicating that many neurodevelopmentally relevant genes undergo methylation changes during developmental transitions.

These developmental categories (from *proliferation* to *neurotransmission*) were also identified when the analysis was repeated with genes that were both differentially methylated and expressed during early differentiation. Consistent with the overall loss of methylation during this stage (Fig. 2.1C), the majority of corresponding DMRxDE genes were hypomethylated, but split to up- and downregulated groups (Fig. 2.4A). Downregulated genes (many of them transcription factors) were enriched in *brain morphogenesis*, in agreement with the closure of major morphogenic processes in the brain by the end of neuronal proliferation (Fig. 2.4B). Upregulated genes represented functions from *neuronal proliferation*, through *migration*, and *neuritogenesis*, to *synaptic transmission.* This analysis was repeated with genes that were DMRxDE during late differentiation/maturation. Though this period is characterized by gains in methylation (Fig. 2.1C), a significant fraction of DExDMR genes were hypomethylated (Fig. 2.4C). We therefor analyzed all combinations of expression and methylation changes by IPA. Although we still identified genes enriched in *neuronal proliferation* and *migration* functions, they were hypermethylated/downregulated, i.e. hyper/down, in contrast to their hypo/up status during the previous progenitor to young neuron transition (Fig. 2.4B, D). This switch from up- to downregulation reflects the cessation of proliferation and migration in both the hippocampal and striatal lineages. Genes associated with ongoing maturation processes (*neuritogenesis and synaptic transmission*) were hypo/up, like in the previous developmental stage. Although most of the hypo/up genes during early and late differentiation (stage-2 and -3) were different, some of them underwent two rounds of changes (red dots in Fig. 2.4C), suggesting a stepwise gene regulatory process, presumably to meet different demands during early and late differentiation.

Figure 2.4. Intersecting DNA methylation and gene expression changes during differentiation identifies developmental stage-specific gene clusters. A. Genes differentially methylated during the progenitor to young neuron transition are mostly hypomethylated, but can be either up- (hypo/up, red) or downregulated (hypo/down, blue). Very few genes are hypermethylated. Numbers in the individual quadrants represent Parson expression vs. methylation correlation *p* values. **B**. IPA analysis of hypo/up and hypo/down genes. Enrichment p values for these two groups of genes for highly significant functional categories are displayed in quadrants that correspond to their expression/methylation status, as in A. No IPA analysis was performed with hyper/up and hyper/down genes because of their low number. Hypo/down genes are associated with the early steps of *brain formation*, while hypo/up genes are enriched in a series of neuronal functions that align with the progressive steps of differentiation from *migration* to *synaptic transmission*. The enrichment score values in the four quadrants are connected, thus areas in the individual quadrants reflect the level of significance for each group of genes. **C**. Genes, differentially expressed during the young to mature neuron transitions are mostly hypermethylated, especially in the striatal lineage, but a substantial number of hypomethylated genes are also present. Genes, previously altered during the progenitor to young neuron transition are highlighted red (previously hypo/up, A) and blue (previously hypo/down). **D**. IPA analysis of genes distributed to four groups in C, based on their expression and methylation. Only highly significant functions are displayed. Hyper/down genes are enriched in functions associated with early *brain development*, *progenitor proliferation* and *migration*. Hypo/up genes are associated with later differentiation processes, from *neuritogenesis* to *synaptic transmission*.

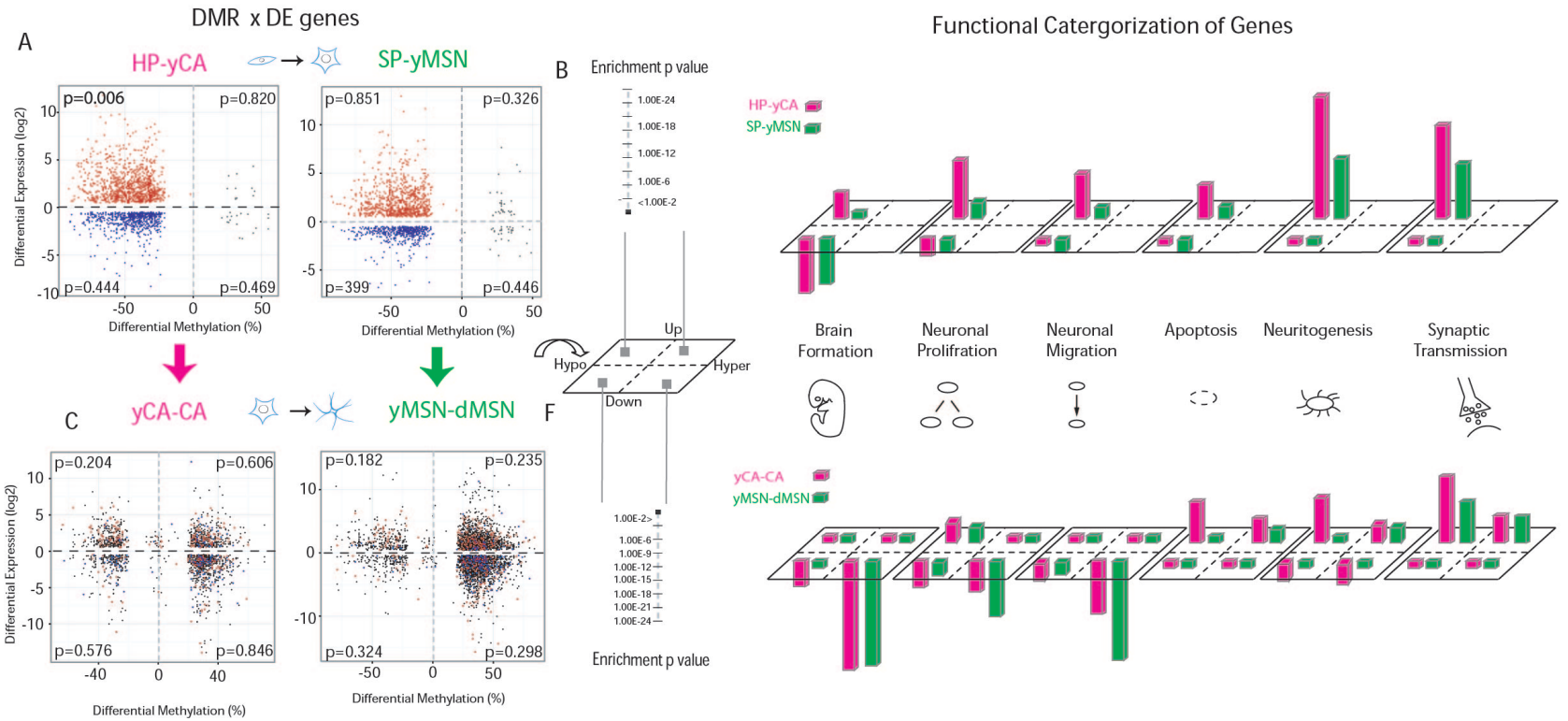
DMR x DE genes
A
HP-yCA
SP-yMSN
p=0.006
p=0.820
p=0.444
p=0.469
p=0.851
p=0.326
p=399
p=0.446
Differential Expression (log2)
Differential Methylation (%)
yCA-CA
yMSN-dMSN
C
p=0.204
p=0.606
p=0.576
p=0.846
p=0.182
p=0.235
p=0.324
p=0.298
B
Enrichment p value
1.00E-24
1.00E-18
1.00E-12
1.00E-6
<1.00E-2
Up
Hypo
Hyper
Down
F
1.00E-2>
1.00E-6
1.00E-9
1.00E-12
1.00E-15
1.00E-18
1.00E-21
1.00E-24
Enrichment p value
Functional Catergorization of Genes
HP-yCA
SP-yMSN
Brain Formation
Neuronal Prolifration
Neuronal Migration
Apoptosis
Neuritogenesis
Synaptic Transmission
yCA-CA
yMSN-dMSN

Taken together, we conclude that differentially methylated genes are enriched in neurodevelopmental functions; upregulated genes representing current and consecutive stage-specific functions, while downregulated genes representing preceding functions that are no longer required. However, these data are only associational. Further studies will be needed to demonstrate that, depending on the developmental stage, both hypomethylation and hypermethylation can downregulate gene expression (i.e. *brain formation* cluster in stage-2 and -3, Fig. 2.4B, D), as well as whether the switch from hypomethylation to hypermethylation at intronic sequences can turn activation to repression (i.e. *proliferation* and *migration* genes in stage-2 and -3).

Neuronal subtype specific DNA methylation and gene expression changes

Methylation differences between the lineages (hippocampal vs. striatal) emerged in substantial numbers, on par with transcriptional changes, during maturation (Fig. 2.1E). Therefore, we analyzed genes DMRxDE between CA1 neurons/GCs and dMSNs by IPA. This analysis identified well known, as well as unexpected gene expression and functional differences. As expected, genes with higher hippocampal expression (CA1>MSN) were enriched at a higher level in the process of *spatial learning* (Fig. 2.5A, upregulated). In contrast, genes upregulated in MSNs (MSN>CA1/GC), were associated with *disorders of the basal ganglia*, *Huntington's disease*, and *movement disorders*, consistent with the specificity of these genes and their expression to the striatum. Because hypomethylated genes, within the upregulated category, had a higher enrichment value, DNA methylation may inversely correlate with expression at many of these neuron-subtype specific genes.

Neuron-subtype specific DMRxDE genes were also enriched in specific cellular functions. Genes, upregulated in hippocampal relative to striatal neurons, were

associated with *neuritogenesis* and *synaptic transmission,* suggesting more robust neuronal plasticity in the hippocampus (Fig. 2.5B). Furthermore, CA1/GC>MSN genes were enriched in the processes of *long-term potentiation (LTP)*, *long-term depression (LTD)*, and *excitatory postsynaptic potential*, distinctive functions in the hippocampus. In contrast, genes upregulated in MSNs relative to CA1/GC were associated with *striatal LTD*, a process that is different from hippocampal LTD. Striatal LTD is postsynaptically induced, but presynaptically expressed, through retrograde endocannabinoid signaling [75]. Hippocampal LTD is postsynaptic and involves internalization of synaptic AMPA receptors [76]. In these categories of genes, upregulated genes were either hypomethylated or hypermethylated.

Next, genes upregulated in hippocampal relative to striatal neurons were enriched in the molecular function of *phosphorylation of proteins* (Fig. 2.5C). In contrast, genes upregulated in the striatum were enriched in *GABA metabolism and cAMP synthesis*, consistent with the neurotransmitter phenotype of MSNs and the Gs/Gi coupling of the striatal dopamine receptors, respectively. Surprisingly, striatal upregulated genes were also enriched in *membrane lipid synthesis* and *steroid biosynthesis*. Besides their role as structural elements, membrane lipids are involved in a multitude of signaling processes and *de novo* steroid biosynthesis of neurons (estrogens, progesterone, and androgens) [77]. Our data suggest that lipid signaling and central steroid biosynthesis could be more prominent in the striatum than in the hippocampus.

Finally, we analyzed genes DExDMR between CA1 neurons and GCs to assess if concurrent methylation and expression differences reflect neuron subtype specificity within the hippocampus (Fig. S2.5C). This analysis identified genes upregulated in GCs relative to CA1 neurons, which were enriched in the biological processes of *proliferation*, *migration* and *neuritogenesis*. These functions are consistent with the

persistent neurogenesis and neuronal replenishment in GCL throughout life, as opposed to the lack of adult neurogenesis in the CA1 layer of the hippocampus. Moreover, genes related to the metabolism of *phosphatidylinositol* membrane lipids were upreglated in GCs suggesting a difference in major signaling pathways, such as AKT, between GCs and CA1. Finally, *sphingolipid* metabolism was also a more prominent function in GCs. Sphingolipids are enriched in raft-like microdomains, specialized membrane domains where transmembrane signaling occurs through receptors and associated signaling components [78]. Genes upregulated in CA1 neurons, relative to GCs, were enriched in only a few specific functions with modest scores. No functional differences were found between dMSNs and vMSN. This is in agreement with the minimal methylation differences between these two closely related neuronal subtypes (Fig. 2.1E).

Figure 2.5. IPA analysis of neuronal subtype-specific DMRxDE genes between the hippocampus and striatum (CA1 vs. dMSN and GC vs. dMSN). Description of the figure is identical to that in Fig. 2.4B.

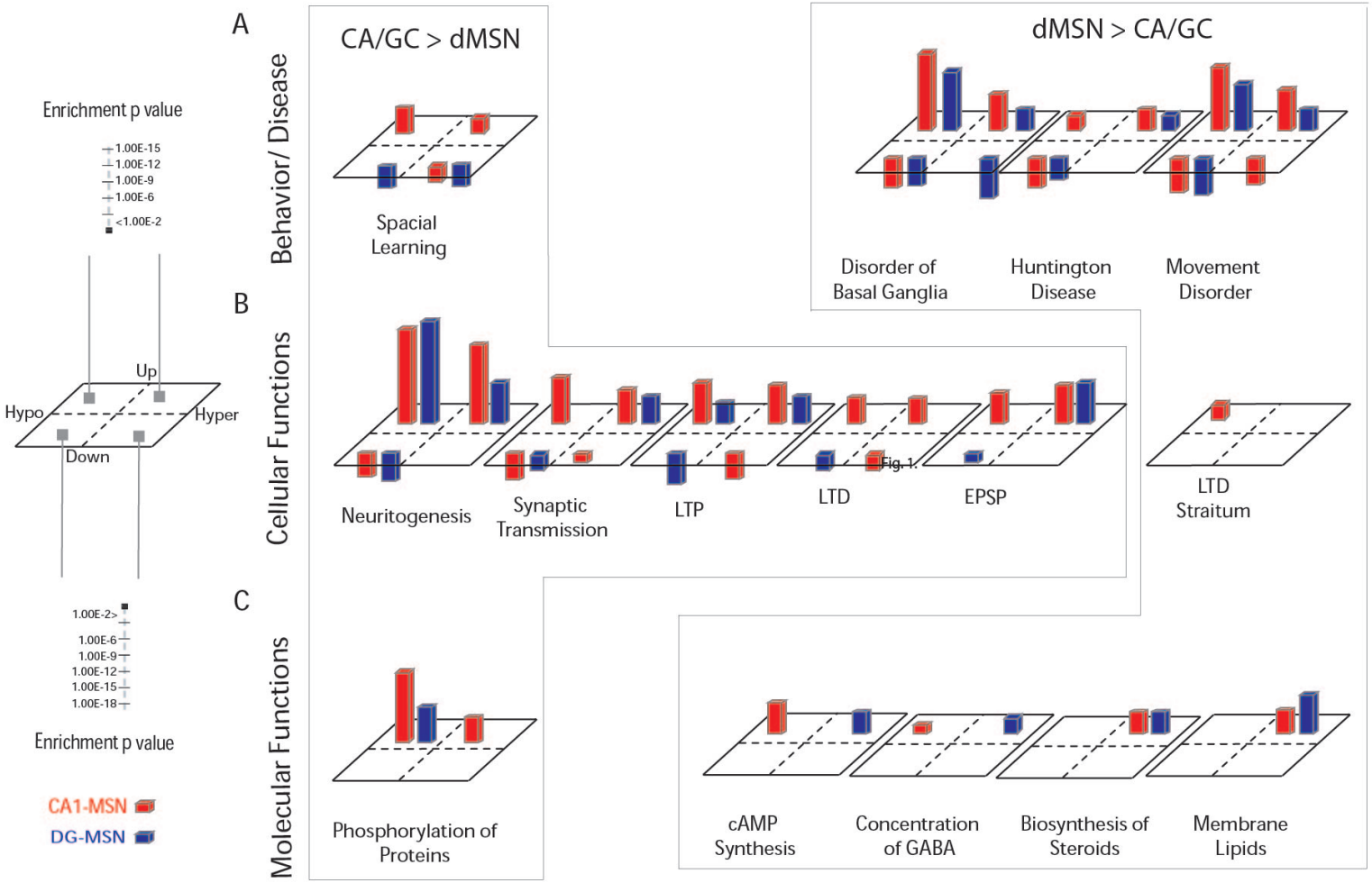
Enrichment p value
1.00E-15
1.00E-12
1.00E-9
1.00E-6
<1.00E-2
Up
Hypo
Hyper
Down
1.00E-2>
1.00E-6
1.00E-9
1.00E-12
1.00E-15
1.00E-18
Enrichment p value
CA1-MSN
DG-MSN
A
Behavior/ Disease
CA/GC > dMSN
Spacial Learning
dMSN > CA/GC
Disorder of Basal Ganglia
Huntington Disease
Movement Disorder
B
Cellular Functions
Neuritogenesis
Synaptic Transmission
LTP
LTD
EPSP
LTD Straitum
C
Molecular Functions
Phosphorylation of Proteins
cAMP Synthesis
Concentration of GABA
Biosynthesis of Steroids
Membrane Lipids

Fig. 1.

2.3 Discussion

Our work describes, for the first time, a set of simple principles that govern *in vivo* DNA methylation and demethylation during neuronal development. By dividing neurodevelopment to 3 major stages and applying the principles to each of these stages, we created a matrix that comprehensively describes DNA methylation and demethylation events in two neuronal lineages and five different neuronal subtypes; a total of ten cell types spanning the entire neurodevelopment (Fig. 2.6).

First, we found alternating large-scale gains and loss of methylation through neuronal development. Although ESCs highly express both Dnmt3a and Dnmt3b, Dnmt3a is the predominant *de novo* DNA methyltransferase involved in the transition of ESCs to neuronal progenitors [79]. Loss of methylation during early differentiation (E10.5-E17.5) was associated with an increase in Tet3 (Fig. 2.1F) suggesting its role in active demethylation, with the potential involvement of passive methylation. Indeed, several lines of evidence indicate a fundamental role for Tet3, and associated active demethylation, during neuronal differentiation and maturation. Genetic deletion of *Tet3* results in neonatal lethality in mice [80], depletion of *Xenopus* xlTet3 causes small head and eyeless phenotype [81], knockdown of TET2 and TET3 expression in E13.5 mouse embryonic cortex leads to abnormal cortical development at E17.5 [82], and *Tet3* knockout ESCs exhibit impaired neurogenesis and increased apoptosis [83]. Methylation during neuronal maturation (from P5 in DG) was likely related to *Dnmt3a* activity because its conditional knockout prevented the gain in methylation that normally occurs when young GCs undergo maturation. Evidence supports the importance of Dnmt3a in neuronal maturation and/or mature neuron functioning. Conditional deletion of *Dnmt3a* in postmitotic excitatory neurons in the mouse forebrain, shortly after birth, caused no apparent behavioral or brain structural abnormalities in one report [84]. However, others described that Dnmt3a deficient ESCs

have impaired neurogenic potential [79] and that Dnmt3a2, the shorter isoform encoded by the *Dnmt3a* gene, is linked to cognitive performance in mice [85]. These data suggest that specific enzymes of the methylation/demethylation machinery may explain the large-scale changes in methylation dynamics through development.

The second principle underlying developmental methylation is related to the dinucleotide context of the methylated and demethylated cytosines. Initially, gain and loss of methylation are limited to CpG sites, while during neuronal maturation changes also occur at a significant number at non-CpG sites in both the hippocampal and striatal lineages. This finding is consistent with previous observations of non-CpG methylation in mouse frontal cortex during fetal to young adult development [30] and with the high mCpH content of the adult brain [62,86]. In summary, these data indicate that CpH methylation ensues after neurons became postmitotic while undergoing field-specific maturation.

The third principle is that the developmental methylation program is remarkably similar in the hippocampus and striatum, with significant divergence only during neuronal maturation. This is in contrast to the transcriptional program that shows substantial lineage differences from the progenitor stage through neurodevelopment. Interestingly, the DNA methylation program of hematopoietic cells is the exact opposite, dominated by lineage specific, over developmental stage specific, methylation changes [87].

Figure 2.6. The five general principles governing DNA methylation during lineage and subtype specific development. These are: i) The program consists of 3-stages (*1+2+3*). An initial genome-wide methylation during progenitor proliferation is followed by a loss of methylation during the transition of regional progenitors to "young" hippocampal and striatal neurons, which is then reversed by a gain in methylation during maturation to subtype specific neurons. ii) At the first two stages, gain and loss of methylation are limited to CpG sites, while during the third maturation stage methylation also occurs at non-CpG sites in both lineages (*1/2+3*). Paralleling these events, iii) targets of methylation/demethylation are initially highly similar in the two lineages, while diversification in methylation during maturation creates subtype specific methylation differences (*1/2+3*). iv) At first, methylation targets all genomic locations, while later, during early and late differentiation the preferred targets are intronic and intergenic sequences with enhancer-like activity (*1+2/3*). v) Differentially methylated genes are enriched in neurodevelopmental functions (from progenitor proliferation, through migration and neuritogenesis, to synaptic transmission); upregulated genes representing current and consecutive stage specific functions, while downregulated genes representing preceding functions that are no longer required (*1+2+3*).

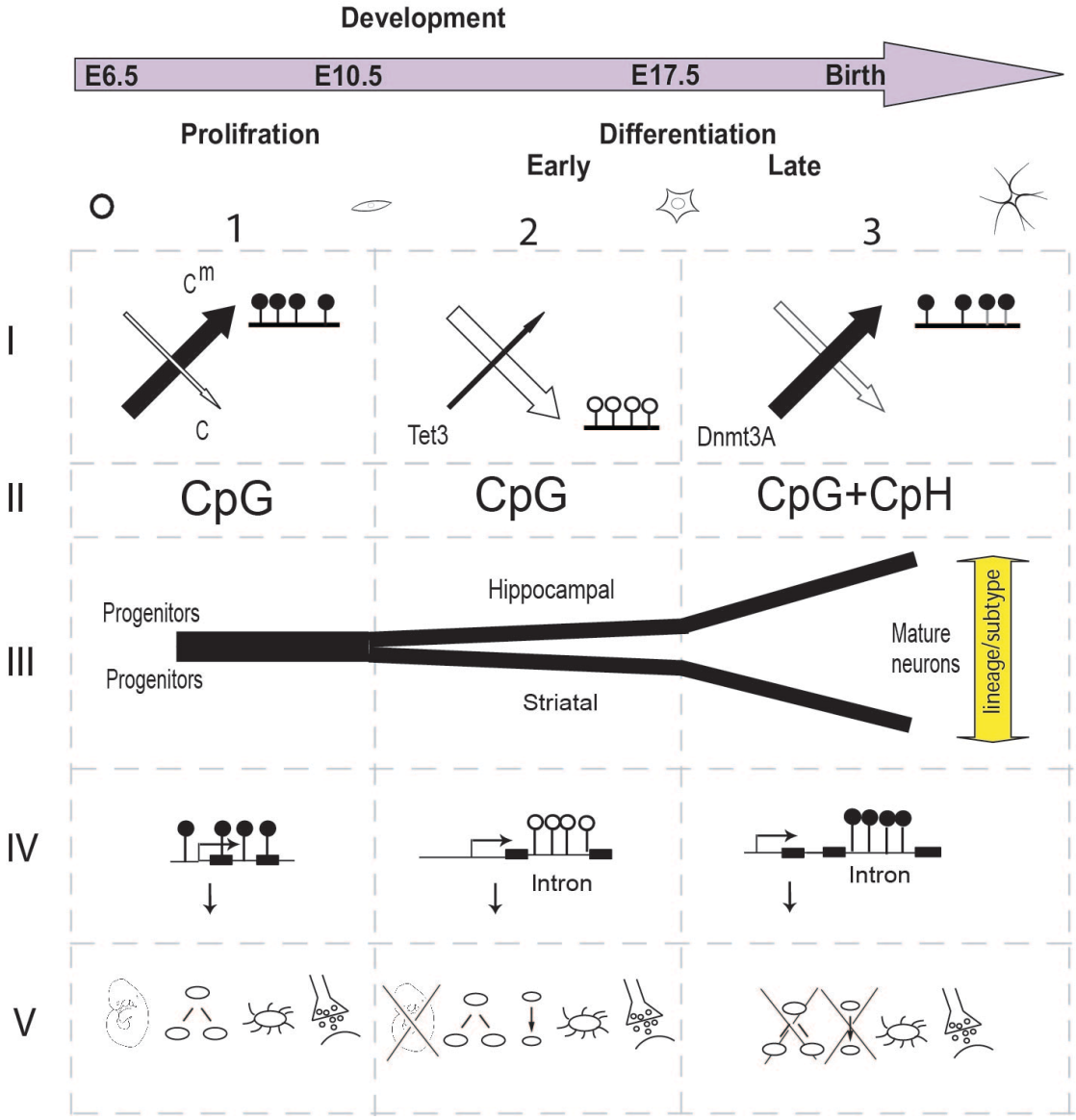
Development
E6.5
E10.5
E17.5
Birth
Prolifration
Differentiation
Early
Late
1
2
3
I
II
III
IV
V
C^m
C
Tet3
Dnmt3A
CpG
CpG
CpG+CpH
Progenitors
Progenitors
Hippocampal
Striatal
Mature neurons
lineage/subtype
Intron
Intron

The fourth principle is that methylation during progenitor proliferation targets most genomic features, except CGI promoters, while later, during young and mature neuron development, loss and gain of methylation occurs preferentially at introns. The initial, large-scale methylation during progenitor proliferation could promote genome integrity since hypomethylated DNA is structurally instable and mutable [88,89]. The targeted methylation changes during differentiation could serve regulatory functions, as some of these sites exhibited enhancer-like activity.

Finally, differentially methylated genes were enriched in neurodevelopmental functions; hypomethylated/upregulated genes representing current and consecutive stage-specific functions, while hypermethylated/downregulated genes representing preceding functions that are no longer required. This indicates that while there is no global correspondence between methylation and expression during neuronal development, methylation correlates with gene expression within specific functional categories. For example, during early differentiation (E10.5-E17.5), genes with functions in neuronal migration, neurite formation, and even synaptogenesis and synaptic transmission underwent intronic hypomethylation and associated activation, well before the manifestation of the associated functions. Adjustments in intronic methylation, again preferential hypomethylation, accompanied by gene activation, continued during maturation (from E17.5) in neuritogenesis and synaptic transmission genes. In contrast, proliferation and migration genes whose expression is no longer required during maturation underwent intronic methylation and downregulation. This suggests that DNA methylation is not secondary to prior, other epigenetic modifications. Rather, consistent with numerous reports [90-93], methylation could be directly involved in modulating the accessibility of transcription factors and co-factors to DNA during neurodevelopment.

The overarching theme emerging from our work is that neuronal methylation/demethylation is principally associated with differentiation, with minimal lineage specificity, but later, during neuronal maturation, methylation contributes to neuron subtype specification. Beyond increasing our understanding of the epigenetic regulation of normal development, this work will be useful in research focused on neurodevelopmental disorders. Neuronal development, like development in general, is highly vulnerable to environmental perturbations. Developmental perturbations can lead to persistent abnormalities, exemplified by autism and schizophrenia stemming from severe maternal gestational infection, or child and adolescent behavioral problems emerging following pre/postpartum maternal stress and maltreatment [42,94,95]. These early life adverse conditions are associated with persistent alterations in the methylome in human and animal models [26,96,97]. Interference with the normal developmental dynamics of DNA methylation or overriding the already established developmental pattern by adverse early life experiences can be fundamental in the etiology of the resulting psychopathology or psychiatric disease-like behaviors in animal models. Our developmental methylation matrix can be cross-referenced with disease associated methylation changes to specify the possible events, and underlying principles, compromised in disease.

2.4 Methods

Mice

Animal experiments were carried out in accordance with the Weill Cornell Medical College Institutional Animal Care and Use Committee guidelines. All mice were group-housed up to five per cage, with 12-h light/dark cycle and with lights on at 6 a.m. Food and water were available ad libitum. Wild-type C57BL/6 males were purchased from The Jackson Laboratory (Bar Harbor, ME). Conditional *Dnmt3a* knockout males were generated by breeding C57BL/6 mice carrying floxed *Dnmt3a* alleles (*Dnmt3a*$^{f/f}$)[98](provided by Riken BioResource Center, Koyadai, Tbukuba, Ibaraki, Japan) and mice heterozygous for the tamoxifen inducible nestin-cre-ERT2 transgene [99](kindly provided by Luis Parada, University of Texas Southwestern Medical Center, Dallas, Texas). Dnmt3a$^{f/f}$;Cre^{-} females were crossed with Dnmt3a$^{f/f}$;Cre^{+} males to obtain Dnmt3a$^{f/f}$;Cre^{-}.and Dnmt3a$^{f/f}$;Cre^{+} littermates. To induce Cre mediated Dnmt3a excision, pregnant females were injected with 6.7ug/kg tamoxifen at E13.5, as described [99]. Since gestational tamoxifen injection interferes with females' maternal care behavior, newborn pups were crossfostered to WT mothers.

Tissue Collection for DNA isolation

ESCs were cultured as described previously [86]. Briefly, E14 ESCs were cultured on feeder cells (mitomycin-inactivated mouse embryonic fibroblasts) for at least two passages after thawing. Cells were split every 2 days with plating densities between 1.5 x 10^6 and 4 x 10^6 cells, on 10-cm cell culture plates. ESC medium was based on DMEM containing 15% ESC quality fetal bovine serum, LIF (1,000 U/ml, Millipore, Billerica, MA, USA), 1X non-essential amino acids, 2mM L-glutamine and β-mercaptoethanol (Invitrogen, Carlsbad, CA, USA).

Hippocampal progenitors were microdissected from the epithelium of the ventricular germinal layer, while striatal neuronal progenitors were isolated from the lateral lateral ganglionic eminence of E10.5 embryos. Young CA neurons and MSNs were dissected from the early hippocampus and striatum respectively from E17.5 embryos. CA1 and CA3 pyramidal neurons and GCs were microdissected and isolated from frozen dorsal and ventral hippocampal 200μm sections of 8-10 week old male mice. MSNs were isolated as described [100,101]. Briefly, dorsal and ventral straitum were dissected and homogenized in lysis buffer (0.32M Sucrose, 5mM$CaCl_2$, 3mM $MgCl_2$, 10mM Tris-HCL-pH8, 0.1M EDTA, 0.1% Triton100 and 1mM DDT in ddH_2O). The homogenate was then resuspended in blocking buffer (1% goat serum, 5mM $MgCl_2$ in PBS) followed by incubating with anti NeuN antibody (Millipore, MAB377X). Nuclei were purified by diluting the lysate in sucrose buffer S1 (0.25M Sucrose, 5mM $MgCl_2$ in PBS) and overlaying it over sucrose buffer S2 (1.1M Sucrose, 2mM $MgCl_2$, 50mM Tris-HCL(pH8), 1mM DTT in ddH_2O). Nuclei were pelleted at 2800g for 15min. Nuclei were then resuspended in resuspension buffer (2mM $MgCl_2$ in TBS), filtered through a 40μ strainer, and FACS sorted at the Weill Cornell Core Facility.

Bisulfite sequencing

DNA was isolated from collected tissue using the DNeasy Blood & Tissue Kit (Qiagen, Valencia, CA). Single end 50bp enhanced reduced representational bisulfite sequencing was performed as described [61], using Illumina HiSeq2000 according to manufacturer instructions. An in-house pipeline was used for methylation calling and alignment to the mm9 reference genome [102]. Differential methylation and statistical analysis were performed using the MethylKit package in R [102] at default setting. Differentially methylated sites were defined as sites where the SLIM corrected p-values were ≥ 0.01 and the difference in methylation between two samples were $\geq$

20%. Differentially methylated regions (DMRs) were defined as regions containing at least four differentially methylated sites with distance no greater than 1kb. Genomic and CGI annotations were based on Ensmbl data downloaded from the UCSC genome browser. Promoters were defined as regions ±2kb from the TSS while exons and introns were defined by reference. The percentage of total differentially methylated sites in a defined genomic feature was divided by the percentage expected to overlap each genomic feature by chance, based on the percentage of genomic space occupied by that feature, to determine the fold change from expected values. Additional methylation datasets were downloaded from the UCSC genome browser DNA methylation track hub [29,103,104]. All graphs and statistical analysis were performed using R (http://ww.r-project.org), Bioconductor (www.bioconductor.org), and ggplot2 (www.ggplot2.org) for visualization, unless stated otherwise.

RNA-Seq

Adult mice were perfused with 30% RNAlater (Ambion, Grand Island, NY) in saline. Embryonic and adult hippocampal samples were isolated as for DNA. Dorsal striatum were microdissected from frozen 200µm adult brain sections. Total RNA was isolated using the RNeasy Mini Kit (Qiagen, Valencia, CA). Single end 50bp RNA sequencing was performed on Illumina HiSeq2000 for HP, SP, yCA and yMSN samples. RNA from dorsal striatum was sequenced using 75bp pair-end sequencing. Adult GC and CA1 pyramidal neuron RNA data were from our previous report (GSE52069ECS)[8]. ESC data were downloaded from GSE20851. All reads were aligned to the mm9 reference genome using TopHat software version 2.0.11 [105]. Default parameters were used with the addition of "--no-novel-juncs" to align exclusively to known genes and isoforms. Gene counts were performed using the HT-seq program [106] with the parameter "intersection-strict". Values for fold-change in gene expression were calculated using the EdgeR [107] package in R, using tagwise

dispersion and default parameters. Differentially expressed genes were defined as genes containing a Benjamini-Hochberg corrected *p-value* ≥ 0.05.

Transfection and Luciferase Reporter Assay

Plasmids were constructed from Basic and Promoter pCpGfree Luciferase Vectors (Invivogen, San Diego, CA) using the In-Fusion Cloning Kit (*Clontech* Laboratories, Mountain View, CA). Intronic DMRs as well as a control drosophila sequence (see table below) were cloned into basic (with no promoter or enhancer activity) and promoter (containing minimal EF1 promoter with no enhancer activities) pCpGfree backbone vectors (InvivogeGen, San Diego, CA).

DMR	Sequence
Drosophila 208bp	ACGCCTAAAGCAACTCCACTGGCTCATCGGTAAAAAGTCAAAGCTGCGAG AGAAACTAAAGATTCTCGTCTACAAGACTATTCTCAAGCCAATCTGGACG TACGGAATTCAGCTGTGGGGCACTGCTTGCACATCACATAGAAGGAAGAT CCAGCGATTTCAAAACAGATGTTTGAGAATAGTCTCCAACGCCCATCCCT ACCACGA
Grid2	CACTGTCTCAATGCAAATCCCAACCCTTTGCATCATCCACCCATCAGTCT TTAATCTGACTCACTATGGTCTCACTTCTCCAAGTTGGACCAGAACCTCT GTGAAGGCAGCAACCACATAGCAGTCTAGGACCATACGTTTGTATTTGGT TTTAAGGGGGGATGGGGGCAATAACACATGACAAAGTGTTCTTAGCCCTG ACTGGGACTGGCCTGGAACTTGCAATGTAAAGCAGGCTGGTTCAAACTCA GAGATCTGCCTGTCTCTGACTCCACAATGCTAGGGTTAATGTTCTTTTAT TAAGTACCATCACCTTGGTGCTATTAGAGATTTACTGGCCAGTTTCATCT GATCCTGGGTTGTCCCAAGAAAT
Htr1	CGGCCTAGCCTCAACTCACTGGCTCGTGTTGAGAGTACTGAGTCAGCTGT ACATTCCACCCTCCCCCTTTTTTTGGAACGAGGAACAAGCCACCTTTTGT GTACTTCTTTTTTTCCTGCTCCCATACTCCTTTCACAGCTCTCTGGGCAA CACTCCCATATGTCCCTGAATTGATGCTGGTCCAGCCACACATCACACGG CTGGCTCCGGTTTTCCAGTTCGTCTCTGAGCTCTCTCCAGCAGCACGCAG ATTGCTTGCCAGGTTCATTGCATTTGTCTCTTGTCCCAAGTACCG
Gria1	TGGAGTCCTCCGGGCTGAGAGCGAACATTTAACTGACATGATGTTGGAGG AGAACCTTTGCTTTTGTGCTTGCTTCCATTTGAGGAACATTTTGCTCCAT TCCTTCCCGCCTGCCTCTGCTCACCTCTTAATTAACTGGAGGTTGCGGGC GAAAGCAGCTGCCGGCTCTTTTCT
Park2	TCAAGTGGTGGAACTGGGTTTTCTCCGGCGAATCTCAGGATTAACACAGT GCTAGGGAGATGCGGGCCCCAGATACAGCTCCGGGTCCTATTCCGCAGCA ACCCGAGGACGTCTTGCCAGAGAACCTGTAGCCGGGATCCTTG
Crhr1	CGGTCCTCGAATTCCTCATCTAATTAGAGCTGGGTTGAGTGTGTGCAGTA ATGAGCTGGCTTTCGCACACTCCGGACTACCCCAAGGCCTCCACTGGGAA CATCCCTAACACAAGCAGGGTATGGGGGCGTACTGAGGGCACACCAAAAG GGTATACTGAGTCATTTTGCTTTTAGAGTGCTAAGGAGGGGTTTTGGCTC TAAGGACAGCTGAGTCACCG

N2A cells were cultured in media containing 88% DMEM + 10mM HEPES, 1% penicillin/streptomycin, 10% fetal bovine serum, and 1% L-Glutamine in a 5% CO_2 37°C incubator. Plasmids were transfected into N2A cell cultures using Lipofectamine Transfection Reagent (Life Technologies, Grand Island, NY) in triplicates. Briefly, 200,000 cells were seeded per well in 12-well plates in 1mL culture media. 24 hours later, 1µg of plasmid DNA was diluted in 85µl Opti-MEM media (Life Technologies) in tubes. After 5 minute incubation, 6µl Lipofectamine Transfection Reagent was added, followed by 20 minute incubation. 85µl of this solution was added to each well of N2a cells. The following day, media was aspirated and replaced with 400µl of culture media. 48 hours after transfection, 20µl aliquots of media were sampled into 96-well plates. 100µl Quanti-Luc luciferase substrate (InvivoGen, San Diego, CA) was added to each well, and plates were read immediately for luciferase activity. Luciferase activity data are shown as mean ± s.e.m. Outlier data was excluded based on ± 2 s.d. from the mean. One-way or repeated measures ANOVAs or *t* tests were used to compare tests. LSD *post hoc* analysis was used to assess statistical significance.

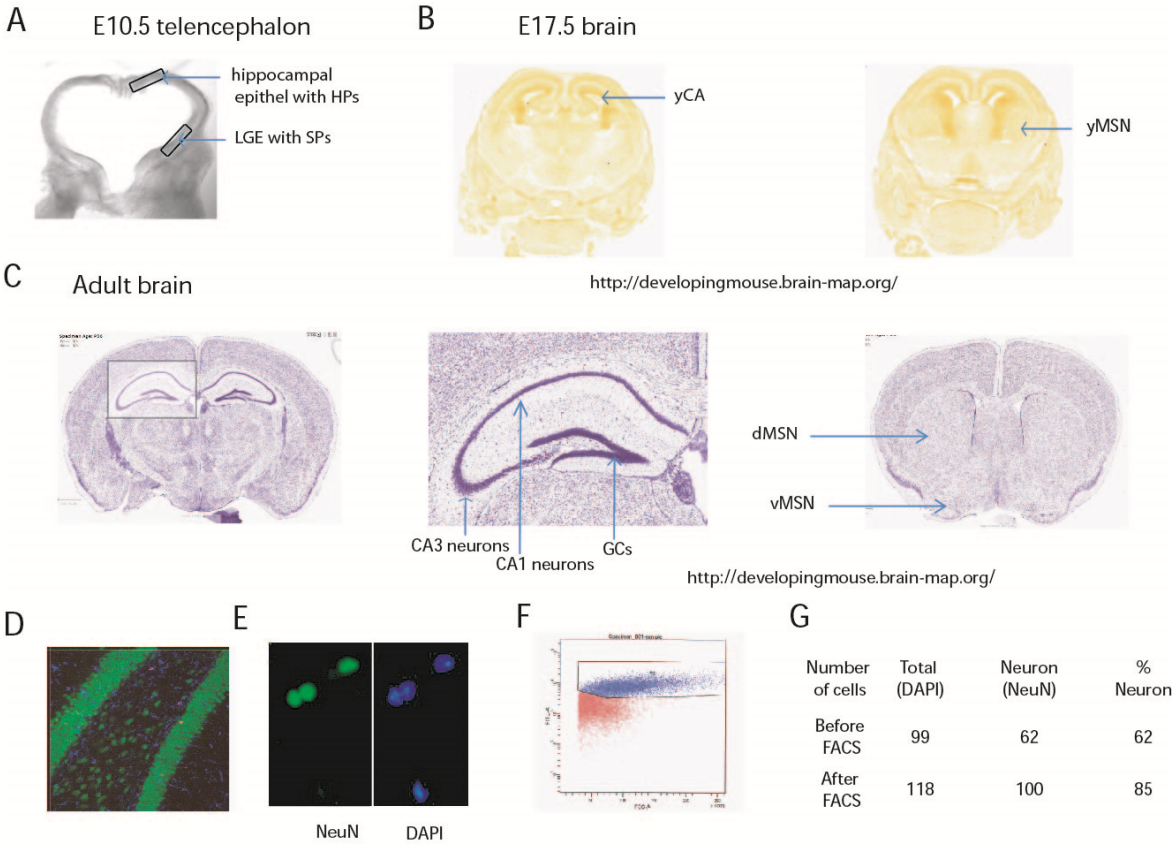

Supplementary Fig. 2.1. Isolation of homogenous populations of neuronal progenitors and neurons. **A.** Photograph of E10.5 telencephalon illustrating the position of the ammonic/ dentate epithelium and LGE, which are the source of hippocampal and striatal progenitors. **B**. E17.5 telencephalon showing the developing hippocampus and striatum and which served as the source of yHNs and yMSNs. **C**. Adult mouse brain illustrating the distinct layers of CA1 and CA3 neurons and GCs, as well as the dorsal striatum and NAc, the source of d- and vMSNs. **D**. The vast majority of nuclei in the GC layer are NeuN positive (intense green nuclear staining) with only a few cells being positive for the glia marker GFAP (blue cytoplasmic staining). BrdU positive cells (red) were also visualized to assess the number of neurons in the S phase of the cell cycle. **E**. Isolation of MSNs from the striatum. DAPI (blue) and NeuN (green) positive nuclei before fluorescence activated cell sorting (FACS), showing that many but not all nuclei are neuronal. **F.** Representative FACS scatter plot from striatal nuclei labeled with a NeuN antibody, according to the protocol of Jiang et al. [101]. Y axis represents FITC intensity at 488nm while the X axis represents size:morphology. NeuN positive cells (blue) can be separated from negative cells (red). **G**. The proportion of NeuN positive nuclei in total DAPI positive nuclei is increased following FACS.

A.

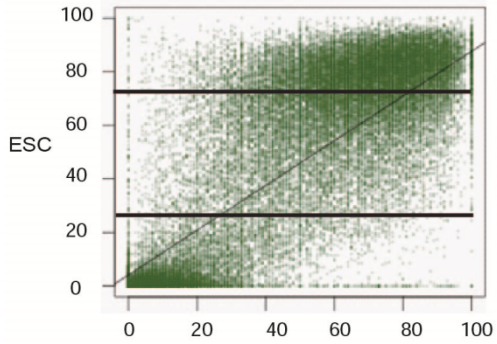

B.

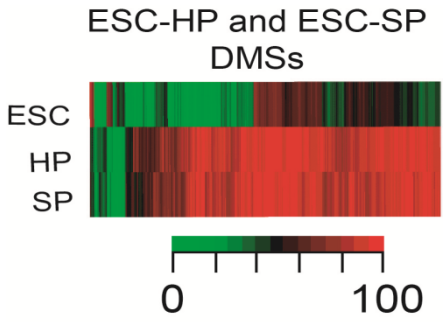

Supplementary Fig. 2.2. Additional methylation data related to the ESC-neuronal progenitor transition. **A.** High concordance (t=586.375, df=79829, p<2.2e-16; r= 0.9008746) between methylation levels in ESCs, cultured in the lab, and E6.5 epiblasts, as reported by Smith et al. [29]. The bimodal distribution of methylation is visible in both cell types, although less prominently in epiblasts. However, a large number of sites with intermediate methylation is also visible indicating that methylation is incomplete. **B**. Heat map representation of methylation levels at all ESC-HP and ESC-SP differentially methylated sites (DMSs) demonstrating a high level of similarity in the two lineages.

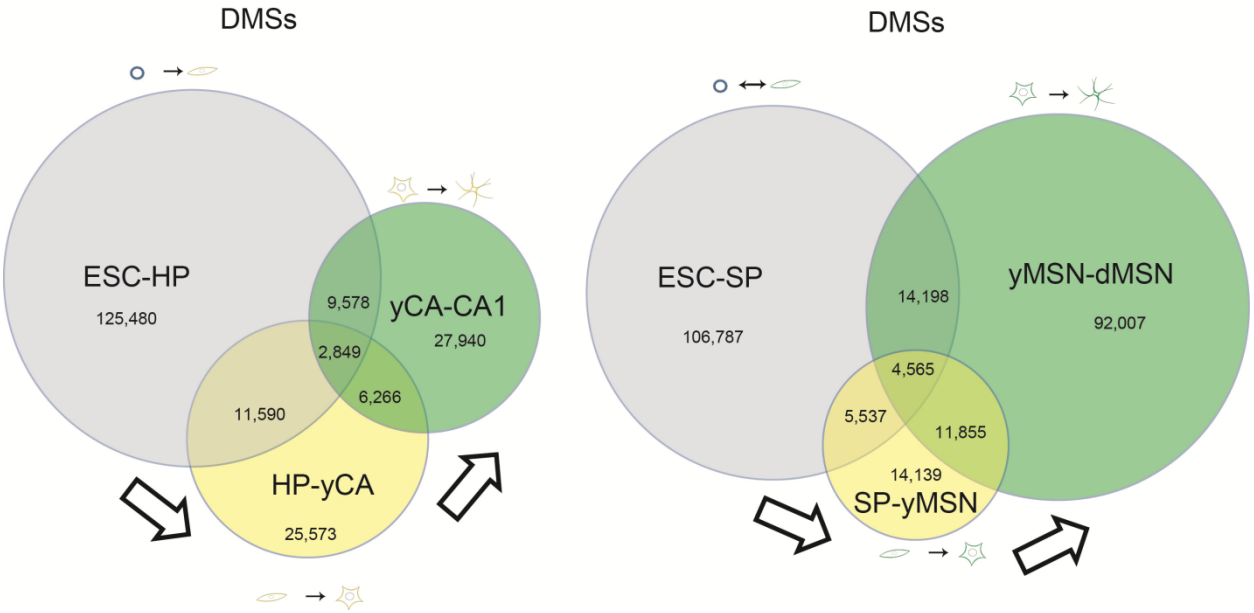

Supplementary Fig. 2.3. Overlap between differentially methylated sites (DMSs) for the three periods of neuronal development indicates that most sites are modified only once during development.

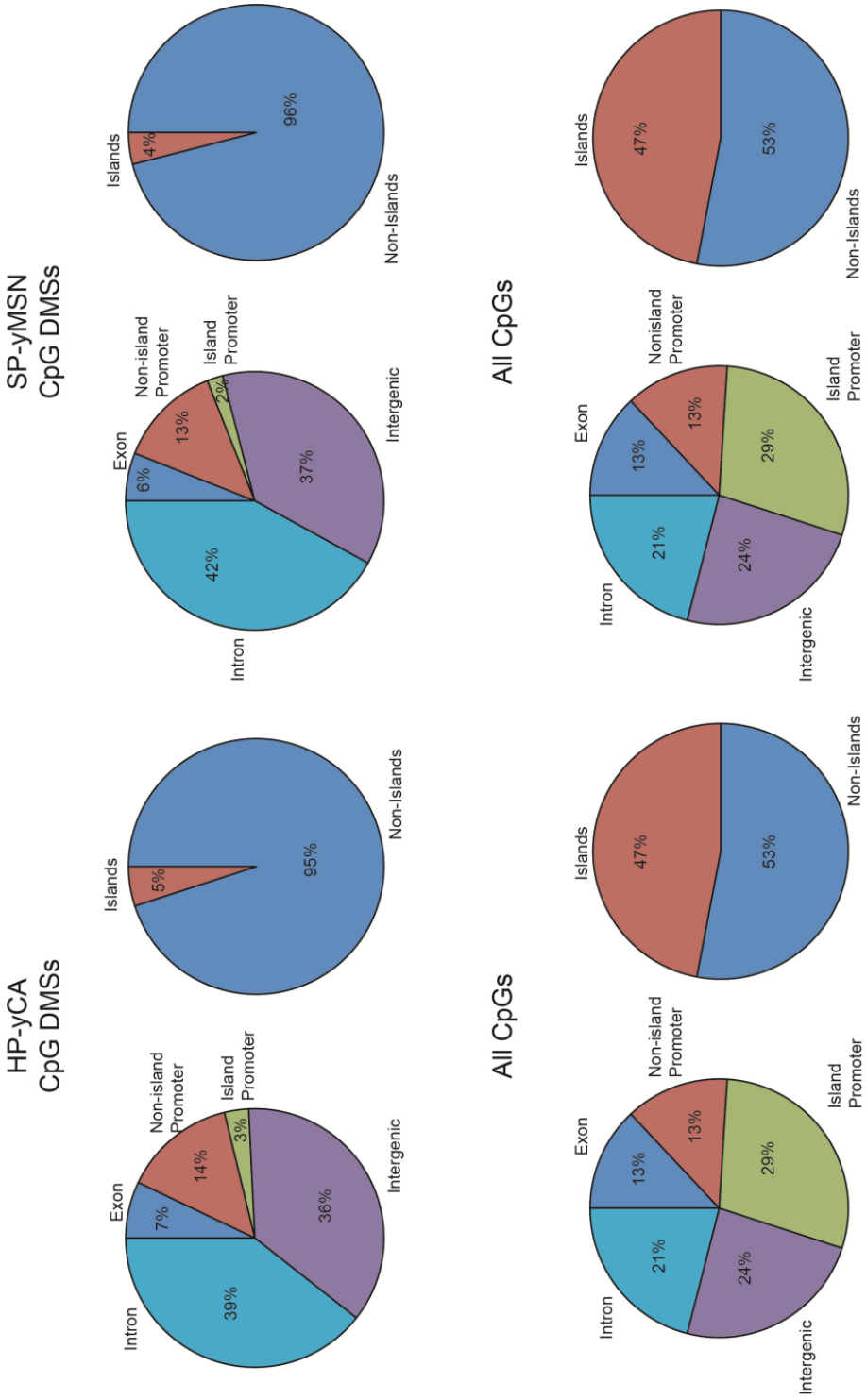

Supplementary Fig. 2.4. Mapping differentially methylated sites (DMSs) associated with the ESC to progenitor transition to genomic features.

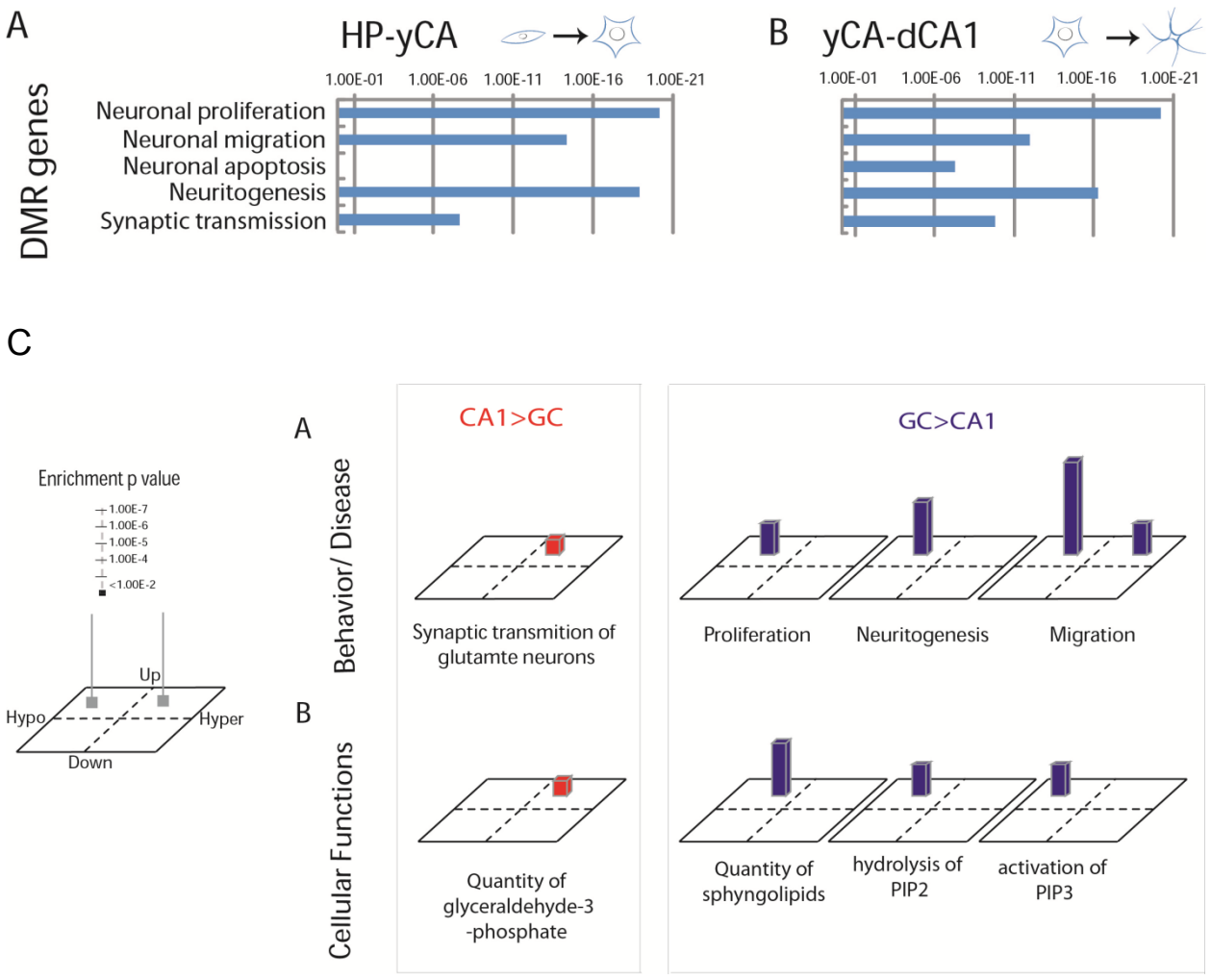

Supplementary Fig. 2.5. Functional analysis of developmental and neuron subtype specific differentially methylated genes. **A, B**. Analysis of intronic/intergenic differentially methylated genes during the progenitor to young neuron (A) and from the young to mature neuron (B) transition. **C**. Analysis of neuronal subtype-specific differentially methylated and differentially expressed (DMR x DE) genes between regions within the hippocampus (CA1 vs. GC). Description of the figure is identical to that of Fig. 4B. G3P, glyceraldehyde-3-phosphate, an intermediate in several central metabolic pathways; PIP2 and PIP3, phosphatidylinositol 4,5-bisphosphate and phosphatidylinositol 3,4,5-trisphosphate.

CHAPTER 3

DIFFERENTIAL GENE BODY METHYLATION AND REDUCED EXPRESSION OF CELL ADHESION AND NEUROTRANSMITTER RECEPTOR GENES IN ADVERSE MATERNAL ENVIRONMENT

** Oh J., Chambwe N., Klein S., Gal J., Andrews S., Gleason G., Shaknovich R., Melnick A., Campagne F., and Toth M. 2013. Differential gene body methylation and reduced expression of cell adhesion and neurotransmitter receptor genes in adverse maternal environment. Published in Translational Psychiatry.*

3.1 Introduction

A significant factor in the development of psychiatric disorders, including anxiety, depression, autism and ADHD is the environment, both prenatally and during early postnatal life[108,109]. Early life adversity, such as maternal stress, maternal infection (e.g. immune activation during pregnancy)[110] and maternal separation during early postnatal life[111], and its behavioral consequences on the offspring can be reproduced in non-human primates and rodents. Although many genetic tools are available for the mouse, establishing early life adversity paradigms with robust and reproducible behavioral outcomes is challenging in this species[112,113]. We have recently developed a mouse model of maternal adversity, that is based on a deficit in the maternal 5-HT_{1A} receptor (R) and which causes innate anxiety, increased stress reactivity and impaired vocal communication in the offspring[12,114]. This model has construct validity because reduced binding of 5-HT_{1A}R has been found in depression, including peri/postpartum depression, a condition that can represent early life adversity for the offspring[12,115]. This model was developed on the outbred Swiss Webster (SW) background (a strain often used in behavioral experiments), to avoid the possible contribution of homozygous genetic variants in inbred strains to behavioral

phenotypes[116]. The unique feature of our maternal adversity model is that the initial trigger is well defined (e.g. maternal receptor deficit as opposed to more complex paradigms such as maternal stress and inflammation) and this gives a foothold from which to investigate the underlying molecular mechanism. A partial receptor deficit (heterozygosity, H) in the mothers is sufficient to elicit the behavioral abnormalities in the wild type (WT) offspring[12] and the behaviors develop independently of the offspring's own receptor genotype (e.g. similar effect in the WT and mutant offspring)[12]. Further studies showed that the anxiety of the offspring of 5-HT_{1A}R-deficient mothers is prenatally determined, is not related to maternal care[114] (a major postnatal factor in anxiety in other models[117]), and is linked to the delayed maturation of dentate granule cells (DGCs) in the ventral but not in the dorsal HIP[12].

The ventral (v)-HIP is part of the distributed and interconnected network of brain regions involved in anxiety. The role for the v-HIP in innate anxiety is supported by the reduced fear and avoidant behavior of rodents following its lesion[118,119]. Sensory inputs, via the entorhinal cortex (EC), arrive to v-DGCs that are connected to v-CA3 and v-CA1 neurons, that together form the classical trisynaptic HIP circuit. This circuit sends direct projections to the medial prefrontal cortex (m-PFC) and activity in the v-HIP is synchronized with m-PFC to produce appropriate defensive and anxiety-related behaviors[120]. Other connections of v-HIP that are relevant to anxiety include those to the amygdala and the bed nuclei of stria terminalis[121].

Previous studies suggested that adverse maternal environment can produce permanent epigenetic changes in neurons[122-125]. Among the various epigenetic modifications, CpG methylation is probably the longest lasting, although it can still be dynamically regulated in certain circumstances[126]. Although DNA methylation assays have long been available, finding methylation changes that underlie environmental effects, including maternal effects, is complicated by the necessity to use homogenous

neuronal populations. Indeed, current knowledge on neuronal methylation is largely limited to whole brain[127,128] and *in vitro* differentiated neurons/neuronal precursors[47,129], although the methylation pattern of mouse DGCs has recently been reported[126]. Also, the effect of early environmental influences on neuronal DNA methylation has mostly been tested with candidate genes[36,125], an approach that does not provide an unbiased survey of epigenetic changes induced by maternal adversity. Here we isolated v-DGCs and performed whole genome representational analyses by using two assays, *HpaII* tiny fragment enrichment by ligation-mediated PCR (HELP assay) and Enhanced Reduced Representation Bisulfite Sequencing (ERRBS), to determine the pattern and developmental dynamics of CpG methylation produced by maternal adversity. We found that the receptor deficient maternal effect induced large-scale methylation changes in exons, introns and gene distal areas while changes were underrepresented in promoters. Methylation changes tended to be clustered and the affected genes encode proteins involved in synapse formation and function.

3.2 Results

Methylation changes in adverse maternal environment in dentate granule cells (DGCs)

Since anxiety in the offspring of 5-HT_{1A}R deficient mothers is associated with the delayed maturation of v-DGCs during early postnatal life, and because genetic interference with v-DGC maturation (by the inactivation of the cyclin dependent kinase inhibitor $p16^{Ink4a}$) is accompanied by increased anxiety[12], we tested v-DGCs for genomic methylation changes associated with the receptor deficient maternal environment. First we used the methylation enzyme based "HELP" assay, to interrogate CpG methylation at 14,392 known RefSeq gene promoters (out of the total of 29,716 based on the NCBI37/mm9 mouse assembly) and 9,114 CpG islands

(promoter and non-promoter, out of 16,026) by using custom arrays[128]. To identify H-maternal specific methylation changes, WT offspring of WT mothers (WT(WT)) were compared to the WT offspring of H mothers (WT(H))(Fig. 1A). WT(WT) samples were also compared to KO(H) and KO(KO) samples because lack of the receptor in the offspring (in KO(H)) and/or the switch of the maternal receptor deficit from partial to complete (in KO(H)) had no additional effect on either the delayed DGC development or the anxiety of the offspring, elicited by the H maternal environment (Fig. 3.1A).

By comparing the methylation level of WT offspring of H and WT mothers (WT(H) vs. WT(WT)), 35 differentially methylated regions (DMRs) were identified (Fig. 3.1B) out of the 25,725 fragments assayed (Benjamini-Hochberg multiple testing, false discovery rate (FDR) <0.5%, methylation ratio >1.5, 3 litters per replicate, 3-4 biological replicates per group, r^2>0.90 between replicates). The majority of the WT(H) specific DMRs represented hypomethylation (29 DMRs). When WT and KO littermates of H mothers were compared (WT(H) vs. KO(H), no DMRs were found indicating that the offspring's own 5-HT_{1A}R genotype elicited no methylation changes that were detectable by HELP (Fig. 3.1B). Importantly, most of the DMRs were also seen when KO offspring of H and KO mothers were compared to WT(WT) offspring ((KO(H) and KO(KO) specific DMRs), indicating that similar methylation changes can be elicited by the H and KO maternal genotype, independently of the offspring genotype, and that there is a good correspondence between methylation changes and anxiety. However, the KO as compared to the H maternal environment caused additional changes in methylation as shown by the heat map representation of all DMRs across the three comparisons (Fig. 3.1C). Approximately half of the DMRs overlapped CpG islands, a distribution similar to that of the assay. Taken together, the methylation changes, similarly to the delayed v-

DGC developmental phenotype and anxiety[12], were elicited by either the H or KO maternal environment and were independent of the offspring genotype.

Figure 3.1. **The 5-HT$_{1A}$R deficient maternal environment results in DNA hypo- and hypermethylation in offspring ventral DGCs**. **A,** WT (and KO) offspring exposed to mutant (H or KO) maternal environment exhibit anxiety. **B**, Exposure to the H maternal environment is associated with differential methylation at 35 DNA fragments in the WT offspring and the majority of these DMRs are also present when the mother and/or the offspring are KO (KO(H) and KO(KO). **C**. Heat map representation of methylation levels at DMRs across biological replicates of the four groups of animals.

A

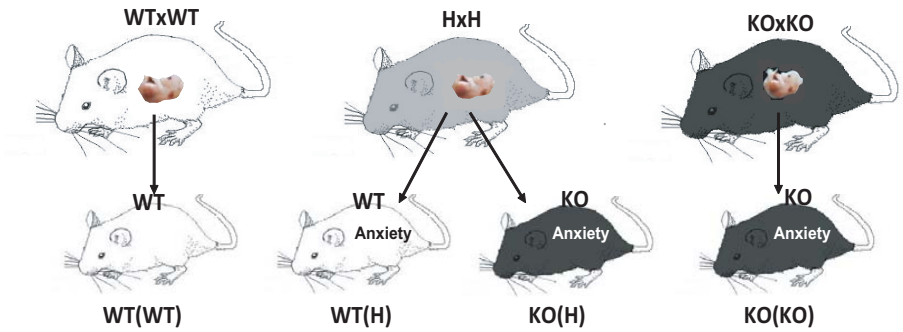
WTxWT
HxH
KOxKO
WT
WT
Anxiety
KO
Anxiety
KO
Anxiety
WT(WT)
WT(H)
KO(H)
KO(KO)

B

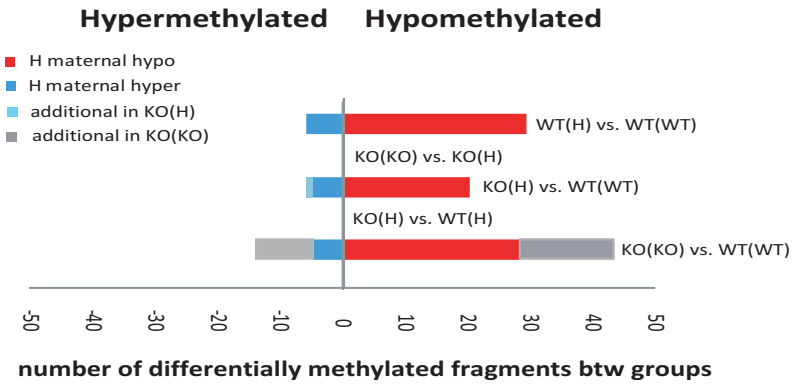
Hypermethylated
Hypomethylated
H maternal hypo
H maternal hyper
additional in KO(H)
additional in KO(KO)
WT(H) vs. WT(WT)
KO(KO) vs. KO(H)
KO(H) vs. WT(WT)
KO(H) vs. WT(H)
KO(KO) vs. WT(WT)
-50
-40
-30
-20
-10
0
10
20
30
40
50
number of differentially methylated fragments btw groups

C

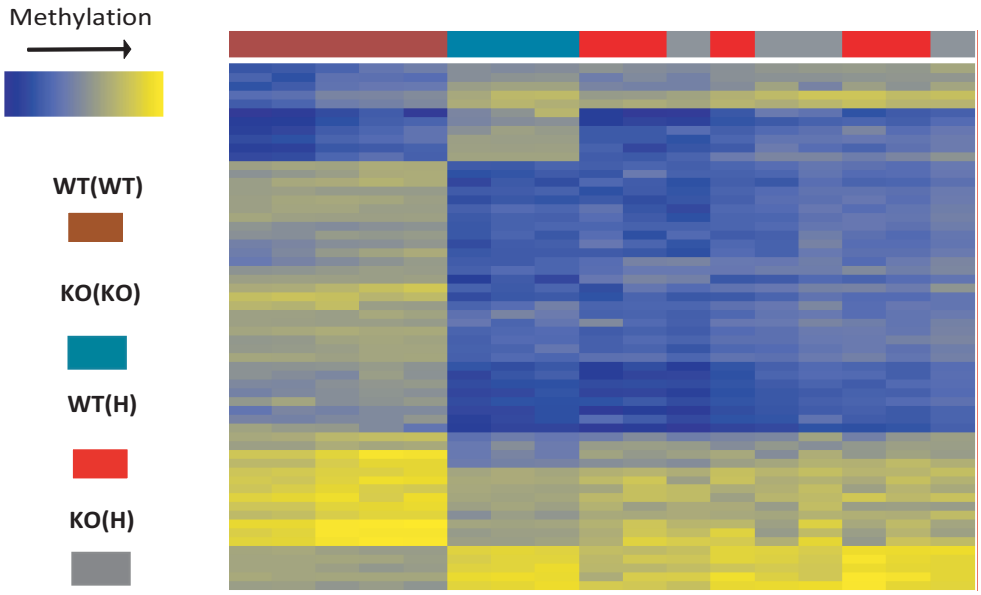
Methylation
WT(WT)
KO(KO)
WT(H)
KO(H)

Since the receptor deficient maternal environment during the prenatal period is necessary and sufficient to elicit the anxiety-like phenotype[12], we tested if prenatal exposure alone can produce hypomethylation at the *Atbf1* and *Smo* DMRs. WT offspring implanted as embryos into the oviducts of KO mothers and then crossfostered at birth to WT mothers (referred to as WT(KO/WT) mice, Fig. 3.2C) showed hypomethylation within both DMRs (Fig. 3.2D). This indicates that exposure to the adverse maternal environment that is limited to the prenatal period is sufficient to elicit not only the anxiety phenotype but also the DNA methylation changes in the offspring.

Figure 3.2. Nucleotide level methylation across DMRs in two genes. **A**, Genomic structure around DMRs. Genomic structure around DMRs. Thick and thin gray bars with red frames indicate the minimal and maximal size of the differentially methylated HELP fragments between HpaII sites. Green boxes represent CpG islands. Blue boxes indicate regions that contained differentially methylated CpG sites, including CpGs at HpaII sites, within the HELP fragments. **B**, Methylation patterns at individual CpG sites in various groups of adult animals across DMRs. Similar patterns were reproduced with independent samples. Columns display mean methylation levels with SE; ANOVA with LSD posthoc: *Atbf1*, $F_{1,3}$=48.00, P<0.00001, N=20; *Smo*, $F_{1,3}$=9.31, P=0.0002, N=8; *p<0.05, **p<0.005, ***p<0.0005 indicate significant differences from the WT(WT) groups. Statistical analyses were performed by using CpG sites that showed a higher than 10% methylation level in WT(WT) samples because hypomethylation can be produced by the H maternal environment only at sites that have a measurable (above the baseline) methylation level when the mother is WT. While all CpG sites within the *Atbf1* DMR, located at the last exon, fulfilled this criterion, the *Smo* DMR, located at the first exon (and close to the promoter), showed an overall lower methylation with measurable methylation only at interspersed CpG sites (indicated by arrows). **C**, Embryo transfer and crossfostering to isolate the effect of the pre- and postnatal receptor deficient maternal environment on DNA methylation. WT embryos were implanted to KO mothers (and to WT to serve as controls) and newborn pups were then crossfosstred to WT foster mothers. Other combinations of the pre- and postnatal maternal environment are listed in panel (D) but not shown here for simplicity. **D**, Offspring exposed to the prenatal KO environment or the combination of the KO pre/postnatal environment show hypomethylation at the *Atbf1* and *Smo* DMRs. Kruskal-Wallis Rank Sum with Tukey posthoc. *Atbf1:* x2=33.4551, P<0.001, **p<0.005 vs. WT(WT/WT), N=20; *Smo*: x2=6.60372, P=0.0102, *p<0.05; N=6.

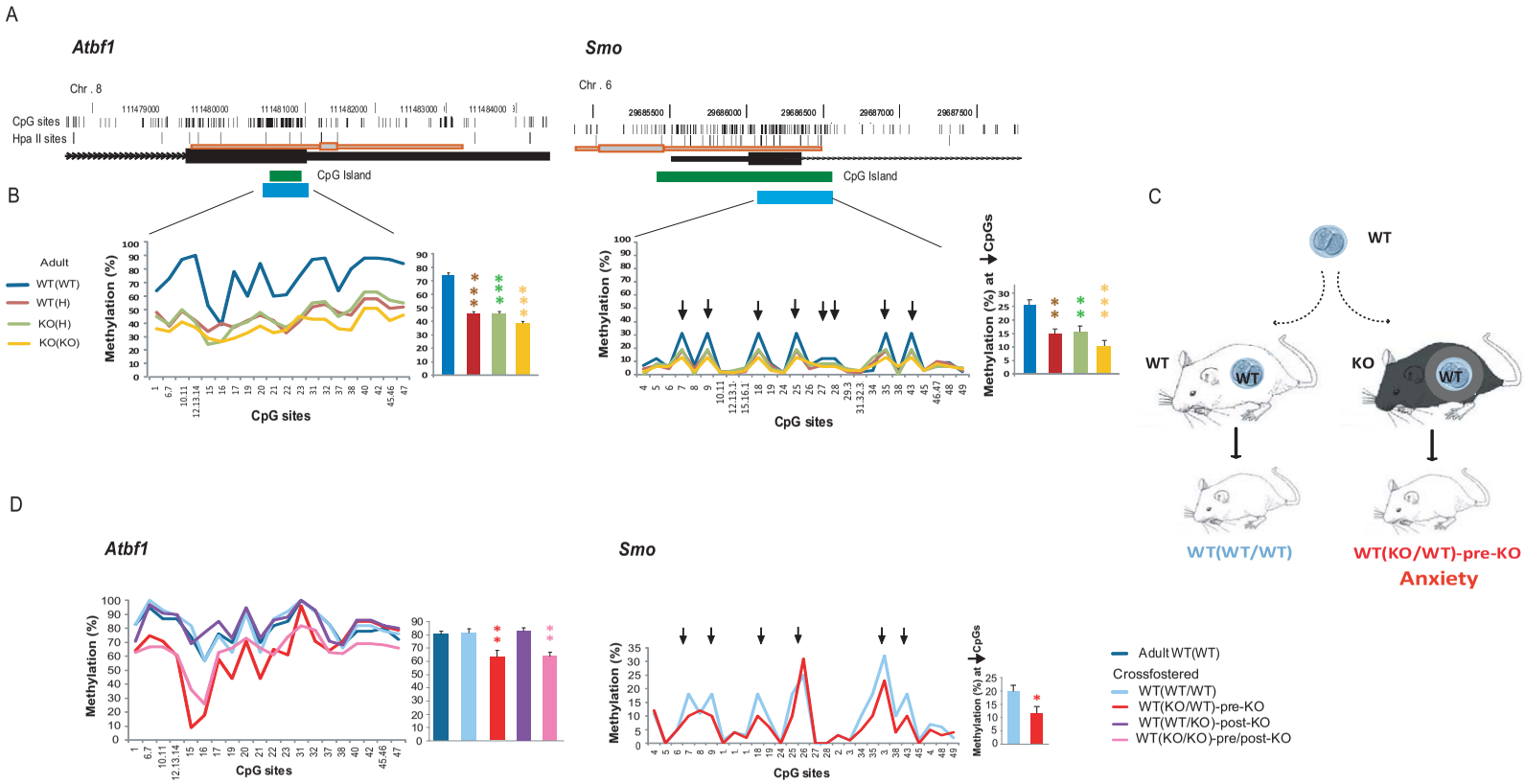
A
Atbf1
Chr . 8
CpG sites
Hpa II sites
CpG Island
Smo
Chr . 6
CpG Island
B
Adult
WT(WT)
WT(H)
KO(H)
KO(KO)
Methylation (%)
CpG sites
Methylation (%) at CpGs
C
WT
WT
KO
WT
WT(WT/WT)
WT(KO/WT)-pre-KO
Anxiety
D
Atbf1
Smo
Methylation (%)
CpG sites
Methylation (%) at CpGs
Adult WT(WT)
Crossfostered
WT(WT/WT)
WT(KO/WT)-pre-KO
WT(WT/KO)-post-KO
WT(KO/KO)-pre/post-KO

Genome-wide differential methylation in adverse maternal environment

We used ERRBS to explore differential methylation at a larger fraction of CpGs and which is not limited to a predetermined set of CpG sites[130]. A total of 376,016,818 aligned sequence reads of 51 bases were obtained from WT(WT), WT(H) and KO(H) v-DGC DNA, which, at ≥35X coverage, reported methylation rates (MR, fraction of methylated cytosines at a site) at 1,740,900 CpG sites (8.4% of all CpGs in the mouse[129]) across the three groups of offspring. We found 2.3% of the CpG sites to be differentially methylated in both WT(H) and KO(H) neurons compared to WT(WT) neurons (BH-FDR $q<0.01$; $\Delta MR \geq 20\%$)(Fig. 3.3A). Island specific DMSs were underrepresented among all DMSs. This finding is in agreement with previous reports showing that islands are typically resistant to methylation; however, if methylated during development, islands usually are not subjected to tissue specific or environmentally induced methylation changes[47,126,131].

Close to half of the DMSs identified in adult DGCs (16,447) were spaced less than 1kb from each other (cl-DMSs; Fig. 3.3B and C) and more than 50% of these "<1 kb" sites had an inter DMS distance between 2 and 100 bps indicating a significant clustering of methylation changes (Supplemental Fig. 3.2). Cl-DMSs specified a total of 6,357 DMRs. ERRBS also detected 4,187 differentially methylated clustered sites when WT(H) and KO(H) samples were compared indicating that the offspring genotype can elicit methylation changes as well. However, this smaller set of sites was not studied further because of lack of the association with the anxiety phenotype (Fig. 3.1A).

Figure 3.3. Genomic features of differentially methylated sites in adverse maternal environment identified by ERRBS. A, CpG island and non-island specific DMSs (WT(WT) vs. WT(H)+KO(H)). **B-C**, Genomic features at clustered (<1kb) DMSs associated with CpG island and non-island sequences.

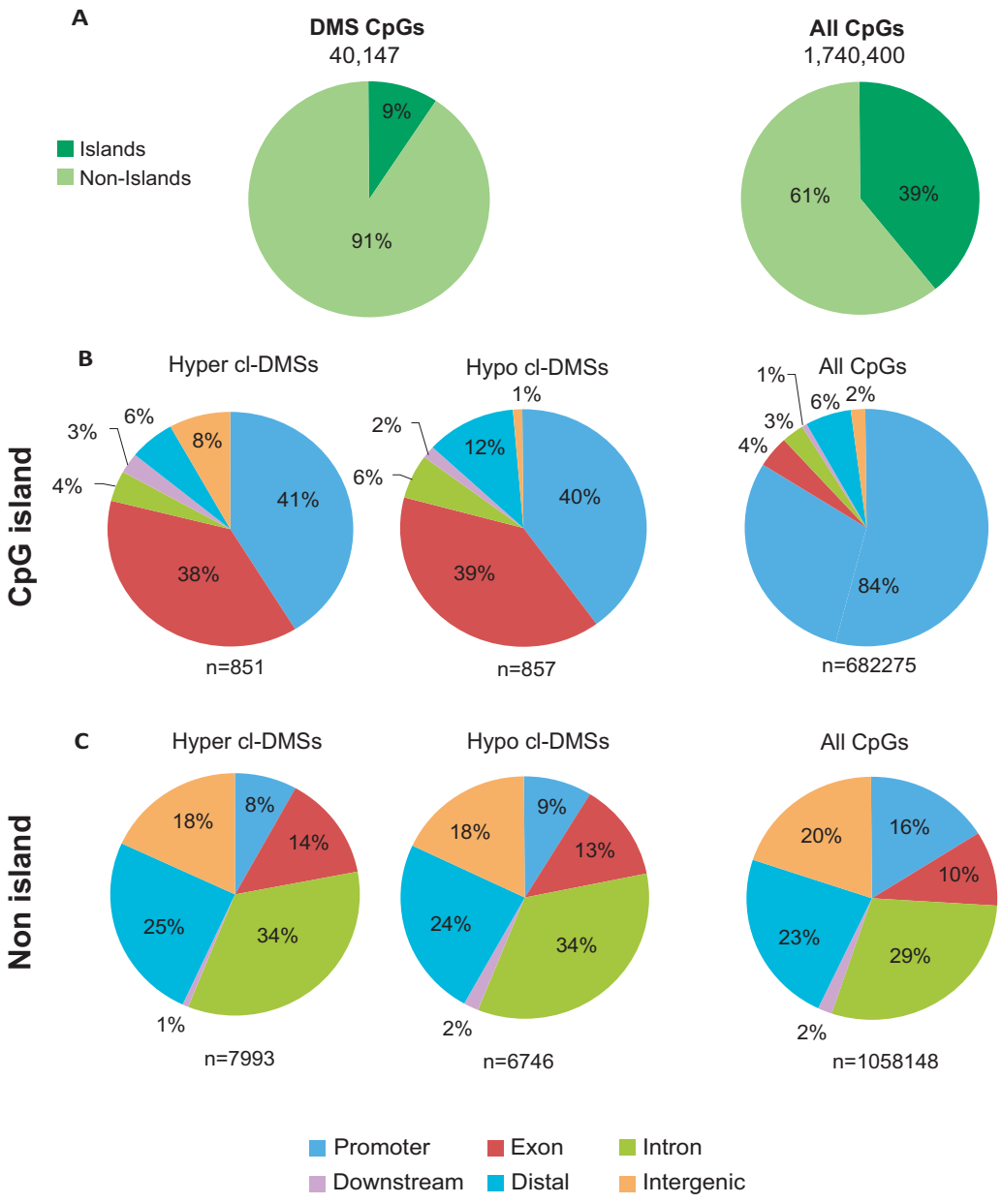
A
DMS CpGs
40,147
All CpGs
1,740,400
Islands
Non-Islands
9%
91%
61%
39%
B
Hyper cl-DMSs
Hypo cl-DMSs
All CpGs
CpG island
41%
38%
8%
6%
3%
4%
n=851
40%
39%
12%
1%
2%
6%
n=857
84%
6%
2%
3%
4%
1%
n=682275
C
Hyper cl-DMSs
Hypo cl-DMSs
All CpGs
Non island
8%
14%
34%
1%
25%
18%
n=7993
9%
13%
34%
2%
24%
18%
n=6746
16%
10%
29%
2%
23%
20%
n=1058148
Promoter
Exon
Intron
Downstream
Distal
Intergenic

The maternally specified cl-DMSs were further analyzed for their genomic features[132]. CpG island-associated DMSs, whether hypo- or hypermethylated, were found more often in exons (~10 x enrichment, compared to all CpGs in islands) and less frequently in promoters (Fig. 3.3B). These findings are consistent with results of the HELP assay that identified DMRs within exons (RRBs also identified the *Atbf1* and *Smo* DMRs). The larger group of non-island DMSs (91%) showed a slight enrichment for intronic and exonic CpGs (34% vs. 29% and 13-14% vs. 10%, respectively), while promoter CpGs were underrepresented in cl-DMSs, at both hypo- and hypermethylated sites (16% vs. 8-9%)(Fig. 3.3C). Overall, these data indicate some preference of the maternal effect to modulate methylation at gene-body CpGs, at both island and non-island sequences.

CpG methylation in the developing dentate gyrus in normal and adverse maternal environment

Majority of adult DGCs are generated during the perinatal and early postnatal period, followed by the gradual maturation of newly born cells[133]. In the maternal $5HT_{1A}R$ deficient model we observed normal proliferation but delayed neuronal maturation at the end of the first week of postnatal life, suggesting that young neurons may already have some epigenetic, either CpG methylation or chromatin, changes. To test this hypothesis, we profiled P7 neurons with ERRBS using the same statistical criteria and parameters that were employed for the analysis of adult DGCs. CpG methylation in both P7 and adult neurons showed the typical bimodal distribution where the majority of CpG sites are either highly methylated (>90%) or methylated at a low level (<10%). However the fraction of highly methylated CpG sites in P7 was slightly lower indicating ongoing methylation in young neurons (Fig. 3.4A). Since many DMSs mapped to introns and exons, the distribution of gene-body CpGs was also assessed and showed a similar pattern (Fig. 3.4C). This analysis also

included E6.5 epiblasts (low coverage; from[29]) and ES cells (high coverage, this study) as references because epiblasts represent the last cell type with multipotency before the onset of gastrulation and cultured ES cells have an epiblast like methylome[31]. In agreement with previous reports, the distribution of methylated CpGs in epiblasts and ES cells indicated an incompletely methylated genome[29,63].

In contrast to the bimodal distribution of methylation at all CpGs, methylation at clustered DMSs (Fig. 3.3B and C) was mostly intermediate in both P7 and adult DGCs (in normal maternal environment) and overall methylation levels were even lower than in epiblasts and ES cells (Fig. 3.4B and D). These data indicate that methylation at environmentally sensitive sites, in contrast to most CpG sites, is typically maintained in the intermediate range up to P7 and beyond. However, a closer inspection revealed significant rearrangements in the methylation of DMSs during development in normal and adverse environment (from P7 to adult). One group of DMSs showed a gain or loss of methylation during normal postnatal development, changes that were inhibited by maternal adversity (Fig. 3.4E and Supplemental Fig. 3.3). These "Type I DMSs" were divided into hypo and hypermethylated subgroups according to the direction of the change in adversity. Sixty percent of DMSs belonged to these categories (33% and 27% for hyper and hypo, respectively). Figs. 3.2B and 3.4G illustrate clusters of type I hypo- and hypermethylated DMSs within the *Atbf1*/*Smo* and the *Grik 4* genes, respectively. Methylation at "Type II DMSs" was not significantly changed during normal postnatal development but the H maternal environment resulted in hyper- or hypomethylation (Fig. 3.4F and Supplemental Fig. 3.3). A total of 40% (20% hypo and 20% hyper) of DMSs were type II. Typical type II hypomethylated DMSs are shown in the *Bsn* gene (Fig. 3.4H).

Although methylation at CpG sites is typically higher in P7 DGCs than in ES cells (and epiblasts) (Fig. 3.4A and C), methylation at DMSs in these cell types was

similar (Fig. 3.4EF and Supplemental Fig. 3.3), suggesting that no significant methylation changes occur at these sites in DGCs, either in normal or adverse environment, before their maturation (e.g. before P7). Thus, the maternal effect, although prenatal in its origin, does not have an impact on methylation at DMSs until neurons develop beyond the young neuronal stage. While Type I and II hypo- and hypermethylated DMSs are quite different in terms of their methylation behavior in adverse maternal environment, we found no obvious sequence context or genomic features that would be group specific or predict the direction of their methylation. Overall, both arrest in developmental methylation/demethylation and abnormal gain/loss of methylation seem to account for producing differential methylation at specific sites in adversity.

Figure 3.4. Methylation at DMSs during development in normal and adverse maternal environment. AB, Histograms with the distribution (% of total) of methylation levels at all CpG sites and DMSs in 10% bins in adult and P7 WT(WT) DGCs, E6.5 epiblasts (E6.5) and ES cells. **BD.** Same as in AB but with gene-body CpGs. **EF**, Methylation in P7 and adult DGCs in normal and adverse maternal environment at Type I and Type II hypo/hypermethylated DMSs. Hierarchical clustering within the four groups of DMSs shows similar methylation levels at P7 in normal and adverse environment and type I and II specific changes in adults. Center: Schematic representation of developmental changes at the four classes of DMSs from P7 to adult age; continuous and dashed lines represent changes in WT and H maternal environment, respectively. **G**, A representative DMR with Type I hyper DMSs in *Girk4*. **H,** A representative DMR with type II hypo DMSs in *Bsn1*.

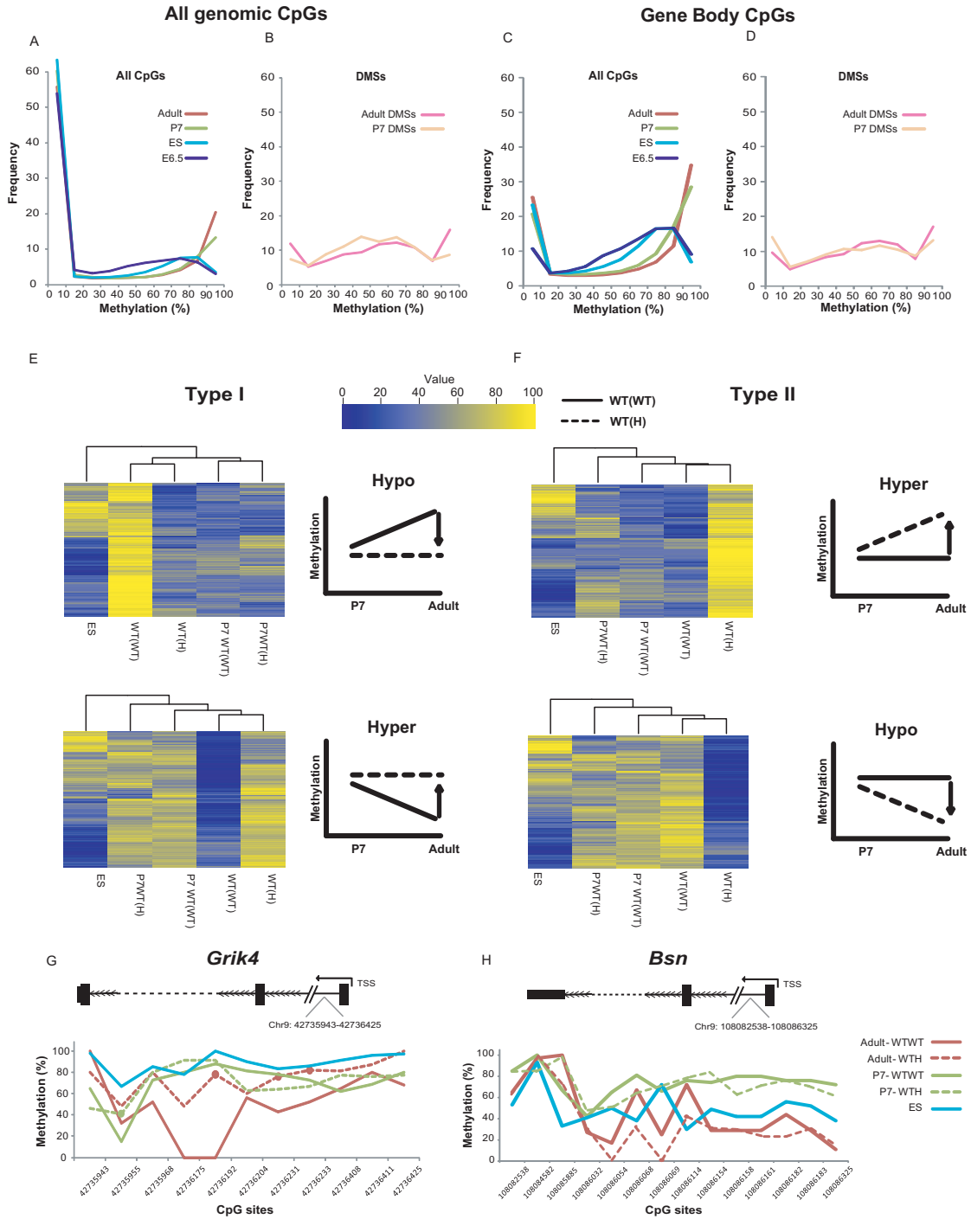
All genomic CpGs
Gene Body CpGs
A
B
C
D
All CpGs
DMSs
Adult
P7
ES
E6.5
Adult DMSs
P7 DMSs
Frequency
Methylation (%)
E
F
Type I
Type II
Value
WT(WT)
WT(H)
Hypo
Hyper
Methylation
P7
Adult
ES
WT(WT)
WT(H)
P7 WT(WT)
P7WT(H)
G
H
Grik4
Bsn
TSS
Chr9: 42735943-42736425
Chr9: 108082538-108086325
Methylation (%)
CpG sites
Adult- WTWT
Adult- WTH
P7- WTWT
P7- WTH
ES

Clusters of DMSs map to cell adhesion molecules and neurotransmitter receptor genes

We used the Ingenuity Knowledge Database to identify genes with relevant biological functions in the list of 1,176 Ensembl genes harboring DMRs. A total of 510 genes belonged to the category of "Nervous System Development and Function" and could be mapped to major steps in neuronal development (Fig. 3.5A). Genes with multiple functions were assigned to multiple developmental processes. This analysis identified neuritogenesis (103 genes with DMRs), migration (61 genes), and pre/postsynaptic differentiation (81 genes) as developmental processes highly enriched in differentially methylated genes. Neuritogenesis, the highest scoring process, is the growth and extension of neurites from the soma by precise cytoskeletal and adhesion dynamics, and guided by external attractive and repulsive cues. Migration and synaptic differentiation are tightly linked to neuritogenesis both in timing and shared molecules.

An independent analysis of the differentially methylated genes by GeneGo MetaCore Process Network Analysis identified essentially the same genes grouped to the functional networks of "Synaptogenesis", "Axonal Guidance" and three "Cell Adhesion" related clusters, "Cadherins", "Attractive and Repulsive Receptors" and "Synaptic Contact" (FDR<0.05)(Fig. 3.5B). Indeed, the "Synaptogenesis" GeneGo category contained synaptic scaffolding proteins and neurotransmitter receptors that were also identified by the Ingenuity "Pre/postsynaptic differentiation" functional category. Similarly, cell adhesion molecules were identified by the Ingenuity analysis in migration, neuritogenesis, and pre/postsynaptic differentiation. Although the genes within these categories were 4.3 times larger than the average gene (138,278 vs. 31,959 bp) and therefore could preferentially harbor DMSs, not all of these large

genes were differentially methylated. Indeed, 556 genes out of the total of 738 within the functional categories in Fig. 3.5B were not modified by methylation. The difference in size between modified and non-modified genes was only ~2-fold (224,942 and 109,909, respectively) which suggests that the differential methylation is not proportionate with gene size. Also, the larger size of genes within the functional categories is mostly due to introns, but more of the gene-associated DMRs (52% of total) were outside of introns in distal sequences (23%), exons (16%), promoters (11%), and downstream sequences (2%) than in introns (31%).

Gene expression analysis of adult DGCs from offspring of WT and H mothers by RNA-Seq showed no overall correlation between expression and methylation at the 3,069 DMR-containing genes, whether the DMRs mapped to promoters, exons, introns or distal sequences (data no shown). However, analysis of the 1,189 differentially expressed genes (>1.3 fold; $q<0.05$, Fisher exact R, BH-FDR; of which 193 contained DMR) with GeneGo Process Network identified "Synaptogenesis" as the top network (Fig. 3.5C). Essentially the same genes were also identified in the "Transmission of nerve impulse" network.

Figure 3.5. Differentially methylated genes encode synaptic proteins. AB, Ingenuity and GeneGo Process Network analysis of DMSs identifies synaptic functions. For the Ingenuity analysis, right-tailed Fisher's exact test was used to calculate a p-value determining the probability that each biological function assigned to the dataset is due to chance alone. For the GeneGo analysis, statistical significance of a process was determined using the Hypergeometric distribution and adjusted for multiple testing by MetaCore. Ratio represents the differentially methylated vs. all genes in the functional categories. **C**, GeneGo Process Network analysis of differentially expressed genes. **D**, Differentially methylated genes encode adhesion molecules (blue) and their effectors (green), presynaptic proteins (pink), scaffolding proteins (grey) and neurotransmitter receptors (yellow). The figure positions the differentially methylated genes/proteins to the pre and postsynaptic compartments, also indicating those that interact with synaptic vesicles within the presynaptic compartment. The effect of cell adhesion molecules converge on the regulation of microtubule and actin organization that are essential in migration, neuritogenesis and synaptic differentiation, identified by functional analysis (panels AB). Cell adhesion molecules are also involved in the recruitment of synaptic receptors whose function controls neuronal excitability. Genes for both inhibitory and excitatory receptors were among those that were differentially methylated. Some of the differentially methylated genes were also downregulated in adult DGCs (red outline and arrow). Other synaptic genes were also downregulated but were not differentially methylated (white background with red outline and arrow). These data indicate a permanent hypofunction at many synaptic genes suggesting a persistent abnormality in synaptic plasticity and neuronal excitability.

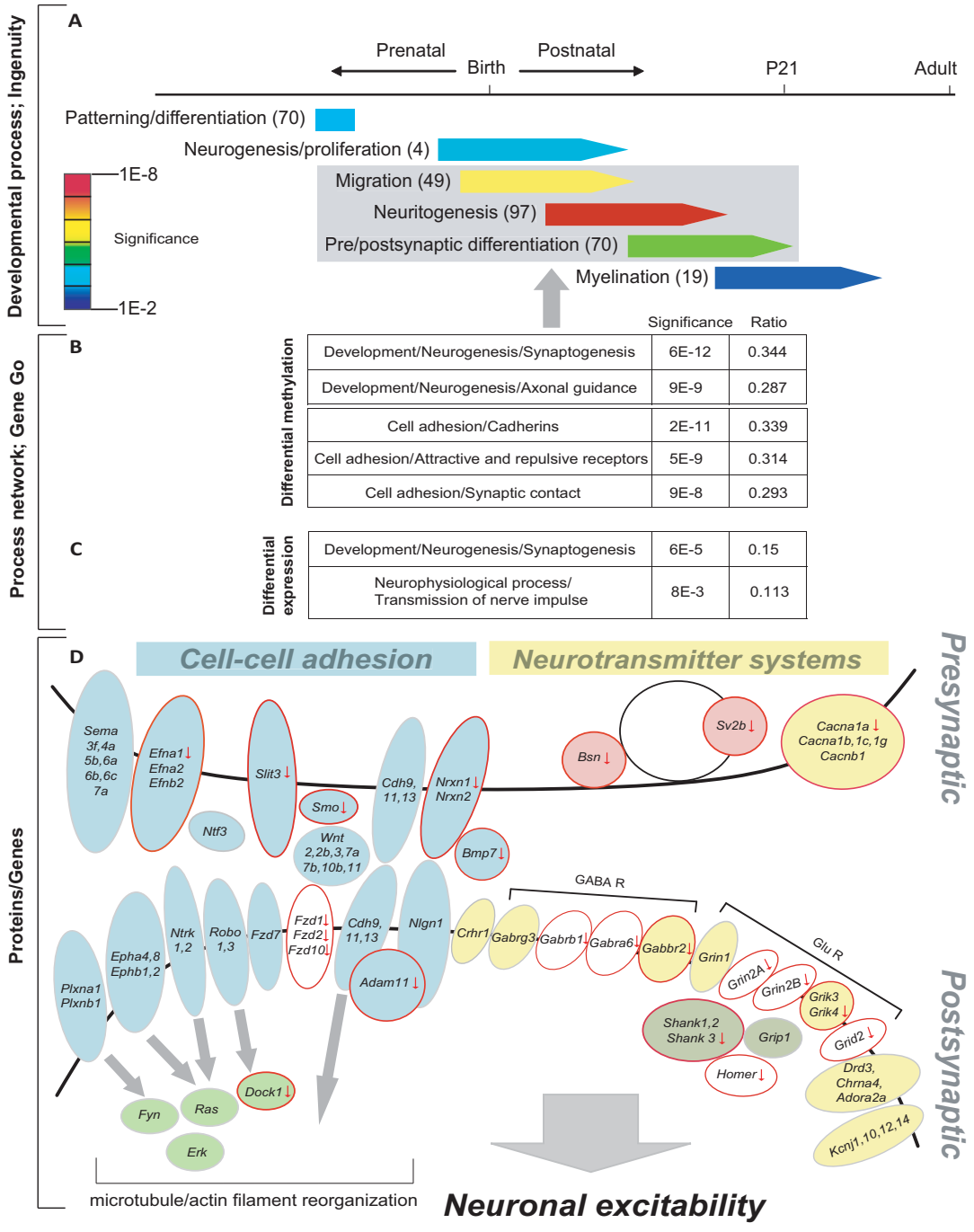
Developmental process; Ingenuity
A
Prenatal
Birth
Postnatal
P21
Adult
Patterning/differentiation (70)
Neurogenesis/proliferation (4)
Migration (49)
Neuritogenesis (97)
Pre/postsynaptic differentiation (70)
Myelination (19)
1E-8
Significance
1E-2
Process network; Gene Go
B
Differential methylation
Significance
Ratio
Development/Neurogenesis/Synaptogenesis
6E-12
0.344
Development/Neurogenesis/Axonal guidance
9E-9
0.287
Cell adhesion/Cadherins
2E-11
0.339
Cell adhesion/Attractive and repulsive receptors
5E-9
0.314
Cell adhesion/Synaptic contact
9E-8
0.293
C
Differential expression
Development/Neurogenesis/Synaptogenesis
6E-5
0.15
Neurophysiological process/ Transmission of nerve impulse
8E-3
0.113
Proteins/Genes
D
Cell-cell adhesion
Neurotransmitter systems
Presynaptic
Postsynaptic
Sema 3f,4a 5b,6a 6b,6c 7a
Efna1↓ Efna2 Efnb2
Slit3↓
Ntf3
Smo↓
Wnt 2,2b,3,7a 7b,10b,11
Cdh9, 11,13
Nrxn1↓ Nrxn2
Bmp7↓
Bsn↓
Sv2b↓
Cacna1a↓ Cacna1b,1c,1g Cacnb1
GABA R
Glu R
Plxna1 Plxnb1
Epha4,8 Ephb1,2
Ntrk 1,2
Robo 1,3
Fzd7
Fzd1↓ Fzd2↓ Fzd10↓
Cdh9, 11,13
Nlgn1
Adam11↓
Crhr1
Gabrg3
Gabrb1↓
Gabra6↓
Gabbr2↓
Grin1
Grin2A↓
Grin2B↓
Grik3 Grik4↓
Grid2↓
Shank1,2 Shank 3↓
Grip1
Homer↓
Drd3, Chrna4, Adora2a
Kcnj1,10,12,14
Dock1↓
Fyn
Ras
Erk
microtubule/actin filament reorganization
Neuronal excitability

Overall, these functional analyses identified two major groups of proteins; cell adhesion molecules and neurotransmitter receptors (Fig. 3.5D). Cell adhesion molecules have pre- and postsynaptic partners, and genes encoding both of these classes were differentially methylated. These included ephrins (EFNA1,A2,B2) and their receptors (EPHA4,A8,B1,B2), semaphorins (SEMA3F,4A,5B,6A,6B,6C,7A), and their plexin receptors (PLXNA1,B1), neurexin (NRXN1,2) and neuroligin (NLGN1), Wnts (WNT2,2b,3,7a,7b,10b,11) and frizzled (FZD7), cadherins (CDH9, 11,13) and slit (SLIT3) and its receptors (ROBO1,3). Neurotransmission related differentially methylated genes included those that encode neurotrophin 3 (NT3*),* the TrkA receptor (TRK1), CRH receptor 1 (CRHR1), GABA-B receptor subunit 2 (GABBR2), an NR1 subunit of the NMDA receptor (encoded by *Grin1*), the dopamine D3 receptor (DRD3), acetylcholine alpha 4 subunit (CHRNA4), adenosine A2 receptor (ADORA2A), a number of calcium channels (CACNA1A,1C,1G,B1) and K channels (KCNJ1,10,12,14), which all have been implicated in neuronal excitability as well as in anxiety[134]. A total of 18 genes within the functional clusters shown in Fig. 3.5A and B were also differentially expressed (Supplemental Table 3.1; see 11 genes in Fig. 3.5D) and almost exclusively downregulated (17 of 18) suggesting hypofunction at these genes. Additional synaptic genes that showed no differential methylation were downregulated, including those that encode the NR2A and 2B NMDA subunits *(Grin2a* and *Grin2b),* HOMER and FZD1, 2 and 10 (Fig. 3.5D). Overall, the differential methylation/expression of a large number of pre- and post synaptic cell adhesion molecule and neurotransmitter receptor genes suggests a wide-ranging and permanent effect of the adverse maternal environment on synaptic plasticity and neuronal excitability.

2.3 Discussion

Pre and early postnatal adversity is a major factor in the development of psychiatric conditions. Offspring development is dependent on the maternal environment during these periods and numerous human and animal studies demonstrate that abnormal maternal physiology and behavior, whether genetic or environmental in nature, result in disruptions in normal brain development, that in turn can result in adolescent and adult behavioral abnormalities[117,135-137].

The development of the hippocampus is particularly sensitive to environmental disruptions, presumably because hippocampal neurons show remarkable structural and functional plasticity[138]. The hippocampal circuit is involved in numerous behaviors including cognitive tasks, evaluation and termination of the stress responses, and emotional behavior[118]. Although the consequences of early life adversity on the hippocampus are relatively well documented at the behavioral and even morphological level[112,117,138], little is known about the underlying molecular mechanisms. Development is programmed by both transcriptional and epigenetic mechanisms and here we studied the developmental dynamics of CpG methylation genome-wide in DGCs in normal and adverse maternal environment. We used a previously established maternal adversity paradigm that is based on a 5-HT_{1A}R deficit in the mother and which produces a delay in the development of the v-DGCs as well as an anxiety-like behavior[12].

The main finding of our work is that, although the receptor deficient maternal environment had a genome-wide effect, DNA methylation changes occurred in specific genomic locations and contexts. Specifically, CpG sites that were targeted by the maternal effect tended to have an intermediate methylation level during neuronal development until P7 and even beyond compared to the majority of the genome that exhibited either high (>90%) or low (<10%) methylation levels early on. Indeed,

methylation at DMSs in developing DGCs was similar or even less than in ES cell or epiblasts, cells that exhibit extensive epigenetic plasticity[63] and we speculate that epigenetic metastability at DMSs explains their sensitivity to disruptions by maternal adversity. Although intermediate methylation can be due to allelic differences documented at dosage compensated and imprinted genes, partial methylation in hematopoietic cells was predominantly associated with stochastic variability in methylation[139]. Since the vast majority of DMSs were not at imprinted genes, and because partial methylation was also seen in males at the X chromosome, we believe that the intermediate methylation at most DMSs is stochastic in nature.

The maternal effect either modified the developmental trajectory of methylation at DMSs by inhibiting programmed hypo/hypermethylation (type I DMSs) or induced abnormal hypo/hypermethylation at sites that normally stay unchanged during postnatal development (type II DMSs). These influences produced relative hypo- and hypermethylation in the H maternal as compared to the WT maternal environment in DGCs. This suggests different mechanisms for the hypo- and hypermethylation and further studies will be needed to determine the factors responsible for the direction of methylation change in adverse maternal environment. Since ERRBS typically profiles one strand, it was not possible to determine if gain in methylation during development, or by the maternal effect at DMSs, was due to de novo methylation or maintenance methylation at asymmetrically methylated sites. On the other hand, loss of methylation at DMSs is likely due to active rather than passive demethylation because in the postnatal gentate gyrus the majority of isolated DGCs are postmitotic and because the number of neuronal precursors, located in the subgranular layer, and glial cells is too low to significantly contribute to the overall signal. Several mechanisms have been shown to account for active demethylation

including oxidative demethylation of cytosines achieved by the ten-eleven-translocation (TET) proteins and repair based mechanisms[140].

DMSs are relatively scarce at promoters and typically found in gene bodies and gene distal areas. This suggests that the maternal effect may not regulate transcription via proximal promoters, but may rather influences expression indirectly by modulating alternative splicing and promoter use, and/or miRNAs expression. Further analysis showed that clusters of DMSs, e.g. DMRs, were enriched in genes that encode proteins involved in adhesion molecules and neurotransmitter receptors. Up to 34% of the genes classified in these categories were differentially methylated suggesting a strong convergence of the maternal effect on these genes and functions. Gene expression studies identified some of the differentially methylated genes and overall differential methylation and expression showed a good correspondence.

It is challenging to establish a causative relationship between the DNA methylation changes in DGCs and innate anxiety, the main phenotype of the offspring of receptor mutant mothers[115], because it is expected that each individual differentially methylated gene contributes only a small fraction of the total phenotype. The association of the differentially methylated genes to the behavioral phenotype is likely similar to that of susceptibility genes to polygenic diseases/conditions. Network and functional analyses have been developed for these situations and we employed two computational models that use different algorithms to identify putative functionally relevant differentially methylated genes. The validity of our approach is strengthened by the fact that many of the differentially methylated/expressed genes and their protein products have individually been linked to anxiety in human or to anxiety-like behavior in animals by pharmacological and/or genetic evidence. The genes for the neurotransmitter receptors/subunits CRHR1, DRD3, ADORA2A, CHRNA4, GABRG3 and GABBR2 were differentially methylated and all of these receptors have

been linked to anxiety. Central administration of CRH in rodents produces behavioral effects via CRHR1/2 that correlate with a state of anxiety, such as a reduction in exploration in a novel environment or an enhanced fear response[141]. Also, genetic studies indicate that CRHR1 is important in regulating anxiety levels[142,143]. Dopamine D3 receptor (DRD3) knockout mice display reduced anxiety in the open field and elevated plus maze associated with increased locomotor activity[144]. Adenosine$_{2a}$ receptor (ADORA2A) null mice show increased anxiety in elevated maze and light dark box[145]. Mice null for the Ach receptor α_4 subunit (CHRNA4), display an increased anxiety in the elevated plus maze test[146]. Inhibitory GABA-A receptors are central in the treatment of anxiety and receptor deficit in the hippocampus and parahippocampus has also been implicated in panic disorder and generalized anxiety disorder[147-149]. Similarly, GABRB2 KO mouse exhibit anxiety[150]. Increased excitability is another mechanism that can lead to anxiety. Differential methylation was detected in *Grin 1*, the gene for the NMDA NR1 subunit, in *Grik3* and *Grik4*, the genes for KA receptor subunits, in genes for glutamate receptor interacting proteins such as *Grip1*, and *Shank1,2,3* as well as in calcium (*Cacna1c*) and potassium channel (*Kcnj)* genes that can all influence neuronal excitability and modulate anxiety[151-154].

Cell adhesion molecules, comprising the other large group of genes with differential methylation, are utilized through many steps during CNS development, including neuronal migration, guidance, neurite outgrowth, and synapse formation. We detected differential methylation at genes encoding cadherins, ephrins, slit-robo, wnts, semaphorins-plexins and neurexin-neuroligins (see Fig. 5). Disruptions of these genes typically result in neurodevelopmental conditions with a wide variety of symptom including cognitive defects, anxiety, and abnormal social behavior. Mutations in some of these genes such as *CDH9* and *NRNX1* in human, that were differentially methylated in the presence of adverse maternal environment in mouse,

have been implicated in autism spectrum disorders and schizophrenia[155-158]. Specifically, loss of function mutations (deletion and CNVs) in *NRXN1*, a gene that was not only differentially methylated but also downregulated in our experiments, have been linked to a number but individually variable ASD symptoms within affected family members resulting in relatively selective behavioral abnormalities such as impaired social interactions, anxiety, or learning and memory deficits in individuals[155,156,159]. Another example of a relatively specific anxiety phenotype associated with an adhesion molecule is the increased avoidance of the open arm of mice with altered EPHB2, an ephrin receptor whose gene was also differentially methylated in the receptor deficient maternal environment[160]. Overall, our finding of differential methylation/expression at a large number of cell adhesion and neurotransmitter receptor genes suggests that some forms of anxiety following maternal adversity could be associated with epigenetic perturbations in multiple synaptic genes, each contributing only a small effect to the overall phenotype.

3.4 Materials and Methods

Animals

Adult, 10-13 week old Swiss Webster male mice were used in all experiments. Animals were generated as described previously[12,114] and housed three-five per cage in a room with controlled temperature and a fixed lighting schedule (lights off from 0600–1800 h). Food and water were available *ad libitum*. All experimental protocols were approved by Research Animal Resource Center (RARC) at the Weill Cornell Medical College.

ES cell culture

E14 ES cells were cultured on feeder cells (mitomycin-inactivated mouse embryonic fibroblasts (MEFs)) for at least two passages after thawing. Cells were split every 2 d with plating densities between 1.5 x 10^6 and 4 x 10^6 cells on 10-cm cell culture plates. ES medium was based on DMEM containing 15% FBS (ES cell qualified), LIF (1,000 U/ml, Millipore, Billerica, MA, USA), 1X non-essential amino acids, 2mM L-glutamine and β-mercaptoethanol (Invitrogen, Carlsbad, CA, USA).

Sample dissection and DNA extraction

Frozen brains were sectioned into 200 μm slices using a CM3050 cryostat (Leica, Germany) and the ventral dentate gyrus (vDG) area from the slices was microdissected using a micro-dissecting knife (FST, Foster City, CA, USA). vDG samples from 3-5 mice from at least 3 litters were pooled into one tube. DNA extraction was carried out with the QIAGEN Puregene Gentra cell kit (Qiagen, Valencia, CA, USA). DNA was dissolved in 10mM Tris (tris[hydroxymethyl]aminomethane)–HCl, pH 8.0, and DNA concentration was measured by using NanoDrop® ND-1000 (Thermo Scientific, Wilmington, DE, USA).

DNA methylation HELP arrays

The HELP (*HpaII* tiny fragment enrichment by ligation-mediated PCR) assay was carried out as previously described[128,161,162] in the Epigenomics Core Facility of the Weill Cornell Medical College. Briefly, two samples of one microgram genomic DNA each were digested overnight with *Hpa*II and *Msp*I (New England Biolabs, Ipswich, MA, USA). Adapters were ligated to the DNA ends and the fragments were amplified by ligation mediated PCR optimized for fragment size between 200 and 2,000 bp. The *Hpa*II and *Msp*I representations were then labeled with Cy5 and Cy3, respectively, followed by the co-hybridization of the labeled fragments to Roche 25K custom arrays representing mouse promoters and CpG islands. The arrays were scanned using a GenePix 4000B scanner (Axon Instruments, Sunnyvale, CA, USA).

HELP data normalization

HELP data were preprocessed and normalized using the HELP data analysis package[163] implemented in R. Normalized HELP methylation signal was compared across groups with the Limma R package. Limma implements moderated variance estimates especially useful with small number of biological replicates in each group. The Limma P-values were adjusted for multiple testing with the Benjamini Hochberg method. HELP fragments were considered differentially methylated if their fold-change crossed zero (indicating a qualitative change in average methylation state for the fragment) and the Limma BH adjusted P-values was $q<0.005$ (stringent estimated false discovery rate of less than 0.5%). Differentially methylated regions (DMRs) were classified based on their CpG density and location. CpG islands were defined as >200bp with GC content of 50% or greater. Islands were divided to strong ($CpG^{o/e}$ >0.80) and weak (0.8 >$CpG^{o/e}$ >0.60) and island shores were defined as 2kb regions around islands. Low CpG regions had a $CpG^{o/e}$ <0.60.

DNA methylation sequencing by MassARRAY EpiTYPER

DNA methylation sequencing by MassARRAY EpiTYPER

MALDI-TOF mass spectrometry based MassARRAY using EpiTYPER (Sequenom, San Diego, CA, USA) was performed on fragments identified by the HELP assay. First, the DNA was bisulfite converted as previously described[164] followed by sequencing. MassARRAY primers were designed to cover the HpaII amplifiable fragments (HAFs) and additional 2,000 bp upstream and downstream sequences in case the sites at HAFs were methylated and the DNA was cut at upstream and/or downstream HpaII sites in the HELP assay. The primers were designed using the Sequenom EpiDesigner beta software (http://www.epidesigner.com/). The primer sequences are displayed below.

Atbf1

1	TTAAGTTTATGTAGTATTTTAGGGGTTTAG	TTCATCTTCAAAACTTACAATCTAAAAAT
2	TTTTAAAAGGATATAATTTAATAGGGTTAG	ACCTCAAATTCATACAACACCTCAA
3	TTTTTTTAAAGGTATTATTGGTTTGG	TTCTCCCCTAAAAATTAACTTCAAC
4	TTGTAATAAGGTGGAGTGTTTTTTT	AAATTATTTTCCCATATACCTATCTATACC
5	GTGGTGAATTTGTAAGAGATGGTGT	AAAACTAAACCCCTAAAATACTACATAAA
6	TTTTTGAGGTGTTGTATGAATTTGA	AAAAACCACCTAAAATCCCTCTACT
7	GTTATTATGGTAATGGTTTTTTAGTTATTT	TAAAAAAACCTCTCCTTTCTCCTTC
8	GTTTTTAAGAAGGAGAAAGGAGAGG	AAAAACAAACCTTCCATACCATACA

Smo

1	GGAATTTATTTTGTAGATTAGGTTGG	AAACTCACAATTCTAAATCATAATCCA
2	AGAAATTTTATGAGGTAGTTGGGTT	AAAACAAACAAAAATTTTCACTCCA
3	TTAAAGATTTAGTTAAGTGTTTTTGGGA	CAACCCCCTAAACTCTCCCTAC
4	TAGTTGGTTTTGTTTTTTGGAATGT	CCAACTAAAAATTCAATCAAATACCTC
5	GAGAGTAGGGTTAGTTAGAGTAATAAAGGA	AAACTATCTTCAACCCTAAAAACC
6	GAAGTTGTTTTTAATTTTGGGAATTT	AAAACTAAAACTCCTCCTCTCCAAC
7	GGAGGGTTTTTAGGGTTGAAGATAG	CCAACAATACCAACAACAACAACTA
8	AGTTGTTGTTGTTGGTATTGTTGG	ACTAACTTCCCTAATCTCTTACCCC
9	TGGTTAAATAGTTAATTTAGTAAAAGTTGA	AAAAATTCCCAAAATTAAAAACAAC
10	AATAGTTTGAGGTTTGAGTTTTTTTT	TCAACTTTTACTAAATTAACTATTTAACCA

Enhanced Reduced Representation Bisulfite Sequencing (ERRBS)

500 ng DNA from each group was processed by the standard RRBS protocol as described[130]DNA was digested with MspI restriction enzyme. This was followed by end repair and ligation of paired end Illumina sequencing adaptors fully methylated at all cytosines. Size selection for library sizes of 150-400 bp was performed followed by a single round of bisulfite treatment using the EZ DNA Methylation Kit (Zymo Research). PCR amplification using Illumina PCR PE1.0 and 2.0 was followed by product isolation using AMPure XP beads per manufacturer's recommended protocol (Agencort). Quality control was performed using quantitation on a Qubit 2.0 fluorometer (Invitrogen) and library visualization using a Quant-iT dsDNA HS Assay Kit for (Agilent 2100 Bioanalyzer). The amplified libraries were sequenced using a 50bp single end read run on a HiSeq2000 per manufacturer's recommended protocol. Image capture, analysis and base calling were performed using Illumina's CASAVA 1.7.

ERRBS read mapping

The last bisulfite plugin parallelizes alignments with the last aligner, and otherwise follows the recommended protocol for aligning bisulfite reads with this aligner (i.e., see http://last.cbrc.jp/doc/bisulfite.txt).

ERRBS methylation rate estimation

Methylation rates were estimated with GobyWeb and the SEQ_VAR_GOBY_METHYLATION plugin. This plugin determine when methylation events occurs at a given genomic location. Events are defined as observing a C in the read when the reference has a C (methylation event on the forward strand) or observing a T in the read when the reference has a C (non-methylation event on the forward strand). Similarly, G/G and G>A observations define methylation and non-methylation events for the reverse strand, respectively.

Methylation rates were estimated for sites were more than 35 events were observed. Methylation rates were estimated as the number of methylation events divided by the sum of non-methylation and methylation events. A methylation rate of 100% indicates that all events support methylation at this site. To identify differentially methylated sites, we calculate a Fisher Exact test comparing the number of methylation events and non-methylation events at a site between two groups of samples as reported earlier[165]. The Fisher p-values are adjusted for multiple testing across all sites observed with more than 35 events across the genome. This is done with the Goby fdr implementation of the Benjamini-Hochberg method (see http://goby.campagnelab.org). Sites are considered significantly differentially methylated when the adjusted q-value is less than 0.01 and the difference in methylation rate is larger than 20% between the groups.

Sample preparation for RNA extraction and RNA-Seq

Mice were perfused with ice-cold saline solution containing 30 % RNAlater (Ambion, Austin, TX, USA) to prevent RNA degradation during microdissection. Brains were rapidly removed, frozen and stored at −80 °C until sectioning. Isolation of vDG was as described above. Ventral DG samples from 3-5 mice from at least 3 litters were pooled.

RNA extraction and RNA sequencing (RNA-Seq)

Total RNA was extracted using Trizol reagent (Invitrogen, Carlsbad, CA, USA). RNA concentration was measured using NanoDrop® ND-1000 (Thermo Scientific, Wilmington, DE, USA) and RNA quality control was performed by using Bioanalyzer 2100 (Agilent Technologies, Palo Alto, California, USA). RNA was fragmented with divalent cations at high temperature and converted to cDNA libraries following the Illumina recommended sample preparation guide (Document 1004898

Rev. D) using Illumina kits (Illumina, San Diego, CA, USA)[164]. The libraries were sequenced on the Illumina GAIIx instrument (one sample per lane), with the single end protocol and 42 cycles of sequencing.

RNA-Seq Data Analysis

RNA-Seq data were received as FASTQ files from the core facility and uploaded to a local instance of GobyWeb (http://gobyweb.campagnelab.org). Alignments were performed with and the bwa aligner[166] against the MM9 mouse reference genome. Alignments were filtered to keep only reads that matched with less than 5% sequence differences (accepting 2 mismatches at most over a 42 bp read) and to exclude those generated from reads that mapped in more than one location in the reference genome. Differential expression analysis was conducted with GobyWeb. Briefly, alignments were used to estimate the number of reads that match gene annotations with the Goby alignment-to-counts mode. Annotations were obtained the Ensembl release corresponding to NCBI37.55/MM9. Gene counts were estimated as the sum of the number of reads that partially overlap with any of the exons of a gene, but do not lie completely within the introns of the gene. Counts were compared between groups with a Fisher exact test (R implementation) adjusted for multiple testing with the method of Benjamini Hochberg (adjusted Fisher exact test P-value<0.01 and fold-change>1.3 in either direction of change).

Statistical analysis

Data are shown as means +/- SE. One way ANOVA or Kruskal-Wallis Rank Sum Test was used in the analyses to compare multiple groups followed by LSD and Tukey posthoc analysis, respectively to assess statistical significance. Differences between groups were considered to be significant when $P<0.05$.

Functional Enrichment Analysis

The list of differentially methylated genes was analyzed through the use of Ingenuity Pathways Analysis (http://www.ingenuity.com). The Functional Analysis identified the biological functions that were most significant to the data set. Right-tailed Fisher's exact test was used to calculate a p-value determining the probability that each biological function assigned to the data set is due to chance alone. Analysis of functional enrichment was carried out using MetaCore from MetaCore from Thomson Reuters (http://www.genego.com/metacore.php, version 6.10) searching for enrichment in the manually curated GeneGO Process Networks, representing a pre-set network of protein interactions. Statistical significance of a process was determined using the Hypergeometric distribution and adjusted for multiple testing by MetaCore.

Data Access

Raw data (HELP, RNA-Seq and RRBS) have been deposited into the GEO database and are included in the super series identified by accession number GSE35856.

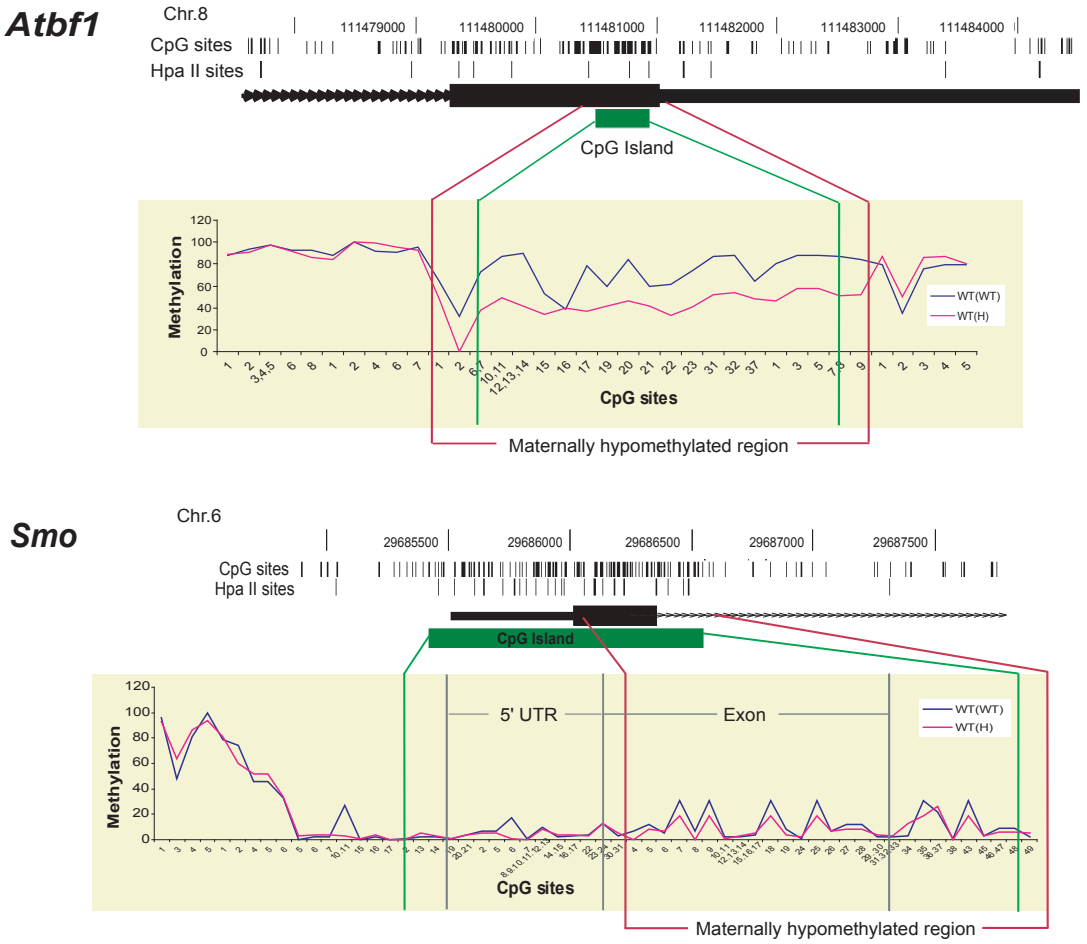

Supplemental Figure 3.1 Differential methylation is restricted to CpG islands in the Atbf1 and Smo DMRs.

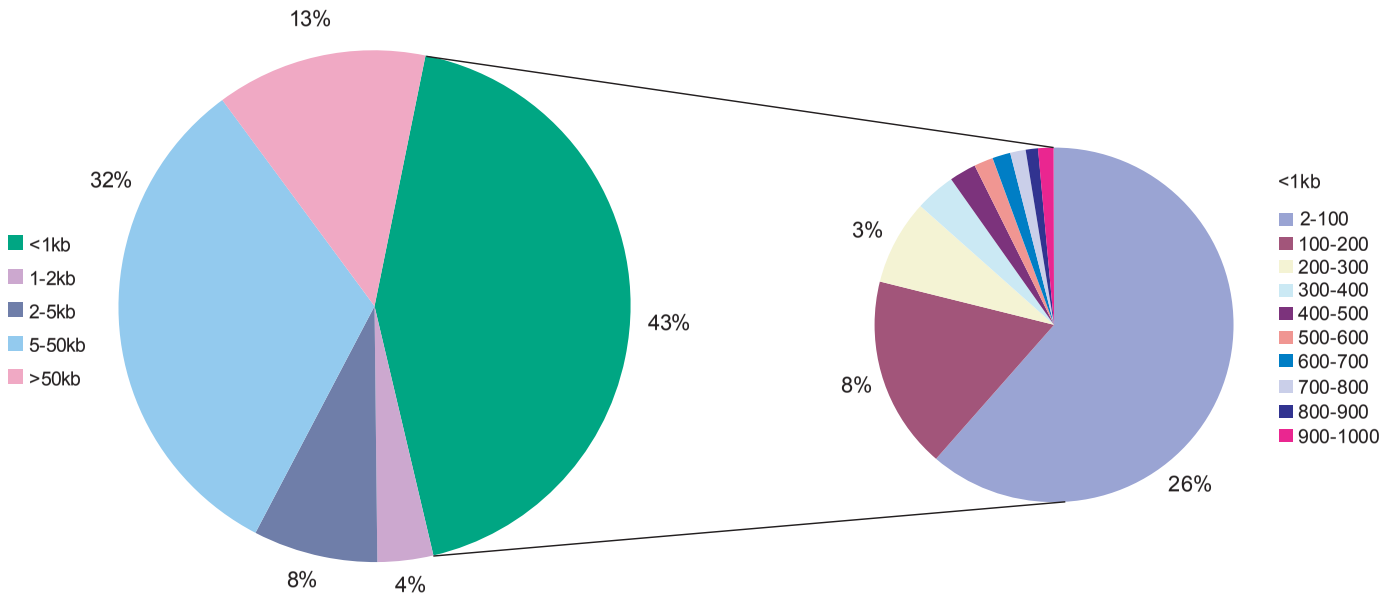

Supplemental Figure 3.2. Distribution of DMSs based on their inter-DMS distance indicates clustering (e.g. over 50% of DMSs are closer than 5 kb). DMSs with an inter-DMS distance of <1kb are further dissected showing that overall, 26% of DMSs are closer than 100 bp to each other.

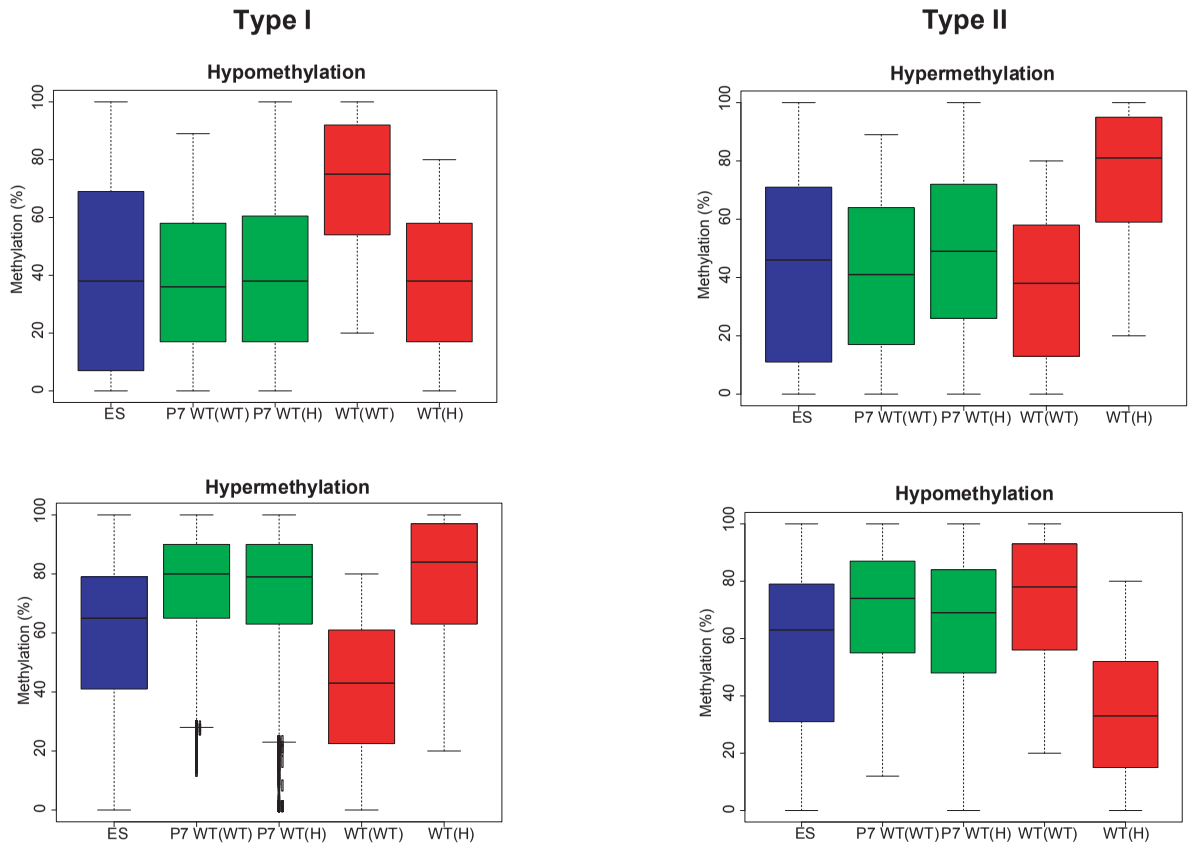

Supplemental Figure 3.3 Boxplot representation of methylation in P7 and adult DGCs in normal and adverse maternal environment at Type I and Type II hypo/hypermethylated DMSs.

Supplemental Table 3.1: List of differentially methylated (ERRBS) and expressed genes encoding synaptic proteins

Gene	Expression wt(wt/wt(h)	Significance		Ensembl gene ID
ADAM11	0.748699135	4.58E-10		ENSMUSG00000020926
SLIT3	0.734192828	2.77E-11		ENSMUSG00000056427
PRKCA	0.578599904	6.59E-42		ENSMUSG00000050965
PRKCH	0.702094347	0.000497419		ENSMUSG00000021108
BMP7	0.637856801	9.53E-05		ENSMUSG00000008999
EFNA1	1.351590619	0.00396434		ENSMUSG00000027954
SMO	0.75645254	0.000290135		ENSMUSG00000001761
DOCK1	0.758581453	0.0011486		ENSMUSG00000058325
APP	0.762555476	6.84E-112		ENSMUSG00000022892
NRXN1	0.766524349	2.42E-16		ENSMUSG00000024109
DNM1	0.731609174	4.17E-169		ENSMUSG00000026825
GABBR2	0.765843385	4.34E-24		ENSMUSG00000039809
SV2B	0.715696659	2.19E-55		ENSMUSG00000053025
BSN	0.709602339	3.05E-157		ENSMUSG00000032589
GRIK4	0.755007588	1.89E-08		ENSMUSG00000032017
CAMK1D	0.709018718	2.37E-32		ENSMUSG00000039145
PTPRF	0.761945399	5.44E-13		ENSMUSG00000033295
FGFR1	0.728395781	5.54E-18		ENSMUSG00000031565

CHAPTER 4

TRAITS OF A PSYCHIATRIC DISEASE-LIKE PHENOTYPE PROPAGATE THROUGH THE MATERNAL LINE VIA SEGREGATED ITERATIVE-SOMATIC AND GAMETIC EPIGENETIC MECHANISMS

** Mitchell E., Klein S., Sharma A., Toth J.G., Argyropoulos K., Chen R., Barboza L., Bavley C., Bortolozzi A., Chen Q., Lodhi N., Ingenito J., Mark W., Dudakov J., Gross S., Paolo G.D., Artigas F., and Toth M. 2015. Manuscript submitted for review.*

4.1 Introduction

The concept of "non-genetic" inheritance of parental behavioral traits is gaining acceptance because it may significantly contribute to the development of disease phenotypes, including psychiatric disorders[4,167]. For example, stress and resulting stress disorders in parents increase the risk for PTSD, depression, and anxiety disorders in their progeny[39,43]. Many aspects of this "intergenerational" transmission paradigm can be reproduced in rodents. In particular, parental stress was shown in several studies to result in abnormal emotional behavior in the offspring[17,40,41]. Some human studies also suggest the transmission of parental behavioral/psychiatric conditions to the grandchildren. As a result, the mechanism of "multigenerational" transmission of parental traits has been extensively studied in rodent models, especially through the male line because of its relatively straightforward interpretation via germ cells and the ease of obtaining sperm for epigenetic studies[17-19,40,41,168,169].

However, epidemiological studies indicate that many inter/multigenerational non-genetic behavioral phenotypes are exclusively or prominently transmitted through the maternal line[4,42,170]. This is not surprising because, in contrast to paternal, maternal conditions can impact the offspring during gametogenesis and through fetal life,

increasing phenotypic complexity and the overall inter/multigenerational effect. One prominent example is the increased vulnerability of the adult children and grandchildren of Holocaust survivors to psychological distress[171,172]. Additional studies suggest that maternal stress[4,39] and infection[95,173] increase the incidence of anxiety, depression, schizophrenia, autism, and attention deficit hyperactivity disorder (ADHD) in the progeny. Non-genetic inheritance can also be initiated by altered "internal" maternal environment, represented by maternal mutations that perturb fetal development, but are not transmitted genetically to the offspring. A recent example relevant to psychiatric conditions is maternal (but not paternal) mutations in tryptophan hydroxylase I (an enzyme responsible for serotonin synthesis in the periphery) resulting in increased risk for ADHD in the offspring[174]. Non-genetic multigenerational transmission of behavior through the female line has also been demonstrated in rodents[40,175].

Although these examples demonstrate the non-genetic transmission of complex behavioral traits via the maternal line across at least two generations and underscore its potential clinical importance in psychiatry, the idea that multifaceted offspring phenotypes can be the aggregate of the consecutive actions of germline and various somatic maternal effects has not been previously studied as a collective basis for complex diseases. Maternal intergenerational effects during pre/postnatal life are believed to be primarily mediated by hormonal and/or cytokine signaling pathways, emanating from the mother and altering the development of the fetal brain[8,176,177]. However, these "somatic" mechanisms are limited to first generation phenotypes, unless the maternal phenotype is self-perpetuating, a possibility that has not been explored comprehensively, presumably because its substantiation requires relatively complex embryo transfer and crossfostering experiments. Therefore the question remains whether multigenerational transmission via the maternal line is gametic, as

was found in a recent animal model[178], and/or somatic, mediated by an iterative process, similar in concept (but not in mechanism) to non-verbal cultural transmission/learning.

To answer this question, we dissected a composite maternally-transmitted psychiatric disease-like phenotype, resembling in dimensions[179] comorbid general anxiety and depression, to elementary behaviors/circuits and their corresponding transmission mechanisms. Depression and stress disorders are associated with reduced postsynaptic serotonin$_{1A}$ receptor (5-HT$_{1A}$R) levels, and we reported that 5-HT$_{1A}$R$^{+/-}$ dams not only exhibit anxiety-like (i.e. increased innate fear) and stress-reactivity traits, but also transmit them non-genetically to their F1 wild-type offspring[12,26,115]. Here we show that, the elementary traits of the composite phenotype are propagated beyond the F1 generation up to the F3 generation, and that, in contrast to Mendelian inheritance, the maternal traits are not inherited in unison, but rather transmitted by segregated somatic and gametic mechanisms, each with generation-dependent penetrance and sex specificity. We also demonstrate that somatic transmission can be iterative and results in a multigenerational phenotype without the involvement of the gametes. Whether iterative somatic or gametic, the transmission mechanisms converge on enhancer-like sequences within synaptic genes, implicating abnormal neuronal signaling in the manifestation of the offspring phenotype. Our data introduce segregated non-genetic transmission of traits as a mechanism that may explain some aspects of the non-Mendelian propagation of behaviors and dimensions of psychiatric diseases across generations.

4.2 Results

Traits of a psychiatric disease-like phenotype are propagated non-genetically across multiple generations in a mouse model

We reported behavioral abnormalities in the genetically wild type (WT) male offspring of 5-$HT_{1A}R^{+/-}$ heterozygote (H) and/or 5-$HT_{1A}R^{-/-}$ knockout (KO) parents[12]. These behaviors included anxiety-like behavior in the elevated plus maze and increased escape directed behavior in the forced swim test. Here we tested if these behaviors propagate to the next (F2) generation through the maternal line. F2 males, produced by mating F1 WT females with control WT males (Supplementary Fig. 4.1), exhibited reduced exploration of the fear-inducing open arm of the elevated plus maze (measured as reduced distance travelled in percent of total distance) (Fig. 4.1a). Total activity was unchanged, indicating that the reduced activity was specific for the open arm and consistent with innate anxiety-like behavior (Supplementary Fig. 4.2). Anxiety of F2 males were comparable to that of KO males (or H males, not shown but see[12]), demonstrating the robustness of the non-genetically transmitted behavior. To test if the anxiety-like behavior is propagated beyond the F2 generation, F3 males, with age-matched F1, as well as WT controls were generated. The anxiety phenotype was not transmitted to the F3 generation, while the F1 males, as in our previous study[12], exhibited the phenotype (Fig. 4.1b). Of note, to avoid genetic drift, the H line was backcrossed every 5-10 generations to WT mice obtained from large colonies kept at Taconic Biosciences (Germantown, NY), and then the H and WT lines were reestablished; non-genetic transmission of anxiety was reproduced following three such backcrosses. Return of open arm behavior in F3 males to the WT level is also consistent with a non-genetic, rather than spurious genetic, transmission. Next, we generated age-matched WT, H, F1, F2, and F3 females (males were used for

epigenetic studies) to study if sex influences transmission. Although F1 females showed a trend for anxiety, F2 and F3 females were indistinguishable from that of WT (Fig. 4.1c), indicating sex differences in the transfer and/or manifestation of anxiety.

We also reported that fetal exposure to the H maternal environment (by embryo transfer and consecutive crossfostering to WT mothers) is sufficient to produce anxiety-like behavior in the elevated plus maze in WT mice[12]. We refer to these mice as F1-S, to indicate their "somatic" "exposure" to the H mothers. In contrast, anxiety did not result when exposure to H maternal environment was limited to the period of gametogenesis (G) and early embryogenesis; up to the 2-4 cell stage (Fig. 4.1d). These F2-G offspring were generated by transferring F2 early embryos from from F1 donors to WT recipients. Overall, these data are most consistent with a model in which anxiety is transmitted via an iterative non-gametic mechanism from H mothers to the F1 generation, and then from the F1 females to the F2 males. Gestational LPS resulted in the similar propagation of anxiety across two generations (Supplementary Fig. 4.3), indicating that the phenomenon of iterative somatic programming of behavior may apply more broadly to adverse early-life experiences.

Figure 4.1. Non-genetic transmission of emotional behavioral traits, associated with maternal 5-HT$_{1A}$R deficit. a. Anxiety in the open arm of the EPM as % of total activity. F2 males, similar to KO males, exhibit increased avoidance of the open arm (group effect in distance traveled; ANOVA: $F_{2,35}$=13.28, P<10^{-4}; LSD *post hoc* ***p<0.005 compared to WT; N=11, 12, and 15 mice per group). All data are presented as mean ± s.e.m. **b.** F1, but not F3, males travel less distance in the open arm (group effect, ANOVA: $F_{2,54}$=6.46, P=0.003; LSD *post hoc* **p<0.01 compared to WT, N=17, 15, and 26 mice per group). **c.** Anxiety of female mice in the elevated plus maze (group effect, ANOVA: $F_{4,57}$=4.22, P=0.0046; N=12 WT, 13 H, 7 F1, 19 F2, and 11 F3). Significant anxiety in H (LSD *post hoc* *p<0.05) and a trend for anxiety in F1 females (^{+}p <0.10). **d.** Males derived by embryo transfer from WT germ-cells that were exposed to H (F2-G), as compared to and WT (WT-G) grand-maternal environment during gametogenesis exhibited no EPM anxiety (distance in open arm in % of total; *t*-test:, T=-0.202, p=0.841, N=16 and 20 animals per group). **e**. Distance traveled in the open field. F2 males, similar to KO males, exhibit reduced activity (ANOVA: $F_{2,47}$=13.47, P<10^{-4}; LSD *post hoc* ***p<0.005, N=17, 17, and 16). **f**. Total activity of F1 and F3 males in open field is not different from that of WT males. **g**. Female H and F3 offspring are hypoactive while F1 offspring exhibit a trend for hypoactivity in the open field (ANOVA: $F_{4,49}$=3.25, P=0.019; LSD *post hoc* **p<0.01, trend ^{+}p<0.10, N=13, 14, 7, 8, and 11). **h**. Hypoactivity is somatically programmed (WT-S vs. F1-S males: *t*-test: T=2.286, *p= 0.036, N=13 and 5 animals per group; WT-G vs. F2-G males: T=-1.279, p=0.208, N=30 and 15. **i**. Stress reactivity, measured as mobility in the forced swim test. F2 males have increased mobility (ANOVA: $F_{2,45}$=10.12, P<0.001; LSD *post hoc* ***p<0.005, N=17, 14, and 17). **j**. No stress phenotype in F1 and F3 males. **k**. Female F1 and F2 have reduced mobility (ANOVA: $F_{4,49}$=7.92, P<10^{-4}; LSD *post hoc* **p<0.01, ***p<0.005, N=14, 14, 7, 9, and 10). **l**. Increased stress reactivity of F2 males is gametically programmed (ANOVA: $F_{2,32}$=3.48, P=0.042; LSD *post hoc* *p<0.05, N=12, 8, and 15).

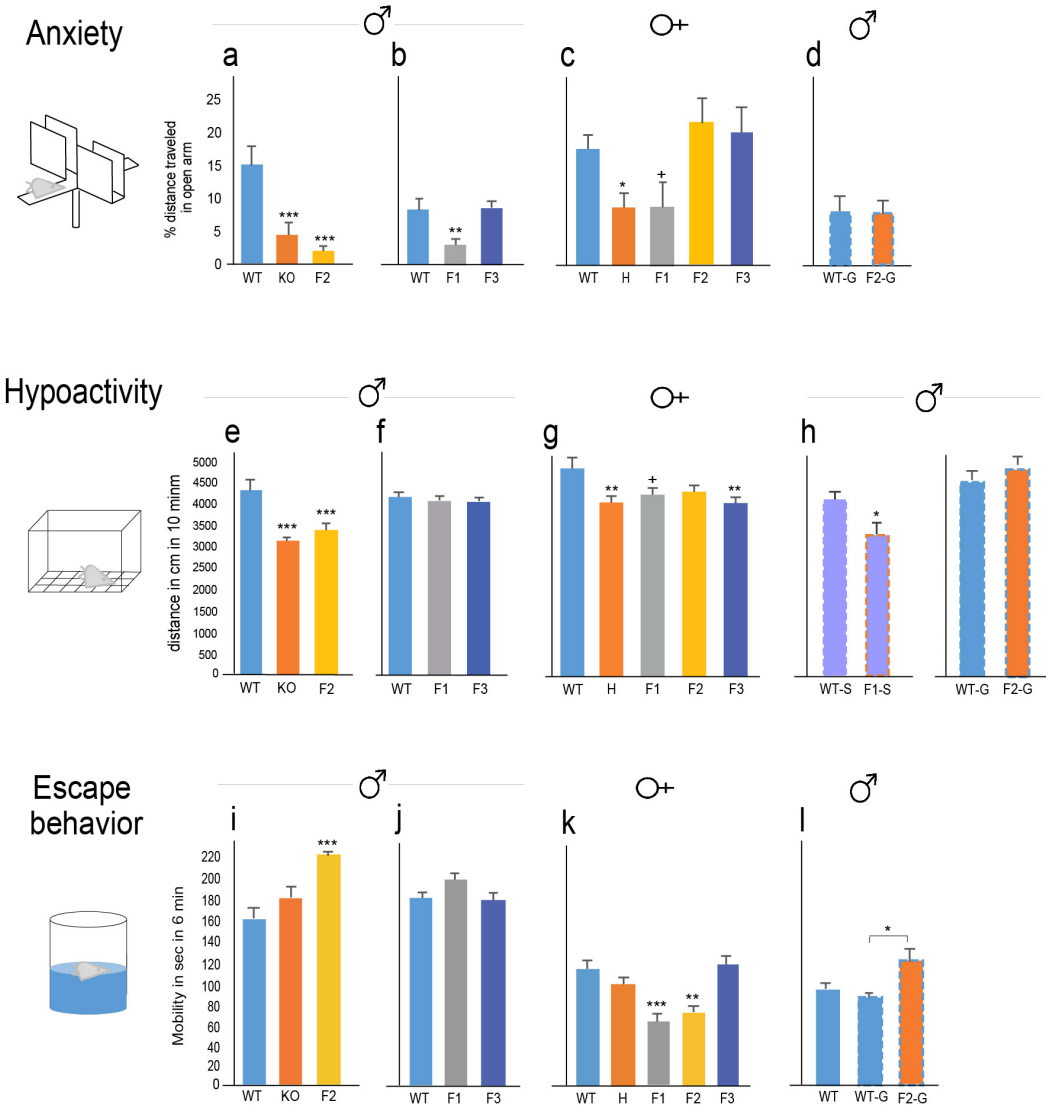
Anxiety
a
b
c
d
% distance traveled in open arm
WT KO F2
WT F1 F3
WT H F1 F2 F3
WT-G F2-G
Hypoactivity
e
f
g
h
distance in cm in 10 minm
WT KO F2
WT F1 F3
WT H F1 F2 F3
WT-S F1-S
WT-G F2-G
Escape behavior
i
j
k
l
Mobility in sec in 6 min
WT KO F2
WT F1 F3
WT H F1 F2 F3
WT WT-G F2-G

Although their overall activity was unchanged in the elevated plus maze, F2 males, similar to KO males, exhibited reduced locomotor activity in the larger and less stressful open field, (Fig. 4.1e). Albeit hypoactivity can be interpreted as a sign of anxiety, in a relatively low stress environment it may rather reflect reduced motivation. In contrast to F2 males, neither F1 nor F3 male offspring showed hypoactivity (Fig. 4.1f). F1 females showed only a trend for reduced activity, while F3, like H females, exhibited significant hypoactivity (Fig. 4.1g). Overall, these data indicate a modest phenotype with variable penetrance and sex specificity across three generations. Interestingly, while F1 males showed no phenotype, hypoactivity was robust in F1-S male offspring, indicating that somatic exposure through fetal life to the H maternal environment is sufficient to elicit hypoactivity (Fig. 4.1h), and that continuous exposure to the H environment during the first three weeks of postnatal life in F1 males may moderate the fetal programming effect (Fig. 4.1f). This could also explain the significant hypoactivity of F2 males (Fig. 4.1e) because they, like F1-S males, are raised by genetically WT mothers. Similar non-genetic transmission to grandchildren that skips the F1 generation (but which is propagated through the paternal line) has previously been suggested in human[180]. Based on the phenotype of F1-S and F2 males, we concluded that the hypoactivity trait is also transmitted by iterative somatic programming. Consistent with somatic transmission, the hypoactivity phenotype was not transmitted to F2-G males (Fig. 4.1h).

An additional variable receptor-associated non-genetic trait is reduced immobility/increased escape-directed behavior in the forced swim test[12]. Though traditionally interpreted as an “antidepressant”-like behavior, it more likely reflects increased reactivity to a stressful environment[12]. Although weak and below significance in F1 and KO males, the escape response was robust in F2 males (Fig. 4.1i,j). F1 and F2 females also exhibited a phenotype, but in the opposite direction,

indicating a sex difference (Fig. 4.1k). We have previously reported that the increased stress reactivity phenotype was absent in F1-S males[12] suggesting that the trait is not somatically transmitted. Here we show that F2-G males have increased stress reactivity (Fig. 4.1l). Lack of increased stress-responsiveness phenotype in F1 males, while present in both F2 and F2-G, supports the possibility that the H maternal fetal/early postnatal environment moderates the gametically programmed phenotype. The increased stress reactivity phenotype, seen in F2-G males was not apparent in the next generation (Supplementary Fig. 4.4), indicating that gametic programming of this phenotype is not strictly transgenerational.

Surprisingly, we also found that, while WT mice predictably responded to the 5-HT_{1A}R agonist 8-OH-DPAT with hypothermia, F2 and F3 males and females, similar to H or KO mice, had a partially/completely blunted drug response (Fig. 4.2a,b). The hypothermic response of the drug is mediated by 5-HT_{1A} presynaptic autoreceptors in the raphe nucleus[181]. Embryo transfer itself induced blunted hypothermic response (presumably because of the surgical/transplantation procedure(s) and the resultant effect on the mother and/or embryo), preventing us from determining the exact transmission mechanism of this particular trait (Supplementary Fig. 4.5). Nevertheless, this data suggests that an environmental perturbation can disturb thermoregulation, revealed by a receptor agonist. To directly test if the blunted drug response in F2 males was due to reduced receptor availability in the raphe, we measured receptor binding by using [^{3}H]-8-OH-DPAT. Indeed, F2 males had significantly reduced receptor binding in the dorsal raphe nucleus (Fig. 4.2c, Supplementary Fig. 4.6). F1 males, consistent with their drug-induced hypothermia response, had normal receptor binding. In F2 males, binding was also reduced in the hippocampus, expressing 5-HT_{1A} postsynaptic receptors, indicating that the non-genetic effect is not restricted to the presynaptic pool. However, levels of postsynaptic

receptors in two cortical areas were unchanged in F2 animals. Since *in situ* hybridization and RNA-Seq showed no receptor mRNA changes in F2 dorsal raphe and hippocampus (Fig. 4.2d), the absence of drug-induced hypothermia/5-HT_{1A}R-binding is not based on a direct transcriptional mechanism, but presumably on impaired translation and/or receptor trafficking/coupling, that can be either a 5-HT_{1A}R specific or a broader mechanism.

Schematic representation of the transmission of the four traits in Fig. 4.2e underscores the variable and sex specific penetrance of the associated behaviors, resulting in a high degree of pleiotropy in the pedigree. The anxiety trait is characterized by fully penetrant but limited intergenerational transmission, as it was present in both male and female F1 offspring, but only in F2 males and not in F3 animals. In contrast, the other traits seem to be partially penetrant but multigenerational because they were weak or not expressed in F1, expressed more robustly in F2 (especially in males), and were occasionally transmitted to the F3 generation. Importantly, the traits were transmitted and/or expressed independently from each other across the generations, even the somatically programmed anxiety and hypoactivity traits, indicating their segregated transmission.

Figure 4.2. Non-genetic transmission of trait associated with the lack of drug-induced hypothermia and summary of transmission of all traits. a. F2, F3, H, and KO males exhibit blunted response (repeated measures ANOVA: group, $F_{5,86}$=23.9, $P<10^{-6}$; dose, $F_{3,258}$=67.9, $P<10^{-6}$; and group x dose, $F_{15,258}$=29.7, $P<10^{-6}$; LSD *post hoc* ***p<0.005, relative to WT at the same dose; N=WT 19, F1 13, F2, 23, F3 12, H 15, KO 16). **b**. F2 and F3 females also exhibit blunted hypothermia response to drug (repeated measures ANOVA: group, $F_{2,24}$=13.7, P=0.0001; dose, $F_{3,72}$=17.1, $P<10^{-6}$; and group x dose, $F_{6,72}$=7.6, P=0.000002; LSD *post hoc* *p<0.05, ***p<0.005, relative to WT at the same dose, N=WT 6, F1 8, F2, 10, F3 11). **c.** F2 males have reduced [^{3}H]-8-OH-DPAT binding (ANOVA: DR, $F_{2,15}$= 6.37, P=0.01; CA, $F_{2,15}$=4.46, P=0.030; LSD *post hoc* *p<0.05, N=6 for all groups), but **d.** not receptor mRNA expression. DR, dorsal raphe; CA, CA subfields of the hippocampus; mPFC, medial prefrontal cortex; EntCtx, entorhinal cortex. **e**. Variable penetrance, gender specificity and different modes of transmission of traits generate a highly variable phenotype in the pedigree. Each quarter circle represents significant phenotype, while trend is represented by one eight of a circle.

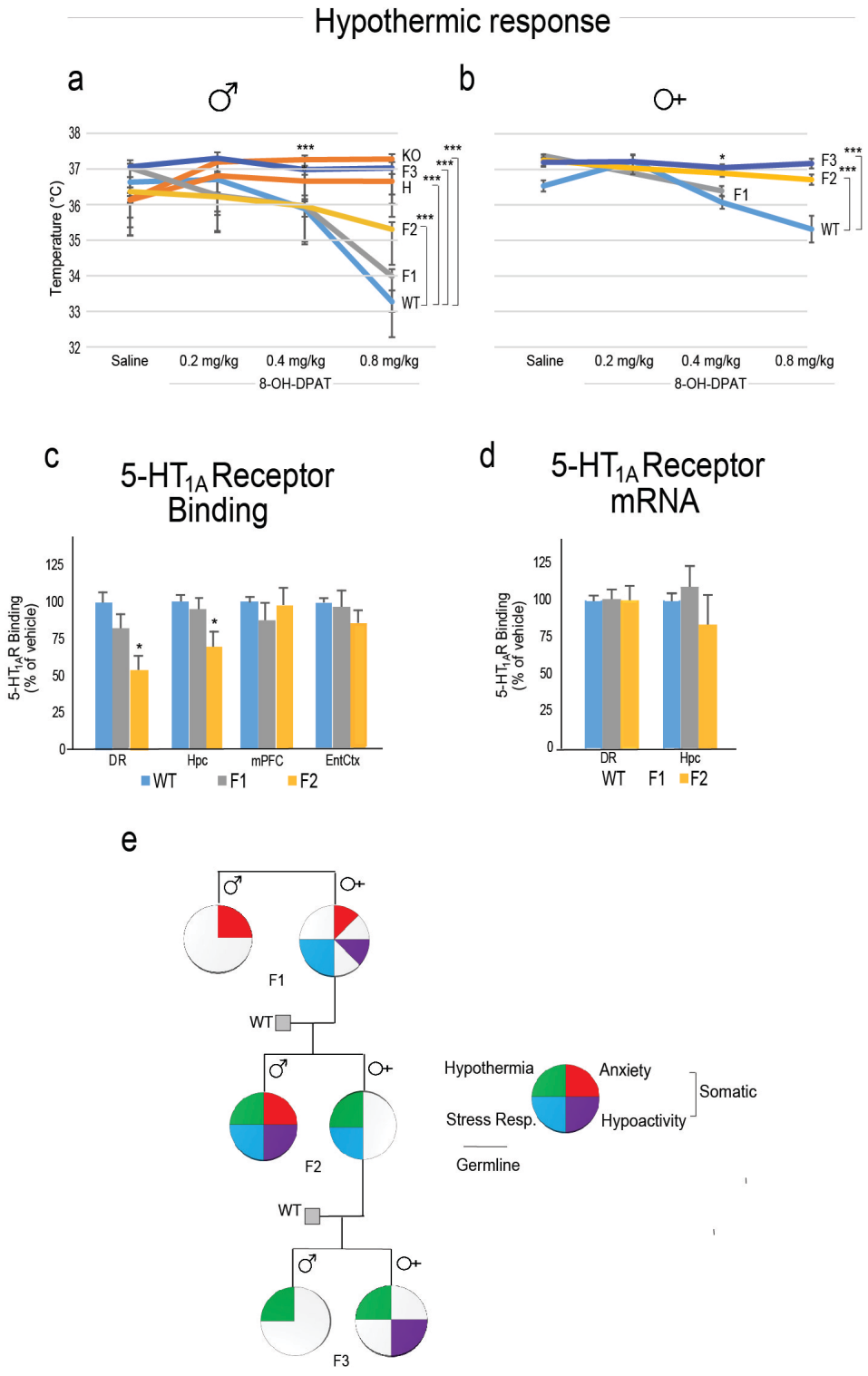
Hypothermic response
a
♂
b
♀+
Temperature (°C)
38
37
36
35
34
33
32
KO
F3
H
F2
F1
WT
***
Saline
0.2 mg/kg
0.4 mg/kg
0.8 mg/kg
8-OH-DPAT
c
5-HT1A Receptor Binding
5-HT1AR Binding (% of vehicle)
125
100
75
50
25
0
DR
Hpc
mPFC
EntCtx
WT
F1
F2
d
5-HT1A Receptor mRNA
e
F1
WT
F2
F3
Hypothermia
Anxiety
Stress Resp.
Hypoactivity
Somatic
Germline

Transmission of the somatic anxiety trait

To gain insight into the mechanism of somatic programming, we focused on the anxiety phenotype because it was robustly transmitted to F1 and F2 males. We hypothesized that transmission of this particular trait is linked to a brain-immune-brain pathway because a deficit in 5-HT_{1A}Rs is associated with depression and stress disorders[182], conditions that can lead to a proinflammatory status in both mother and offspring[183], and because immune activation in the offspring can result in abnormal emotional behaviors[184]. Indeed, F1 and F2 neonates (3 days old), similarly to 5-HT_{1A}R H or KO pups, had elevated peripheral neutrophil and monocyte counts, indicating a proinflammatory status (Fig. 4.3a). Flow analysis of neonatal spleens showed similar myeloid (neutrophil, monocyte, macrophage) changes, together with an elevated number of NK and T cells (Fig. 4.3b). Notably, a significant number of monocytes transmigrated to F1 and F2 brains suggesting their activated state (Fig. 4.3c). This finding may provide a plausible mechanism to explain the anxiety-like phenotype of F1 and F2 males because the presence of activated monocytes and their development to macrophages in brain parenchyma have been shown to cause anxiety-like behavior in mice[185].

Figure 4.3. Neonatal immune alterations in the F1 and F2 offspring of 5-HT_{1A}R deficient H mothers. a,b. Blood and spleen of F1 and F2 P3 neonates have increased number of neutrophils and monocytes (Blood, ANOVA: $F_{4,72}$=9.99, P=0.000002; LSD *post hoc* ***p<0.01, trend +p<0.10, N=15, 22, 15, 8, and 14; Spleen, ANOVA: $F_{2,12}$=6.53, P=0.012; LSD *post hoc* **p<0.01 and *p<0.05, N=6, 3, and 6). **c**. Brains of F1 and F2 P3 neonates have transmigrated monocytes (ANOVA: $F_{2,12}$= 10.07, P=0.0027; LSD *post hoc* ***p<0.005 and *p<0.05, N=6, 3, 6). Lower panels show the gating strategy.

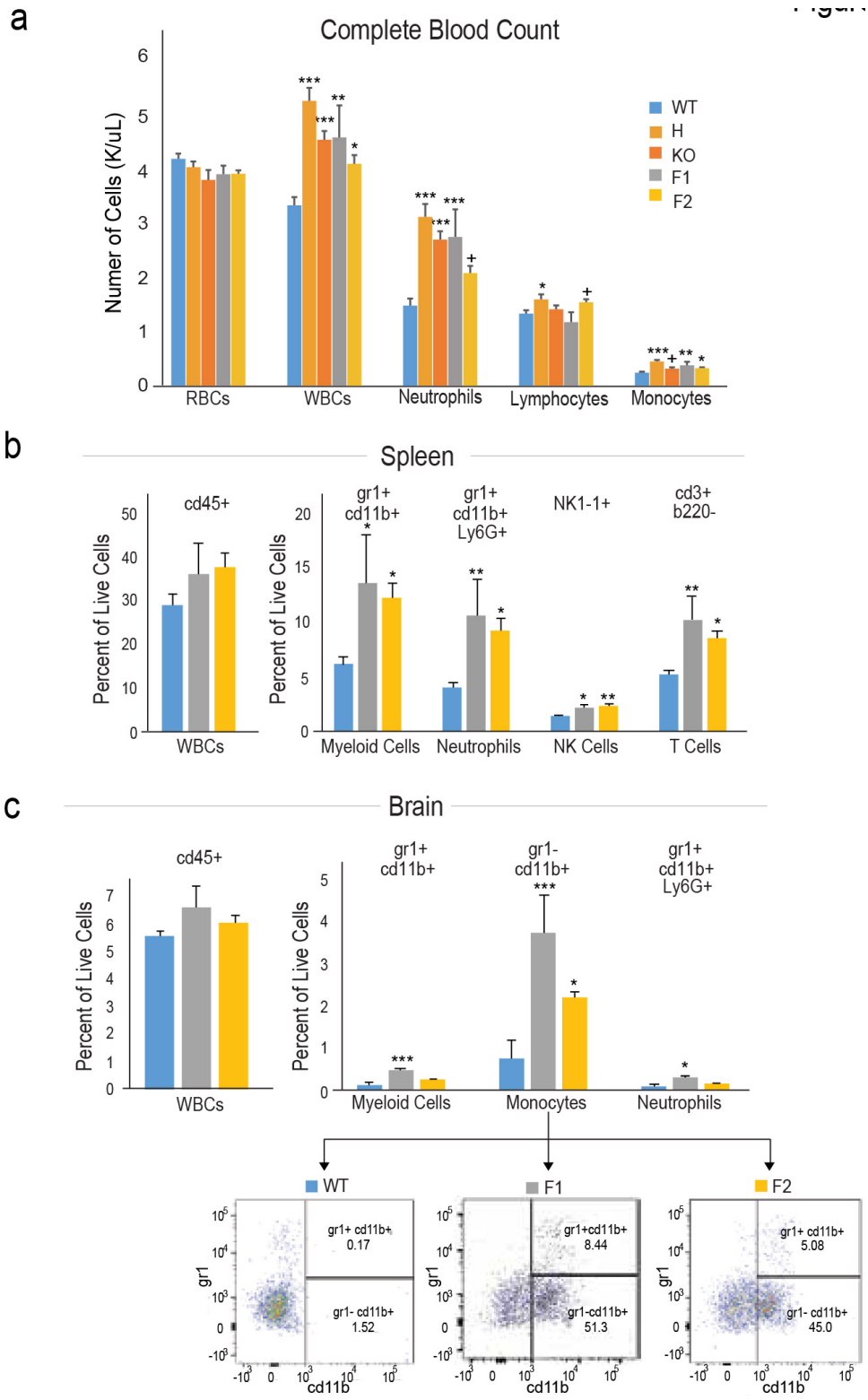
a
Complete Blood Count
Numer of Cells (K/uL)
WT
H
KO
F1
F2
RBCs
WBCs
Neutrophils
Lymphocytes
Monocytes
b
Spleen
Percent of Live Cells
cd45+
WBCs
gr1+ cd11b+
gr1+ cd11b+ Ly6G+
NK1-1+
cd3+ b220-
Myeloid Cells
Neutrophils
NK Cells
T Cells
c
Brain
Percent of Live Cells
cd45+
WBCs
gr1+ cd11b+
gr1- cd11b+
gr1+ cd11b+ Ly6G+
Myeloid Cells
Monocytes
Neutrophils
WT
F1
F2
gr1
cd11b
gr1+ cd11b+ 0.17
gr1- cd11b+ 1.52
gr1+cd11b+ 8.44
gr1-cd11b+ 51.3
gr1+ cd11b+ 5.08
gr1- cd11b+ 45.0

Neuronal transcriptome and metabolome changes in lipid signaling track the anxiety-like phenotype across generation

Anxiety in the elevated plus maze has been linked to dentate gyrus granule cells, in particular in the ventral hippocampus, in lesion, pharmacological and optogenetic studies[119,186]. Consistent with this association, we reported delayed granule cell maturation, specifically in the ventral hippocampus, in F1 offspring[12]. Delayed hippocampal development in turn may result in persistent transcriptional abnormalities that could contribute to the F1 adult anxiety phenotype.

The high density and clustering of granule cell bodies in the granule cell layer of the dentate gyrus and their separation from most other cell types (Fig. 4.4a) allowed us to microdissect them from cryosections and then assess gene expression, primarily in this cell type, as a function of prior maternal environment. RNA-Seq identified ~3,000 differentially expressed genes in both F1 and F2 adult males (FDR $q<0.01$), with a significant (2/3) overlap, consistent with the shared anxiety phenotype of these mice (Fig. 4.4a). Surprisingly, differentially expressed genes in both F1 and F2 (same direction of change) were primarily enriched in membrane lipid-related functions, including *sphingolipid,* glycerophospholipid (i.e. *phosphatidylethanolamine)* and *diacylglycerol metabolism* (Ingenuity Functional Analysis, $p=0.000037$, 0,00019, and 0.0045, respectively; Supplementary Table 4.1). Although anxiety is typically viewed as a dysfunction in neurotransmission, membrane lipids and their metabolizing enzymes are known to regulate membrane receptor function and intracellular signaling[78] and have been implicated in psychiatric diseases, including anxiety [187,188].

Figure 4.4. The impact of the receptor deficient maternal environment on the F1/F2 neuronal transcriptome and metabolome. **a**. A sagittal section of the ventral hippocampus highlighting the location of ventral granule cells, the source of mRNAs and metabolites. Granule cells can be isolated as a homogenous population because of their clustering in the granule cell layer (cells are highlighted by their green NeuN positive nuclei). Only a few cells positive for the glia marker GFAP present within the granule cell layer (blue cytoplasmic staining). Most of the differentially expressed F1 and F2 genes overlap. **b**. Ingenuity functional analysis of differentially expressed overlapping F1-F2 genes identified enrichment in functions related to sphingolipid metabolism (right), receptor signaling (center) and glycerophospholipids (left), indicated by solid grey circles, as a result of the maternal effect. Gene/protein nomenclature, see Supplementary Table 2. Lipid changes shown in panel c are also highlighted (blue box represents reduced and red increased levels in both F1/F2 granule cells, while red/blue boxes with staggered outline represent changes in either F1 or F2. Cer, ceramide; DAG, diacylglycerol; ETA, ethanolamine; GalCer, galactosylceramide, GM3, monosialodihexosylganglioside; MAG, monoacylglycerol; PA, phosphatidic acid; PE, phosphatidylethanolamine, PEp, plasmalogen phosphatidylethanolamine; PG, phosphatidylglycerol; PI, phosphatidylinositol; PS, phosphatidylserine; SM, sphingomyelin. **c.** Glycerophospholipid and sphingolipid composition of F1 and F2 ventral granule cells, relative to WT cells. BMP, bis(monoacylglycero)phosphate; LPI, lysophosphatidylinositol. N=6 per group. Columns represent total levels of lipid subclasses. Results are presented as mean and bars as s.e.m, *p≤ 0.05; and trend +p 0.1 by ANOVA with Bonferroni *posthoc* test (α: 0.0166). Blue and red boxes in insets represent significantly reduced and increased levels in specific lipid species within lipid subclasses; see also Supplementary Table 4 for the extent of changes.

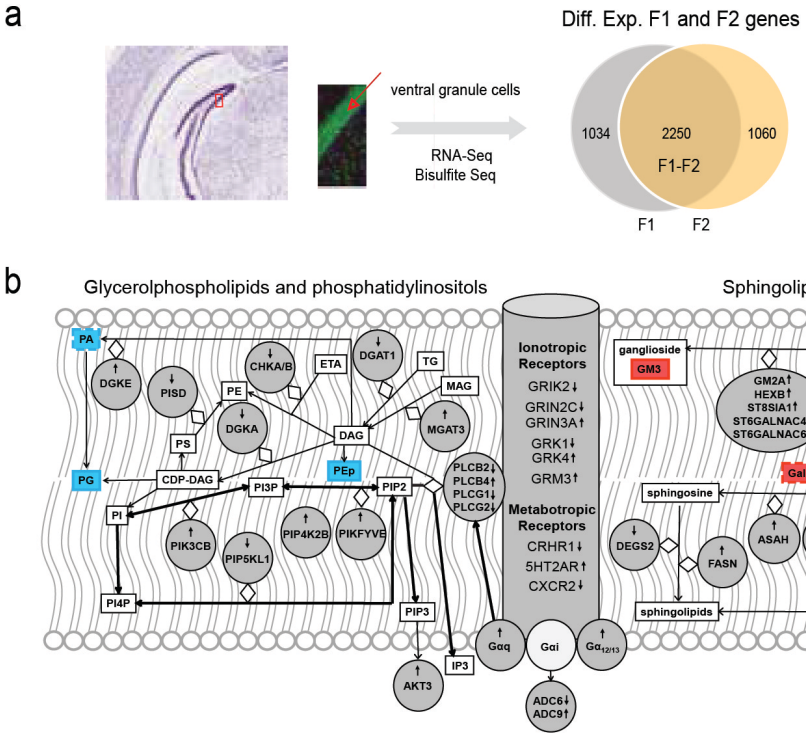
a
Diff. Exp. F1 and F2 genes
ventral granule cells
RNA-Seq
Bisulfite Seq
1034
2250
1060
F1-F2
F1
F2
b
Glycerolphospholipids and phosphatidylinositols
Sphingolipids
PA
DGKE
PISD
CHKA/B
ETA
DGAT1
TG
MAG
PE
DGKA
MGAT3
PS
DAG
PG
CDP-DAG
PI3P
PEp
PIP2
PI
PIK3CB
PIP5KL1
PIP4K2B
PIKFYVE
PI4P
PIP3
IP3
AKT3
PLCB2↓
PLCB4↑
PLCG1↓
PLCG2↓
Ionotropic Receptors
GRIK2↓
GRIN2C↓
GRIN3A↑
GRK1↓
GRK4↑
GRM3↑
Metabotropic Receptors
CRHR1↓
5HT2AR↑
CXCR2↓
Gαq
Gαi
Gα12/13
ADC6↓
ADC9↑
ganglioside
GM3
cerebroside
UGT8
GM2A↑
HEXB↑
ST8SIA1↑
ST6GALNAC4↑
ST6GALNAC6↑
CerP
CERK
GalCer
sphingosine
Cer
SMPD 1/2/3/4 ↑↓↑↓
NSMAF
DEGS2
FASN
ASAH
CLN3
sphingolipids
SM
c
WT
F1
F2
Relative lipid levels
5.5
5.0
1.5
1.0
0.5
0
PA
PEp
PG
BMP
LPI
SM
GalCer
GM3

Differentially expressed genes encoded key enzymes in sphingolipid metabolism (*Smpd1-4, Cerk, Nsmaf, Asah2, Degs2, Fasn, Scd and Cln3*; see genes with expression changes in Fig. 4.4b, and the list of all genes in Supplementary Table 4.2). Regulation was complex, with both up and downregulation, even within gene families (e.g. *Smpd1-4),* suggesting microdomain specific rather than global changes in corresponding lipids. Interestingly, we also found seven genes, all upregulated, that are involved in the metabolism of the glycosphingolipid GM3 (*UGT8, HexB*, *Gm2A*, *Large*, *St6galnac4, St6galnac6*, and *St8sia1*), suggesting a possible coregulation of these genes. Additional differentially expressed genes were associated with glycerophospholipid metabolism (*Dgke, Chka, Chkb, Pisd, Dgat1, Dgka, Mgat3, Mgll,* and *Pla2g3).* Moreover, Ingenuity analysis identified the canonical *Superpathway of Inositol Phosphate Compounds* (p=0.00014, see within the glycerophosholipid network in Fig. 4.4b), represented by a substantial number of genes (*Plcb2, Plcb4, Plcg1, Plcg2, Pik3cb, Pip4k2b, Pip5kl1, Pikfyve, Ppip5k1* and *2).* Phosphoinositol signaling is triggered by receptor activation, and we also found a number of differentially expressed genes encoding membrane receptors, including GPCRs and their downstream signaling molecules, such as Gαq, Gα12/13, adenylate cyclase 6/9, AKT3, embedded into the lipid networks (Supplementary Table 5.1, Fig. 4.4b). In sum, the transcriptome data suggest a broad dysfunction in lipid signaling in F1 and F2 ventral granule cells.

Next, we performed untargeted profiling of 3,156 metabolites in granule cells from individual WT and F1 mice that identified 21 differentially-expressed metabolites ($p \leq 0.05$), of which 11 were structurally-defined, and which confidently distinguished F1 from WT granule cells (Supplementary Fig. 4.6 and Supplementary Table 4.3). Remarkably, 9/11 of the structurally-defined molecules were recognized as membrane/bioactive lipids, comprised of 5 glycerophospholipids, phosphatidic acid

43:2, phosphatidylethanolamine 38:5, phosphatidylcholine 38:6, diacylglycerol 40:8 and 40:7, 3 lactosylceramides (differing in carbon chain length and degree of unsaturation), and 1 lipid metabolite (3-phosphoglyceroinositol), all diminished in F1 as compared to WT granule cells by 10-90%.

A more comprehensive targeted lipidomic study assessed the levels of a large number of lipid species in both F1 and F2 granule cells. Phosphatidic acid levels (measured in the range of 30-42 in total fatty acid chain length) again were reduced, but reached statistical significance only in F2 neurons (Fig. 4.4c, Supplementary Table 4.4), in line with the generally more robust behavioral phenotype of the F2 offspring (Fig. 4.2e). Phosphatidic acid is known to play major roles in regulating membrane trafficking and cellular signaling through interaction with effector proteins or by direct effects on lipid bilayers[189]. Levels of specific plasmalogen phosphatidylethanolamine (36:1 and 36:3) and phosphatidylglycerol (34:0, 34:1, 36:1) species were reduced in both F1 and F2 granule cells. Levels of some bis(monoacylglycerol)phosphate species were also generally reduced, but reached statistical significance only in F2. In contrast, different lysophosphatidylinositol species were increased in both F1 and F2 neurons. Although untargeted metabolomics suggested reductions in the levels of specific molecular species of phosphatidylcholine and diacylglycerol as well, these changes were not verified by targeted lipidomics (however, the diacylglycerol species identified in untargeted metabolomics were not analyzed in the targeted lipidomics experiment). In sum, levels of major glycerophospholipids were reduced in F1 and F2 neurons, in some cases only in F2 neurons (Fig. 4.4c). Regarding sphingolipids, sphingomyelin levels were reduced, but only in F2 neurons, while galactoceramide levels were increased in F1 GCs. However, levels of another glycosphingolipid, GM3, were increased in both F1 and F2 neurons and represented the largest changes in the F1/F2 lipidome (Fig. 4.4c). GM3 and other sphingolipids are enriched in raft-like

microdomains, specialized membrane domains where transmembrane signaling occurs through receptors and associated signaling components[78]. Taken together, the deficit in major glycerophospholipids and the surplus in some glycosphingolipids in F1/F2 granule cells suggest an imbalance between two major classes of membrane lipids. These data, in combination with the transcriptional findings, strongly implicate abnormal neuronal signaling through altered lipid metabolites and/or lipid-receptor interactions in F1 and F2 granule cells, possibly underlying the iterative anxiety phenotype.

DNA methylation changes in lipid and transmembrane signaling genes cosegregate with the anxiety phenotype

We have previously reported permanent DNA methylation changes in adult F1 ventral granule cells[26]. Here we profiled F1, F2, and F3 ventral granule cells from adult males and followed the segregation of methylation signatures with the anxiety phenotype across generations. Methylation at ~1.5 million CpGs and 6-7 million non-CpGs was measured genome-wide by bisulfite sequencing[61]. Differentially methylated sites ($\geq$15%, q<0.01) tended to be clustered ($\geq$4), forming differentially methylated regions (DMRs, average size 200-300bp). DMRs were present in all F1, F2 and F3 neurons (Fig. 4.5a). The change in methylation occurred at CpGs (>95%), either hypomethylation or hypermethylation (55% and 45%), and was unidirectional in all differentially methylated sites at 87% of the DMRs. Thus the methylation landscape in F1-F3 ventral granule cells was characterized by mostly uniformly hypomethylated or hypermethylated DMRs distributed across the genome.

Most DMRs (>80%) mapped to intragenic sequences and therefore could be assigned to specific genes. We hypothesized that DMRs and their genes are associated with anxiety if present in both F1 and F2 granule cells, while the set of DMR genes present in all F1, F2 and F3 neurons may lack key differentially methylated genes

required for the development of anxiety (F3 males do not exhibit anxiety). Approximately half of the 659 F2 DMRs was also present in F1 neurons, of which the majority was absent in F3 neurons, demonstrating the existence of a substantial pool of genes that meets the criteria for association (Fig. 4.5a). As Fig. 4.5b shows, functional analysis of DMRs present in both F1 and F2 neurons identified *sphingolipid/ceramide*-related processes (Supplementary Table 4.5) and included genes previously identified by the transcriptome analysis (*Cerk, Smpd3, St8sia1, Dgke*). In contrast, these functions were not identified by DMRs present across all the F1-F3 neurons. These data indicate the cosegregation of differentially methylated membrane lipid genes with anxiety and further strengthen the association between these genes and the phenotype, first suggested by the transcriptome and lipidomics studies.

Besides membrane lipid related functions, F1-F2 shared DMR genes were also enriched in neurotransmission and synaptic functions (Supplementary Table 4.5). Furthermore, the F1-F2 DMR gene dataset also identified *anxiety* (p=0.00002), the very trait that was transmitted to the F1 and then to the F2 generation, as the top associated behavior (Supplementary Table 4.5). Of note, the transcriptome analysis did not recognize these networks, suggesting that although differentially methylated in a significant number, *neurotransmission/synaptic function* and *anxiety* related genes are not differentially expressed in high enough numbers to produce statistically significant enrichment. The broader functional categories identified by differential DNA methylation, relative to differential expression, could be due to persistent hypo/hypermethylation from early life at genes that regulate synaptic development but which are no longer required in mature neurons, or simply to subtle or isoform specific changes that were not detected in our transcriptome studies.

Figure 4.5. Impact of the receptor deficient maternal environment on the F1/F2 neuronal methylome. **a**. Overlap of genes with differentially methylated regions (DMRs) in F1, F2 and F3 ventral granule cells. **b**. Overrepresentation of DMR genes in F1 and F2, but not in all F1, F2 and F3 granule cells, in the process of *sphingolipid/ceramide*-related processes (see list of genes in Supplementary Table 5.5). The short and long columns indicate the lowest and highest significance levels for these processes. **c.** Similar changes in DNA methylation and gene expression in F1 and F2 neurons. F1 and F2 overlapping differentially methylated and expressed genes are distributed to four quadrants, according to their expression (up/downregulated) and average methylation at differentially methylated sites within DMRs (hyper/hypomethylated; +/-). Color of genes is rendered according to their differential expression/differential methylation values in F1 (blue, up/hypo quadrant; purple: down/hypo; green, down/hyper; and red, up/hyper), while their actual positions reflect values in F2. Most genes in a quadrant are of a similar color, indicating similar expression and methylation changes in F1 and F2 neurons. **d.** F1/F2 overlapping DMRs are overrepresented at exonic regions. **e.** Selected DMRs from *Cerk* and *Dgke* (Fig. 5.4b) have no promoter, but significant enhancer-like, effects on the EF1 promoter, similar to that of the CMV enhancer, in transfected 293 cells (ANOVA: $F_{4.49}$=163.16, $P<10^{-4}$; LSD *post hoc* ***$p<0.005$ for both CERK and DGKE, in addition to the positive control CMV). An intergenic *Drosophila* sequence has neither promoter nor enhancer activity.

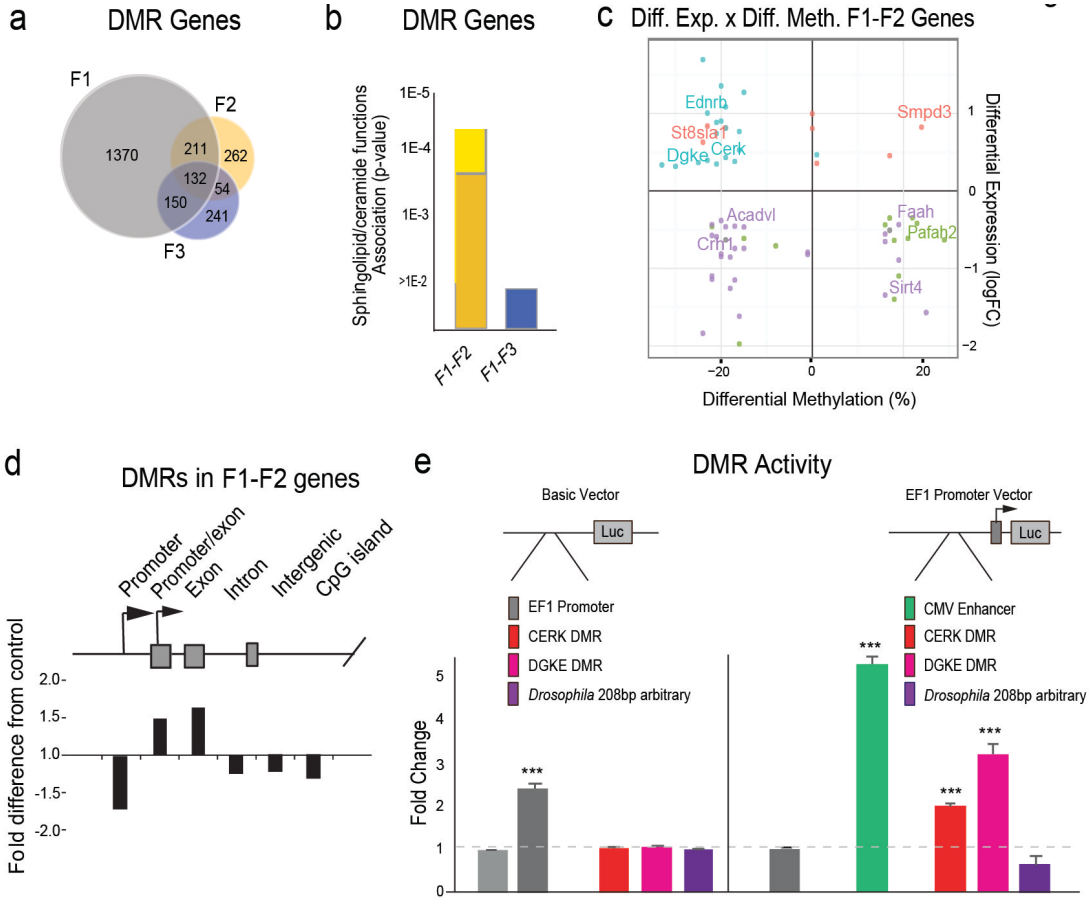
a
DMR Genes
F1
F2
F3
1370
211
262
132
54
150
241
b
DMR Genes
Sphingolipid/ceramide functions Association (p-value)
1E-5
1E-4
1E-3
>1E-2
F1-F2
F1-F3
c
Diff. Exp. x Diff. Meth. F1-F2 Genes
Ednrb
St8sia1
Dgke
Cerk
Smpd3
Acadvl
Cnr1
Faah
Pafah2
Sirt4
Differential Expression (logFC)
Differential Methylation (%)
d
DMRs in F1-F2 genes
Promoter
Promoter/exon
Exon
Intron
Intergenic
CpG island
Fold difference from control
e
DMR Activity
Basic Vector
EF1 Promoter Vector
Luc
EF1 Promoter
CERK DMR
DGKE DMR
Drosophila 208bp arbitrary
CMV Enhancer
Fold Change

Next, we intersected the DNA methylation and gene expression data that again identified *sphingolipid* and *glycerophospholipid* related functions (Supplementary Table 4.6). There was no direct correlation between methylation and expression changes (Fig. 4.5c); not an unexpected finding, given the multitude of possible effects of intragenic methylation on gene expression. However, these data showed that the direction of expression changes was identical and the overall methylation changes largely the same in F1 and F2 neurons, indicating that programming of the transcriptome and methylome, similar to that of anxiety, is iterative.

Anxiety associated DMRs map to exons and have enhancer-like activity

Since most DMRs were intragenic, assignment of DMRs to specific gene features may shed light on their function. As Fig. 4.5d shows, F1-F2 shared DMRs were enriched in exons, including those that map to alternative promoters, but excluded from proximal promoters, introns, and intergenic areas. DMRs from *Cerk* and *Dgke*, two representative DMRs (~200 bp), from differentially expressed and methylated genes associated with lipid signaling (Fig. 4.4b), were selected for further studies. They reside within H3K4me3/H3K27ac/H3K9ac and H3K27ac/H3K4me1 peaks, respectively, in both neuronal (cerebellar neurons) and non-neuronal cells (ENCODE[190]). These chromatin signatures are typically associated with promoter and enhancer sequences. In a luciferase reporter assay, these DMRs exhibited no promoter activity, while enhancing the activity of the EF1 promoter in 293 cells (Fig. 4.5e). An arbitrary 208bp intergenic *drosophila* sequence had neither promoter nor enhancer activity. These data suggest that at least some of the DMRs represent regulatory elements associated with enhancers and that their enhancer-like activity is not limited to neurons and could contribute to gene regulation in multiple tissues.

DNA Methylation at Gametically Programmed Genes

Altered stress reactivity of the F2 offspring in the forced swim test is gametically transmitted through the maternal line (Fig. 4.1i,l). Since the genome of female primordial germ cells (PGCs), following an almost complete demethylation by E12.5-13.5, is gradually remethylated reaching partial methylation in oocytes, we tested if this process is altered in PGCs exposed to the H grandmaternal environment. We isolated E18.5 F2 and WT PGCs from pregnant H and WT mothers by FACS[191] and identified 220 gametically programmed DMRs (Fig. 4.6a). Methylation at differentially methylated sites within these DMRs was partial in WT PGCs, while mostly unmethylated in F2 PGCs, with some sites methylated completely (Fig. 4.6b), suggesting dysregulated remethylation/reprogramming in female PGCs at specific regions. DMR associated genes were enriched in few functions, most prominently in *imprinting* (p=0.00034) and *fertility* (p=0.00042), encompassing some of the same genes (Supplementary Table 4.7). These DMR genes regulate proliferation, growth and differentiation and imprinted genes are known to be essential in early embryonic growth and development[192]. Although CpG islands were underrepresented in PGC DMRs, 3 out of the 5 within imprinted loci (*Airn/Igfr2, Dio,* and *Blcap/Nnat*) were mapped to islands, which however were not the imprinted control regions and were not imprinted.

Next we asked if PGC DMRs survive reprogramming in the early F2 embryo and propagate to somatic cells. Methylation at CpG sites that were differentially methylated in PGCs was similar (FDR >0.05, <15%) between F2 and WT and F2-G and WT-G granule cells. Moreover, methylation at these sites had the typical bimodal distribution in neurons, independent of whether the offspring were the granddaughter of WT or H mothers (Fig. 4.6b). These data indicate that the initial methylation differences at PGC DMRs were later corrected.

Since PGC DMRs, by altering embryonic development, may produce secondary neuronal DMRs[193] or perhaps neuronal DMRs are tagged in the gametes by an epigenetic mark other than DNA methylation, we mapped gametically programmed DMRs in hippocampal granule cells. We reasoned that such DMRs (referred to as neuronal gametically programmed DMRs) should be present in the brain of two independent sets of animals with H grandmaternal ancestry, F2 and F2-G, both exhibiting increased stress reactivity (Fig. 4.1i,l). F2 mice, derived by normal breeding, carry both somatic and gametically programmed DMRs, while F2-G animals, obtained through embryo transfer, harbor gametically programmed DMRs and perhaps DMRs that are produced by the embryo transfer procedure[194]. By overlapping these two DMR sets, one can identify common DMRs that are directly or indirectly related to gametic programming, while eliminating obvious confounds. This approach identified 17 overlapping DMRs (FDR $q<0.05$, overlap Fisher exact test $p=0.0065$, odds ratio 4.11) representing 21 genes, none of which matched PGC DMRs, as expected (Fig. 4.6a). These data also suggest that the much larger group of F2 DMRs represents mostly non-gametic (i.e. somatic) DMRs (see also the large F1-F2 overlap for iterative DMRs, Fig. 4.5a).

Differentially methylated CpGs within neuronal gametically programmed DMRs were mostly hypomethylated (80%)(Fig. 4.6c). Though the low number of gametic DMRs prevented us to analyze their association with genomic features, we found that three representatives of neuronal gametic DMRs, located at distal promoter/exon sequences, all enhanced the activity of the EF1 promoter in luciferase assays (Fig. 4.6d), indicating that, similar to somatic DMRs, they represent regulatory elements, presumably enhancers.

Figure 4.6. **Characteristics of gametically-programmed DMRs**. **A**. PGC DMRs are unrelated to neuronal gametically programmed DMRs, which are defined as overlapping DMRs in F2 and F2-G neurons. **b**. Distribution of methylation levels at individual CpG sites, differentially methylated in F2 PGCs, in PGCs and hippocampal granule cells. **c**. Methylation changes at neuronal gametically programmed sites are predominantly hypomethylation. **d**. Neuronal gametically programmed DMRs have no promoter, but significant enhancer, activity (ANOVA: $F_{5,57}$=170.82, P<10^{-4}; LSD *post hoc* ***p<0.005 for KIF19, SRCIN1, and MGMT).

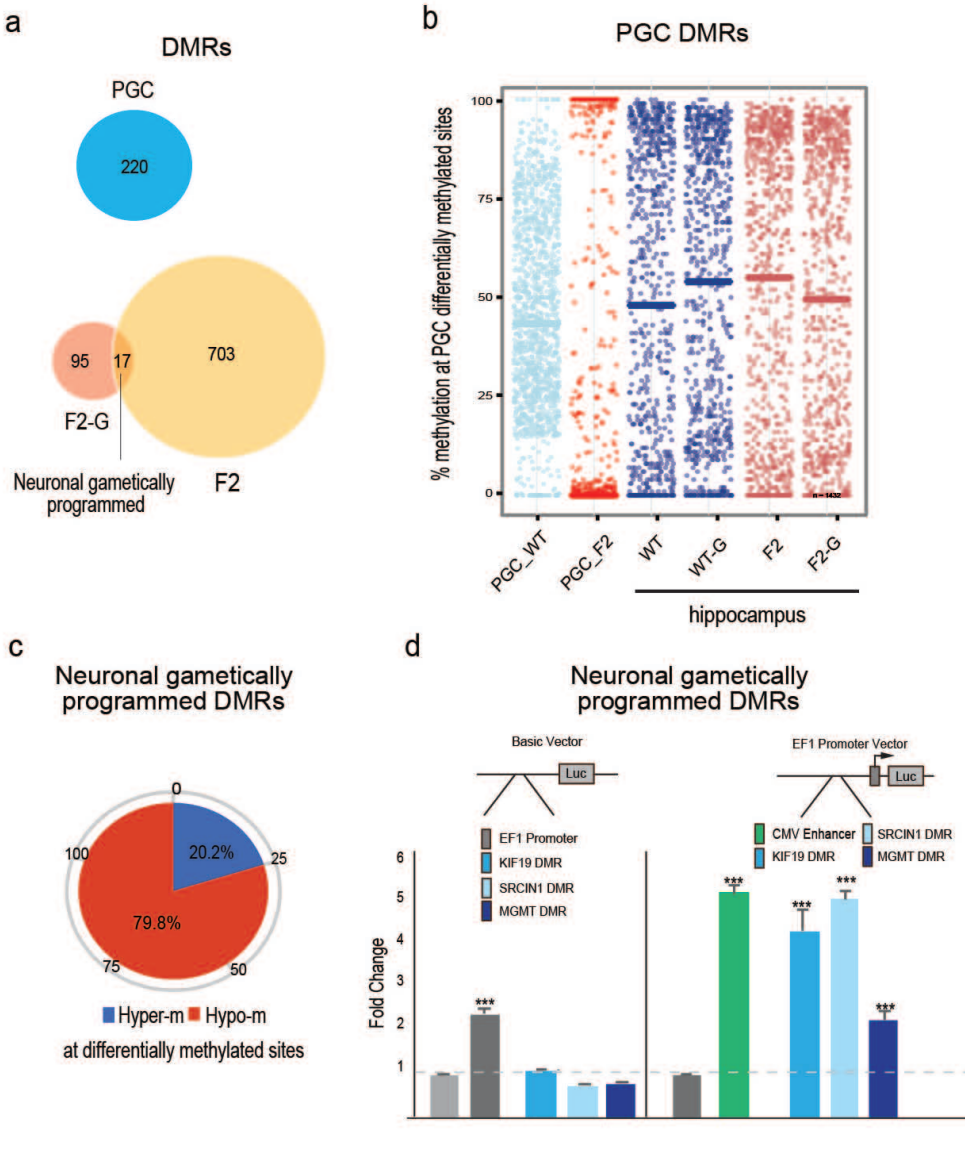
a
DMRs
PGC
220
95
17
703
F2-G
Neuronal gametically programmed
F2
b
PGC DMRs
% methylation at PGC differentially methylated sites
100
75
50
25
0
PGC_WT
PGC_F2
WT
WT-G
F2
F2-G
hippocampus
c
Neuronal gametically programmed DMRs
0
25
50
75
100
20.2%
79.8%
Hyper-m
Hypo-m
at differentially methylated sites
d
Neuronal gametically programmed DMRs
Basic Vector
Luc
EF1 Promoter
KIF19 DMR
SRCIN1 DMR
MGMT DMR
EF1 Promoter Vector
Luc
CMV Enhancer
SRCIN1 DMR
KIF19 DMR
MGMT DMR
Fold Change
1
2
3
4
5
6
***

Unlike somatic, neuronal gametically programmed DMR genes were not enriched in membrane lipid signaling and neurotransmission related functions. Rather, 9/21 of these genes mapped directly to synaptic morphology-related functions and/or neuropsychiatric risk genes. Specifically, *Disc1* and *Srcin1* are involved in spine maintenance and morphogenesis, respectively (Ingenuity p=0.00085 and 0.0034); *Itga6* in neurite morphogenesis (p=0.00085); *Gng7* and *Soc5* in transmembrane signaling (p=0.0084 and p=0.025), *Kif19* in microtubule dynamics (p=0.00338); while, *Disc1*, *Pias4*, *Rsrc1* and *Frem* have been implicated in autism, schizophrenia and neurological disorders. Intriguingly, *Disc1* was also associated with *adaptive behavior* and *immobility in the forced swim test*[195,196] (p=0.00069 and p=0.0014), the very trait identified as gametically programmed. However, escape directed behavior in the forced swim test has been linked to multiple brain regions, including the prefrontal cortex, raphe and the hippocampus; thus it will be important to test if the hippocampal gametically programmed DMRs are also present in other relevant brain regions.

4.3 Discussion

Here we address a central problem in the epidemiology and diagnosis of psychiatric disorders; particularly, how their symptoms are propagated across generations, even in the absence of plausible genetic factors[197,198], and why they may present differently in individuals, even those in the same family tree. For example, family members can have various combinations of anxiety, depression, bipolar disease, and schizophrenia symptoms, complicating diagnosis and treatment.

While the behavioral manifestations associated with a genetic risk factor are transmitted together, here we show that the individual traits of a complex psychiatric disease-like phenotype are propagated across multiple generations by parallel non-genetic mechanisms. The “anxiety” and “hypoactivity” traits were transmitted by a

somatic, while the "increased stress-reactivity" trait was transmitted by a gametic, mechanism. In humans, these traits transcend diagnostic categories and are found in comorbid generalized anxiety and depression disorders and other psychiatric conditions. Since the individual traits/pathways each have their own generation-dependent penetrance and gender specificity, the resulting cumulative phenotype is pleiotropic. Pleiotropy, which refers to the ability of a single gene or factor to produce multiple phenotypic outcomes[199], is a commonly occurring phenomenon in psychiatric disorders[200], complicating diagnosis and treatment. It is typically assumed that this phenomenon in the context of genetic disease arises from individual differences in vulnerability to the various effects of the causative gene. However, the work presented here reveals that pleiotropy can be produced by the variable distribution and segregated transmission of behavioral traits.

Although some of the maternal traits propagated to the F2 and even to the F3 generation (i.e. hypoactivity), contrary to our expectation, this was not based on a true transgenerational mechanism, but rather on the reiteration of single generational somatic transmission, referred here to as iterative somatic transmission. The iterative propagation of anxiety is most compatible with a model in which, the inflammatory state is acquired by F1 males from their H mothers and then by the F2 males from their F1 mothers. The increased number of monocytes and their transmigration to the brain parenchyma in F1 and F2 males could be central to the transmission mechanism and the resulting anxiety phenotype. Monocytes develop to macrophages in the brain and activate resident microglia, as reported in various animal models of psychiatric disorders[185,201,202]. Because microglia participate in programmed cell death, survival, axon remodeling, pruning, and synaptogenesis in various brain regions, including the hippocampus[203], it is reasonable to hypothesize that the increased number of peripheral monocytes and their transmigration to the brain contributes, via microglia

activation, to the development of anxiety-like phenotype in the F1 and F2 male offspring. The hypoactivity trait also followed a somatic programming scheme, but its manifestation was highly variable across generations, which contributed to the pleiotropy.

The somatically programmed behaviors, in particular the anxiety-like behavior that can be linked to the ventral hippocampus, were accompanied by DNA methylation changes that converged on the functional networks of lipid signaling and synaptic/neurotransmission in hippocampal granule cells. Corresponding transcriptional and lipidomics changes further argue for the role of the lipid signaling network in somatic programming. However, complexity and high redundancy in the regulation of lipid metabolic pathways[204] complicate linking the specific transcriptional changes directly to the lipid alterations. Nevertheless, studies implicate membrane lipids and their metabolites in psychiatric diseases, including anxiety[187,188].

Embryo transfer experiments showed that the increased stress reactivity trait was propagated to the F2 generation by gametic transmission in our model. This indicates that gametically programmed information survives reprogramming in the early embryo and persists into adulthood. However, it was erased in the F3 germline, therefore the transmission is not strictly transgenerational. Although we identified gametically programmed DMRs in both F2 PGCs and adult hippocampal neurons, their dissimilarity makes it difficult to link them causally. However, it has recently been suggested that primary PGC epigenetic signatures may initiate a cascade of developmental changes in the early zygote and later development, leading to secondary epigenetic signatures in adult tissues[205]. Indeed, PGC DMRs were associated with imprinted genes that are known to be essential in early growth and development[192]. Alternatively, epigenetic changes other than alterations in DNA methylation could be formed in PGCs at neuronal DMR regions that later, during

neuronal development, acquire the adult neuronal DNA methylation signatures. Whether derived from PGC DMRs indirectly or from other "primed" regions, neuronal gametically programmed DMRs map to genes whose dysfunctions can be linked to the altered stress reactive phenotype.

In summary, our data introduce segregated non-genetic transmission of traits as a mechanism that may explain the non-Mendelian propagation and pleiotropy of behavioral/psychiatric phenotypes across generations. A transmission-pathway based concept can complement the current gene-centered view of inheritance in psychiatric disease, as well as facilitate the development of animal models with better construct validity[206] and novel therapeutic approaches.

4.4 Methods

Mice

Animal experiments were carried out in accordance with the Weill Cornell Medical College Institutional Animal Care and Use Committee guidelines. All mice were group housed up to five per cage with 12-h light/dark cycle with lights on at 6 a.m. Food and water were available ad libitum. 5-HT_{1A}R KO mice were originally generated on the 129SvEv background[207] and backcrossed to the Swiss–Webster (SW, Taconic Biosciences, Germantown, NY) background >10 times. We used the outbred SW background (a strain often used in behavioral experiments), to avoid the possible contribution of homozygous genetic variants in inbred strains to behavioral phenotypes[116]. Of note, the H line was backcrossed every 5-10 generations to WT mice obtained from large colonies kept at Taconic Biosciences (Germantown, NY), and the H and WT lines were reestablished, to avoid genetic drift. The F1 generation consisted of littermate *5-$HT_{1A}R^{+/+}$* (F1-wild-type; F1), *5-$HT_{1A}R^{+/-}$* (H, heterozygote) and *5-$HT_{1A}R^{-/-}$* (knockout; KO) mice (generated as previously described[12,207]), all

exposed to the receptor deficient H maternal environment. F1 females were crossed with WT males to generate F2 offspring (all WT). F2 females were crossed with WT males to generate F3 offspring. A separate WT lineage provided control WT offspring exposed to normal, WT gestational environment. Typically, 1-2 animals were randomly selected from litters; thus at least 3 litters were used per group. Since many groups consisted of more than 10 animals, the number of litters typically exceeded 6-8.

Behavioral Procedures

All tests were conducted using offspring aged 8-12 weeks. During all behavioral tests the investigators who performed the tests were blind to the genotype and treatment of the animals. Moreover, all behavioral tests are fully automatized with no human input on data collection. Behavioral tests were conducted during the light on phase, between 10am and 4pm. Mice were first tested in open field for overall activity, followed by elevated plus maze and forced swim test, followed by the drug-induced hypothermia test. At least 24 hours rest was allotted between different tests. All tests were conducted between 9 a.m and 6 p.m (i.e. during the light cycle). Offspring were selected from $\geq$5 litters. The elevated plus maze[12] was performed using a cross maze with 12 x 2 inch arms at dim light (50 lux). Animals were introduced to the middle portion of the maze facing an open arm and allowed to freely explore for 10 minutes. Time spent and distance traveled in the open and closed arms were measured by a video-tracking system (Noldus Information Technology, Wageningen, The Netherlands.). The open-field test[12] used a 15 x 21 inch black box, divided into 12 even-sized (4 x 3 inch) rectangles. The time spent in and distance traveled in the two rectangles at the center of the field at 150 lux were recorded by the video-tracking system to evaluate anxiety, and data was presented as a percentage of total distance traveled. In the forced swim test[12], mice were placed into a clear, water-

filled cylinder (diameter, 20.3 cm; depth, 10 cm), essentially as described by Porsolt at al.[208]. In this test, immobility of the mice is scored by an observer in two minute bins for a total of six minutes. On test days, animals were transported to the dimly illuminated behavioral laboratory and left undisturbed for at least 1 hr before testing.

Hypothermic Response

Hypothermic response[209] was assessed at different dosages of 8-OH-DPAT over the course of four days because the response does not show habituation. Animals were individually housed 1-2 hours prior to the start of the experiment. On Day 1, animals were injected (i.p.) with 100uL saline. After 30 minutes, rectal temperature was measured. On Day 2-4, mice were administered 0.8mg/kg, 0.4mg/kg, and 0.2mg/kg 8-OH-DPAT, respectively, prior to taking temperature measurements.

Embryo Transfer

Two types of embryo transfers were performed[12]. SW WT embryos (E0.5-E2.5) were implanted into pseudopregnant 5-$HT_{1A}R^{+/-}$ females (7-9 weeks old) to generate F1-S (somatically-exposed) offspring. To generate F2-G (gametically-exposed) offspring, embryos (E0.5-E2.5), derived from female PCGs/oocytes exposed to the 5-$HT_{1A}R^{+/-}$ grandmaternal environment (within the WT F1 female fetus) were implanted into pseudopregnant SW WT females (7-9 weeks old).

5-HT_{1A}R Receptor Binding/*5-HT1AR* Expression

Tissue preparation, *in situ* hybridization, and receptor autoradiography procedures were performed as previously described[209]. Briefly, mice were killed by pentobarbital overdose and brains rapidly removed, frozen on dry ice and stored at -80ºC. Coronal tissue sections (14µm) were cut using a microtome-cryostat (HM500-OM, Microm, Walldorf, Germany), thaw-mounted onto 3-aminopropyltriethoxysilane (Sigma-Aldrich)-coated slides and kept at -20ºC until use. For 5-HT_{1A}R mRNA, antisense oligoprobe was complementary to bases 1780-1827 (GenBank accession

NM_008308). Oligonucleotide was labeled (2 pmol) at the 3'-end with [^{33}P]-dATP (>2500 Ci·mmol^{-1}; DuPont-NEN, Boston, MA) using terminal deoxynucleotidyltransferase (TdT, Calbiochem, La Jolla, CA). The autoradiographic binding assays for 5-HT$_{1A}$R was performed using [^{3}H]-8-OH-DPAT (233 Ci·mmol^{-1}), Autoradiograms were analyzed and relative optical densities (ROD) were obtained using a computer assisted image analyzer (MCID; Mering, Germany). The system was calibrated with ^{3}H-microscales standards to obtain fmol/mg protein equivalents from ROD data. The slide background and non-specific densities were subtracted. ROD were evaluated in two or three adjacent sections by duplicate of each mouse and averaged to obtain individual values.

Complete Blood Count (CBC)

All neonatal CBCs were performed on pups between 3-4 days old. Blood was collected from the trunk via decapitation. Total red blood cells, white blood cells, neutrophils, lymphocytes, monocytes, eosinophils, and basophils were quantified by both automated (IDEXX ProCyte Dx Hematology Analyzer, Westbrook, ME) and manual counts.

Flow Cytometry

The presence of immune subsets in spleens and brains was assessed in 3-4 day old pups by flow cytometry. All pups were anesthetized and perfused with saline in order to flush out circulating blood cells from the organs. Spleen cells were collected by homogenization and filtering through a 40μm cell strainer into FACS buffer (PBS with 0.5% BSA). Brains were harvested in FACS buffer followed by three sequential digestion steps in RPMI + 25mM HEPES + Collagenase D (1mg/mL) + DNAase 1 (0.2mg/mL) at 37^{o}C for 5 minutes each. Spleen and brain single cell suspensions were counted using a Z2 Coulter Counter (Beckman Coulter, Jersey City, NJ) and subsequently stained with a 10-color panel with the following antibodies: Ly6G-FITC,

Gr1-PE, NK1.1-PerCP-Cy5.5, CD11c-PE-Cy7, CD11b-APC (all from BD Biosciences, Franklin Lakes, NJ) and CD45-APC-Cy7, CD3-BV570, B220-BV650, CD4-BV711 and CD8-BV780 (all from BioLegend, San Diego, CA). Samples were acquired within an hour after staining in an LSR-II flow cytometer (BD Biosciences) and analyzed on FlowJo 9.7.6 software.

Isolation of PGCs

PGCs were isolated from E18.5 F1 and WT fetal ovaries based on side and forward scatter differences between germ cells and somatic cells in cell suspension, essentially as described[191]. This method provides higher than 90% purity of isolated PGCs, which was verified in our experiments by stationing sorted cells for VASA, a gemline specific marker[210]. Following sorting of PGCs from individual embryos, the genotype of the embryo was determined, and only F2 PGCs from WT F1 fetuses were used for DNA isolation. Because of the relative low number of germ cells per embryo, 45 F1 and 31 WT female fetuses were used.

Enhanced Reduced Representation Bisulfite Sequencing

Brains from adult male WT, F1, F2, F3, WT-S, F1-S, and F2-G offspring (8-12 weeks old) from at least three different litters were quick frozen on dry ice and sectioned (200μM) in cryostat. The ventral dentate gyrus was microdissected from the sections. DNA was isolated using the DNeasy Blood & Tissue Kit (Qiagen, Valencia, CA). Single end 50bp eRRBS sequencing was performed as described[61], using Illumina HiSeq2000 and 2500 machines according to manufacturer instructions. An in-house pipeline (R MethylKit) was used for methylation calling and alignment to the mm9 reference genome[102]. Differential methylation and statistical analysis were performed using default setting. Differentially methylated sites were defined as sites where the corrected p-value is $\geq$ 0.01 (0.05 in the gametically programmed data) and the difference in methylation between two samples is $\geq$ 15%. Differentially

methylated regions (DMRs) were calculated as regions containing at least four differentially methylated sites, where the distance between two neighboring sites was no greater than 1kb. Genomic and CpG island annotations were based on Ensmbl data downloaded from the UCSC genome browser. Promoters were defined as regions ±2kb from the TSS; exons and introns were defined by reference; upstream regions were defined as extending 50kb from promoter regions; and downstream regions were 50kb from the TES. The percentage of total differentially methylated sites in a defined genomic feature was divided by the percentage expected to overlap each genomic feature by chance, based on the percentage of genomic space occupied by that feature, to determine the fold change from expected values. Additional methylation datasets were downloaded from the UCSC genome browser DNA methylation track hub[29,103,104]. Data have been deposited: GSE68713.

RNA-Seq

WT, F1, and F2, adult offspring (8-12 weeks old) from at least three different litters were perfused with 30% RNAlater (Ambion, Grand Island, NY) in saline. Brains were frozen on dry ice and sectioned (200μM). The ventral dentate gyrus was microdissected from the sections. Total RNA was isolated using the RNeasy Mini Kit (Qiagen, Valencia, CA). Single end 50bp RNA sequencing was performed on Illumina HiSeq2000 and 2500 machines and aligned to the mm9 reference genome using TopHat software version 2.0.11[105]. Default parameters were used with the addition of "--no-novel-juncs" to align exclusively to known genes and isoforms. Genes were counted using HT-seq program[106] with the parameter "intersection-strict". Values for gene expression were calculated using EdgeR[107] package in R using tagwise dispersion and default parameters. Differentially expressed genes were determined using Benjamini-Hochberg corrected p=0.05 threshold. Data have been deposited: GSE68713.

Transfection and Luciferase Reporter Assay

Plasmids were constructed using the In-Fusion Cloning Kit (*Clontech* Laboratories, Mountain View, CA). HEK293 cells (American Tissue Type Collection) were cultured in culture media containing 88% DMEM + 10mM HEPES, 1% penicillin/streptomycin, 10% FBS, and 1% L-Glutamine in a 5% CO_2 37°C incubator. Plasmids were transfected into HEK293 cell cultures using Lipofectamine Transfection Reagent (Life Technologies, Grand Island, NY) in triplicates. Briefly, 0.2E6 cells were seeded in 12-well plates in 1mL of culture media. 24 hours later, 1µg of plasmid DNA was diluted in 85µl Opti-MEM media (Life Technologies) in tubes. After 5 minute incubation, 6µl Lipofectamine Transfection Reagent was added, followed by 20 minute incubation. 85µl of this solution was added to each well of HEK293 cells. The following day, media was aspirated and replaced with 400µl of culture media. 48 hours after transfection, 20µl aliquots of media were sampled into 96-well plates. 100µl of Quanti-Luc luciferase substrate (InvivoGen, San Diego, CA) was added to each well, and plates were read immediately for luciferase activity.

Metabolomics

Brain metabolite extraction

Hippocampal ventral granule cell bodies/nuclei were isolated by microdissection from adult male WT and F1 brain sections and washed twice with ice-cold PBS, followed by metabolite extraction using -70ºC 80% methanol in water (LC-MS grade methanol, Fisher Scientific, Grand Island, NY). The tissue–methanol mixture was subjected to bead-beating for 45 sec using a *Tissuelyser* cell disrupter (Qiagen, Valencia, CA). Extracts were centrifuged for 5 min at 5,000 rpm to pellet insoluble material and supernatants were transferred to clean tubes. The extraction procedure was repeated two additional times and all three supernatants were pooled, dried in a *Vacufuge* (Eppendorf) and stored at -80ºC until analysis. The methanol-

insoluble protein pellet was solublized in 0.2M NaOH at 95ºC for 20 min and quantified using the BioRad DC assay. On the day of metabolite analysis, dried cell extracts were reconstituted in 70% acetonitrile with 0.2% ammonium hydroxide at a relative protein concentration of 3µg/ml and 3µl of the reconstituted extract was injected for LC/MS-based untargeted metabolite profiling.

LC/MS metabolomics platform for untargeted metabolite profiling

Brain extracts were analyzed by LC/MS as described previously [211,212] using a platform comprised of an Agilent Model 1200 liquid chromatography system coupled to an Agilent 6230 time-of-flight MS analyzer. Chromatography of metabolites was performed using aqueous normal phase (ANP) gradient separation, on a *Diamond Hydride* column (Microsolv, Eatontown, NJ). Mobile phases consisted of: (A) 50% isopropanol, containing 0.025% acetic acid, and (B) 90% acetonitrile containing 5 mM ammonium acetate. To eliminate the interference of metal ions on the chromatographic peak integrity and electrospray ionization, EDTA was added to the mobile phase at a final concentration of 6 µM. The following gradient was applied: 0-1.0 min, 99%B; 1.0-15.0 min, to 20%B; 15.0 to 29.0, 0%B; 29.1 to 37min, 99%B. Raw data were analyzed using MassHunter Profinder 6.0 and MassProfiler Professional 13.0 software package (MPP; Agilent Technologies, Santa Clara, CA). Unpaired t-tests ($p<0.05$) were used to determine significant differences between groups.

Differentially expressed metabolite identification

To ascertain the identities of differentially expressed metabolites ($P<0.05$) between F1 cross vs. wildtype vGC samples, molecular features were searched against an in-house *METLIN* Personal Metabolite Database (Agilent Technologies, Santa Clara, CA), annotated with accurate monoisotopic neutral masses (<5 ppm) and chromatographic retention times. A molecular formula generator (MFG) algorithm in

MPP was used to generate and score empirical molecular formulae based on a weighted consideration of monoisotopic mass accuracy, isotope abundance ratios, and spacing between isotope peaks. A tentative compound ID was assigned when *METLIN* and MFG scores concurred for a given candidate molecule. Tentatively assigned molecules were verified based on a match of LC retention times and/or MS/MS fragmentation spectra to that of pure molecule standards.

Analysis of lipids by high-performance liquid chromatography–mass spectrometry

Tissue lipid extracts from isolated ventral granule cells were prepared using a modified Bligh/Dyer procedure, spiked with appropriate internal standards, and analyzed using a 6490 Triple Quadrupole LC/MS system (Agilent Technologies, Santa Clara, CA, USA). Glycerophospholipids and sphingolipids were separated with normal-phase HPLC as before [213,214] with a few changes. An Agilent Zorbax Rx-Sil column (inner diameter 2.1 × 100 mm) was used under the following conditions: mobile phase A (chloroform:methanol:1 M ammonium hydroxide, 89.9:10:0.1, v/v) and mobile phase B (chloroform:methanol:water: ammonium hydroxide, 55:39.9:5:0.1, v/v); 95% A for 2 min, linear gradient to 30% A over 18 min and held for 3 min, and linear gradient to 95% A over 2 min and held for 6 min. Sterols and glycerolipids were separated with reverse-phase HPLC using an isocratic mobile phase as before [213] except with an Agilent Zorbax Eclipse XDB-C18 column (4.6 × 100 mm). Individual lipid species were measured by multiple reaction monitoring transitions and lipid concentration was calculated by referencing to appropriate internal standards: D5-cholesterol, CE 17:0, 4ME 16:0 diether DAG, D5-TAG 16:0/18:0/16:0, PA 14:0/14:0, PC 14:0/14:0, PE 14:0/14:0, PG 15:0/15:0, PS 14:0/14:0, LPC 17:0, LPE 14:0, LPI 13:0, BMP 14:0/14:0, SM d18:1/12:0, dhSM d18:0/12:0, Cer d18:1/17:0, GalCer d18:1/12:0, LacCer d18:1/12:0 and Sulf

d18:1/17:0 (Avanti Polar Lipids, Alabaster, AL, USA). PI 16:0/16:0 was purchased separately (Echelon Biosciences, Salt Lake City, UT, USA). Some lipid classes did not have commercially available internal standards and hence these lipids were referenced to standards that are closely eluted in the liquid chromatography–mass spectroscopy method: Ether-linked species were normalized to corresponding acyl-linked standards: GM3 to PI 16:0/16:0. Lipid concentration was normalized by molar concentration across all species for each sample, and the final data are presented as mean mol%.

Data Analysis.

Data are shown as mean ± s.e.m. Outlier data was excluded based on ± 2 s.d. from the mean. One-way or repeated measures ANOVAs or *t* tests were used to compare tests. LSD or Bonferroni *post hoc* analyses were used to assess statistical significance. Sample size was based on prior data and by using power calculation All graphs and statistical analysis were performed using R (http://ww.r-project.org), Bioconductor (www.bioconductor.org), and ggplot2 (www.ggplot2.org) for visualization, unless stated otherwise.

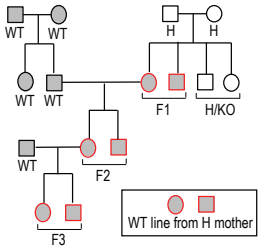

Supplementary Figure. 1. Breeding strategy of F1-F3 WT animals. Shaded boxes indicate genetically WT individuals.

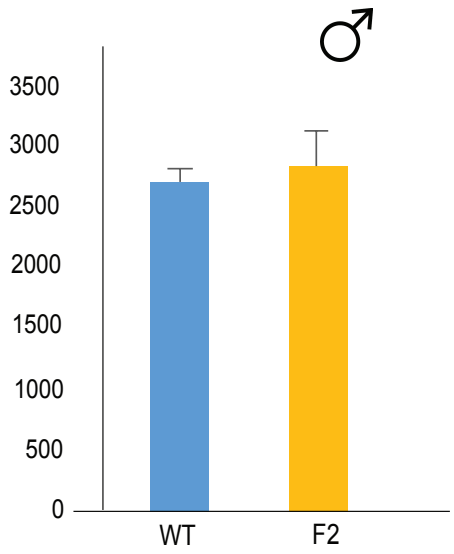

Supplementary Figure. 2. Total locomotor activity of F2 males are not different from that of WT males, *t*-test, p=0.645.

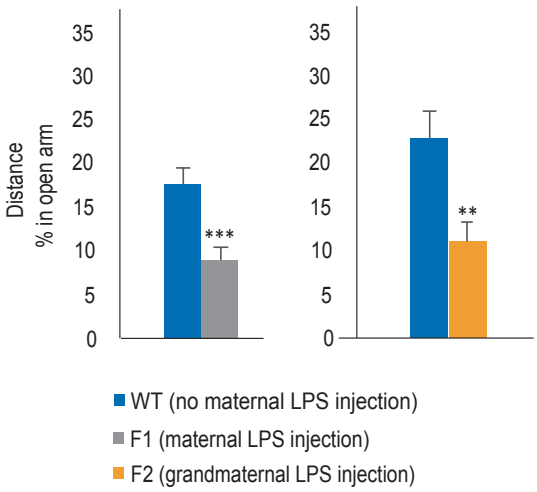

Supplementary Figure. 3. Gestational LPS results anxiety in the elevated plus maze in both F1 (distance in the open arm in % of total; *t*-test, *T*=3.571, ****P*<0.005, *N*=35 and 34 mice per group) and F2 (*t*-test, *T*=3.033, ***P*<0.01, *N*=13 mice per group) offspring.

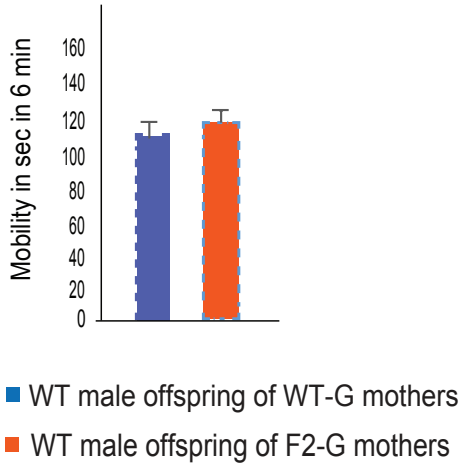

Supplementary Figure. 4. The increased stress reactivity phenotype seen in F2-G males is not transmitted to the next generation.

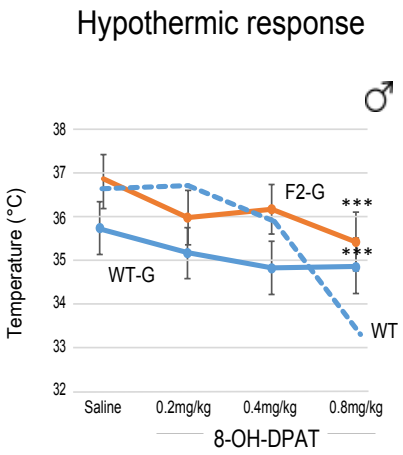

Supplementary Figure. 5. Blunted hypothermic response to the 5-HT_{1A}R agonist 8-OH-DPAT following embryo transfer in both F2-G mice and their WT-G controls (repeated measures ANOVA: group, $F_{2,129}$=10.8, P=0.0002; dose, $F_{3,129}$=24.4, $P<10^{-6}$; and group x dose, $F_{6,129}$=8.4, $P<10^{-6}$; LSD *post hoc* ***p<0.005 for both groups, relative to WT at the same dose. N=18, 12, and 10 animals per group).

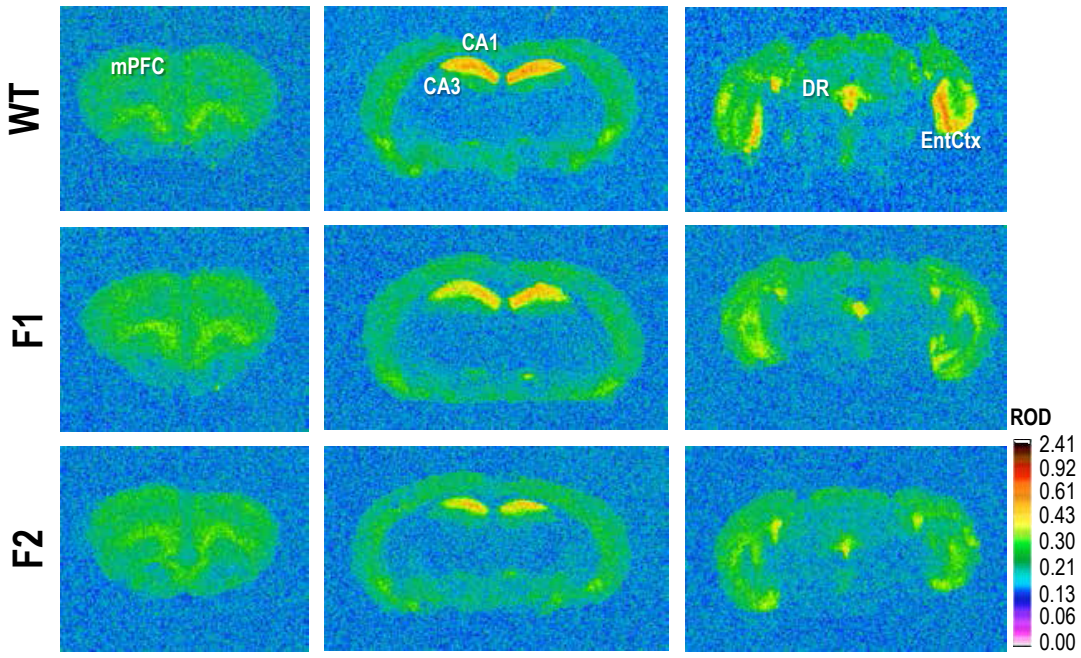

Supplementary Figure. 6. Representative coronal brain sections showing reduced 5-HT_{1A}R expression in hippocampus and dorsal raphe nuclei assed by [^{3}H]-8-OH-DPAT binding.

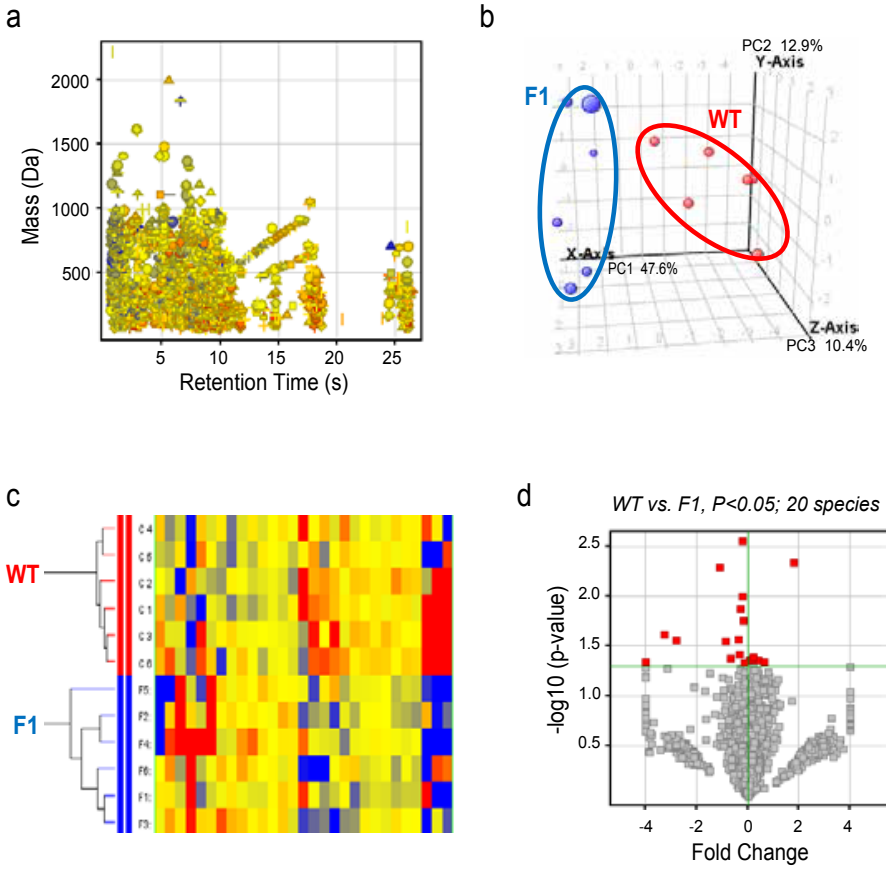

Supplementary Figure. 7. Untargeted metabolite profiling identifies differentially-expressed metabolites in GCs from F1 vs. WT mice (n = 6 mice/group). **a**. A total of 3,156 distinct molecular features were aligned and quantified by untargeted molecular feature extraction in all samples from at least one group, as either positive ions (1,726) or negative ions (1,503). **b**. Principal component analysis (PCA) shows within group clustering and between group separation of GC extracts from WT and F1 brains, considering the relative abundances of 21 differentially-expressed features from among the 3,156 species in panel a ($P < 0.05$). Each point corresponds to an individual mouse brain extract. **c**. Unsupervised hierarchical clustering analysis (HCA) according to Euclidean distance metric and Ward's linkage rule with samples color-coded by phenotype, displays expression patterns and clustering of the differentially-expressed metabolites ($p<0.1$). Feature intensity depicted as a heat map, ranging from red to blue, where red represents an expression level greater than the mean value and blue represents expression levels below the mean value. **d**. Volcano analysis of all 3,156 detected brain features, where between group differences in metabolite expression are plotted at the -log of fold-change vs. log of the p-value. Notably, of the 21 molecules that fulfill the criteria of differential expression with a p-value ≤ 0.05 (indicated in red), 9 were identified as lipids with diminished abundance in F1 vs. WT brain samples while 11 were not structurally confirmed (see Extended Data Table 4).

Supplementary Table 1. Functions enriched in overlapping F1 and F2 differentially expressed genes			
Functional Annotation	p-Value	Molecules	# Molecules
hydrolysis of lipid	3.75E-05	ABHD4,ACAA1,AGT,ARFRP1,ARRB2,CHRM2,CXCR2,ENPP6,FAAH,GBA2,GM2A,GNA12,GNAQ,GPT,GRK4,HEXB,HTR2A,IKBKB,LDL,LPL,MGLL,NAAA,NSMAF,PAFAH1B1,PAFAH2,PLA2G3,PLCB4,PLCG1,PLCG2,PNPLA6,PPT1,PRKAA2,RGS4,SMPD1,SMPD2,UNC5B	36
neuronal ceroid lipofuscinosis	6.10E-05	CLCN7,CLN3,CLN5,CTSD,PPT1,SMPD1,TPP1	7
synthesis of glycosphingolipid	6.65E-05	ABCA8,ABCB1,BCL2L1,CD82,CERK,CLN3,DEGS2,FASN,LARGE,NSMAF,PRKCD,PRKDC,SCD,SLC27A1,SMPD1,SMPD2,SMPD3,SMPD4,ST6GALNAC6,ST8SIA1,UGT8	21
metabolism of sphingomyelin	7.76E-05	CLN3,SMPD1,SMPD2,SMPD3,SMPD4	5
synthesis of glycolipid	7.89E-05	ABCA8,ABCB1,BCL2L1,CD82,CERK,CLN3,DEGS2,FASN,GPAA1,HEXB,LARGE,NSMAF,PIGL,PIGO,PRKCD,PRKDC,SCD,SLC27A1,SMPD1,SMPD2,SMPD3,SMPD4,ST6GALNAC6,ST8SIA1,UGT8	25
cleavage of lipid	8.03E-05	ABHD4,ACAA1,AGT,ARFRP1,ARRB2,CHRM2,CXCR2,ENPP6,FAAH,GBA2,GM2A,GNA12,GNAQ,GPT,GRK4,HEXB,HTR2A,IKBKB,LDLR,LPL,MGLL,NAAA,NSMAF,PAFAH1B1,PAFAH2,PLA2G3,PLCB4,PLCG1,PLCG2,PNPLA6,PPT1,PRKAA2,PTGS1,RGS4,SMPD1,SMPD2,UNC5B	37
metabolism of sphingolipid	1.31E-04	ABCA8,ABCB1,BCL2L1,CD82,CERK,CLN3,DEGS2,FASN,GBA2,GM2A,HEXB,LARGE,NSMAF,PPT1,PRKCD,PRKDC,SCD,SLC27A1,SMPD1,SMPD2,SMPD3,SMPD4,ST6GALNAC6,ST8SIA1,UGT8	25
synthesis of phosphatidylethanolamine	1.93E-04	CHKA,CHKB,PCYT2,PISD,SLC27A1	5
sialylation of ganglioside	6.02E-04	ST6GALNAC4,ST6GALNAC6,ST8SIA1	3
concentration of lipid	8.64E-04	ABCA7,ABCB1,ABCC8,ACP6,ADIPOR2,AGT,AKT3,ALDH1A1,AMH,APAF1,ARNT,BCAT2,BCL2L1,CASP9,CERK,CHKA,CHRNA7,CLN3,CLU,CRHR1,CRTC2,CTSD,CXCL12,CYP27B1,DAGLB,DGAT1,DGAT2,DGKE,DHCR24,DIO2,DLG2,DLK1,DNM2,EDN3,EPB41,FA2H,FAAH,FADS2,FAM57B,FASN,FGF7,GAD2,GBA2,GNAQ,GPR116,GPX1,HEXB,HMGA1,HMGCR,HSD3B7,IL18,IL18BP,INHA,INPP5B,INSIG1,IRS2,LBP,LDLR,LPGAT1,LPL,MAG,MGAT3,MGLL,MRAS,NAA40,NEIL1,NKX2-1,NPC1L1,NSMAF,NTRK2,PCYT2,PDGFRA,PEX5L,PIKFYVE,PIP5KL1,PLA2G3,PLD2,PLIN5,PLP1,PLSCR3,PNPLA6,PNPLA8,PPP1R3C,PRKAA2,PRKCD,PROKR2,PTGS1,PTPN11,QKI,RGS4,RORA,RPS6KB2,SAFB,SAT1,SCD,Scd2,SCG5,SCNN1A,SIRT6,SLC1A2,SLC27A1,SLC6A11,SLCO2A1,SMPD1,SMPD2,SMPD3,SOAT2,ST8SIA1,TAZ,TGFA,TGFBR2,TRIB1,TYK2,UCP2,UGT8,UHMK1,WNK4	117
hydrolysis of phospholipid	1.23E-03	AGT,ARRB2,CHRM2,CXCR2,ENPP6,GNA12,GNAQ,GPT,GRK4,HTR2A,LPL,NSMAF,PAFAH1B1,PAFAH2,PLA2G3,PLCB4,PLCG1,PLCG2,PNPLA6,RGS4,SMPD1,SMPD2,UNC5B	23
synthesis of ceramide	2.73E-03	BCL2L1,CERK,CLN3,DEGS2,FASN,NSMAF,PRKCD,PRKDC,SCD,SMPD1,SMPD2,SMPD3,SMPD4	13
quantity of polyunsaturated fatty acids	3.34E-03	AGT,CERK,DAGLB,DGKE,DNM2,FAAH,FADS2,GNAQ,GPX1,IL18,IL18BP,LDLR,LPL,PNPLA8,PTGS1,SCD,SLCO2A1,TAZ,TGFA,TGFBR2	20
metabolism of phospholipid	3.35E-03	ABCA8,ACP6,AGT,ASPG,CHKA,CHKB,CLN3,DGKE,FASN,FGF7,GPAA1,HEXB,KDR,LPCAT4,LPL,NKX2-1,PCYT2,PIGL,PIGO,PIK3CB,PIKFYVE,PIP4K2B,PISD,PLA2G4B,PLCB2,PLCG1,PLCG2,PLD2,PNPLA6,SLC27A1,SMPD1,SMPD2,SMPD3,SMPD4,TAZ	35
hydrolysis of diacylglycerol	4.52E-03	PAFAH1B1,PAFAH2,PLCG1,PLCG2	4
degradation of 2-arachidonoylglycerol	7.13E-03	FAAH,MGLL	2

Receptors, including GPCRs

Supplementary Table 2. List of overlapping F1 and F2 differentially expressed genes

Sphingolipid metabolism	
Smpd1	sphingomyelinase 1
Smpd2	sphingomyelinase 2
Smpd3	sphingomyelinase 3
Smpd4	sphingomyelinase 4
Nsmaf	neutral sphingomyelinase activation associated factor
Cerk	ceramide kinase
Asah2	ceramidase
Degs2	sphingolipid delta 4-desaturase
Fasn	fatty acid synthase
Scd	fatty acid desaturase
Cln3	neuronal ceroid-lipofuscinosis 3

Monosialodihexosylganglioside (GM3) metabolism	
UGT8	ceramide glucosyltransferase
HexB	hexosaminidase
Gm2A	GM2 ganglioside activator
Large	glucuronosyltransferase
St6galnac4	glycosyltransferase
St6galnac6	glycosyltransferase
St8sia1	glycosyltransferase

Glycerophospholipid metabolism	
Dgke	diacylglycerol kinase
Chka	ethanolamine kinase
Chkb	ethanolamine kinase
Pisd	phosphatidylserine (PS) decarboxylase
Dgat1	DAG acyltransferase1
Dgka	DAG kinase
Mgat3	monoacylglycerol acyltransferase 3
Mgll	monoglyceride lipase
Pla2g3	phospholipase A2

Inositol Phosphate Compounds	
Plcb2	phospholipase C (PLC) beta 2
Plcb4	phospholipase C (PLC) beta 4
Plcg1	phospholipase C (PLC) gamma 1
Plcg5	phospholipase C (PLC) gamma 2
Pik3cb	phosphatidylinositol (PI) kinase
Pip4k2b	phosphatidylinositol phosphate (PIP) kinase
Pip5kl1	phosphatidylinositol phosphate (PIP) kinase
Pikfyve	phosphoinositide kinase
Ppip5k1	diphosphoinositol pentakisphospate kinase 1
Ppip5k2	diphosphoinositol pentakisphospate kinase 2

Supplementary Table 3. LC/MS-based untargeted metabolite profiling of GCs

Mass	RT	Compound Name	P-value	Fold Change	WT1	WT2	WT3	WT4	WT5	WT6	F1	F2	F3	F4	F5	F6
805.5551	1.315	Lactosylceramide (d18:1/12:0)	0.001025	0.69	13517	18559	15358	14822	13922	12009	11975	9750	10421	9637	8659	10040
612.523	1.15	612.5229@1.153	0.001568	0.5	6890.6735	5870.279	8942.492	4751.243	6024.913	7343.214	4593.72	3594.054	3083.091	4511.239	2788.455	1285.39
105.041	8.48	L-SERINE	0.002494	0.86	545548.43	587575.4	509347.5	521087.4	519365.1	574056.4	442161.9	411167.2	501405.5	482729.2	459559.8	495996.5
480.2392	1.058	unknown	0.006169	0.58	10783	10497	7867	9628		13051	6008	6630	5628	7343	8297	2104
801.5451	1.338	Lactosylceramide (d18:1/12:2)	0.008609	0.86	27496	32597	29496	29890	30061	32112	25241	21882	29258	28627	25620	24868
815.636	1.020	unknown	0.008859	0.11	16202	14977	20811	305	3882	16565	845	1522	1422	312	423	3357
798.618	1.03	PA(43:2)	0.016535	0.1	37769.091	52442.19	27925.48	4068.157	1216.652	33153.52	1417.756	1980.147	3674.196	95.3798	1690.984	6445.085
789.567	7.07	PC(P-38:6)	0.017049	0.89	122285.75	140459.7	143802.6	123432.4	125386	135811.7	104296	121513.2	128133.7	120223.3	118336.7	109796.8
803.5448	1.338	Lactosylceramide (d18:1/12:1)	0.018018	0.81	33854	43909	34323	35551	31237	32581	26588	27149	34666	31336	26588	24662
428.364	9.98	428.3637@9.973	0.026209	1.1	24399.941	23841.34	24728.2	22941.06	25642.19	21499.89	24054.94	27151.02	27890.5	27945.03	24366.23	26039.64
394.2711	1.140	unknown	0.029537	0.77	88244	83537	81142	123530	99894	112448	86668	80670	62641	59516	68930	93978
322.197	1.42	322.198@1.4279999	0.03479	1.22	76005.85	49532.1	50517.36	67714.51	55098.65	45310.54	77237.3	71048.51	71473.84	64304.92	66765.49	69545.95
334.063	7.04	3-Phosphoglyceroinositol	0.036676	0.81	145326.88	154173.3	161708	121876.6	140880.5	138160.1	85926.69	107675.1	100675	127789.5	127333.5	151891.4
164.055	1.5	L-RHAMNOSE	0.043106	1.26	54934.681	47735.53	43796.99	45206.76	43313.29	21780.19	61212.03	56025.19	54001.76	52133.35	51993.01	48962.68
537.326	8.75	537.3266@8.748	0.044886	1.03	209433.44	209559.7	213559.2	218249.7	217456.3	209986.3	219850.1	213039.2	218410.3	215239	229806.5	221948.9
148.035	7.49	Methylmalate?	0.046224	1.69	238616.71	200796.6	226369.7	230282.5	256008.5	288905	223375	582056.7	273894.6	588074.9	527560.7	243984.3
749.5342	4.323	PE(P-38:5)	0.046778	0.92	606099	665298	745203	607464	659355	703771	568651	624384	593099	634252	624278	611696
705.528	7.74	705.5278@7.7409997	0.047103	1.11	343946.15	355845.8	375849.5	415715.8	376188.3	384007.2	438353.8	462037.8	441811.2	408325.7	392708.7	358888.6
666.5191	1.013	DG(40:7)	0.048597	0.64	6735	6754	11698	5242	5752	8225	4978	3262	2436	5224	7075	5612
664.5067	1.013	DG(40:8)	0.04449	0.72	9100	9391	14301	8087	10119	14045	7995	7990	4283	8710	8942	9048
311.236	1.25	311.2383@1.269	0.049318	1.34	23188.898	19393.18	26637.56	27256.28	20932.58	14530.15	25061.86	26581.5	41815.93	23363.96	28941.9	30960.58

PA: phosphatidic acid; PC: phosphatidylcholine; PE: phosphatidylethanolamine; DG: diacylglycerol
Statistically significant increase (fold change vs WT)
Decrease
Unpaired t-tests ($p<0.05$)

PA: phosphatidic acid
PC: phosphatidylcholine
PE: phosphatidylethanolamine
DG: diacylglycerol

Supplementary Table 4. Lipidomics data complementing Fig. 4e.

Species	F1/WT	F2/WT		Species	F1/WT	F2/WT		Species	F1/WT	F2/WT		Species	F1/WT	F2/WT
PA 36:1	1.0	0.6		PEp 36:0	2.3	1.2		PG 34:0	0.8	0.8		BMP 34:1	1.0	0.7
PA 36:2	0.9	0.6		PEp 36:1	0.8	0.7		PG 34:1	0.7	0.8		BMP 34:2	0.8	0.7
PA 36:3	0.8	0.6		PEp 36:2	1.2	0.9		PG 34:2	0.7	0.8		BMP 36:0	1.0	0.8
PA 36:4	0.8	0.6		PEp 36:3	0.6	0.7		PG 36:0	0.6	0.5		BMP 36:1	1.0	0.6
PA 38:0	0.9	0.6		PEp 36:4	1.0	1.2		PG 36:1	0.7	0.6		BMP 36:2	0.9	0.7
PA 38:1	0.8	0.5		PEp 38:0	1.2	1.0		PG 36:2	0.6	0.6		BMP 36:4	1.0	1.0
PA 38:2	0.9	0.5		PEp 38:1	0.8	0.7		PG 36:3	0.7	0.7		BMP 38:0	1.0	1.1
PA 38:3	0.8	0.6		PEp 38:2	1.0	0.6		PG 36:4	0.9	1.1		BMP 38:2	1.0	0.6
PA 38:4	0.9	0.5		PEp 38:3	1.1	1.1						BMP 38:3	0.8	0.6
PA 38:5	0.9	0.5		PEp 38:4	0.9	1.1						BMP 38:4	0.9	0.7
PA 38:6	1.0	0.7		PEp 38:5	0.9	1.1						BMP 38:6	0.9	0.9
PA 40:4	1.1	0.5		PEp 38:6	1.0	1.2						BMP 40:4	1.0	0.6
PA 40:5	1.0	0.5										BMP 40:5	1.0	0.8
PA 40:6	1.0	0.5										BMP 40:6	1.0	0.6
PA 40:7	1.1	0.4										BMP 40:7	1.0	1.0
PA 42:5	1.1	0.5												
Species	**F1/WT**	**F2/WT**		**Species**	**F1/WT**	**F2/WT**		**Species**	**F1/WT**	**F2/WT**		**Species**	**F1/WT**	**F2/WT**
LPI 16:0	1.4	1.1		SM d18:1/20:0	1.0	0.8		GalCer d18:1/20:0	1.4	0.9		GM3 d18:1/18:0	5.6	1.7
LPI 18:0	4.0	1.4		SM d18:1/20:1	0.9	0.9		GalCer d18:1/20:1	1.5	1.0		GM3 d18:1/20:0	3.8	1.8
LPI 18:1	1.1	1.2		SM d18:1/22:0	1.0	0.8		GalCer d18:1/22:0	1.2	0.9		GM3 d18:1/24:0	1.8	2.1
LPI 20:4	0.9	1.3		SM d18:1/22:1	1.0	0.7		GalCer d18:1/22:1	1.3	1.0				
				SM d18:1/24:0	1.1	0.9								
				SM d18:1/24:1	1.0	0.8								
				SM d18:1/26:0	1.0	0.8								
				SM d18:1/26:1	1.0	0.7								

Statistically significant increase (fold change vs WT)
Decrease
ANOVA, Bonferroni $p<0.05$.

PA: phosphatidic acid
PEp:plasmalogen phosphatidylethanolamine
PG: phosphatidylglycerol
BMP: bis(monoacylglycerol)phosphate
LPI: lysophosphatidylinositol
SM: sphingomyelin
GalCer: galactoceramide
GM3: monosialodihexosylganglioside

Supplementary Table 5. Functions enriched in DMR genes present in both F1 and F2 neurons		
Functional Annotation	p-Value	Molecules
Behavior		
anxiety	2.01E-05	ADORA2A,CAMK2A,CRHR1,DRD2,GRIN3B,LMTK3,NFATC2,NPAS3,OPRD1,PCSK1N,RAI1,SHANK1,SLC6A4
hypoactivity of mice	6.89E-05	ADORA2A,DLG4,DRD2,GNAS,GRIN3B,HCN2,NR4A2,SHANK1,SLC6A4,SOCS7,SRGAP3
prepulse inhibition	1.60E-04	ADORA2A,DLG4,DRD2,GNAS,NTSR1,SLC6A4,SRGAP3
social exploration	5.03E-04	DLG4,GRIN3B,NPAS3,SLC6A4,SRGAP3
hypothermia	7.55E-04	DRD2,GALP,NTSR1,PPARA,SLC6A4
emotional behavior	1.66E-03	ADORA2A,CAMK2A,CRHR1,DLG4,DRD2,GALP,LMTK3,NPAS3,NR4A2,RIMS2,SHANK1,SLC6A4
Lipid Metabolism		
phosphorylation of sphingolipid	6.71E-04	CERK,SPHK1
concentration of lipid	1.67E-03	ABHD5,ADORA2A,BRD2,CEBPA,CERK,CRHR1,CXCL14,CYP26B1,DGKE,DLG4,DLK1,DRD2,GNAS,LTC4S,MBP,mir-33,NGFR,PLA2G1B,PPARA,RAI1,SIRT4,SLC5A10,SLC6A4,SMARCD3,SMPD3,SPHK1,SREBF2,SRGAP3,ST8SIA1
synthesis of ceramide	3.84E-03	CERK,DRD2,NGFR,SMPD3,SPHK1
synthesis of lipid	3.93E-03	ABHD5,ACADVL,BRD2,CEBPA,CERK,CRHR1,DGKE,DRD2,EDNRB,ITGA6,LTC4S,MAP3K1,NFATC2,NGFR,NR4A2,PDGFB,PIGY,PLA2G1B,PPARA,SIRT4,SLC22A2,SMPD3,SPHK1,SREBF2,ST8SIA1
synthesis of glycolipid	4.41E-03	CERK,DRD2,NGFR,PIGY,SMPD3,SPHK1,ST8SIA1
synthesis of glycosphingolipid	4.69E-03	CERK,DRD2,NGFR,SMPD3,SPHK1,ST8SIA1
Neurotransmission, synapse/neuronal development		
neurotransmission of axons	6.71E-04	EPHB2,RIMS2
proliferation of neuronal cells	1.05E-03	ADORA2A,BRSK1,CAMK2A,DLG4,DRD2,DVL2,EML1,EPHB2,GNAS,ITGA6,KIF26A,MID1,MYLIP,NFATC2,NGFR,OPRD1,PCSK1N,PDGFB,PXN,SMARCD3,SRGAP3,TIAM1,ZNF423
metabolism of dopamine	1.15E-03	DRD2,NR4A2,SLC6A4,SNCB
morphogenesis of neurites	1.87E-03	ADORA2A,ATXN10,BRSK1,CAMK2A,CRHR1,CUL7,CUX2,DLG4,DRD2,EPHB2,FGF13,MID1,NGFR,PTPN20B,SDK2,TIAM1,USP21
neurotransmission	1.98E-03	ADORA2A,CAMK2A,CRHR1,DLG4,DRD2,EPHB2,HCN2,MBP,MYH14,NGFR,NTSR1,RIMS2,RXRB,SCN8A,SLC6A4,SNCB,SNPH
neuritogenesis	2.05E-03	ADORA2A,ATXN10,BRSK1,CAMK2A,CRHR1,CUL7,CUX2,DLG4,DRD2,EPHB2,FGF13,MBP,MID1,NGFR,PTPN20B,PXN,SDK2,SNCB,ST8SIA1,STMN1,TIAM,USP21
abnormal pruning of axons	2.19E-03	EPHB2,NGFR
transport of monoamines	2.74E-03	DRD2,SLC22A2,SLC6A4
plasticity of synapse	2.75E-03	ADORA2A,CAMK2A,CRHR1,DLG4,DRD2,EPHB2,NGFR
size of dendritic spines	4.52E-03	CAMK2A,DLG4

Supplementary Table 6. Functions enriched in F1-F2 differentially expressed and differentially methylated genes			
Functional Annotation	p-Value	Molecules	# Molecules
Lipid Metabolism			
synthesis of glycosphingolipid	3.89E-04	CERK,SLC27A1,SMPD3,ST8SIA1	4
quantity of diacylglycerol	6.97E-04	DGKE,FAAH,SLC27A1	3
synthesis of lipid	9.22E-04	ACADVL,CERK,CRHR1,DGKE,EDNRB,FAAH,SIRT4,SLC27A1,SMPD3,ST8SIA1	10
concentration of arachidonic acid	2.42E-03	CERK,DGKE	2
hydrolysis of 1,2-dioctanoyl-sn-glycerol	6.66E-03	PAFAH2	1
phosphorylation of ceramide to ceramide-1-P	6.66E-03	CERK	1
synthesis of ganglioside GD1b,GD2,GT1,GD3	9.97E-03	ST8SIA1	1
catabolism of sphingomyelin	1.98E-02	SMPD3	1

Supplementary Table 7. Functions enriched in PGC differentially methylated genes			
Functional Annotation	p-Value	Molecules	# Molecules
Imprinting	3.37E-04	Blcap,Nnat, Airn/Igfr2, Ccdc40, Dio3, Wt1	5
Fertility	4.16E-04	Airn/Igfr2, Dio, Cnaz, Lhcgr, Parp1, Sulf2, Wt	7
Morphogenesis of genital organ	2.58E-03	Lhcgr, Wt	2

CHAPTER 5

ENVIRONMENTALLY MALLEABLE EPIGENOMIC REGIONS IN THE MAMMALIAN BRAIN

** Klein S.L., Sharma A., Mitchell E., Lodhi N., Bovinico C., Barboza L., Bavely C., O'Dell S., and Toth M. 2015. Environmentally malleable epigenomic regions in the mammalian brain. Manuscript in preparation.*

5.1 Introduction

The perinatal and early postnatal periods are highly sensitive to environmental influences which can lead to life-long behavioral and cognitive abnormalities[109]. Children of overtly stressed and/or anxious parents frequently display increased behavioral abnormalities including anxiety, hyperactivity, attention deficits, and drug abuse[4,215,216]. Maternal stress and/or anxiety can be caused by a variety of factors including reduced expression of the 5HT1A serotonin receptor that results in elevated and anxiety and depressive behavior[12,182,217,218]. In previous work we have shown that MA in mice due to 5HT1A-R deficiency results in elevated anxiety in genetically wild-type offspring that mirrors the human condition[219,220].

Maternal gestational infections have been linked to increased incidents of schizophrenia and autism in the offspring that are associated with increased anxiety-like behavior[38]. Several mouse models of maternal infection have been used including injection of the bacterial mimetic, lipopolysaccharide (LPS), to induce an immunological response[221]. LPS administration leads to activation of the innate immune system through cytokine induction, fever, complement cascade activation and HPA axis activation. Offspring of mothers injected with LPS have increased numbers of activated microglia and decreased hippocampal neurogenesis, dendritic length,

arborization, and spine density[221-223]. Behaviorally, they display increased anxiety, deficits in social interaction and learning impairments[221].

Maternal neglect can result in mild neurocognitive impairment, impulsivity, as well as anxiety, attention, and social deficits[224,225]. The effects of maternal neglect were described in several studies, including one that followed children raised in Romanian orphanages who experienced limited human physical contact and care[225]. The children exhibited mild neurocognitive impairment, impulsivity, as well as anxiety, attention, and social deficits, including indiscriminate friendliness[224,225]. Animal models of maternal neglect include maternal separation (MS), where offspring are separated from their mothers for several hours per day in the early weeks of life. MS in several animal species, including mice, rats and monkeys, result in anxiety and behavioral abnormalities in adult offspring[11,226,227].

The various forms of adverse early life experiences differ from each other in many respects, including their timing (gestational, perinatal, early postnatal), duration, and severity. However, the repertoire of behavioral abnormalities exhibited by the offspring often overlap. In particular, anxiety is a frequent endophenotype of early life adversity[136,228-230], suggesting a molecular convergence that results in altered expression of gene networks, circuitry, and behavior.

Conceivably, the long-lasting behavioral effects of maternal MA, LPS, and MS may be explained by stable epigenetic changes in offspring neurons. Early life adversity induced epigenetic changes at candidate genes have been documented in rodent models, as well as postmortem human studies[36,125,231,232]. Some of these gene-specific epigenetic changes correlated with the offspring's phenotype[96,123,125,233-236]. However, no fundamental epigenetic signatures have been associated with early life adversity conditions, and it is unclear if certain genomic domains are particularly responsive to adverse environments.

Of the different epigenetic modifications, DNA methylation is relatively stable and closely associated with gene transcription[237]. The genomic localization of DNA methylation is important in the regulation of gene expression[74]. Promoter DNA methylation is a key regulator of gene expression during development and is contingent on CpG density[31,74]. However non-promoter/gene body DNA methylation is an important regulator of at neural gene expression[24]. Intragenic DNA methylation at intronic and exonic sequences may regulate isoform specific expression through their activity as enhancers or splice site regulators[74].

In Chapter 3 we described maternal environment-induced DNA methylation changes in homogenous populations of hippocampal neurons in the MA model. Here we show that the concept of epigenetic maleability at DMRs can be extended to additonal models of early life adveristies; specifically to the MS and LPS models. Furthermore we show that there are common regions of early environemtnally sensitive DMRs (E-DMRs) that may underlie the common anxiety phenotype.

5.2 Results

Behavioral phenotypes overlap in three models of early life adversity

We tested the behavioral phenotypes of offspring exposed to maternal MA, LPS and MS to determine all possible convergent behavioral phenotype. We chose a panel of behavioral tests that measure innate anxiety, stress responsiveness/coping, and social anxiety. To better represent a natural population and avoid the spurious effects of recessive alleles in our behavioral studies, we used the outbred Swiss Webster (SW) strain of mice[238,239].

We previously reported increased innate anxiety in MA and LPS offspring[12,240] (see Chapter 4, Fig 4.1b and Sup Fig. 4.3), measured as increased avoidance of the fear-inducing open and raised arms of the elevated plus maze (EPM). Here we show

that the MS offspring also exhibit increased EPM anxiety (Fig. 5.1A, Fig. S5.1A). Innate anxiety can also be assessed, under less stressful conditions, in the open field (OF) test. Less exploration of the open center area, as compared to the more protected peripheral area, is interpreted as increased anxiety. LPS and MS offspring exhibited more center exploration; i.e. less anxiety (Fig. 5.1A, Fig. S5.1B), while the MA offspring were similar to controls[12]. The opposite behavioral changes in the OF and EPM tests indicate that anxiety *per se* is not an obligatory association of early life adversity. Rather, depending on the context, adversity could lead to less anxiety, interpreted in the clinical literature as the inability to correctly assess novel environment/situation or risk taking behavior. Early childhood adversity is a recognized risk factor for risk taking behavior, including drug addiction[241,242]. Consistent with this interpretation, MS in rodents has been reported to result in increased risk taking behavior[243,244].

We previously reported increased escape behavior in the forced swim test (FST) of MA offspring[12] (Fig. 4.1j). Here we observed a similar phenotype in MS offspring, while LPS offspring exhibited no significant behavioral change (Fig. 5.1A, Fig. S5.1C). We interpret this behavior as increased stress reactivity and lack of habituation to an otherwise inescapable situation. These data are consistent with the increased stress reactivity seen in many psychiatric disorders.

Figure 5.1. Convergence of anxiety and differential DNA methylation in three models of early life adversity: A. Summary of behavioral tests and their outcomes. EPM, elevated plus maze; OF, open field; FST, forced swim test. See Chapter 5 and Supplementary Figure 1 for details and statistics. **B.** Differentially methylated (DM) regions (DMRs) are defined as regions with ≥4 clustered DM sites (DMSs) where two DMSs are no greater than 1kb apart. **C**. E-DMRs (152, corresponding to 249 genes) are defined as overlapping DMRs from at least two of the three early adversity models. **D.** DMS CpGs within E-DMRs display an overall trend toward hypomethylation versus hypermethylation in all three models, though a substantial portion is differentially methylated in opposing directions in at least one of the early life adversity models. **E.** Methylation distribution of hyper- and hypomethylated E-DMR DMSs in individual models relative to control. Distribution of all CpGs, which follow a bimodal arrangement, is also shown. **F.** Methylation distribution of control (gray) and E-DMR DMSs (blue) on the autosomes (solid) and X-chromosome (dashed). **G.** Correlation plot of E-DMR DMSs in six individual animals and in a pooled sample indicate that intermediate methylation is not due to inter-animal differences. Methylation at all CpGs from the pooled sample is also included to show the lack of correlation with methylation at E-DMR DMSs. Boxed numbers denote Pearson regression coefficient r^2.

A

Innate Anxiety EPM	MA	LPS	MS
Risk Taking OF		LPS	MS
Stress Responsiveness FST	MA		MS
Sociability 3 Chamber			MS
Social Anxiety 3 Chamber	MA	LPS	

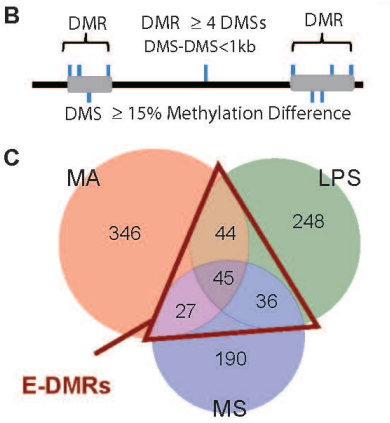

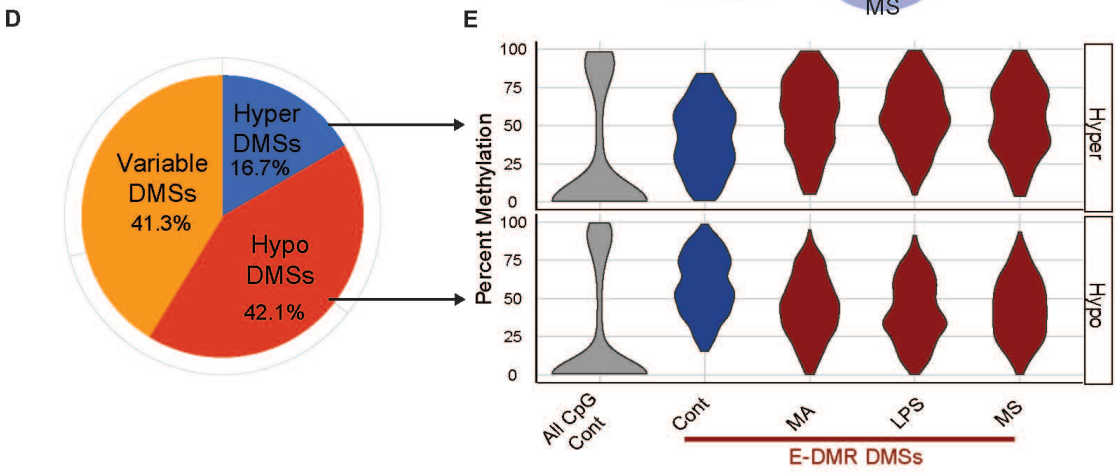

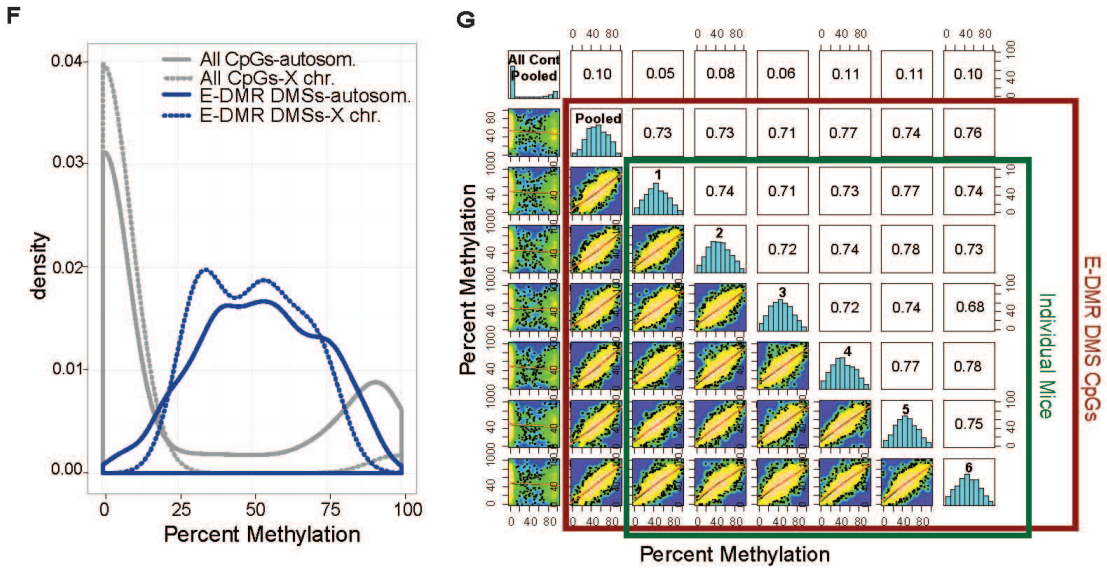

Another overlap between two adversity models, specifically between MA and LPS, occurred in the 3 chamber social interaction test[245]. Although mice typically prefer to interact with a conspecific stranger as opposed to an inanimate object, both MA and LPS offspring exhibited absence of preference, interpreted as social anxiety (Fig. 5.1A, Fig. S5.1D). Social anxiety is a well-documented consequence of early life adversity, exemplified by autism, which is often associated with gestational infection[38,246,247]. However, MS offspring, similar to neglected children[216], exhibited no anxiety towards strangers, or as referred in clinical literature, showed lack of stranger anxiety or indiscriminate friendliness.

Taken together, profiling a range of emotional behaviors in MA, LPS, and MS offspring revealed EPM anxiety as a common behavioral outcome across the three models. EPM anxiety has been linked to the ventral hippocampus by lesion, pharmacological, electrophysiological, and more recently optogenetic studies[119,186,248,249]. These data suggest that all three adversity conditions may target the ventral portion of the hippocampus. Ventral hippocampal granule cells (v-GCs) play a central role in processing and distributing incoming tactile, olfactory and visual information to downstream v-CA neurons[186,250].

Three early life adversity conditions alter DNA methylation at shared DNA domains

GC neuronal bodies were microdissected from the ventral dentate gyrus (DG) of adult animals and assayed for differential methylation by enhanced reduced representation bisulfite sequencing (eRRBS)[61,130]. DMRs were defined as genomic regions with $\geq$4 clustered differentially methylated sites (DMSs), each with $\geq$15 % methylation difference between control and adversity exposed animals, and SLIM corrected p-value of < 0.01[251], where the distance between two DMSs in no greater than 1kb (Fig. 5.1B).

All three early life adverse conditions produced DMRs in adult v-GCs. The average size of the DMRs, depending on the model, was 286-304 bp and contained 4.7-5.2 DMSs. Furthermore, a total of 1.7% of eRRBS-profiled CpGs were differentially methylated in at least one model. Similar to the behavioral overlap, some of the model-specific DMRs intersected, indicating that the shared behavioral phenotypes may correspond to common DMRs (Fig. 5.1A and C). Specifically, 152 DMRs (9.3 DMSs/DMR) were shared by at least 2 models. Because of their inherent sensitivity across at least two early life adversity models, we refer to these overlapping DNA blocks as "environmentally-sensitive" or E-DMRs.

Early life adversity caused both hypomethylation and, to a lesser extent, hypermethylation at DMSs within E-DMRs (Fig. 5.1D). Approximately 60% of the DMSs were unidirectionally modified across models, while the rest were methylated variably between models.

Environmentally malleable domains have intermediate levels of DNA methylation

Environmentally malleable CpG sites in all three models, independently of whether shared or model specific, displayed intermediate methylation, between 25 and 75%, that shifted to higher and lower levels following adversity (Fig. 5.1E and Fig. S5.2A). This is in contrast to the canonical bimodal distribution of DNA methylation, at majority of CpG sites, that are either fully methylated (>75%) or unmethylated (<25%). This raised the possibility that the intermediate methylation may be a proxy, or perhaps even a prerequisite, for epigenetic malleability by the environment.

DNA methylation at an individual site is binary, therfore we sought to explain the nature of the observed intermediate methylation. Since each cell contains two

alleles the intermediate methylation phenomenon could be due mono-allelic methylation, similar to imprinting, resulting in intermediate methylation around 50%. However, DMSs within E-DMRs were in a range of 25-75%, rather than peaking at 50% (Fig. 5.1E) and did not map to known imprinting control regions (Xie et al., 2012). Furthermore, E-DMRs were also intermediately methylated, and bidirectionally modified by adversity, when present in single copies on the X chromosome in males, suggesting that the intermediate methylation is allele independent (Fig. 5.1F). Another possibility for the observed intermediate methylation is inter-animal variability resulting from pooled samples. However, DMSs within E-DMRs were highly correlated between individual mice (Fig. 5.1G). The only remaining explanation is neuron-to-neuron methylation variability in the hippocampus.

The association of DMSs with intermediately methylated regions suggest that the intermediate methylation may be a marker of, or perhaps even a prerequisite for, epigenetic malleability by early life adversity. E-DMRs may underly an epigenetic mosaicism in the GC layer of the hippocampus as evidenced by the inter-neuronal methylation variability.

E-DMRs are enriched in exonic sequences

DMSs within E-DMRs were enriched at exons and distal promoters, while excluded from proximal promoters, introns and integenic regions (Fig. 5.2A). A similar pattern was seen within DMRs in individual models (Fig. S5.2B). The exonic and distal promoter enrichment of E-DMRs suggests a role in transcriptional regulation, perhaps via alternative promoter use or enhancer activity. To test this notion, we cloned several exonic E-DMRs into luciferase constructs to determine their

effect on transcription in 293 T-cells[240]. Exonic E-DMRs from the cadherin-related 23 (*Cdh23*) and cytohesin-4 (*Cyth4)* genes exhibited no promoter activity, but resulted in significantly increased activity of a minimal EF1 promoter (Fig. 5.2B). In contrast, an arbitrary 208 bp intergenic drosophila sequence had no effect on luciferase activity. We previously reported similar activity of the *Kif19* E-DMR[240]. Although the selected E-DMRs all enhanced luciferase activity, their effect on neuronal transcription is difficult to predict. For example, enhancers may promote the transcription of certain RNA isoforms at the expense of others, or promote transcription of nearby genes rather than their own. Therefore, further studies will be needed to understand how differential methylation at exonic E-DMRs regulate gene expression in the hippocampus.

Figure 5.2. Genomic features of E-DMRs. **A.** Enrichment and exclusion of E-DMR DMSs relative to control CpGs at genomic features. **B.** E-DMRs have no promoter but increased enhancer activity **C.** Merged canonical pathways obtained with E-DMR genes using IPA: Ephrin Receptor Signaling (p=5.6-E3), BMP Receptor Signaling (p=7.4-E3), RAR Activation (p=8.1-E3), Integrin Signaling (p=1.0-E2), Notch Signaling (p=2.3-E2), IGF Signaling (p=2.5-E2) and NGF Signaling (p=3.3-E2).

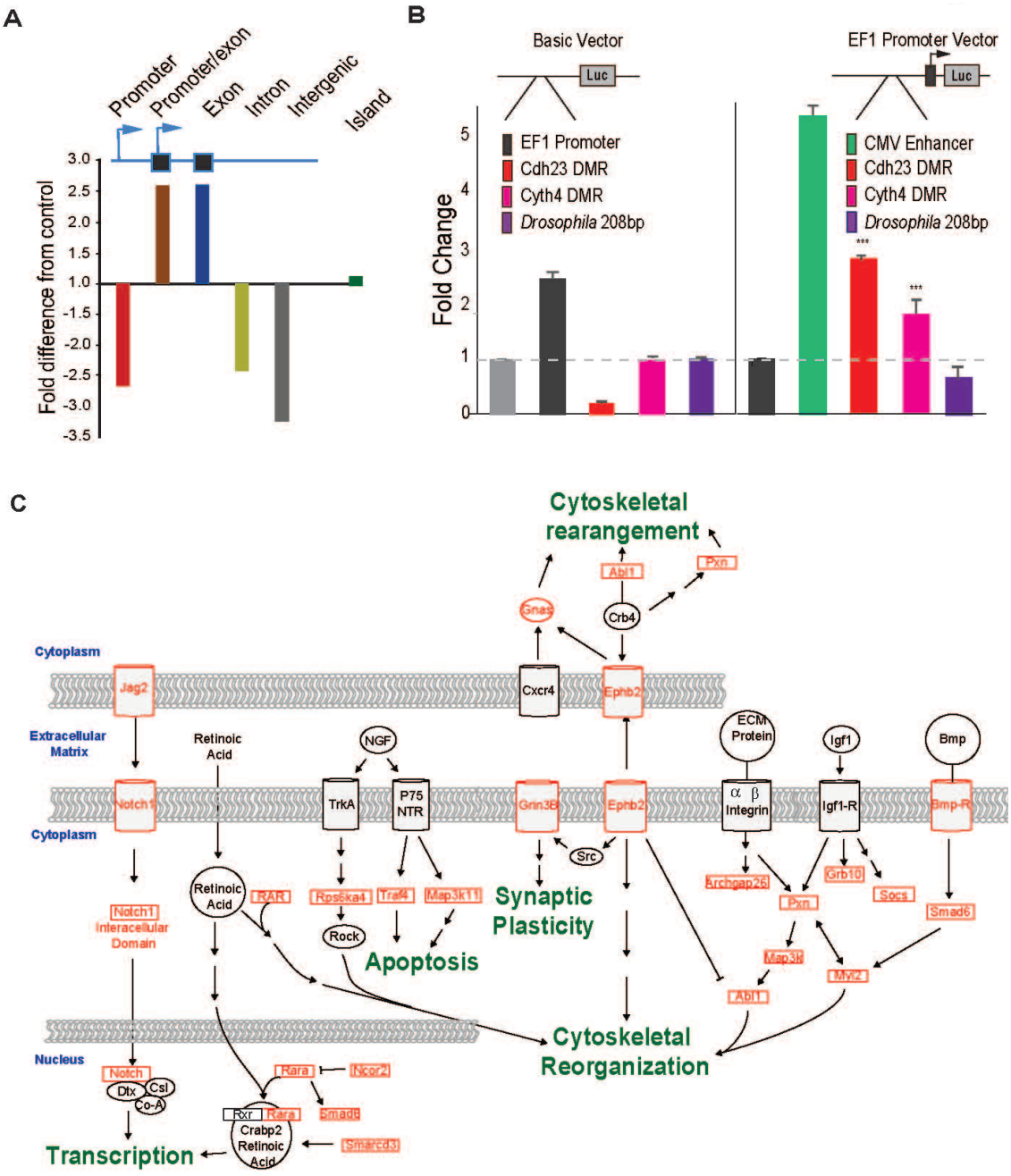
A
Promoter
Promoter/exon
Exon
Intron
Intergenic
Island
Fold difference from control
3.0
2.5
2.0
1.5
1.0
-1.5
-2.0
-2.5
-3.0
-3.5
B
Basic Vector
Luc
EF1 Promoter
Cdh23 DMR
Cyth4 DMR
Drosophila 208bp
EF1 Promoter Vector
Luc
CMV Enhancer
Cdh23 DMR
Cyth4 DMR
Drosophila 208bp
Fold Change
5
4
3
2
1
0
***
***
C
Cytoskeletal rearangement
Abl1
Pxn
Gnas
Crb4
Cytoplasm
Jag2
Cxcr4
Ephb2
Extracellular Matrix
Retinoic Acid
NGF
ECM Protein
Igf1
Bmp
Notch1
TrkA
P75 NTR
Grin3B
Ephb2
α β Integrin
Igf1-R
Bmp-R
Cytoplasm
Src
Archgap26
Grb10
Socs
Pxn
Smad6
Notch1 Interacellular Domain
Retinoic Acid
RAR
Rps6ka4
Traf4
Map3k11
Rock
Synaptic Plasticity
Apoptosis
Map3k
Myl2
Abl1
Cytoskeletal Reorganization
Nucleus
Notch
Dtx
Csl
Co-A
Rara
Ncor2
Rxr
Rara
Smad8
Crabp2 Retinoic Acid
Smarcd3
Transcription

E-DMRs are associated with genes regulating cell-to-cell adhesion and signaling

Ingenuity Pathway Analysis (IPA) revealed that E-DMRs were enriched in a subset of genes involved almost exclusively in cell-to-cell adhesion/signaling and regulation of synaptic plasticity (Fig. 5.2C). Specifically, E-DMR genes mapped to the canonical pathways of *Ephrin Receptor Signaling* (p=5.6-E3; *Abl1, Ephb2, Gnas, Grin3B, Pxn*), *BMP (bone morphogenic protein) Receptor Signaling* (p=7.4-E3; *Myl2, Smad6*), *RAR (retinoic acid receptor) Activation* (p=8.1-E3; *Gnas, Ncor2, Rara, Smad6, Smarcd3*), *Integrin Signaling* (p=1.0-E2; *Abl1,Archgap26, Map3K11, Myl2, Pxn*), *Notch Signaling* (p=2.3-E2; *Jag2, Notch1*), *IGF Signaling* (p=2.5-E2; *Grb10, Pxn, Socs7*) and *NGF Signaling* (p=3.3-E2; *Map3K11, Rps6ka4, Traf4*). Although individually moderate, the combination of E-DMR associated pathways offers a compelling argument for a regulatory role in cell-to-cell adhesion and signaling. Importantly, these molecular pathways regulate the RHO-family GTPases and other downstream cytoskeletal stabilizing proteins and serve to control spinoskeletal actin structure and long-term spine maintenance [252].Taken together, we identified common epigenetic gene targets of the different models that may directly correspond to the regulation of spine cytoskeletal structure and the convergent EPM anxiety phenotype.

Intermediate methylation of E-DMRs are formed during neuronal maturation

To determine whether methylation at E-DMRs are intermediate from early development, or become intermediate later during neuronal differentiation, we analyzed embryonic stem cells (ESCs), embryonic day 10.5 hippocampal precursors (HPs), postnatal day 7 “young” immature GCs (yGCs), and adult mature GCs (Fig. 5.3A). Methylation at “all” profiled CpG sites followed previously described methylation distributions through development. However, environmentally malleable CpGs, within E-DMRs, gradually assumed intermediate methylation from their mostly

hypomethylated state in ESCs (Fig. 5.3A). Specifically, intermediate methylation was established during development largely through the partial methylation of unmethylated sites. The *de-novo* methyltransferase most active during neuronal differentiation is Dnmt3a[84,253]. Therefore, we conditionally deleted *Dnmt3a* by tamoxifen-induced nestin-Cre-ERT2 (*Dnmt3a*$^{f/f}$,T-*cre*$^{+}$; 75-85% efficiency), to test if formation of intermediate methylation at E-DMRs is disrupted. We took advantage of the delayed development of GCs and administered tamoxifen at embryonic day 13.5, thus avoiding possible undesirable effects during brain (for example cortical) development, while still influencing DNA methylation through most of GC development[57,254]. Conditional deletion of *Dnmt3a* substantially reduced the developmental gain in methylation, resulting in an incomplete formation of intermediate methylation in *Dnmt3a*$^{f/f}$,T-*cre*$^{+}$, relative to control *Dnmt3a*$^{f/f}$,T-*cre*$^{-}$ GCs (Fig. 4.3B). The reduced methylation at E-DMRs suggests a role of Dnmt3a in the establishment of the intermediate methylation state at environmentally malleable CpG sites.

Intermediate methylation of E-DMRs are tissue specific

Although we used SW mice, E-DMR-associated malleable intermediate methylation sites were also present in v-GCs derived from inbred B6 mice (which are preferred in genomic studies). Hierarchical clustering, based on the methylation level of malleable CpGs in E-DMRs, showed high similarity between the two strains at both young and mature neuronal stages (Fig. 5.3C). However, methylation levels were different in SW blood leukocytes, indicating tissue specific differences.

Figure 5.3. Development and tissue specificity of E-DMRs. **A.** Methylation distribution of E-DMR DMSs and control CpG sites through neuronal development in the hippocampus. **B.** Methylation distribution of E-DMR DMSs following the conditional inactivation of *Dnmt3a* in the DG. **C.** Dendrogram of intermediately methylated sites in C57B6 and Swiss Webster mice indicates a high degree of similarity of E-DMR DMSs at two different stages of GC development. **D.** PCA plot based on methylation levels at E-DMR DMSs in multiple tissues suggests a high degree of similarity between ventral and dorsal GCs, extending to hippocampal CA3 pyramidal cells as well striatal MSNs. **E-F.** Methylation of E-DMR DMSs in blood leukocytes of control and MA offspring are not intermediate, but blood has intermediate CpGs that are malleable by MA. **G**. Conservation of E-DMRs compared to random control regions sampled by eRRBS. Student T-test p-value 1.22×10^{-71}.

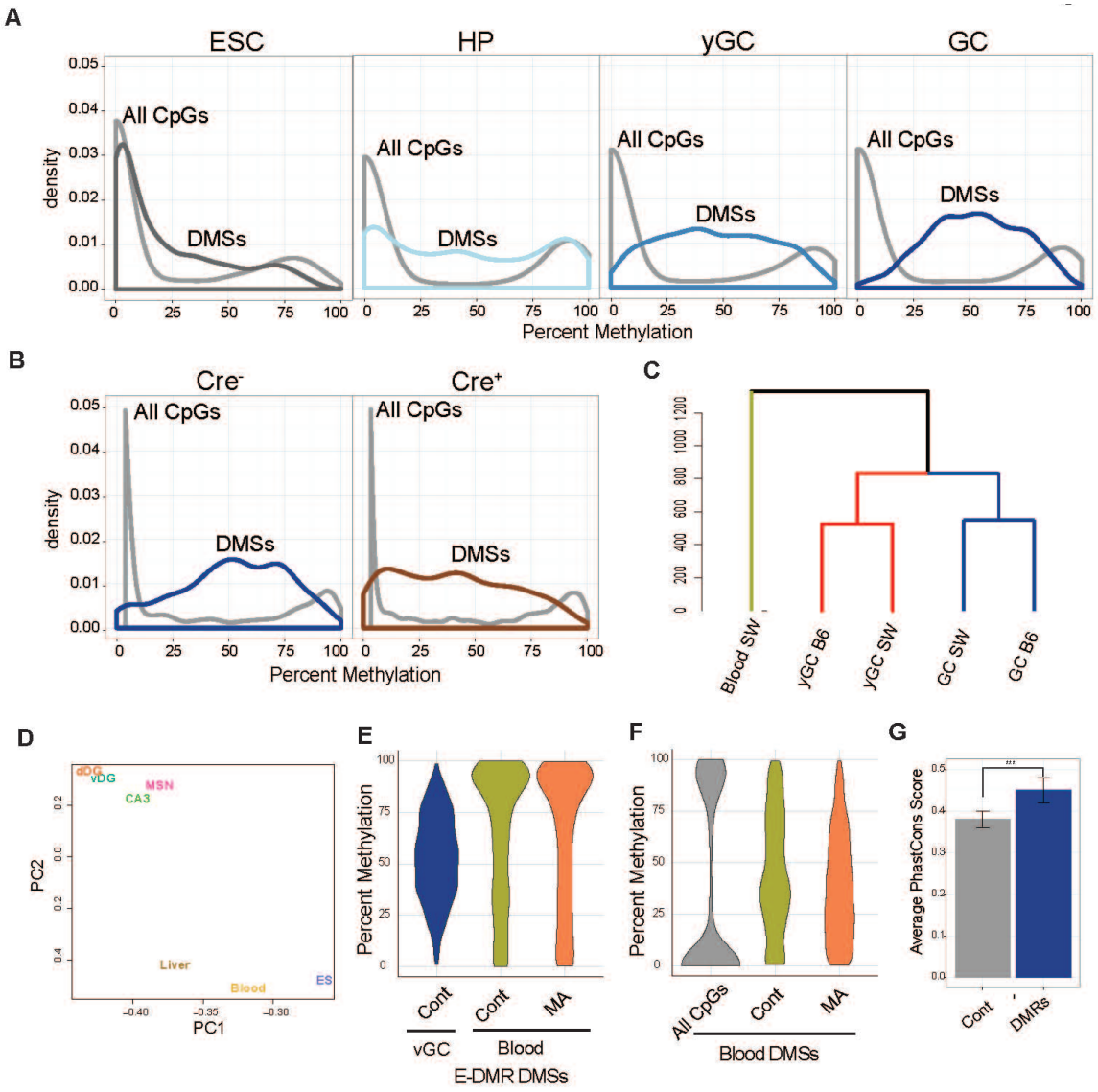
A
ESC
HP
yGC
GC
All CpGs
DMSs
density
Percent Methylation
B
Cre-
Cre+
C
Blood SW
yGC B6
yGC SW
GC SW
GC B6
D
PC1
PC2
Liver
Blood
ES
E
Percent Methylation
Cont
MA
vGC
Blood
E-DMR DMSs
F
All CpGs
Blood DMSs
G
Average PhastCons Score
DMRs

To determine the location and tissue specificity of E-DMRs, DNA methylation levels were compared in multiple tissue types. Another group of GCs reside in the dorsal (d) part of the DG/hippocampus. While v-GCs are associated with emotional behaviors, d-GCs regulate cognitive behaviors[118]. PCA analysis showed similar methylation levels at E-DMR DMSs in v- and d-GCs (Fig. 5.3D). This is consistent with their shared origin from HPs in the dorsal telencephalon early in development. CpG methylation levels at E-DMR DMSs were also similar in hippocampal CA3 neurons (originate from HPs but born earlier than GCs[57,254]), and even in striatal medium spiny neurons (MSNs), originating from the ventral telencephalon[49]. However, the methylation level of malleable CpGs were different in liver, blood leukocytes and ESCs (see also Fig. 5.3C). Specifically, these sites were mostly unmethylated in ESCs (Fig. 5.3A) and mostly methylated in blood leukocytes, in both the control and MA offspring (Fig. 5.3E). Overall, these data indicate that the methylation status of DMSs within E-DMRs are similar across different neuronal subtypes, but the similarity does not extend to non-neuronal tissue. More specifically, the more similar the tissue the greater the similarity of DNA methylation at E-DMRs. However, methylation profiling of blood leukocytes in the MA model revealed that blood leukocytes do have malleable intermediately methylated regions, but at different genomic locations (Fig. 5.3F). Taken together, environmentally malleable intermediate methylated sites are not limited to neurons, but their genomic location is tissue specific.

Finally, we assessed the evolutionary conservation of neuronal malleable intermediately methylated regions by calculating the average PhastCons scores, generated by comparing 30 mammalian species (UCSC genome browser), at E-DMRs and control eRRBS regions of similar size. Although control sequences had a relatively high conservation score, due to eRRBS bias towards regions with higher

than average CpG content (for example exons), E-DMRs had a significantly higher score suggesting greater evolutionary conservation across mammalian species (Fig. 5.3G).

5.3 Discussion

These results support the original hypothesis that different environmental conditions converge at the epigenetic level. While they each differed in timing, severity, and behavior, and resulted in unique DMRs, the overlap between the three adversities suggests an epigenetic convergence that may in part underlie the anxiety-like behavior. We identified E-DMRs that have specific characteristics that distinguish them from the rest of the genome. Depending of the neuronal subtype, timing and strength of input, different regions will exhibit features that render them malleable and responsive to the environmental input.

However, clustered intermediately methylated sites alone may not be sufficient to produce an E-DMR. Indeed, while a total of 2-3% of CpGs are malleable (which is close to the ~10% total intermediately methylated clustered CpGs, given that only three environmental conditions were tested), only 0.2% of CpGs are in E-DMRs. Additional features that may be required for environmental sensitivity across multiple adverse conditions include, histone modifications, RNA associations, protein-binding, and unique chromatin conformations. In fact many studies have demonstrated the inter-relatedness between DNA methylation and other epigenomic signatures. However, further studies will be needed to determine other unique and specific epigenomic features E-DMRs.

Since CpG methylation at E-DMRs are not allele specific, intermediate methylation at the tissue level reflects epigenetic mosaicism consisting of neurons with methylated and unmethylated CpGs. Because the methylation status of neighboring CpGs in an allele tends to be similar (as determined from single molecule

Illumina reads); the inter-neuron variability in methylation could be extended to E-DMRs (i.e. all or most CpGs in a specific E-DMR are either methylated or unmethylated in a cell). Furthermore, preliminary evidence (not shown) suggests E-DMRs exhibit methylation dependent enhancer activity. Therefore, the ratio of neurons with a methylated vs. unmethylated E-DMRs may determine the number of cells expressing the associated gene or gene isoform(s) at high or low levels, essentially creating transcriptional mosaicism on top of the epigenetic mosaicism. E-DMRs were mapped to genes involved in cell-to-cell adhesion and signaling that are highly regulated in neuronal cells. Therefore, neurons expressing high and low levels of a gene and/or isoform can differ in neuronal functions.

Furthermore, the methylated vs. unmethylated allele ratio at each E-DMR may shift following a sustained environmental influence. Since environmental challenges primarily hypomethylate CpGs within E-DMR, the number of neurons with an unmethylated E-DMR, at the expense of methylated, can increase. The change in the ratio of cells with methylated E-DMRs may alter the topology of the epigenetic and transcriptional mosaicism in the DG. This in turn can have a substantial effect on network function due to sparse coding in GCs, where neurons encode sensory information using a small number of active neurons[255]. The phenomenon of environmental malleability of intermediately methylated CpG sites may help to answer a long standing question in neuroscience regarding how prior experience is stored via epigenetic memory in neuronal networks.

However, there is a delay between the early environmental adversity and differential methylation at E-DMRs after P7, in the adult animal. Furthermore, we were able to show that the overall developmental methylation patterns remain unperturbed until that time point. However, we show that three different stressors, at different time points in development, lead to similar epigenetic changes. This suggests

an intermediate step that connects the initial stressors to the delayed appearance of epigenetic changes in the hippocampus.

Previous studies of the three models of early life adversity report HPA axis activation and elevated proinflammatory markers in both human and animal studies[11,220,222]. In fact exposure of animals to proinflammatory agents, such as IL-6 or IL-10, is sufficient to produce behavioral abnormalities[223,256], while increased inflammatory cytokine expression has been shown to increase anxiety-like behavior[257].Additionally, administration of anti-proinflammatory agents, such as anti-IL-6 or IL-ra, can mitigate early environment induced behavioral abnormalities[223]. Therefore, it is conceivable that there is an immunological intermediary between the initial environmental insult and resulting neurological affect. One mode of transmission could be through the increased number of monocytes in the affected offspring and their transmigration to the brain. Monocytes may develop into macrophages in the brain and activate resident microglia[203]. Microglia participate in programmed cell death, survival, axon remodeling, pruning, and synaptogenesis in various brain regions, including the hippocampus[10,185,203]. Therefore, it is reasonable to hypothesize that an increased number of peripheral monocytes and their transmigration to the brain may contribute, via microglia activation, to the development of anxiety phenotype in affected offspring (Fig. 5.4).

Intermediate methylation at E-DMRs were present not only in GCs, but also in hippocampal CA3 neurons and even in more distant striatal MSNs, indicating that it is a panneuronal feature. However, these genomic regions were not intermediately methylated or malleable in non-neuronal cells. Nonetheless, non-neuronal cells, specifically blood leukocytes, had their own environmentally sensitive intermediately methylated regions. This suggests that malleability at intermediately methylated regions is a general phenomenon. Furthermore, it is possible that tissue-specific

environmentally malleable DMRs may play important roles in tissue specific environmental response. For instance, differential methylation in blood leukocytes, in response to a stressful environment, may trigger an adaptive immunological response.

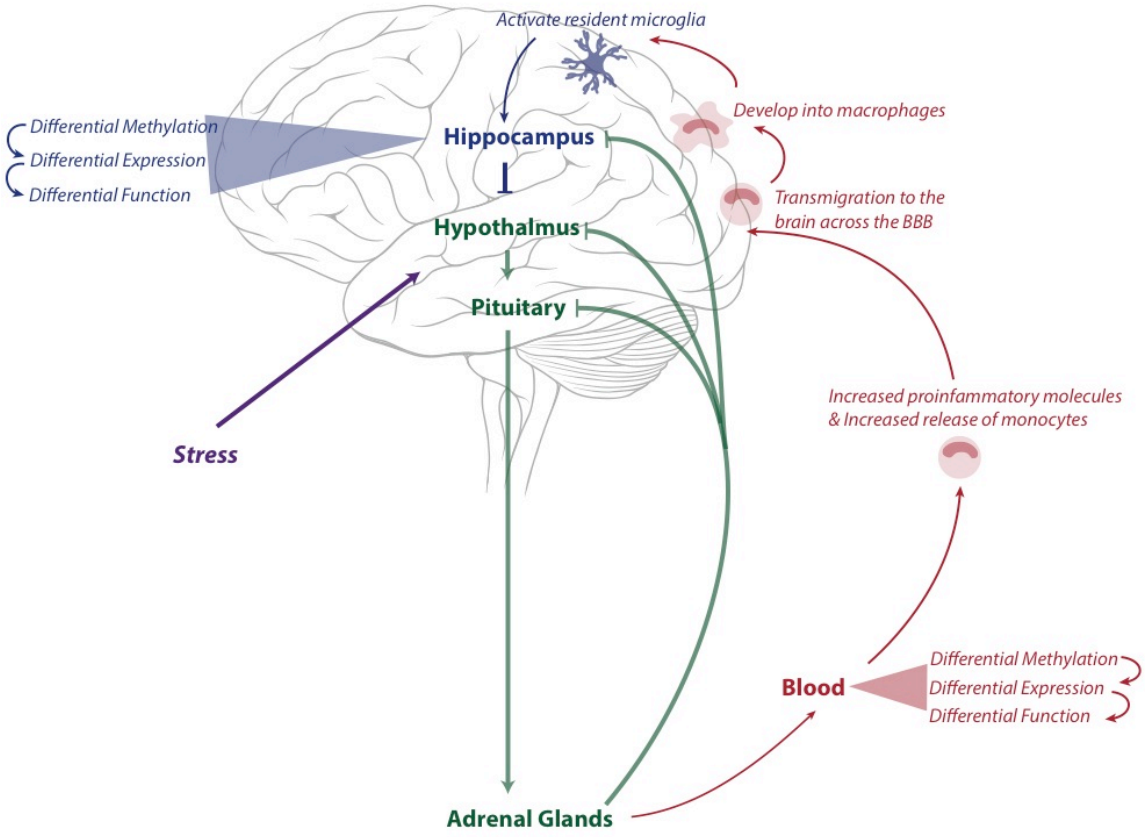

Figure 5.4: Summary of proposed mechanism of stress induced methylation changes in brain. Stress activates the HPA axis (green) resulting in the release of proinflammatory molecules such as glucocorticoids into the blood stream. Environmentally sensitive regions in the blood may respond to these proinflammatory molecules by undergoing differential methylation that may alter the transcriptional profile of the affected genes resulting in the increased release of monocytes into the bloodstream. The monocytes will then transmigrate to the brain where they will transverse the blood brain barrier and develop into macrophages and activate resident microglia. The activated microglia may release factors that will affect neurons in the hippocampus via the differential methylation at E-DMRs.

5.4 Methods

Mice

Animal experiments were carried out in accordance with the Weill Cornell Medical College Institutional Animal Care and Use Committee guidelines. All mice were group housed up to five per cage with 12-hour light/dark cycle with lights on at 6 a.m. Food and water were available ad libitum. Male MA, LPS, and MS mice were generated on the Swiss-Webster (SW, Taconic Biosciences, Germantown, NY) background. The MA offspring were wild-type (WT) mice born to 5-HT1AR$^{+/-}$ parents generated as previously described[220]. The LPS offspring were generated following maternal injection of 50μg/mg of LPS once a day from E16 to E18 as previously described[110,221]. For the MS model, newborn pups were removed from the maternal cage for 3 hours per day and placed on a warming pad from P1 to P14[111]. A separate SW WT line provided control WT offspring exposed to normal, WT, early-life environment. Adult mice exposed to chronic unpredictable stress and voluntary wheel running were 8 week old SW males, obtained from Jackson Laboratory. After a 3 day acclimation period, mice were either kept at control conditions or exposed to running or a CUS protocol[258] for 4 weeks. Stressors used for chronic unpredictable stress were: restraint, cold (9 ˚C for 1-2 h), cage shake, forced swim, bobcat odor, lights off, white noise (3-5 h), food deprivation, wet bedding, overnight light, overnight cage tilt, overnight light on, overnight strobe and overnight overcrowding. Two stressors were administered each day. Running animals were kept at similar conditions but in larger cages to accommodate the running wheels.

Behavioral Procedures

All tests for early life adversity models were conducted using offspring aged 8-12 weeks. For adult models of environmental perturbation tests were carried out 12 weeks after exposure to stress or running. Mice were first tested in open field for

overall activity, followed by elevated plus maze and forced swim test, followed by the 3-chamber social interaction test. At least 24 hours rest was allotted between different tests. All tests were conducted between 9 a.m. and 6 p.m. (i.e. during the light cycle). Offspring were selected from ≥ 5 litters. The elevated plus maze was performed using a cross maze with 12 x 2 inch arms at dim light (50 lux)[207]. Animals were introduced to the middle portion of the maze facing an open arm and allowed to freely explore for 10 minutes. Time spent and distance traveled in the open and closed arms were measured by a video-tracking system (Noldus Information Technology, Wageningen, The Netherlands.). The open-field test[12] used a 15 x21 inch black box, divided into 12 even-sized (4 x 3 inch) rectangles. The time spent in and distance traveled in the two rectangles at the center of the field at 150 lux were recorded by the video tracking system to evaluate anxiety, and data was presented as a percentage of total time spent in the field or total distance traveled. In the forced swim test[12] mice were forced to swim in a clear, water-filled cylinder (diameter, 20.3 cm; depth 10cm), essentially as described by Porsolt et.[208]. In this test, immobility of the mice was scored by a blindsided observer for a total of six minutes. The three chamber test was conducted as described[245]. On test days, animals were transported to the dimly illuminated behavioral laboratory and left undisturbed for at least 1 hour before testing.

eRRBS

Brains from naïve male WT, MA, LPS, MS, Stress and Run mice (8-12 weeks old) from at least three different litters were flash frozen on dry ice and cryosectioned (200μM). The v-GC neuronal bodies were microdissected from the sections. DNA was isolated using the DNeasy Blood & Tissue Kit (Qiagen, Valencia, CA). Single end 50bp eRRBS sequencing was performed as described[61], using Illumina HiSeq2000 and 2500 machines according to manufacturer instructions. An in-house pipeline was used for methylation calling and alignment to the mm9 reference genome[102].

Differential methylation and statistical analysis were performed using the MethylKit package in R[102] at default settings. Differentially methylated (DM) sites were defined as sites where the corrected p-value was ≥0.01 and the difference in methylation between two samples was ≥15%. DMRs were calculated as regions containing at least four DMSs, where the distance between two neighboring DMSs was no greater than 1kb. Genomic and CpG island annotations were based on Ensmbl data downloaded from the UCSC genome browser. Promoters were defined as regions ±2kb from the TSS while exons and introns were defined by reference. The percentage of total DM sites in a defined genomic feature was divided by the percentage expected to overlap each genomic feature by chance, based on the percentage of genomic space occupied by that feature, to determine the fold change from expected values. Additional methylation datasets were downloaded from the UCSC genome browser DNA methylation track hub[29,103,104].

RNA-Seq

Naïve adult MA offspring (8-12 weeks old) from at least three different litters were perfused with 30% RNAlater (Ambion) in saline. Brains were frozen on dry ice and sectioned (200μM). The GC layer from V-DG was microdissected from the sections. Total RNA was isolated using the RNeasy Mini Kit (Qiagen). Single end 50bp RNA sequencing was performed on Illumina HiSeq2000 and 2500 machines and aligned to the mm9 reference genome using TopHat software version 2.0.11[105]. Default parameters were used with the addition of "--no-novel-juncs" to align exclusively to known genes and isoforms. Genes were counted using HT-seq program[106] with the parameter "intersection-strict". Values for gene expression were calculated using EdgeR[107] package in R using tagwise dispersion and default parameters. Differentially expressed genes were determined using Benjamini-Hochberg corrected p=0.05 threshold.

Transfection and Luciferase Reporter Assay

Plasmids were constructed using the In-Fusion Cloning Kit (*Clontech* Laboratories, Mountain View, CA). HEK293 cells were cultured in culture media containing 88% DMEM + 10mM HEPES, 1% penicillin/streptomycin, 10% FBS, and 1% L-Glutamine in a 5% CO_2 37°C incubator. Plasmids were transfected into HEK293 cell cultures using Lipofectamine Transfection Reagent (Life Technologies, Grand Island, NY) in triplicates. Briefly, 0.2-E6 cells were seeded in 12-well plates in 1mL of culture media. 24 hours later, 1µg of plasmid DNA was diluted in 85µl Opti-MEM media (Life Technologies) in tubes. After 5 minute incubation, 6µl Lipofectamine Transfection Reagent was added, followed by 20 minute incubation. 85µl of this solution was added to each well of HEK293 cells. The following day, media was aspirated and replaced with 400µl of culture media. 48 hours after transfection, 20µl aliquots of media were sampled into 96-well plates. 100µl of Quanti-Luc luciferase substrate (InvivoGen, San Diego, CA) was added to each well, and plates were read immediately for luciferase activity.

Data Analysis

Data are shown as mean ± s.e.m. Outlier data was excluded based on ± 2 s.d. from the mean. One-way or repeated measures ANOVAs or *t* tests were used to compare tests. LSD or Bonferroni *post hoc* analyses were used to assess statistical significance. All graphs and statistical analysis were performed using R (http://ww.r-project.org), Bioconductor (www.bioconductor.org), and ggplot2 (www.ggplot2.org) for visualization, unless stated otherwise.

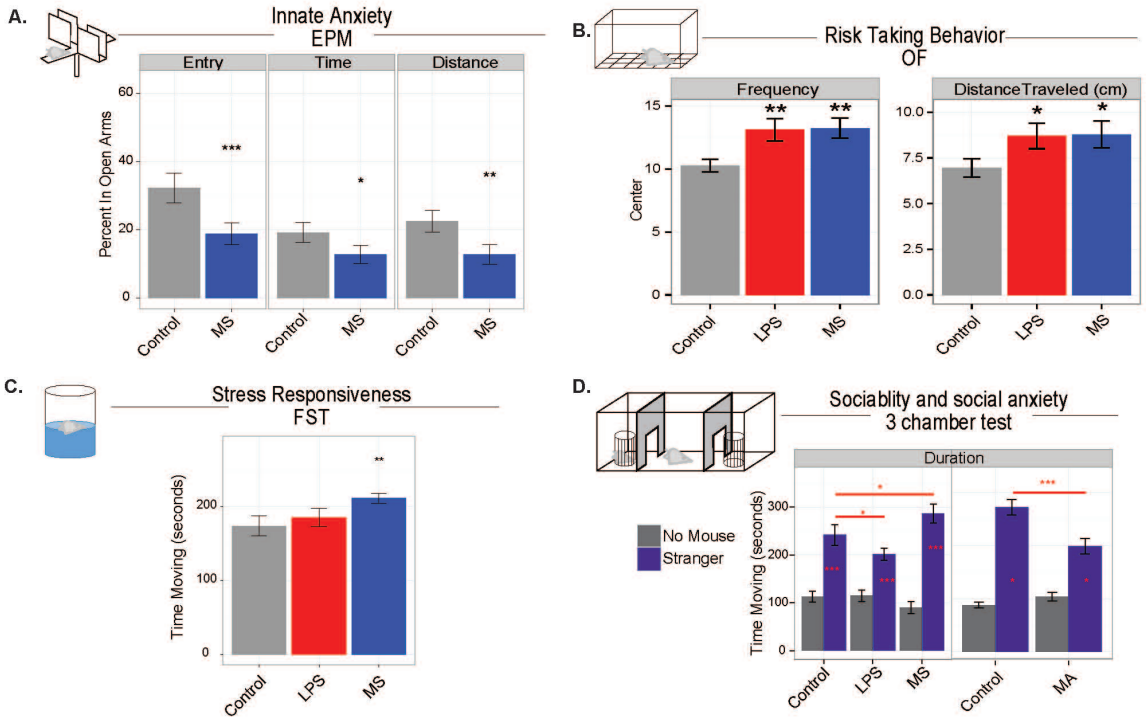

Supplementary Figure 5.1: Behavioral analysis of adult offspring exposed to early life adversity. **A.** Distance traveled in the center field, a measure of exploratory activity (ANOVA: F=3.77, P=0.333, N=10, 15 and 14). LPS offspring exhibit reduced activity (LSD post hoc p=0.018), as well as MS offspring (LSD post hoc p=0.021). **B.** Stress reactivity, measured as mobility in FST (ANOVA: F= 2.86, P=0.0698, N= 13, 15, and 14). LPS mice do no exhibit reduced activity (LSD post hoc p=0.47427). MS offspring exhibit reduced stress reactivity (LSD post hoc p=0.02577). **C.** Social interaction, measured as interaction with stranger mice in the three-chamber sociability and social novelty test (group effect of entry time and distance using Levenes's Test of equality of error variances: F= 3.12, P = 0.013, F=2.98, P = 0.016, F = 2.638, P = 0.029, N = 26, 30 and 30). LPS mice display decreased sociability (LSD post hoc p= 0.661, p = 0.069, p = 0.81) while MS mice display increased sociability (LSD post hoc p= 0.048 , p= 0.045, p = 0.154). **D.** EPM - risk avoidance of the open arm in the EPM as % of total activity. MS mice exhibit increased risk avoidance (group effect of entry, time, and distance; ANOVA: F = 4.12, P= 0.024, F= 2.42, P = 0.10, F= 3.04, P = 0.059; LSD post hoc p=0.009, p = 0.09, p = 0.02, compared to WT; N=13, 15, and 15 mice per group).

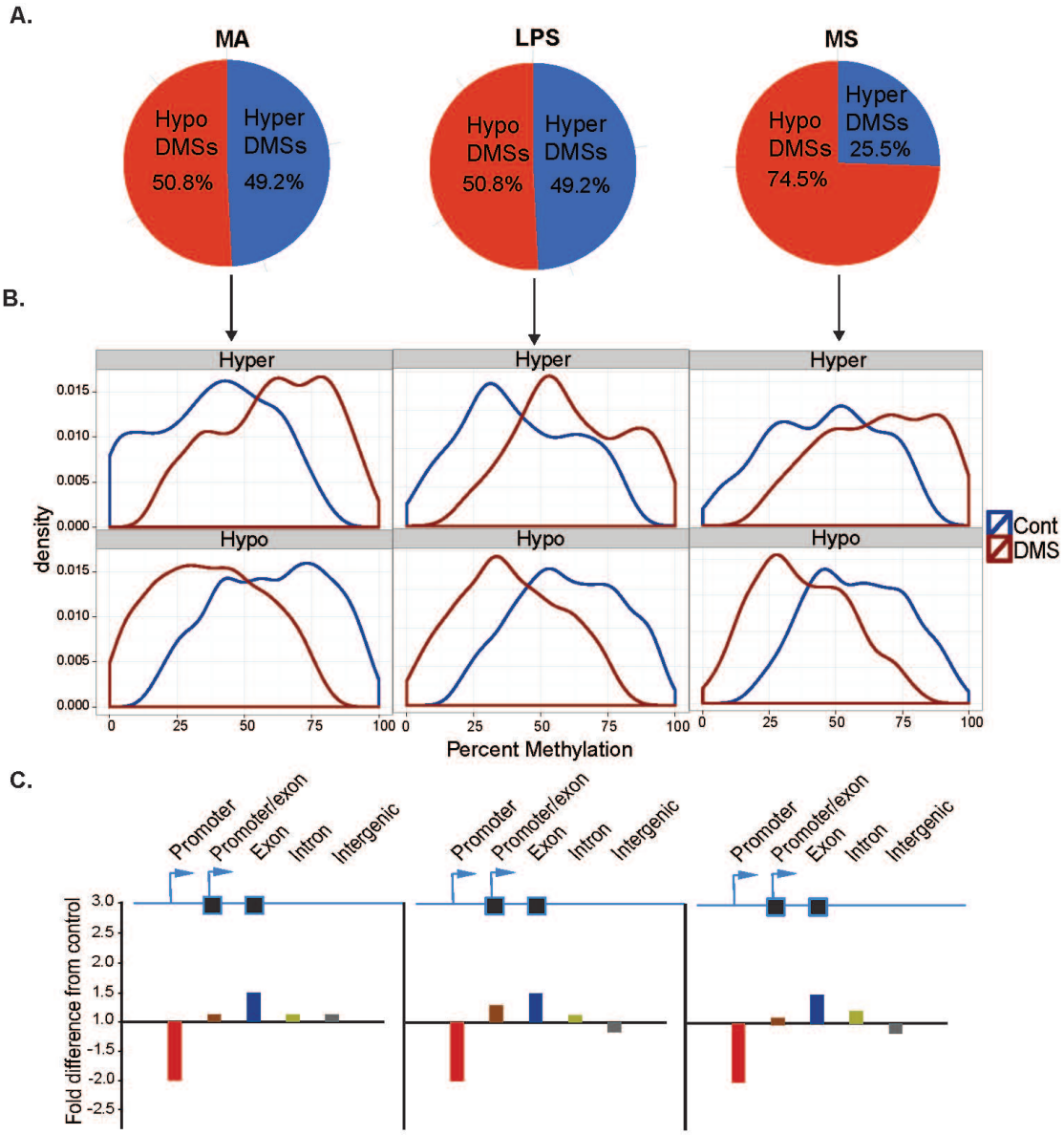

Supplementary Figure 5.2: Differentially methylated regions following individual early life adversities. **A.** Methylation distribution of clustered hyper- and hypo-methylated sites; from left to right: MA, LPS and MS. **B.** Proportion of hyper and hypo methylated sites; from left to right: MA, LPS and MS. Both MA and LPS have a fairly even divide, MS mice have a strong bias toward hypomethylation. **C.** Genomic distribution of DMSs, from left to right: MA, LPS and MS. All three adversities result in exonic enrichment of DMRs.

CHAPTER 6

DISCUSSION

6.1 Brief summary of novel findings

First, Chapter 2 of this work identifies several principles of DNA methylation during development and lineage specification in the brain that have never been described before. This provides a foundation upon which we can understand how the process can be dysregulated in abnormal situations, such as neurodevelopmental disorders. Second, several studies have attempted to specify the epigenetic signature of regions that are sensitive and responds to environmental challenges, such as early life adversity, and which may also store prior environmental experience[16,17,25,259]. However, most of these studies used candidate gene approaches and were unable to define a single characteristic feature that would define regions of environmental sensitivity[16,25,259]. Chapters 3 and 4 identify several features that define environmentally (E) malleable regions. Their most prominent characteristic is an overall intermediate methylation profile due to inter-cellular mosaicism within affected tissue. While intermediately methylated regions have previously been documented in the brain and other tissues[260], no functional role has been associated with them. Beyond their inherent sensitivity and responsiveness, E-DMRs may also explain how a stable, life-long, molecular "memory" of an early environmental insult is maintained in neurons and/or neuronal networks. Based on the data in Chapters 3 and 4, a molecular and network model is proposed that attempts to explain how E-DMRS sense and respond to environmental effects at the molecular level and how their epigenetic changes alter neuronal and network functions that eventually lead to the associated behavioral manifestations (see below). Finally, findings in Chapter 5 support a non-genetic model of heritability by which DNA methylation signatures, and associated behavioral phenotypes, are passed from one generation to the next,

resembling genetic inheritance, but which is based on somatic and gametic parallel epigenetic pathways.

6.2 Molecular Model

Based on the results described in Chapters 3 and 4, there appear to be regions in the genome that display an inherent sensitivity and responsiveness to environmental conditions. Here, a molecular model is proposed that explains the a) sensitivity and b) responsiveness of E-DMRs and c) their capacity to store prior environmental information permanently. This model is proposed here, in the general discussion, because this project is still in progress and would be premature to include in the regular discussion. However, this line of thinking represents the future direction of our work and therefore appropriate to describe here.

Sensitivity: DNA methylation is a highly regulated process. Within a single tissue, majority of CpG sites normally display a fully methylated or unmethylated state[74]. The default state for CpG sites is methylation and mechanisms are in place to prevent methylation where necessary, such as at active gene promoters and CpG islands[74]. The presence of intermediately methylated sites at E-DMRs, represents inter-cellular variability and suggests a greater degree of regulation at these regions. This sensitivity can be due to the local chromatin and/or protein environment of the region. For instance, the local presence of DNA binding proteins such as MeCP2, HDACs as well as histones and their modifications can affect how easily DNA methyltransferases and demethylase enzymes can access and/or change the methylation status of a CpG site[261]. The malleability of these regions suggests a semi-permissive state in which there is a stoichiometric probability that a site will be methylated. The environmentally induced cellular changes could result in a change in the binding affinity of one more factors at E-DMRs, which in turn may change the

affinity of the region to DNA methyltransferases or demethylation components. Alternatively, the environmental stimulus may directly affect the concentration and/or binding affinity of DNA methyltransferases and/or demethylase components, thereby affecting their binding equilibrium. The change in binding and activity of the factors bound at these malleable regions can then have a direct effect on the methylation status of nearby CpG sites.

Responsiveness: The environmental input may change the methylation pattern at one or more E-DMRs within a subpopulation of the cells. Since E-DMRs are located at gene regulatory sequences, and because methylation of E-DMRs modulates gene activity (unpublished data), environmentally induced methylation changes can have a profound effect on gene expression at a fraction of cells within each subpopulation.

Based on previous studies we know that changes in DNA methylation can result in altered gene expression[262,263]. Several studies have described activity mediated activation of synaptic receptors resulting in an intercellular signal cascade resulting in the altered DNA methylation and expression of neuronal genes[24,264]. For instance, neuronal activity of hippocampal granule cell resulted in increased Gadd45b expression[24], which is believed to be a component of a demethylation pathway[265,266]. This in turn was associated with the demethylation of exon IX of the BDNF gene resulting in increased BDNF expression and activity[24].

Memory: The inherent malleability of E-DMRs may be characterized by the stochastic binding and unbinding of local chromatin bound proteins. The binding affinity of these proteins and modifications may be dependent on the presence of additional proteins, co-factors and modifications, as well as local transcriptional activity. Based on some preliminary experiments we know that the changes following acute stress are not the same as those following chronic stress. It is conceivable that

following acute stress there are some local changes at E-DMRs resulting in temporary transcriptional and epigenetic changes. However chronic stress may elicit transcriptional activity or silencing, concurrent with changes at the local chromatin level, that may lead to more stable chromatin modifications. For instance due the inherent sensitivity of these regions in the affected tissue, chronic transcriptional activity will shift the stoichiometric balance of the bound proteins and co-factors. Chromatin associated proteins, histone modifications, RNA binding and DNA methylation are co-regulated. Therefore, the persistent shift in the highly malleable local protein environment may shift the affinity of DNA methyltransferases and demethylases at these regions resulting in a stable shift in local DNA methylation. Unlike the initial stochastic nature of DNA methylation at a particular E-DMR, following chronic environmental stimuli, in the form of early life adversity, will result in a stable shift in a subpopulation of cells in the affected tissue. This will shift the stoichiometric balance of CpGs between the methylated versus unmethylated CpG state in one direction.

6.3 Network Model

The molecular model can be extended to a network model that eventually may explain the environmentally induced behavioral manifestations. Based on theories of processing and sparse coding of information in a neuronal network, sustained environmental input is expected to target a particular subset of cells based on their intrinsic properties, such as the cell type, location as well as proteins and receptors present[255]. Because of the mosaicism in E-DMR methylation, cells that have E-DMRs in a malleable epigenetic state will be affected through the gain and/or loss methylation at particular E-DMRs or clusters of CpG sites within E-DMRs. Interestingly, little to no overlap between E-DMRs and regions that change during

normal neural development and differentiation were observed. This suggests that the methylation pattern develops undisturbed until postnatal development, when, in a delayed fashion, the earlier environmental insult, "overwrites" the developmental pattern. We speculate that the delay is due to an immunological mechanism that links the environmental insult to the brain.

Since E-DMRs are found at highly regulated synaptic genes, this model would explain how the brain can respond to the environment that could be, at least initially, adaptive. However, early life adaptation may result in alternative developmental trajectories that appear to cause disease, and thus maladaptive later in life. For instance in a stressful situation, such as in a war, a mother will display increased anxiety and stress pathology that will be transmitted to the offspring[267,268]. The child will then display similar increased anxiety and stress responsivity as the mother, so as to be better adapted to a volatile and potentially dangerous situation. Similarly, in the case of maternal neglect or abuse the child may seem to adapt by displaying a lack of stranger anxiety or indiscriminate friendliness and sociability to strangers[216,225]. This is perhaps a way to increase the probability of interacting with another individual(s) who may partially compensate for their lack of parental care. It is only when the early life environmental adversity does not match the adult environmental conditions that the initial adaptation becomes a maladaptation. For instance, in the maternal stress situation the increased anxiety and stress-responsivity is ill-suited to a peaceful environment. Similarly, children exposed to maternal neglect early in life, who are subsequently exposed to a stable and nurturing environment, are no longer benefited by increased anxiety and indiscriminate friendliness, which may do them more harm than good. This theory is supported only empirically in humans, but a number of well-controlled ecological studies seem to support it[269-271]. For instance a study of squirrel populations found that mothers in high-density populations released more

glucocorticoids that resulted in increased growth rates in their offspring[271]. This provides their children with an adaptive advantage to the environmental conditions with the tradeoff of shorter lifespan.

In summary, the experience dependent variations in DNA methylation may prime the genome for differential transcriptional response to later events. This metaplasticity may be especially important in brain regions responsible for processing environmental input to elicit a behavioral response.

6.4 Implications

The presence of environmentally sensitive DMRs in blood at hematopoietic genes suggests that each tissue type may have its own environmentally sensitive regions (Fig. 4.3F). Similar to our findings in the brain and blood (Fig. 4.3E and 4.3F), these regions may be responsible for tissue-specific responses to the environment. We, and others[260], have identified similar regions of intermediate methylation in other neuronal tissues as well as others such as the heart, liver. These tissue specific regions of intermediate methylation were enriched at exonic regions of tissue specific genes in multiple species, including humans[260]. If this mode of environmental regulation is similar to that described in this work, it is conceivable that they can be similarly dysregulated by adverse environmental conditions, specific to the affected tissue. Therefore, blood mononuclear cell DMRs could be used as a proxy to determine if neuronal DMRs were affected by the environmental insult.

In a heterogeneous population of individuals not all of those exposed to early environmental adversity will exhibit behavioral pathology. For instance, not all children exposed to a traumatic early life environment such as war or abuse will display adult behavioral pathologies[267]. However, it would be useful to identify which children, who experienced early trauma, have been affected at the molecular level that

may predispose them for subsequent adult psychiatric abnormalities. Obtaining neural tissue, even neurons from olfactory epithelia, is not feasible (or ethical) in these circumstances. Therefore, identification of blood-specific environmentally sensitive regions (Chapter 4) may provide a useful diagnostic tool. By identifying and classifying adversity-specific blood DMRs in affected populations versus non-affected, we can create a reference for which to compare the blood of children exposed to adversity but do not yet exhibit any symptoms. In this way a simple blood test can be designed to determine the methylation at adversity-specific blood DMRs.

Another area of translating our E-DMR data to the clinic is the development of therapeutics that target the epigenetically modified genes, mostly involved in synaptic functions. These include neuronal adhesion molecules, receptors and intracellular signaling. Another possible application is methyl donor therapy[234]. Although it is nonspecific, our work suggests that in the adult CNS, regions with intermediate methylation preferentially respond to the level of methyl donors, while fully methylated and non-methylated areas remain stable. As discussed earlier, only 1-2% of the genome is in intermediate level of methylation. Therefore, a treatment that is considered non-specific, may actually be relatively selective to malleable regions with relatively moderate side effects. Indeed, a number of papers reported behavioral normalization in animal models following environmental insults following a methyl treatment[234,272,273]. For example, in one study of maternal separation in rats, the increased anxiety was mitigated by feeding them a methyl supplementation diet[234]. Another study of rats that displayed anxiety following early life exposure to low licking and grooming mothers found that the anxiety phenotype, and associated differential methylation, could be reversed through a methyl supplementation diet later in life[234].

In summary, the advances presented in this work may provide to foundation and knowledge necessary to make significant advances in the identification and treatment of individuals affected by adverse early life experiences.

BIBLIOGRAPHY

1 Kessler, R. C. *et al.* Lifetime and 12-month prevalence of DSM-III-R psychiatric disorders in the United States. Results from the National Comorbidity Survey. *Arch Gen Psychiatry* **51**, 8-19 (1994).

2 Baker-Andresen, D., Ratnu, V. S. & Bredy, T. W. Dynamic DNA methylation: a prime candidate for genomic metaplasticity and behavioral adaptation. *Trends in neurosciences* **36**, 3-13 (2013).

3 Tsuang, M. T., Bar, J. L., Stone, W. S. & Faraone, S. V. Gene-environment interactions in mental disorders. *World psychiatry : official journal of the World Psychiatric Association* **3**, 73-83 (2004).

4 Toth, M. Mechanisms of non-genetic inheritance and psychiatric disorders. *Neuropsychopharmacology : official publication of the American College of Neuropsychopharmacology* **40**, 129-140 (2015).

5 Lv, J., Xin, Y., Zhou, W. & Qiu, Z. The epigenetic switches for neural development and psychiatric disorders. *Journal of genetics and genomics = Yi chuan xue bao* **40**, 339-346 (2013).

6 Fuccillo, M., Joyner, A. L. & Fishell, G. Morphogen to mitogen: the multiple roles of hedgehog signalling in vertebrate neural development. *Nature reviews. Neuroscience* **7**, 772-783, doi:10.1038/nrn1990 (2006).

7 Charron, F. & Tessier-Lavigne, M. Novel brain wiring functions for classical morphogens: a role as graded positional cues in axon guidance. *Development* **132**, 2251-2262, doi:10.1242/dev.01830 (2005).

8 Liu, B. *et al.* Maternal hematopoietic TNF, via milk chemokines, programs hippocampal development and memory. *Nature neuroscience* **17**, 97-105 (2014).

9 Bale, T. L. Epigenetic and transgenerational reprogramming of brain development. *Nature reviews. Neuroscience* **16**, 332-344, doi:10.1038/nrn3818 (2015).

10 Knuesel, I. *et al.* Maternal immune activation and abnormal brain development across CNS disorders. *Nature reviews. Neurology* **10**, 643-660, doi:10.1038/nrneurol.2014.187 (2014).

11 Kalinichev, M., Easterling, K. W., Plotsky, P. M. & Holtzman, S. G. Long-lasting changes in stress-induced corticosterone response and anxiety-like behaviors as a consequence of neonatal maternal separation in Long-Evans rats. *Pharmacology, biochemistry, and behavior* **73**, 131-140 (2002).

12 Gleason, G. *et al.* The serotonin1A receptor gene as a genetic and prenatal maternal environmental factor in anxiety. *Proc Natl Acad Sci U S A* **107**, 7592-7597 (2010).

13 Abdolmaleky, H. M., Thiagalingam, S. & Wilcox, M. Genetics and epigenetics in major psychiatric disorders: dilemmas, achievements, applications, and future scope. *Am J Pharmacogenomics* **5**, 149-160, doi:532 [pii] (2005).

14 Craddock, N. & Owen, M. J. The Kraepelinian dichotomy - going, going... but still not gone. *The British journal of psychiatry : the journal of mental science* **196**, 92-95 (2010).
15 Kapur, S., Phillips, A. G. & Insel, T. R. Why has it taken so long for biological psychiatry to develop clinical tests and what to do about it? *Molecular psychiatry* **17**, 1174-1179 (2012).
16 Dias, B. G. & Ressler, K. J. Parental olfactory experience influences behavior and neural structure in subsequent generations. *Nature neuroscience* **17**, 89-96, doi:10.1038/nn.3594 (2014).
17 Franklin, T. B. *et al.* Epigenetic transmission of the impact of early stress across generations. *Biological psychiatry* **68**, 408-415, doi:10.1016/j.biopsych.2010.05.036 (2010).
18 Gapp, K. *et al.* Implication of sperm RNAs in transgenerational inheritance of the effects of early trauma in mice. *Nature neuroscience* **17**, 667-669, doi:10.1038/nn.3695 (2014).
19 Guerrero-Bosagna, C., Settles, M., Lucker, B. & Skinner, M. K. Epigenetic transgenerational actions of vinclozolin on promoter regions of the sperm epigenome. *PLoS One* **5**, doi:10.1371/journal.pone.0013100 (2010).
20 Walker, A. K., Hawkins, G., Sominsky, L. & Hodgson, D. M. Transgenerational transmission of anxiety induced by neonatal exposure to lipopolysaccharide: implications for male and female germ lines. *Psychoneuroendocrinology* **37**, 1320-1335 (2012).
21 Smrt, R. D. *et al.* Mecp2 deficiency leads to delayed maturation and altered gene expression in hippocampal neurons. *Neurobiology of disease* **27**, 77-89 (2007).
22 Blackman, M. P., Djukic, B., Nelson, S. B. & Turrigiano, G. G. A critical and cell-autonomous role for MeCP2 in synaptic scaling up. *J Neurosci* **32**, 13529-13536 (2012).
23 Bienvenu, T. & Chelly, J. Molecular genetics of Rett syndrome: when DNA methylation goes unrecognized. *Nat Rev Genet* **7**, 415-426 (2006).
24 Ma, D. K. *et al.* Neuronal activity-induced Gadd45b promotes epigenetic DNA demethylation and adult neurogenesis. *Science* **323**, 1074-1077 (2009).
25 Novikova, S. I. *et al.* Maternal cocaine administration in mice alters DNA methylation and gene expression in hippocampal neurons of neonatal and prepubertal offspring. *PLoS One* **3**, e1919 (2008).
26 Oh, J. E. *et al.* Differential gene body methylation and reduced expression of cell adhesion and neurotransmitter receptor genes in adverse maternal environment. *Translational psychiatry* **3**, e218 (2013).
27 Goldberg, A. D., Allis, C. D. & Bernstein, E. Epigenetics: a landscape takes shape. *Cell* **128**, 635-638 (2007).
28 Seisenberger, S. *et al.* Reprogramming DNA methylation in the mammalian life cycle: building and breaking epigenetic barriers. *Philosophical transactions of the Royal Society of London. Series B, Biological sciences* **368**, 20110330 (2013).

29 Smith, Z. D. *et al.* A unique regulatory phase of DNA methylation in the early mammalian embryo. *Nature* **484**, 339-344, doi:10.1038/nature10960 (2012).
30 Lister, R. *et al.* Global epigenomic reconfiguration during mammalian brain development. *Science* **341**, 1237905, doi:10.1126/science.1237905 (2013).
31 Borgel, J. *et al.* Targets and dynamics of promoter DNA methylation during early mouse development. *Nat Genet* **42**, 1093-1100 (2010).
32 Paulsen, M. & Ferguson-Smith, A. C. DNA methylation in genomic imprinting, development, and disease. *J Pathol* **195**, 97-110 (2001).
33 Casey, B. J., Tottenham, N., Liston, C. & Durston, S. Imaging the developing brain: what have we learned about cognitive development? *Trends Cogn Sci* **9**, 104-110 (2005).
34 Forster, E., Zhao, S. & Frotscher, M. Laminating the hippocampus. *Nature reviews. Neuroscience* **7**, 259-267 (2006).
35 Ji-eun Oh, N. C., Judit Gal, Stuart Andrews, Georgia Gleason, Rita & Shaknovich, A. M., Fabien Campagne, Miklos Toth. Maternal Serotonin1A Receptor Programs the Level of Anxiety via Exonic CpG-Island Methylation in the Offspring Hippocampus. (2011).
36 Murgatroyd, C. *et al.* Dynamic DNA methylation programs persistent adverse effects of early-life stress. *Nature neuroscience* **12**, 1559-1566 (2009).
37 Halmoy, A. *et al.* Attention-deficit/hyperactivity disorder symptoms in offspring of mothers with impaired serotonin production. *Arch Gen Psychiatry* **67**, 1033-1043 (2010).
38 Atladottir, H. O. *et al.* Maternal infection requiring hospitalization during pregnancy and autism spectrum disorders. *Journal of autism and developmental disorders* **40**, 1423-1430 (2010).
39 Bowers, M. E. & Yehuda, R. Intergenerational Transmission of Stress in Humans. *Neuropsychopharmacology : official publication of the American College of Neuropsychopharmacology*, doi:10.1038/npp.2015.247 (2015).
40 Wehmer, F., Porter, R. H. & Scales, B. Pre-mating and pregnancy stress in rats affects behaviour of grandpups. *Nature* **227**, 622 (1970).
41 Morgan, C. P. & Bale, T. L. Early prenatal stress epigenetically programs dysmasculinization in second-generation offspring via the paternal lineage. *J Neurosci* **31**, 11748-11755, doi:10.1523/JNEUROSCI.1887-11.2011 (2011).
42 Yehuda, R., Bell, A., Bierer, L. M. & Schmeidler, J. Maternal, not paternal, PTSD is related to increased risk for PTSD in offspring of Holocaust survivors. *Journal of psychiatric research* **42**, 1104-1111, doi:10.1016/j.jpsychires.2008.01.002 (2008).
43 Yehuda, R., Schmeidler, J., Wainberg, M., Binder-Brynes, K. & Duvdevani, T. Vulnerability to posttraumatic stress disorder in adult offspring of Holocaust survivors. *The American journal of psychiatry* **155**, 1163-1171 (1998).

44 Moore, L. D., Le, T. & Fan, G. DNA methylation and its basic function. *Neuropsychopharmacology* **38**, 23-38, doi:10.1038/npp.2012.112 (2013).
45 Stadler, M. B. *et al.* DNA-binding factors shape the mouse methylome at distal regulatory regions. *Nature* **480**, 490-495 (2011).
46 Thurman, R. E. *et al.* The accessible chromatin landscape of the human genome. *Nature* **489**, 75-82, doi:10.1038/nature11232 (2012).
47 Mohn, F. *et al.* Lineage-specific polycomb targets and de novo DNA methylation define restriction and potential of neuronal progenitors. *Molecular cell* **30**, 755-766 (2008).
48 Hirabayashi, Y. & Gotoh, Y. Epigenetic control of neural precursor cell fate during development. *Nature reviews* **11**, 377-388 (2010).
49 Wilson, S. W. & Rubenstein, J. L. Induction and dorsoventral patterning of the telencephalon. *Neuron* **28**, 641-651 (2000).
50 Bayer, S. A. Development of the hippocampal region in the rat. II. Morphogenesis during embryonic and early postnatal life. *J Comp Neurol* **190**, 115-134 (1980).
51 Deacon, T. W., Pakzaban, P. & Isacson, O. The lateral ganglionic eminence is the origin of cells committed to striatal phenotypes: neural transplantation and developmental evidence. *Brain Res* **668**, 211-219 (1994).
52 Campbell, K. Dorsal-ventral patterning in the mammalian telencephalon. *Current opinion in neurobiology* **13**, 50-56 (2003).
53 Galceran, J., Miyashita-Lin, E. M., Devaney, E., Rubenstein, J. L. & Grosschedl, R. Hippocampus development and generation of dentate gyrus granule cells is regulated by LEF1. *Development (Cambridge, England)* **127**, 469-482 (2000).
54 Ericson, J. *et al.* Sonic hedgehog induces the differentiation of ventral forebrain neurons: a common signal for ventral patterning within the neural tube. *Cell* **81**, 747-756 (1995).
55 Yun, K., Potter, S. & Rubenstein, J. L. Gsh2 and Pax6 play complementary roles in dorsoventral patterning of the mammalian telencephalon. *Development* **128**, 193-205 (2001).
56 Horton, S., Meredith, A., Richardson, J. A. & Johnson, J. E. Correct coordination of neuronal differentiation events in ventral forebrain requires the bHLH factor MASH1. *Mol Cell Neurosci* **14**, 355-369, doi:10.1006/mcne.1999.0791 (1999).
57 Altman, J. & Bayer, S. A. Prolonged sojourn of developing pyramidal cells in the intermediate zone of the hippocampus and their settling in the stratum pyramidale. *J Comp Neurol* **301**, 343-364 (1990).
58 Wichterle, H., Turnbull, D. H., Nery, S., Fishell, G. & Alvarez-Buylla, A. In utero fate mapping reveals distinct migratory pathways and fates of neurons born in the mammalian basal forebrain. *Development* **128**, 3759-3771 (2001).
59 Kamiya, D. *et al.* Intrinsic transition of embryonic stem-cell differentiation into neural progenitors. *Nature* **470**, 503-509 (2011).

60 Papaioannou, V. E., McBurney, M. W., Gardner, R. L. & Evans, M. J. Fate of teratocarcinoma cells injected into early mouse embryos. *Nature* **258**, 70-73 (1975).
61 Akalin, A. *et al.* Base-pair resolution DNA methylation sequencing reveals profoundly divergent epigenetic landscapes in acute myeloid leukemia. *PLoS Genet* **8**, e1002781 (2012).
62 Xie, W. *et al.* Base-resolution analyses of sequence and parent-of-origin dependent DNA methylation in the mouse genome. *Cell* **148**, 816-831, doi:10.1016/j.cell.2011.12.035 (2012).
63 Lister, R. *et al.* Human DNA methylomes at base resolution show widespread epigenomic differences. *Nature* **462**, 315-322 (2009).
64 Harris, R. A. *et al.* Comparison of sequencing-based methods to profile DNA methylation and identification of monoallelic epigenetic modifications. *Nat Biotechnol*.
65 Ramsahoye, B. H. *et al.* Non-CpG methylation is prevalent in embryonic stem cells and may be mediated by DNA methyltransferase 3a. *Proc Natl Acad Sci U S A* **97**, 5237-5242 (2000).
66 Ziller, M. J. *et al.* Genomic Distribution and Inter-Sample Variation of Non-CpG Methylation across Human Cell Types. *PLoS Genet* **7**, e1002389 (2011).
67 Fritz, E. L. & Papavasiliou, F. N. Cytidine deaminases: AIDing DNA demethylation? *Genes Dev* **24**, 2107-2114 (2010).
68 Nabel, C. S. *et al.* AID/APOBEC deaminases disfavor modified cytosines implicated in DNA demethylation. *Nat Chem Biol* **8**, 751-758, doi:10.1038/nchembio.1042 (2012).
69 Kohli, R. M. & Zhang, Y. TET enzymes, TDG and the dynamics of DNA demethylation. *Nature* **502**, 472-479, doi:10.1038/nature12750 (2013).
70 Arand, J. *et al.* In vivo control of CpG and non-CpG DNA methylation by DNA methyltransferases. *PLoS Genet* **8**, e1002750 (2012).
71 Grove, E. A. & Tole, S. Patterning events and specification signals in the developing hippocampus. *Cereb Cortex* **9**, 551-561 (1999).
72 Gutierrez-Arcelus, M. *et al.* Passive and active DNA methylation and the interplay with genetic variation in gene regulation. *eLife* **2**, e00523.
73 Gutierrez-Arcelus, M. *et al.* Passive and active DNA methylation and the interplay with genetic variation in gene regulation. *Elife* **2**, e00523, doi:10.7554/eLife.00523 (2013).
74 Jones, P. A. Functions of DNA methylation: islands, start sites, gene bodies and beyond. *Nat Rev Genet* **13**, 484-492 (2012).
75 Gerdeman, G. L., Ronesi, J. & Lovinger, D. M. Postsynaptic endocannabinoid release is critical to long-term depression in the striatum. *Nat Neurosci* **5**, 446-451, doi:10.1038/nn832 (2002).
76 Malenka, R. C. & Bear, M. F. LTP and LTD: an embarrassment of riches. *Neuron* **44**, 5-21, doi:10.1016/j.neuron.2004.09.012 (2004).
77 Do Rego, J. L. *et al.* Neurosteroid biosynthesis: enzymatic pathways and neuroendocrine regulation by neurotransmitters and neuropeptides.

Front Neuroendocrinol **30**, 259-301, doi:10.1016/j.yfrne.2009.05.006 (2009).
78 Sonnino, S., Mauri, L., Chigorno, V. & Prinetti, A. Gangliosides as components of lipid membrane domains. *Glycobiology* **17**, 1R-13R, doi:10.1093/glycob/cwl052 (2007).
79 Wu, H. *et al.* Dnmt3a-dependent nonpromoter DNA methylation facilitates transcription of neurogenic genes. *Science* **329**, 444-448 (2010).
80 Gu, T. P. *et al.* The role of Tet3 DNA dioxygenase in epigenetic reprogramming by oocytes. *Nature* **477**, 606-610, doi:10.1038/nature10443 (2011).
81 Xu, Y. *et al.* Tet3 CXXC domain and dioxygenase activity cooperatively regulate key genes for Xenopus eye and neural development. *Cell* **151**, 1200-1213, doi:10.1016/j.cell.2012.11.014 (2012).
82 Hahn, M. A. *et al.* Dynamics of 5-hydroxymethylcytosine and chromatin marks in Mammalian neurogenesis. *Cell Rep* **3**, 291-300, doi:10.1016/j.celrep.2013.01.011 (2013).
83 Li, T. *et al.* Critical role of Tet3 in neural progenitor cell maintenance and terminal differentiation. *Mol Neurobiol* **51**, 142-154, doi:10.1007/s12035-014-8734-5 (2015).
84 Feng, J. *et al.* Dnmt1 and Dnmt3a maintain DNA methylation and regulate synaptic function in adult forebrain neurons. *Nature neuroscience* **13**, 423-430 (2010).
85 Oliveira, A. M., Hemstedt, T. J. & Bading, H. Rescue of aging-associated decline in Dnmt3a2 expression restores cognitive abilities. *Nat Neurosci* **15**, 1111-1113, doi:10.1038/nn.3151 (2012).
86 Varley, K. E. *et al.* Dynamic DNA methylation across diverse human cell lines and tissues. *Genome Res* **23**, 555-567, doi:10.1101/gr.147942.112 (2013).
87 Bock, C. *et al.* DNA methylation dynamics during in vivo differentiation of blood and skin stem cells. *Mol Cell* **47**, 633-647, doi:10.1016/j.molcel.2012.06.019 (2012).
88 Eden, A., Gaudet, F., Waghmare, A. & Jaenisch, R. Chromosomal instability and tumors promoted by DNA hypomethylation. *Science (New York, N.Y* **300**, 455 (2003).
89 Li, J. *et al.* Genomic hypomethylation in the human germline associates with selective structural mutability in the human genome. *PLoS genetics* **8**, e1002692 (2012).
90 Ramirez-Carrozzi, V. R. *et al.* A unifying model for the selective regulation of inducible transcription by CpG islands and nucleosome remodeling. *Cell* **138**, 114-128, doi:10.1016/j.cell.2009.04.020 (2009).
91 Baubec, T., Ivánek, R., Lienert, F. & Schübeler, D. Methylation-dependent and -independent genomic targeting principles of the MBD protein family. *Cell* **153**, 480-492, doi:10.1016/j.cell.2013.03.011 (2013).

92 Lewis, J. D. *et al.* Purification, sequence, and cellular localization of a novel chromosomal protein that binds to methylated DNA. *Cell* **69**, 905-914 (1992).
93 Hu, S. *et al.* DNA methylation presents distinct binding sites for human transcription factors. *Elife* **2**, e00726, doi:10.7554/eLife.00726 (2013).
94 Cicchetti, D. & Toth, S. L. Child maltreatment. *Annu Rev Clin Psychol* **1**, 409-438, doi:10.1146/annurev.clinpsy.1.102803.144029 (2005).
95 Atladóttir, H. O. *et al.* Maternal infection requiring hospitalization during pregnancy and autism spectrum disorders. *J Autism Dev Disord* **40**, 1423-1430, doi:10.1007/s10803-010-1006-y (2010).
96 Roth, T. L., Lubin, F. D., Funk, A. J. & Sweatt, J. D. Lasting epigenetic influence of early-life adversity on the BDNF gene. *Biol Psychiatry* **65**, 760-769 (2009).
97 McGowan, P. O. *et al.* Promoter-wide hypermethylation of the ribosomal RNA gene promoter in the suicide brain. *PLoS One* **3**, e2085, doi:10.1371/journal.pone.0002085 (2008).
98 Kaneda, M. *et al.* Essential role for de novo DNA methyltransferase Dnmt3a in paternal and maternal imprinting. *Nature* **429**, 900-903 (2004).
99 Chen, J., Kwon, C. H., Lin, L., Li, Y. & Parada, L. F. Inducible site-specific recombination in neural stem/progenitor cells. *Genesis* **47**, 122-131 (2009).
100 Matevossian, A. & Akbarian, S. Neuronal nuclei isolation from human postmortem brain tissue. *J Vis Exp*, doi:10.3791/914 (2008).
101 Jiang, Y., Matevossian, A., Huang, H. S., Straubhaar, J. & Akbarian, S. Isolation of neuronal chromatin from brain tissue. *BMC Neurosci* **9**, 42 (2008).
102 Akalin, A. *et al.* methylKit: a comprehensive R package for the analysis of genome-wide DNA methylation profiles. *Genome biology* **13**, R87, doi:10.1186/gb-2012-13-10-r87 (2012).
103 Seisenberger, S. *et al.* The dynamics of genome-wide DNA methylation reprogramming in mouse primordial germ cells. *Mol Cell* **48**, 849-862, doi:10.1016/j.molcel.2012.11.001 (2012).
104 Song, Q. *et al.* A reference methylome database and analysis pipeline to facilitate integrative and comparative epigenomics. *PLoS One* **8**, e81148, doi:10.1371/journal.pone.0081148 (2013).
105 Kim, D. *et al.* TopHat2: accurate alignment of transcriptomes in the presence of insertions, deletions and gene fusions. *Genome Biol* **14**, R36, doi:10.1186/gb-2013-14-4-r36 (2013).
106 Anders, S., Pyl, P. T. & Huber, W. HTSeq--a Python framework to work with high-throughput sequencing data. *Bioinformatics* **31**, 166-169, doi:10.1093/bioinformatics/btu638 (2015).
107 Robinson, M. D., McCarthy, D. J. & Smyth, G. K. edgeR: a Bioconductor package for differential expression analysis of digital gene expression

data. *Bioinformatics* **26**, 139-140, doi:10.1093/bioinformatics/btp616 (2010).
108 Gilbert, R. *et al.* Burden and consequences of child maltreatment in high-income countries. *Lancet* **373**, 68-81 (2009).
109 Green, J. G. *et al.* Childhood adversities and adult psychiatric disorders in the national comorbidity survey replication I: associations with first onset of DSM-IV disorders. *Arch Gen Psychiatry* **67**, 113-123 (2010).
110 Chen, G. H. *et al.* Acceleration of age-related learning and memory decline in middle-aged CD-1 mice due to maternal exposure to lipopolysaccharide during late pregnancy. *Behavioural brain research* **218**, 267-279, doi:10.1016/j.bbr.2010.11.001 (2011).
111 Veenema, A. H., Reber, S. O., Selch, S., Obermeier, F. & Neumann, I. D. Early life stress enhances the vulnerability to chronic psychosocial stress and experimental colitis in adult mice. *Endocrinology* **149**, 2727-2736, doi:10.1210/en.2007-1469 (2008).
112 Millstein, R. A. & Holmes, A. Effects of repeated maternal separation on anxiety- and depression-related phenotypes in different mouse strains. *Neurosci Biobehav Rev* **31**, 3-17 (2007).
113 Priebe, K. *et al.* Maternal influences on adult stress and anxiety-like behavior in C57BL/6J and BALB/cJ mice: a cross-fostering study. *Dev Psychobiol* **47**, 398-407 (2005).
114 van Velzen, A. & Toth, M. Role of maternal 5-HT(1A) receptor in programming offspring emotional and physical development. *Genes Brain Behav* **9**, 877-885 (2010).
115 Gleason, G., Zupan, B. & Toth, M. Maternal genetic mutations as gestational and early life influences in producing psychiatric disease-like phenotypes in mice. *Frontiers in psychiatry / Frontiers Research Foundation* **2**, 25 (2011).
116 Zoghbi, H. Y. & Warren, S. T. Neurogenetics: advancing the "next-generation" of brain research. *Neuron* **68**, 165-173 (2010).
117 Meaney, M. J. Maternal care, gene expression, and the transmission of individual differences in stress reactivity across generations. *Annu Rev Neurosci* **24**, 1161-1192 (2001).
118 Bannerman, D. M. *et al.* Regional dissociations within the hippocampus--memory and anxiety. *Neurosci Biobehav Rev* **28**, 273-283 (2004).
119 Kjelstrup, K. G. *et al.* Reduced fear expression after lesions of the ventral hippocampus. *Proc Natl Acad Sci U S A* **99**, 10825-10830 (2002).
120 Adhikari, A., Topiwala, M. A. & Gordon, J. A. Synchronized activity between the ventral hippocampus and the medial prefrontal cortex during anxiety. *Neuron* **65**, 257-269 (2010).
121 Ishikawa, A. & Nakamura, S. Ventral hippocampal neurons project axons simultaneously to the medial prefrontal cortex and amygdala in the rat. *J Neurophysiol* **96**, 2134-2138 (2006).

122 Elliott, E., Ezra-Nevo, G., Regev, L., Neufeld-Cohen, A. & Chen, A. Resilience to social stress coincides with functional DNA methylation of the Crf gene in adult mice. *Nat Neurosci* **13**, 1351-1353 (2010).
123 Oberlander, T. F. *et al.* Prenatal exposure to maternal depression, neonatal methylation of human glucocorticoid receptor gene (NR3C1) and infant cortisol stress responses. *Epigenetics* **3**, 97-106 (2008).
124 Zhang, T. Y. *et al.* Maternal care and DNA methylation of a glutamic acid decarboxylase 1 promoter in rat hippocampus. *J Neurosci* **30**, 13130-13137 (2010).
125 McGowan, P. O. *et al.* Epigenetic regulation of the glucocorticoid receptor in human brain associates with childhood abuse. *Nat Neurosci* **12**, 342-348 (2009).
126 Guo, J. U. *et al.* Neuronal activity modifies the DNA methylation landscape in the adult brain. *Nat Neurosci* **14**, 1345-1351 (2011).
127 Rollins, R. A. *et al.* Large-scale structure of genomic methylation patterns. *Genome research* **16**, 157-163 (2006).
128 Khulan, B. *et al.* Comparative isoschizomer profiling of cytosine methylation: the HELP assay. *Genome Res* **16**, 1046-1055 (2006).
129 Meissner, A. *et al.* Genome-scale DNA methylation maps of pluripotent and differentiated cells. *Nature* **454**, 766-770 (2008).
130 Gu, H. *et al.* Preparation of reduced representation bisulfite sequencing libraries for genome-scale DNA methylation profiling. *Nature protocols* **6**, 468-481 (2011).
131 Irizarry, R. A. *et al.* The human colon cancer methylome shows similar hypo- and hypermethylation at conserved tissue-specific CpG island shores. *Nature genetics* **41**, 178-186 (2009).
132 Giannopoulou, E. G. & Elemento, O. An integrated ChIP-seq analysis platform with customizable workflows. *BMC bioinformatics* **12**, 277 (2011).
133 Muramatsu, R., Ikegaya, Y., Matsuki, N. & Koyama, R. Neonatally born granule cells numerically dominate adult mice dentate gyrus. *Neuroscience* **148**, 593-598 (2007).
134 Wood, S. J. & Toth, M. Molecular pathways of anxiety revealed by knockout mice. *Molecular neurobiology* **23**, 101-119 (2001).
135 Charil, A., Laplante, D. P., Vaillancourt, C. & King, S. Prenatal stress and brain development. *Brain research reviews* **65**, 56-79 (2010).
136 Phillips, N. K., Hammen, C. L., Brennan, P. A., Najman, J. M. & Bor, W. Early adversity and the prospective prediction of depressive and anxiety disorders in adolescents. *J Abnorm Child Psychol* **33**, 13-24 (2005).
137 Nemeroff, C. B. Early-Life Adversity, CRF Dysregulation, and Vulnerability to Mood and Anxiety Disorders. *Psychopharmacol Bull* **38 Suppl 1**, 14-20 (2004).
138 McEwen, B. S. Stress and hippocampal plasticity. *Annu Rev Neurosci* **22**, 105-122 (1999).

139 Hodges, E. *et al.* Directional DNA methylation changes and complex intermediate states accompany lineage specificity in the adult hematopoietic compartment. *Molecular cell* **44**, 17-28 (2011).
140 Niehrs, C. & Schafer, A. Active DNA demethylation by Gadd45 and DNA repair. *Trends in cell biology* **22**, 220-227 (2012).
141 Sutton, R. E., Koob, G. F., Le Moal, M., Rivier, J. & Vale, W. Corticotropin releasing factor produces behavioural activation in rats. *Nature* **297**, 331-333 (1982).
142 Smith, G. W. *et al.* Corticotropin releasing factor receptor 1-deficient mice display decreased anxiety, impaired stress response, and aberrant neuroendocrine development. *Neuron* **20**, 1093-1102 (1998).
143 Timpl, P. *et al.* Impaired stress response and reduced anxiety in mice lacking a functional corticotropin-releasing hormone receptor 1. *Nature genetics* **19**, 162-166 (1998).
144 Accili, D. *et al.* A targeted mutation of the D3 dopamine receptor gene is associated with hyperactivity in mice. *Proceedings of the National Academy of Sciences of the United States of America* **93**, 1945-1949 (1996).
145 Ledent, C. *et al.* Aggressiveness, hypoalgesia and high blood pressure in mice lacking the adenosine A2a receptor. *Nature* **388**, 674-678 (1997).
146 Ross, S. A. *et al.* Phenotypic characterization of an alpha 4 neuronal nicotinic acetylcholine receptor subunit knock-out mouse. *J Neurosci* **20**, 6431-6441 (2000).
147 Schlegel, S. *et al.* Decreased benzodiazepine receptor binding in panic disorder measured by IOMAZENIL-SPECT. A preliminary report. *European archives of psychiatry and clinical neuroscience* **244**, 49-51 (1994).
148 Kaschka, W., Feistel, H. & Ebert, D. Reduced benzodiazepine receptor binding in panic disorders measured by iomazenil SPECT. *Journal of psychiatric research* **29**, 427-434 (1995).
149 Tiihonen, J. *et al.* Cerebral benzodiazepine receptor binding and distribution in generalized anxiety disorder: a fractal analysis. *Molecular psychiatry* **2**, 463-471 (1997).
150 Mombereau, C. *et al.* Altered anxiety and depression-related behaviour in mice lacking GABAB(2) receptor subunits. *Neuroreport* **16**, 307-310 (2005).
151 Barkus, C. *et al.* Hippocampal NMDA receptors and anxiety: at the interface between cognition and emotion. *Eur J Pharmacol* **626**, 49-56 (2010).
152 Lee, A. S. *et al.* Forebrain elimination of cacna1c mediates anxiety-like behavior in mice. *Mol Psychiatry* (2012).
153 Dong, Y. *et al.* CREB modulates excitability of nucleus accumbens neurons. *Nature neuroscience* **9**, 475-477 (2006).
154 Catches, J. S., Xu, J. & Contractor, A. Genetic ablation of the GluK4 kainate receptor subunit causes anxiolytic and antidepressant-like behavior in mice. *Behavioural brain research* **228**, 406-414 (2012).
155 Szatmari, P. *et al.* Mapping autism risk loci using genetic linkage and chromosomal rearrangements. *Nature genetics* **39**, 319-328 (2007).

156 Kim, H. G. *et al.* Disruption of neurexin 1 associated with autism spectrum disorder. *American journal of human genetics* **82**, 199-207 (2008).
157 Morrow, E. M. *et al.* Identifying autism loci and genes by tracing recent shared ancestry. *Science (New York, N.Y* **321**, 218-223 (2008).
158 Wang, K. *et al.* Common genetic variants on 5p14.1 associate with autism spectrum disorders. *Nature* **459**, 528-533 (2009).
159 Wisniowiecka-Kowalnik, B. *et al.* Intragenic rearrangements in NRXN1 in three families with autism spectrum disorder, developmental delay, and speech delay. *Am J Med Genet B Neuropsychiatr Genet* **153B**, 983-993 (2010).
160 Attwood, B. K. *et al.* Neuropsin cleaves EphB2 in the amygdala to control anxiety. *Nature* **473**, 372-375 (2011).
161 Figueroa, M. E., Melnick, A. & Greally, J. M. Genome-wide determination of DNA methylation by Hpa II tiny fragment enrichment by ligation-mediated PCR (HELP) for the study of acute leukemias. *Methods Mol Biol* **538**, 395-407 (2009).
162 Figueroa, M. E. *et al.* An integrative genomic and epigenomic approach for the study of transcriptional regulation. *PLoS ONE* **3**, e1882 (2008).
163 Thompson, R. F. *et al.* An analytical pipeline for genomic representations used for cytosine methylation studies. *Bioinformatics (Oxford, England)* **24**, 1161-1167 (2008).
164 Ehrich, M. *et al.* Quantitative high-throughput analysis of DNA methylation patterns by base-specific cleavage and mass spectrometry. *Proceedings of the National Academy of Sciences of the United States of America* **102**, 15785-15790 (2005).
165 Gu, H. *et al.* Genome-scale DNA methylation mapping of clinical samples at single-nucleotide resolution. *Nature methods* **7**, 133-136 (2010).
166 Li, H. & Durbin, R. Fast and accurate short read alignment with Burrows-Wheeler transform. *Bioinformatics* **25**, 1754-1760 (2009).
167 Bohacek, J., Gapp, K., Saab, B. J. & Mansuy, I. M. Transgenerational epigenetic effects on brain functions. *Biol Psychiatry* **73**, 313-320, doi:10.1016/j.biopsych.2012.08.019 (2013).
168 Dias, B. G. & Ressler, K. J. Parental olfactory experience influences behavior and neural structure in subsequent generations. *Nat Neurosci*, doi:10.1038/nn.3594 (2013).
169 Petropoulos, S., Matthews, S. G. & Szyf, M. Adult glucocorticoid exposure leads to transcriptional and DNA methylation changes in nuclear steroid receptors in the hippocampus and kidney of mouse male offspring. *Biol Reprod* **90**, 43, doi:10.1095/biolreprod.113.115899 (2014).
170 Yehuda, R. *et al.* Influences of maternal and paternal PTSD on epigenetic regulation of the glucocorticoid receptor gene in Holocaust survivor offspring. *Am J Psychiatry* **171**, 872-880, doi:10.1176/appi.ajp.2014.13121571 (2014).

171 Scharf, M. Long-term effects of trauma: psychosocial functioning of the second and third generation of Holocaust survivors. *Development and psychopathology* **19**, 603-622 (2007).
172 Sigal, J. J., DiNicola, V. F. & Buonvino, M. Grandchildren of survivors: can negative effects of prolonged exposure to excessive stress be observed two generations later? *Canadian journal of psychiatry* **33**, 207-212 (1988).
173 Brown, A. S. *et al.* Elevated maternal interleukin-8 levels and risk of schizophrenia in adult offspring. *Am J Psychiatry* **161**, 889-895 (2004).
174 Halmoy, A. *et al.* Attention-deficit/hyperactivity disorder symptoms in offspring of mothers with impaired serotonin production. *Arch Gen Psychiatry* **67**, 1033-1043 (2011).
175 Liu, D. *et al.* Maternal care, hippocampal glucocorticoid receptors, and hypothalamic-pituitary-adrenal responses to stress. *Science* **277**, 1659-1662 (1997).
176 Owen, D., Andrews, M. H. & Matthews, S. G. Maternal adversity, glucocorticoids and programming of neuroendocrine function and behaviour. *Neuroscience and biobehavioral reviews* **29**, 209-226, doi:10.1016/j.neubiorev.2004.10.004 (2005).
177 Smith, S. E., Li, J., Garbett, K., Mirnics, K. & Patterson, P. H. Maternal immune activation alters fetal brain development through interleukin-6. *J Neurosci* **27**, 10695-10702, doi:10.1523/JNEUROSCI.2178-07.2007 (2007).
178 Padmanabhan, N. *et al.* Mutation in folate metabolism causes epigenetic instability and transgenerational effects on development. *Cell* **155**, 81-93, doi:10.1016/j.cell.2013.09.002 (2013).
179 Casey, B. J. *et al.* DSM-5 and RDoC: progress in psychiatry research? *Nat Rev Neurosci* **14**, 810-814, doi:10.1038/nrn3621 (2013).
180 Kaati, G., Bygren, L. O. & Edvinsson, S. Cardiovascular and diabetes mortality determined by nutrition during parents' and grandparents' slow growth period. *Eur J Hum Genet* **10**, 682-688 (2002).
181 Martin, K. F., Phillips, I., Hearson, M., Prow, M. R. & Heal, D. J. Characterization of 8-OH-DPAT-induced hypothermia in mice as a 5-HT1A autoreceptor response and its evaluation as a model to selectively identify antidepressants. *Br J Pharmacol* **107**, 15-21 (1992).
182 Drevets, W. C. *et al.* Serotonin-1A receptor imaging in recurrent depression: replication and literature review. *Nucl Med Biol* **34**, 865-877 (2007).
183 Merlot, E., Couret, D. & Otten, W. Prenatal stress, fetal imprinting and immunity. *Brain Behav Immun* **22**, 42-51, doi:10.1016/j.bbi.2007.05.007 (2008).
184 Malkova, N. V., Yu, C. Z., Hsiao, E. Y., Moore, M. J. & Patterson, P. H. Maternal immune activation yields offspring displaying mouse versions of the three core symptoms of autism. *Brain Behav Immun* **26**, 607-616 (2012).
185 Wohleb, E. S., Powell, N. D., Godbout, J. P. & Sheridan, J. F. Stress-induced recruitment of bone marrow-derived monocytes to the brain promotes

anxiety-like behavior. *J Neurosci* **33**, 13820-13833, doi:10.1523/JNEUROSCI.1671-13.2013 (2013).
186 Kheirbek, M. A. *et al.* Differential control of learning and anxiety along the dorsoventral axis of the dentate gyrus. *Neuron* **77**, 955-968 (2013).
187 Mühle, C., Reichel, M., Gulbins, E. & Kornhuber, J. Sphingolipids in psychiatric disorders and pain syndromes. *Handb Exp Pharmacol*, 431-456, doi:10.1007/978-3-7091-1511-4_22 (2013).
188 Bennett, C. N. & Horrobin, D. F. Gene targets related to phospholipid and fatty acid metabolism in schizophrenia and other psychiatric disorders: an update. *Prostaglandins Leukot Essent Fatty Acids* **63**, 47-59, doi:10.1054/plef.2000.0191 (2000).
189 Ammar, M. R., Kassas, N., Bader, M. F. & Vitale, N. Phosphatidic acid in neuronal development: a node for membrane and cytoskeleton rearrangements. *Biochimie* **107 Pt A**, 51-57, doi:10.1016/j.biochi.2014.07.026 (2014).
190 Consortium, E. P. An integrated encyclopedia of DNA elements in the human genome. *Nature* **489**, 57-74, doi:10.1038/nature11247 (2012).
191 Wojtasz, L., Daniel, K. & Toth, A. Fluorescence activated cell sorting of live female germ cells and somatic cells of the mouse fetal gonad based on forward and side scattering. *Cytometry A* **75**, 547-553, doi:10.1002/cyto.a.20729 (2009).
192 Ferguson-Smith, A. C. Genomic imprinting: the emergence of an epigenetic paradigm. *Nat Rev Genet* **12**, 565-575 (2011).
193 Rodgers, A. B. & Bale, T. L. Germ Cell Origins of Posttraumatic Stress Disorder Risk: The Transgenerational Impact of Parental Stress Experience. *Biol Psychiatry* **78**, 307-314, doi:10.1016/j.biopsych.2015.03.018 (2015).
194 Rivera, R. M. *et al.* Manipulations of mouse embryos prior to implantation result in aberrant expression of imprinted genes on day 9.5 of development. *Hum Mol Genet* **17**, 1-14, doi:10.1093/hmg/ddm280 (2008).
195 Clapcote, S. J. *et al.* Behavioral phenotypes of Disc1 missense mutations in mice. *Neuron* **54**, 387-402, doi:10.1016/j.neuron.2007.04.015 (2007).
196 Clapcote, S. J. & Roder, J. C. Survey of embryonic stem cell line source strains in the water maze reveals superior reversal learning of 129S6/SvEvTac mice. *Behav Brain Res* **152**, 35-48 (2004).
197 Danchin, E. *et al.* Beyond DNA: integrating inclusive inheritance into an extended theory of evolution. *Nat Rev Genet* **12**, 475-486 (2011).
198 Manolio, T. A. *et al.* Finding the missing heritability of complex diseases. *Nature* **461**, 747-753 (2009).
199 Stearns, F. W. One hundred years of pleiotropy: a retrospective. *Genetics* **186**, 767-773, doi:10.1534/genetics.110.122549 (2010).
200 Consortium, C.-D. G. o. t. P. G. Identification of risk loci with shared effects on five major psychiatric disorders: a genome-wide analysis. *Lancet* **381**, 1371-1379, doi:10.1016/S0140-6736(12)62129-1 (2013).

201 Hsiao, E. Y., McBride, S. W., Chow, J., Mazmanian, S. K. & Patterson, P. H. Modeling an autism risk factor in mice leads to permanent immune dysregulation. *Proc Natl Acad Sci U S A* **109**, 12776-12781, doi:10.1073/pnas.1202556109 (2012).
202 Meyer, U. *et al.* Relative prenatal and postnatal maternal contributions to schizophrenia-related neurochemical dysfunction after in utero immune challenge. *Neuropsychopharmacology* **33**, 441-456, doi:10.1038/sj.npp.1301413 (2008).
203 Beumer, W. *et al.* The immune theory of psychiatric diseases: a key role for activated microglia and circulating monocytes. *J Leukoc Biol* **92**, 959-975, doi:10.1189/jlb.0212100 (2012).
204 Köberlin, M. S. *et al.* A Conserved Circular Network of Coregulated Lipids Modulates Innate Immune Responses. *Cell* **162**, 170-183, doi:10.1016/j.cell.2015.05.051 (2015).
205 Rodgers, A. B., Morgan, C. P., Bronson, S. L., Revello, S. & Bale, T. L. Paternal stress exposure alters sperm microRNA content and reprograms offspring HPA stress axis regulation. *J Neurosci* **33**, 9003-9012, doi:10.1523/JNEUROSCI.0914-13.2013 (2013).
206 Kaiser, T. & Feng, G. Modeling psychiatric disorders for developing effective treatments. *Nat Med* **21**, 979-988, doi:10.1038/nm.3935 (2015).
207 Parks, C. L., Robinson, P. S., Sibille, E., Shenk, T. & Toth, M. Increased anxiety of mice lacking the serotonin1A receptor. *Proc Natl Acad Sci U S A* **95**, 10734-10739 (1998).
208 Porsolt, R. D., Anton, G., Blavet, N. & Jalfre, M. Behavioural despair in rats: a new model sensitive to antidepressant treatments. *Eur J Pharmacol* **47**, 379-391 (1978).
209 Bortolozzi, A. *et al.* Selective siRNA-mediated suppression of 5-HT1A autoreceptors evokes strong anti-depressant-like effects. *Mol Psychiatry* **17**, 612-623, doi:10.1038/mp.2011.92 (2012).
210 Toyooka, Y. *et al.* Expression and intracellular localization of mouse Vasa-homologue protein during germ cell development. *Mech Dev* **93**, 139-149 (2000).
211 Chen, Q. *et al.* Untargeted plasma metabolite profiling reveals the broad systemic consequences of xanthine oxidoreductase inactivation in mice. *PLoS One* **7**, e37149, doi:10.1371/journal.pone.0037149 (2012).
212 Ismailoglu, I. *et al.* Huntingtin protein is essential for mitochondrial metabolism, bioenergetics and structure in murine embryonic stem cells. *Developmental biology* **391**, 230-240, doi:10.1016/j.ydbio.2014.04.005 (2014).
213 Chan, R. B. *et al.* Comparative lipidomic analysis of mouse and human brain with Alzheimer disease. *J Biol Chem* **287**, 2678-2688, doi:10.1074/jbc.M111.274142 (2012).
214 Dumont, M. *et al.* Bezafibrate administration improves behavioral deficits and tau pathology in P301S mice. *Hum Mol Genet* **21**, 5091-5105, doi:10.1093/hmg/dds355 (2012).

215 Weinstock, M. The potential influence of maternal stress hormones on development and mental health of the offspring. *Brain, behavior, and immunity* **19**, 296-308 (2005).
216 Humphreys, K. L. & Zeanah, C. H. Deviations from the expectable environment in early childhood and emerging psychopathology. *Neuropsychopharmacology : official publication of the American College of Neuropsychopharmacology* **40**, 154-170 (2015).
217 Moses-Kolko, E. L. *et al.* Serotonin 1A receptor reductions in postpartum depression: a positron emission tomography study. *Fertil Steril* **89**, 685-692 (2008).
218 Neumeister, A. *et al.* Reduced serotonin type 1A receptor binding in panic disorder. *J Neurosci* **24**, 589-591 (2004).
219 Savitz, J., Lucki, I. & Drevets, W. C. 5-HT(1A) receptor function in major depressive disorder. *Progress in neurobiology* **88**, 17-31 (2009).
220 Toth, M. 5-HT1A receptor knockout mouse as a genetic model of anxiety. *Eur J Pharmacol* **463**, 177-184 (2003).
221 Enayati, M. *et al.* Maternal infection during late pregnancy increases anxiety- and depression-like behaviors with increasing age in male offspring. *Brain research bulletin* **87**, 295-302 (2012).
222 Guha, M. *et al.* Lipopolysaccharide activation of the MEK-ERK1/2 pathway in human monocytic cells mediates tissue factor and tumor necrosis factor alpha expression by inducing Elk-1 phosphorylation and Egr-1 expression. *Blood* **98**, 1429-1439 (2001).
223 Girard, S., Tremblay, L., Lepage, M. & Sebire, G. IL-1 receptor antagonist protects against placental and neurodevelopmental defects induced by maternal inflammation. *J Immunol* **184**, 3997-4005 (2010).
224 Olsavsky, A. K. *et al.* Indiscriminate amygdala response to mothers and strangers after early maternal deprivation. *Biological psychiatry* **74**, 853-860 (2013).
225 Chugani, H. T. *et al.* Local brain functional activity following early deprivation: a study of postinstitutionalized Romanian orphans. *NeuroImage* **14**, 1290-1301 (2001).
226 Laudenslager, M. L., Reite, M. & Harbeck, R. J. Suppressed immune response in infant monkeys associated with maternal separation. *Behavioral and neural biology* **36**, 40-48 (1982).
227 Romeo, R. D. *et al.* Anxiety and fear behaviors in adult male and female C57BL/6 mice are modulated by maternal separation. *Hormones and behavior* **43**, 561-567 (2003).
228 Beydoun, H. & Saftlas, A. F. Physical and mental health outcomes of prenatal maternal stress in human and animal studies: a review of recent evidence. *Paediatr Perinat Epidemiol* **22**, 438-466 (2008).
229 Davis, E. P. *et al.* Prenatal exposure to maternal depression and cortisol influences infant temperament. *J Am Acad Child Adolesc Psychiatry* **46**, 737-746 (2007).

230 Halligan, S. L., Murray, L., Martins, C. & Cooper, P. J. Maternal depression and psychiatric outcomes in adolescent offspring: a 13-year longitudinal study. *J Affect Disord* **97**, 145-154 (2007).
231 Klein, D. N. *et al.* Early adversity in chronic depression: clinical correlates and response to pharmacotherapy. *Depress Anxiety* **26**, 701-710 (2009).
232 Mueller, B. R. & Bale, T. L. Sex-specific programming of offspring emotionality after stress early in pregnancy. *J Neurosci* **28**, 9055-9065 (2008).
233 Weaver, I. C. *et al.* Epigenetic programming by maternal behavior. *Nature neuroscience* **7**, 847-854, doi:10.1038/nn1276 (2004).
234 Weaver, I. C. *et al.* Reversal of maternal programming of stress responses in adult offspring through methyl supplementation: altering epigenetic marking later in life. *J Neurosci* **25**, 11045-11054 (2005).
235 Radtke, K. M. *et al.* Transgenerational impact of intimate partner violence on methylation in the promoter of the glucocorticoid receptor. *Translational Psychiatry* **Published online 19 July** (2011).
236 Whitelaw, N. C. & Whitelaw, E. Transgenerational epigenetic inheritance in health and disease. *Curr Opin Genet Dev* **18**, 273-279 (2008).
237 Cedar, H. & Bergman, Y. Linking DNA methylation and histone modification: patterns and paradigms. *Nat Rev Genet* **10**, 295-304 (2009).
238 Jacome, L. F., Burket, J. A., Herndon, A. L. & Deutsch, S. I. Genetically inbred Balb/c mice differ from outbred Swiss Webster mice on discrete measures of sociability: relevance to a genetic mouse model of autism spectrum disorders. *Autism research : official journal of the International Society for Autism Research* **4**, 393-400 (2011).
239 Rice, M. C. & O'Brien, S. J. Genetic variance of laboratory outbred Swiss mice. *Nature* **283**, 157-161 (1980).
240 Mitchell, E. *et al.* **Propagation of Anxiety Traits through the Maternal Line via Segregated and Parallel Epigenetic Mechanisms**. *submitted* (2015).
241 Agid, O. *et al.* Environment and vulnerability to major psychiatric illness: a case control study of early parental loss in major depression, bipolar disorder and schizophrenia. *Mol Psychiatry* **4**, 163-172 (1999).
242 Kessler, R. C., Davis, C. G. & Kendler, K. S. Childhood adversity and adult psychiatric disorder in the US National Comorbidity Survey. *Psychol Med* **27**, 1101-1119 (1997).
243 Cruz, F. C., Quadros, I. M., Planeta, C. a. S. & Miczek, K. A. Maternal separation stress in male mice: long-term increases in alcohol intake. *Psychopharmacology (Berl)* **201**, 459-468, doi:10.1007/s00213-008-1307-4 (2008).
244 Moffett, M. C. *et al.* Maternal separation alters drug intake patterns in adulthood in rats. *Biochem Pharmacol* **73**, 321-330, doi:10.1016/j.bcp.2006.08.003 (2007).

245 Moy, S. S. *et al.* Sociability and preference for social novelty in five inbred strains: an approach to assess autistic-like behavior in mice. *Genes Brain Behav* **3**, 287-302, doi:10.1111/j.1601-1848.2004.00076.x (2004).
246 Brown, A. S. Epidemiologic studies of exposure to prenatal infection and risk of schizophrenia and autism. *Developmental neurobiology* **72**, 1272-1276 (2012).
247 Chess, S. Follow-up report on autism in congenital rubella. *J Autism Child Schizophr* **7**, 69-81 (1977).
248 Bannerman, D. M. *et al.* Ventral hippocampal lesions affect anxiety but not spatial learning. *Behav Brain Res* **139**, 197-213 (2003).
249 Gordon, J. A., Lacefield, C. O., Kentros, C. G. & Hen, R. State-dependent alterations in hippocampal oscillations in serotonin 1A receptor-deficient mice. *J Neurosci* **25**, 6509-6519 (2005).
250 Adhikari, A., Topiwala, M. A. & Gordon, J. A. Single units in the medial prefrontal cortex with anxiety-related firing patterns are preferentially influenced by ventral hippocampal activity. *Neuron* **71**, 898-910 (2011).
251 Wang, H. Q., Tuominen, L. K. & Tsai, C. J. SLIM: a sliding linear model for estimating the proportion of true null hypotheses in datasets with dependence structures. *Bioinformatics* **27**, 225-231, doi:10.1093/bioinformatics/btq650 (2011).
252 Koleske, A. J. Molecular mechanisms of dendrite stability. *Nature reviews. Neuroscience* **14**, 536-550 (2013).
253 Okano, M., Bell, D. W., Haber, D. A. & Li, E. DNA methyltransferases Dnmt3a and Dnmt3b are essential for de novo methylation and mammalian development. *Cell* **99**, 247-257 (1999).
254 Altman, J. & Bayer, S. A. Migration and distribution of two populations of hippocampal granule cell precursors during the perinatal and postnatal periods. *J Comp Neurol* **301**, 365-381 (1990).
255 Olshausen, B. A. & Field, D. J. Sparse coding of sensory inputs. *Current opinion in neurobiology* **14**, 481-487, doi:10.1016/j.conb.2004.07.007 (2004).
256 Samuelsson, A. M., Jennische, E., Hansson, H. A. & Holmang, A. Prenatal exposure to interleukin-6 results in inflammatory neurodegeneration in hippocampus with NMDA/GABA(A) dysregulation and impaired spatial learning. *American journal of physiology. Regulatory, integrative and comparative physiology* **290**, R1345-1356 (2006).
257 Sakic, B. *et al.* Disturbed emotionality in autoimmune MRL-lpr mice. *Physiology & behavior* **56**, 609-617 (1994).
258 Duman, C. H. *et al.* Peripheral insulin-like growth factor-I produces antidepressant-like behavior and contributes to the effect of exercise. *Behav Brain Res* **198**, 366-371 (2009).
259 Chen, J. *et al.* Maternal deprivation in rats is associated with corticotrophin-releasing hormone (CRH) promoter hypomethylation and enhances CRH transcriptional responses to stress in adulthood. *Journal of neuroendocrinology* **24**, 1055-1064 (2012).

260 Elliott, G. *et al.* Intermediate DNA methylation is a conserved signature of genome regulation. *Nature communications* **6**, 6363 (2015).
261 Maunakea, A. K., Chepelev, I., Cui, K. & Zhao, K. Intragenic DNA methylation modulates alternative splicing by recruiting MeCP2 to promote exon recognition. *Cell research* **23**, 1256-1269, doi:10.1038/cr.2013.110 (2013).
262 Bird, A. DNA methylation patterns and epigenetic memory. *Genes Dev* **16**, 6-21 (2002).
263 Ntanasis-Stathopoulos, J., Tzanninis, J. G., Philippou, A. & Koutsilieris, M. Epigenetic regulation on gene expression induced by physical exercise. *Journal of musculoskeletal & neuronal interactions* **13**, 133-146 (2013).
264 Cortes-Mendoza, J., Diaz de Leon-Guerrero, S., Pedraza-Alva, G. & Perez-Martinez, L. Shaping synaptic plasticity: the role of activity-mediated epigenetic regulation on gene transcription. *International journal of developmental neuroscience : the official journal of the International Society for Developmental Neuroscience* **31**, 359-369, doi:10.1016/j.ijdevneu.2013.04.003 (2013).
265 Barreto, G. *et al.* Gadd45a promotes epigenetic gene activation by repair-mediated DNA demethylation. *Nature* **445**, 671-675 (2007).
266 Rai, K. *et al.* DNA demethylation in zebrafish involves the coupling of a deaminase, a glycosylase, and gadd45. *Cell* **135**, 1201-1212 (2008).
267 Werner, E. E. Children and war: risk, resilience, and recovery. *Development and psychopathology* **24**, 553-558, doi:10.1017/S0954579412000156 (2012).
268 Essex, M. J., Klein, M. H., Cho, E. & Kalin, N. H. Maternal stress beginning in infancy may sensitize children to later stress exposure: effects on cortisol and behavior. *Biological psychiatry* **52**, 776-784 (2002).
269 Caldji, C. *et al.* Maternal care during infancy regulates the development of neural systems mediating the expression of fearfulness in the rat. *Proc Natl Acad Sci U S A* **95**, 5335-5340 (1998).
270 Careau, V., Buttemer, W. A. & Buchanan, K. L. Early-developmental stress, repeatability, and canalization in a suite of physiological and behavioral traits in female zebra finches. *Integrative and comparative biology* **54**, 539-554, doi:10.1093/icb/icu095 (2014).
271 Dantzer, B. *et al.* Density triggers maternal hormones that increase adaptive offspring growth in a wild mammal. *Science* **340**, 1215-1217, doi:10.1126/science.1235765 (2013).
272 Weaver, I. C., Meaney, M. J. & Szyf, M. Maternal care effects on the hippocampal transcriptome and anxiety-mediated behaviors in the offspring that are reversible in adulthood. *Proc Natl Acad Sci U S A* **103**, 3480-3485 (2006).
273 Downing, C. *et al.* Subtle decreases in DNA methylation and gene expression at the mouse Igf2 locus following prenatal alcohol exposure: effects of a methyl-supplemented diet. *Alcohol* **45**, 65-71, doi:10.1016/j.alcohol.2010.07.006 (2011).